

AD 625782

FINAL REPORT

to

Office of Civil Defense  
Contract OCD-PS-64-217  
157

YIELDING MEMBRANE ELEMENTS  
IN  
PROTECTIVE CONSTRUCTION

OCD REVIEW NOTICE

This report has been reviewed in the  
Office of Civil Defense and approved for publication.  
Approval does not signify that the content necessarily  
reflects the views and policies of the Office of Civil  
Defense.

ENGINEERING RESEARCH LABORATORY  
UNIVERSITY OF ARIZONA  
TUCSON, ARIZONA

MAY 28, 1965

**DISTRIBUTION OF THIS DOCUMENT IS UNLIMITED**

The following persons have participated directly  
in the development of the findings reported in  
this document.

**Principal Investigators:**

H. Harrenstien  
R. Gunderson  
S. Hansen  
J. Burns  
J. Salmons  
D. Nielson

**Consultants:**

R. Richard  
D. Linger

**Engineering Editor:**

G. Sheets

## TABLE OF CONTENTS

### CHAPTER I INTRODUCTION

	page
General	1
Traditional Configurations	1
Design Economy	1
Efficient Protective Structures Configurations	1
The Contract	2

### CHAPTER II SHELTER APPLICATIONS AND CONSTRUCTION TECHNIQUES

General	3
Circular Membrane Structure	3
Rectangular Membrane Structure	3
Other Applications	6

### CHAPTER III ENGINEERING ANALYSES

Introduction	7
General Membrane Theory	7
Membrane Analysis of a Thin Plate	7
Two-Way Circular Membrane	8
General Theory of Funicular Shells	10
Solutions and Design Curves	11
Membranes Supported by Yielding Beams	13
Boundary Conditions	13
Yielding Membranes Supported by Concrete Arch Rings	14
Yielding Membranes Supported by Straight Edge Beams	16
Yielding Membranes Supported by Curved Edge Beams	17
Yielding Membranes Supported by Reinforced Concrete Shear Slabs	18
Yielding Membranes Supported by Membrane Elements	18
Dynamic Tests	20

### CHAPTER IV SUMMARY AND CONCLUSIONS

### APPENDIX A YIELDING MEMBRANE FORCES

Introduction	A-1
Yielding Membrane Theory	A-1
Formulation of the Problem	A-1
Yielding Edge Beams	A-8
Finite Difference Equations	A-8
Computer Results	A-10
Equivalent Curves for Other Materials	A-20

APPENDIX A  
(continued)

	page
Experimental Analysis	A-21
Introduction	A-21
Test Equipment	A-21
Test Procedure	A-22
Experimental Observations	A-22
Membrane Boundary Conditions	A-25
Analytical and Experimental Comparisons	A-26
Updating Previous Work	A-26
Comparison of Test Results and Computer Results	A-31

APPENDIX B  
YIELDING MEMBRANE PROGRAM

Abstract	B-1
Introduction	B-1
Mathematical Formulation of the Problem	B-1
Discussion of the Computer Program	B-4
Capacity	B-6
Detailed Procedure	B-6
Output	B-10
Relaxation Factors	B-17
Strain	B-17
Modifications to the Program	B-17
Two Parallel Edges Free	B-20
Plastic Beams Across Two Parallel Edges	B-27

APPENDIX C  
SOIL-STRUCTURE INTERACTION

Introduction	C-1
Soil-Structure Interaction Forces	C-1
Effective Soil-Structure Interaction Pressures	C-1
Types of Buried Structures	C-1
Rigid Buried Structures	C-1
Rigid Flexible Buried Structures	C-1
Flexible Buried Structures	C-1
Settlement Ratios	C-1
The Positive Settlement Ratio	C-3
The Negative Settlement Ratio	C-4
Zero Settlement Ratio	C-4
Soil-Structure Interactions	C-5
Rigid Fully-Buried Structures	C-5
Flexible Buried Structures	C-6
Rigid-Flexible Buried Structures	C-6
Summary of Effects	C-6
Analysis Features	C-6
Design Features	C-7

APPENDIX D  
HISTORICAL REVIEW OF MEMBRANE THEORY

Bibliography	D-4
--------------	-----

# CHAPTER I

## INTRODUCTION

### General

When the design of protective structures to resist blast and other close-in nuclear weapons effects is considered, it is only logical to realize that simultaneously large amounts of initial and fallout radiation may be inevitable realities. The shielding that is required to provide adequate resistance to close-in radiological effects, and the structural strength required to properly resist the blast effects in these regions, suggest buried structures as the most feasible solution. It is observed that the buried structure, in addition to providing resistance to these effects, possesses a hardness which is applicable to resisting other effects, for example those from the immediate thermal pulse and the effects of later fires.

Laymen, and engineers alike, have for years concluded that such shelters are beyond the reach of economical programs. This in fact is reflected in current national OCD policy and the National Shelter Program. However, such reasoning is usually not based on studies which consider true minimum cost structures. In general, the structures on which these conclusions are based are traditional in concept. These traditional structures in general grew from application of traditional design procedures to situations in which loadings are of one or two orders of magnitude greater than traditional.

### Traditional Configurations

Traditional building configurations or shapes were originally conceived and generated to house man in everyday functions; and were called upon, structurally, to resist only natural and self induced loads of moderate magnitude. Most of the engineering technology developed for traditional or conventional design was directed toward the development of procedures and methodologies to adequately assure the designer that this structure, which for example was composed of beams and slabs, would properly resist these conventional loads. The magnitude of load rarely affected very greatly the choice of structural type. When overpressures from nuclear bursts are considered, and then the existing design procedures are applied to design traditional type structures for these higher loadings, there is little wonder that expensive designs result.

### Design Economy

Two aspects (among others) are present in the design of all civil engineering structures. They are the selection of configuration, and the determination of size. The configuration, or shape, is a qualitative matter which describes in general terms the nature of the structure such as a flat slab, beam slab, concrete joist, or dome type. The other aspect is size of the structural components which are contained in the shape. These are aspects such as thicknesses, amounts and location of reinforcement, etc. In the traditional civil engineering structure, the shape decision has generally been somewhat arbitrary. The size decision, within the shape, has been determined by more or less rigorous calculations. This procedure results in reasonably economical solutions if loads and spans are small. In the case of design for blast resistance, the loads are significantly higher than any considered previously. The spans may be shortened, but usually at a loss of functional value. Thus it is not surprising to discover that selection of configuration can no longer be as arbitrary.

In summary, if the structural configuration is selected without regard to the magnitude and type of loading, the resulting size determinations will invariably lead to the requirement of a great amount of material, and therefore higher cost. If, however, structural configurations are chosen out of proper respect for loads, the resulting sizes will be reasonable and hence material quantities which are related to cost will be reduced and held near a minimum.

### Efficient Protective Structures Configurations

The most efficient forms that man knows to resist pressures are doubly-curved shell structures. A shell structure achieves its efficiency by resisting loads primarily through the development of direct stress. Examples of these types are the spherical and parabolic domes that are common in civil engineering solutions to the problem of spanning large arenas with a minimum of material. The shell of an egg is another common example of this form which exhibits the same type of structural efficiency. Among the classes of doubly-curved shells, which are available, are some which exhibit truly the ultimate in structural efficiency. These are the constant-stress funicular shells. The spherical pressure vessel is an example of this type.

Constant stress funicular shells resist pressure loads by either developing uniform tensile or uniform compressive stresses depending on the particular configuration. The concrete shell works best in compression; the steel shell in tension.

Unfortunately, compressive funicular shells which have low thickness to curvature ratios tend to buckle on overload. As a general statement, a shell structure (or any structure) in a state of compression may buckle catastrophically if certain combinations of geometric and material parameters are ill chosen. Because the calculation or prediction of this tendency is a complex procedure for all but the simplest of structures; and at best is an approximation, it is probably better to avoid the problem entirely by insisting that tensile funicular shells be used. These structures cannot buckle.

### The Contract

This report is the result of a contract, a quote from which follows. It investigates the feasibility of the application of these funicular structures to the problem of sheltering people from dynamic overpressures caused by nearby nuclear or conventional bursts.

- "A. The contractor, in consultation and cooperation with the Government, shall furnish all engineering, labor, equipment, tools, materials, supplies, facilities, and services necessary for a feasibility study relating to optimizing shelter design. The work and services shall pertain to the analysis and design of flexible yielding membrane elements of a shelter to resist normal dynamic effects not unlike those which may result at the soil-structure interface as a result of a nuclear blast.
- B. The general areas of investigation shall include, but not be limited to the following:
1. Investigate the theoretical prediction of the configuration of a yielding membrane and determine its application to the shelter.
  2. Perform certain loading simulator studies to corroborate the intuitive fact that yielding buried structures are efficient structural systems.
  3. Extend the theory of studies involving the investigations of the membrane supported on yielding boundaries.
  4. Determine the feasibility of future possible exploitation in this area."

## CHAPTER II

### SHELTER APPLICATIONS AND CONSTRUCTION TECHNIQUES

#### General

In the course of introducing new concepts, such as that of the yielding membrane, it is often desirable (from a presentation standpoint) to indicate the ultimate uses of the product before the involved supporting calculations and data are presented. This pattern is used here; therefore, the material in this Chapter serves in part as illustration of an application of the concept. Models are used as examples of possible shelter applications.

The first example illustrates the rather limited application of a discontinuous circular dish membrane as the roof structure of a community shelter which is designed to resist 55 psi blast overpressure from a 5 MT nuclear weapon which is detonated as a surface burst. The second is an attempt at approaching the ultimate in efficiency of this application. This approach involves a multistory cubicle structure in which the yielding membrane is continuous and completely encloses the cubicle volume.

#### Circular Membrane Structure

The model shown in Figures 1 through 6 illustrates the application of the concept through the use of a dished membrane as a roof structure. Although blast simulator studies (Chapter III) indicate that the preliminary dishing is in fact unnecessary, from a structural standpoint, the application shown is a conservative one and is to be recommended until more test and analytical data are obtained.

The steel cap or membrane carries blast overpressure loadings primarily by the development of direct uniform tensile stress. Little or no bending exists; hence little or no shear is present. In the application shown, the membrane is not continuous. That is, it is a series of individually dished elements. This break in continuity requires the use of boundary arch structures which are the reinforced-concrete edge rings. They are, in fact, concrete arches which lie in a horizontal plane. They eventually transmit the vertical component of the load to the supporting wall structure. Note the visual expression of structural efficiency which is present when steel is used in tension and concrete in compression.

To provide added toughness in design concept, the modular system is used. Nature has used the same system, that of duplication of self sustaining elements, in many naturally occurring designs; in order to assure survival of the function of the overall product against attacks by facets of hostile environments. These modular units are 30 feet in diameter and conservatively use 3/8 inch steel membrane roofs. Each unit is an independent structure which does not rely upon the strength of adjacent units to provide a reaction or to contribute to the support of external forces. The particular advantage of this independent action is that the other elements of structure would not collapse if one unit failed. It must be noted here that large structures would be subjected to unsymmetrical loading caused by the transient nature of the blast wave, which would tend to shear each unit from the other vertically. The design suggested adjusts to this shearing tendency.

The prototype, which the model illustrates, would lend itself readily to precast and prefabricated construction methods. The entire wall structure can be constructed from one basic shape. Precast concrete piers may be set in place. Roof caps may be field welded to attachment points. A variation of this concept includes a membrane floor of the same configuration, and material, as the roof. An internal floor system would be required as well as other changes in construction technique. Cost estimates for this structure were reported previously on other contracts.\*

#### Rectangular Membrane Structure

If optimization of efficiency of configuration and application to the total shelter is attempted in concept, one solution which results is that presented in Figures 7 through 9. These are views of a model which is nearly the shape of a cube. The cube is the rectilinear solid which has the maximum interior volume for the minimum exterior surface. Because blast overpressures in shelters are hopefully resisted only at the exterior surfaces, the structure that incorporates a minimum of these surfaces uses a minimum of material within the configuration or shape classification. Such is a fundamental requirement of material cost minimization.

---

\* Final Report, "Local Civil Defense Systems," Contract OCD-OS-62-232, University of Arizona, June, 1964 and Final Report, "Cost Studies in Protective Construction Systems," Subcontract Institute for Defense Analysis, 138-4, January, 1965.

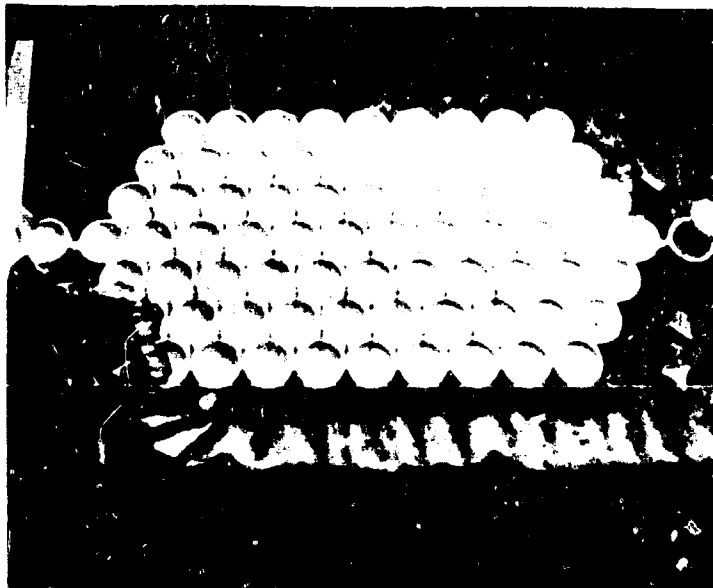


Figure 1 . Community shelter for 4,500 persons

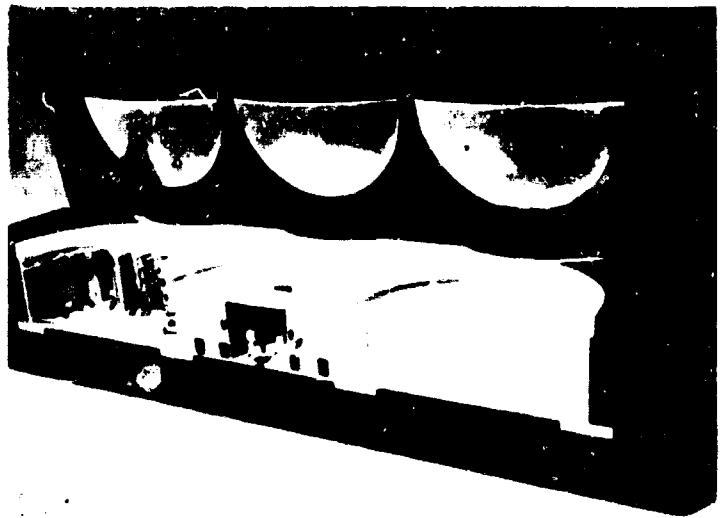


Figure 2 . Cross-section of community shelter module

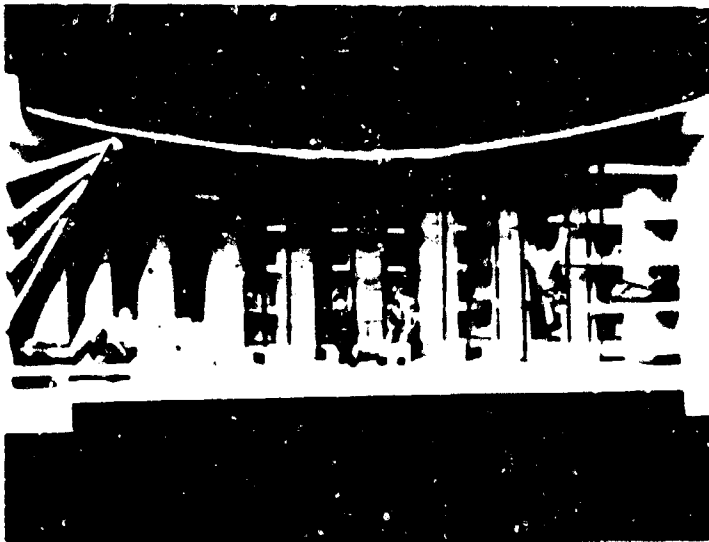


Figure 3 . Cross-section of community shelter module showing dish-type membrane roof structure.



Figure 4 . Close-up of construction procedure



Figure 5 . Construction procedure and sloping entrance



Figure 6 . Precast column which assembles to form all interior walls

Figure 7 (Right). A cutaway view of a model which illustrates the concept of the use of rectangular yielding membranes as exterior structural parts of a shelter complex. This model uses a minimum of exterior skin to a maximum of interior volume. The "egg crate" walks and floors provide the needed rigidity to keep the membrane in place.

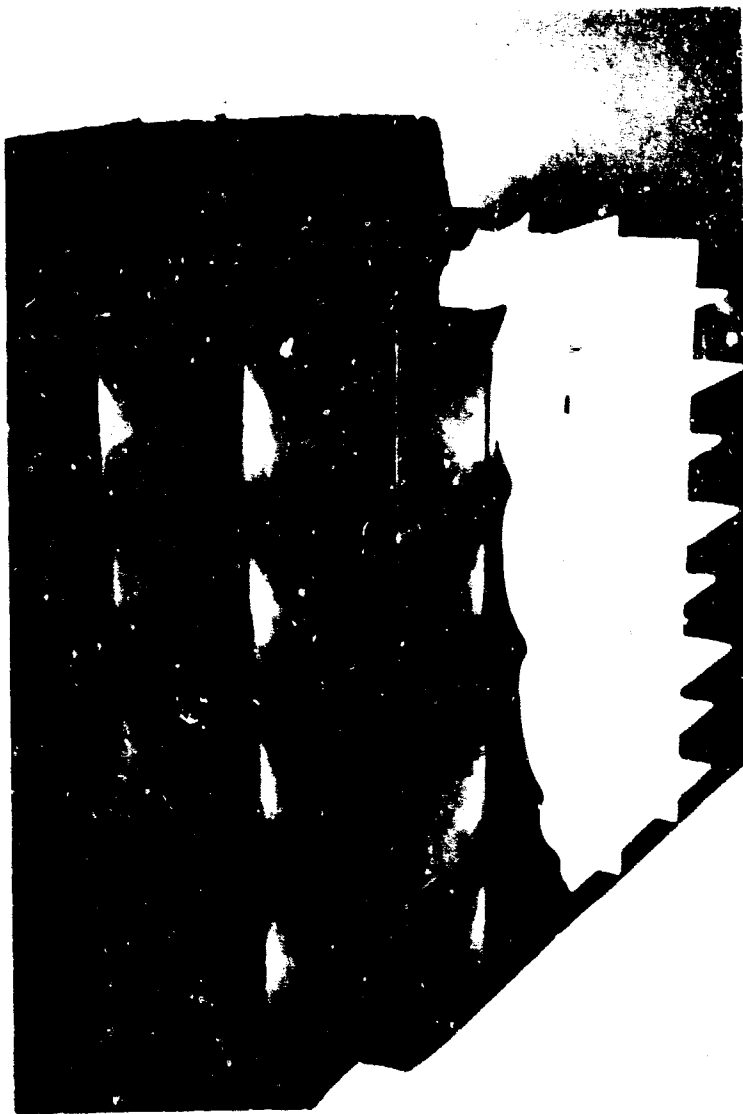


Figure 8 (Left). The membranes take a dished form as indicated in this photograph when they are subjected to external pressure. This dishing process promotes favorable soil-structure interaction behavior.



Figure 9 (Above). Requirements of flexibility in connections are crudely illustrated by this detail. It is necessary to use flexible links between the basic shelter and its somewhat disconnected entrance.

To further optimize the use of material, the exterior skin of this shelter is a continuous yielding membrane. As in the previous example, dished elements are used even though tests indicate such preliminary dishing is unnecessary. The advantages of continuity are apparent in the savings produced by the lack of reinforced concrete supporting edge rings. The interior walls and floors, which are of reinforced concrete, transfer the thrust through the entire shelter where it is equilibrated by the loads on the opposite sides. This shelter overcomes, in part, many of the structural disadvantages of large one-story structures. Aside from using a minimum of exterior surface, it resists the "slicing up" shears that occur in most large structures as the blast wave travels across the shelter. It is noted in passing that these can be extremely large but they are not usually considered in normal routine design practice.

The structural shell as illustrated possesses reserve strength to resist all conceivable ground motions associated with any overpressures for which it is designed. Interior details, of course, must be designed in such a way that the creation of interior missiles and associated damage to occupants is prevented.

#### Other Applications

No doubt, in the review of the applications presented in this Chapter, other applications of the membrane concept are indicated. These, in fact, do exist and include such items as blast doors, end walls to tube structures and above-ground protective enclosures for supplies; and other items which are unaffected by such factors as electromagnetic pulse, initial nuclear radiation, and fallout gamma radiation. Extremely thin membranes can resist very high overpressure in such applications but they must be shielded from missile penetration. In most cases, it is not necessary for such membranes to be pre-formed. Their ultimate resistance to blast overpressures is unaltered by leaving them initially flat.

CHAPTER III  
ENGINEERING ANALYSES

Introduction

Intuitively, it appears that yielding membranes are technically sound protective structure components. To support this intuitive reasoning, it is appropriate to consider certain supporting calculations and analyses of an engineering nature. In addition to the analysis of the continuum, attention must be given to the boundaries where the membranes terminate.

With respect to these problems the details of the historical development of analysis of these structures, together with specific developments for the instant shapes, are presented at length in Appendices A and D to this report. A summary of some of the more essential engineering features, which are in part abstracted from this analysis, are included in this Chapter.

General Membrane Theory

Flexible buried structures, because of yielding characteristics which produce negative settlement ratios, offer the ultimate in economy in view of the way in which they force the soil to resist the overload. The most efficient flexible structure is that which simultaneously yields under constant stress at every point in its plane. The behavior of such a structure may be predicted in advance by an inverse solution of the differential equations for stress in shell structures under normal pressure loadings. These structures by definition are called funicular.

For an example of the structural efficiency of a system such as this, consider the following simple comparisons. These structures are intentionally not buried for simplicity of presentation.

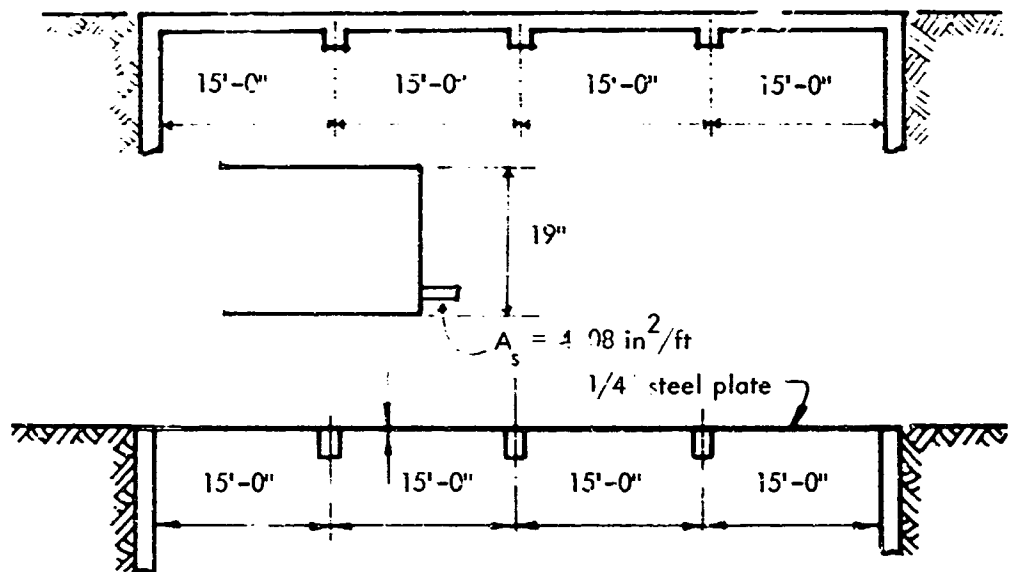
Membrane Analysis of a Thin Plate

For a comparison consider a previously designed one-way fiat slab.

Where under a standard design with  $p_o = 50$  psi the resulting section is as follows:

Now consider the same span covered with a thin steel plate.

Assume that when the load is applied the plate will yield into a circular arc. Consider a free body of the loaded section, as shown on the next page.



By static Equilibrium:

$$\sum F_v = 0$$

$$P_o(L) - 2(10,000 \frac{L/2}{R}) = 0$$

$$P_o = \frac{10,000}{R} \quad \text{or} \quad R = \frac{10,000}{P_o}$$

For this particular case of loading:

$$P_o = 50 \text{ psi} \quad \therefore R = \frac{10,000}{50} = 200 \text{ in.}$$

This determines the Radius as a function of the load only, independent of the length (L). This condition in itself is insufficient since no consideration is given to the percentage elongation. To determine this percentage, consider the equation of the triangle bounded by R and R-h.

$$(R-h)^2 = R^2 - (\frac{L}{2})^2$$

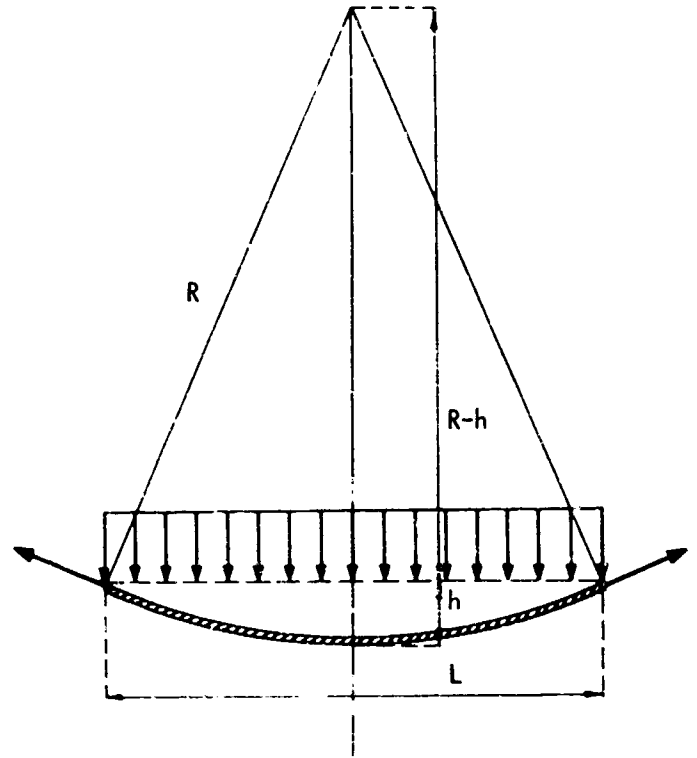
$$h = R - \sqrt{R^2 - (\frac{L}{2})^2}$$

h for this case is given by  $h = 200 - [(200)^2 - (90)^2]^{1/2} = 200 - 178 = 22"$   
 Calculation of the percentage of elongation:

$$\% e = \frac{Q-L}{L} \quad \text{where } Q \text{ is the arc length of the membrane}$$

$$Q = R\theta = (200) 2 \tan^{-1} \frac{90}{178} (\frac{\pi}{180}) = 187.2"$$

$$\% e = \frac{187.2 - 180}{180} = \frac{7.2}{180} = 0.04 = 4\% \quad \therefore \text{O.K.}$$



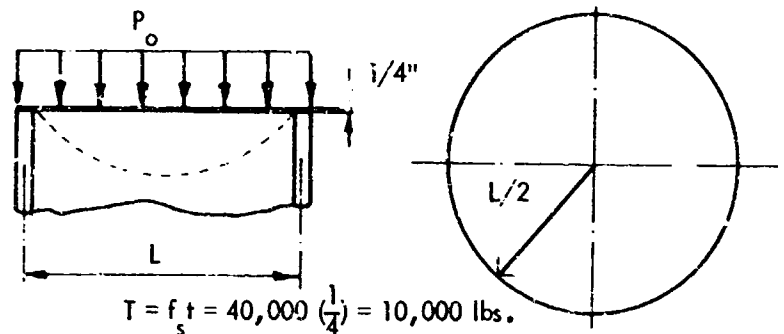
$$\text{At yield } T = f_s t = 40,000 (\frac{1}{4}) = 10,000 \text{ lbs./in.}$$

Thus it is seen that a 1/4" steel membrane is capable of resisting as great a load as a 19" reinforced concrete slab which is reinforced at a rate of 4.08 in<sup>2</sup>/ft. The plate contains 3.0 in<sup>2</sup>/ft. -- less steel than in the reinforced slab. The strain of 4% is less than the ultimate uniaxial strain capacity of most structural steel plate.

For increased efficiency of steel membrane, it may be used in a biaxial state of stress -- such as that found in a circular diaphragm, an example of which follows.

### Two-Way Circular Membrane

Consider a circular plate of diameter L subjected to a load of  $p_o$  psi and clamped around the circumference, as shown at the right.



$$T = f_s t = 40,000 (\frac{1}{4}) = 10,000 \text{ lbs.}$$

From static equilibrium:

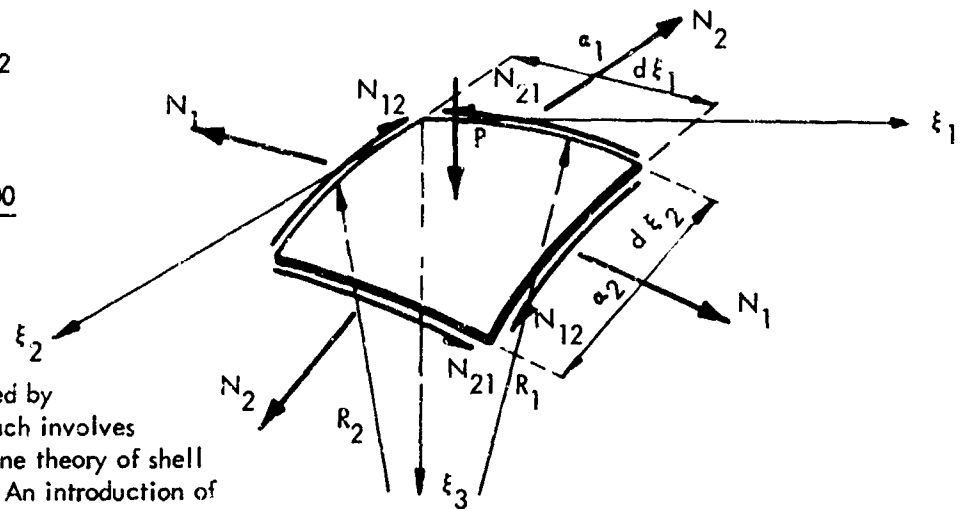
$$\sum F_v = 0$$

$$P_o \pi \left(\frac{L}{2}\right)^2 = 10,000 \left(\frac{L/2}{R}\right) \pi \left(\frac{L}{2}\right)^2$$

$$\therefore P_o = \frac{20,000}{R} \quad \text{or} \quad R = \frac{20,000}{P_o}$$

$$\text{For } P_o = 50 \text{ psi, } R = 400 \text{ in.}$$

The same examples may be solved by a more general approach. This approach involves the application of the general membrane theory of shell structures to the situation presented. An introduction of this approach to design was made at the Symposium on Shell Research, Delft, The Netherlands, August 30, 1961.\* The application at that time was directed toward the "Configuration of Shell Structures for Optimum Stress." Basically, the approach involves the initial assignment of a given final stress state, such as that of constant stress. The search is then made for the shell structure which exhibits this final state of stress under a previously assigned normal pressure loading.



Consider a free-body of an element of a shell, as shown above. From the equilibrium conditions, if

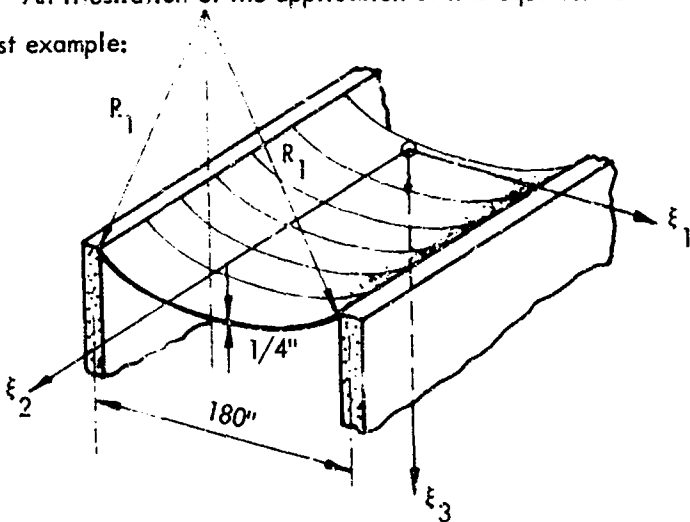
$$N_1 = N_2 = +S \text{ (constant), and } N_{12} = N_{21} = 0$$

then 
$$\frac{1}{R_1} + \frac{1}{R_2} = -\frac{P}{S}$$

Note that in this equation,  $R_1$  and  $R_2$  are the principal radii of curvature of the final deflected surface.  $P$  is the normal pressure on the surface and  $S$  is the membrane tension in dimensions of force per unit length.

An illustration of the application of this equation is now made with reference to the previous two examples.

First example:



$$R_2 = \infty \quad P = P_o \quad S = 10,000 \text{ lb/in.}$$

$$\therefore \frac{1}{R_1} + \frac{1}{R_2} = -\frac{P}{S} \text{ becomes}$$

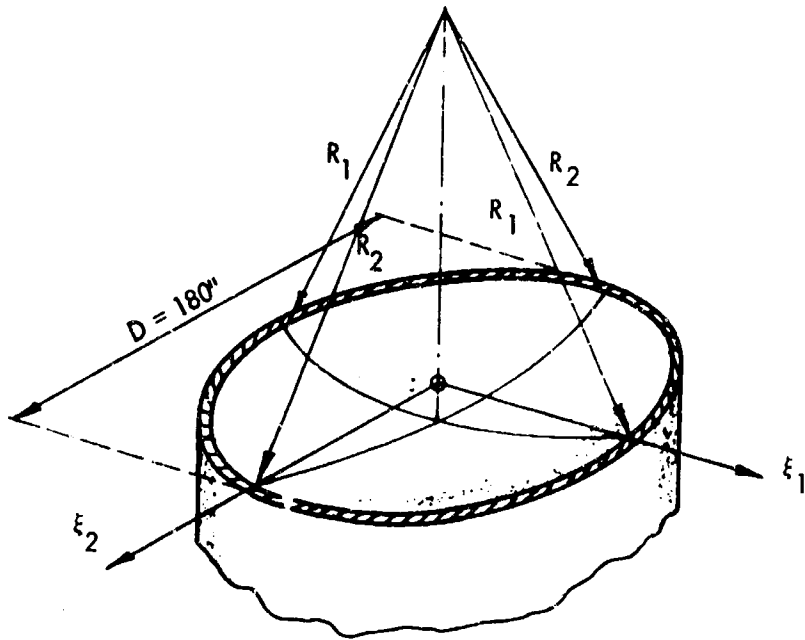
$$\frac{1}{R_1} + \frac{1}{\infty} = -\frac{P_o}{S}, \quad \frac{1}{R_1} = -\frac{P_o}{S}$$

$$\therefore R_1 = -\frac{S}{P_o}$$

$$R_1 = -\frac{10,000}{50} = -200 \text{ in., as before.}$$

\* H. P. Harrenstien, "Configuration of Shell Structures for Optimum Stresses," Proceedings of the Symposium on Shell Research, Delft, The Netherlands, 1961.

Second Example:



$$R_1 = R, R_2 = R, P = P_o = 50 \text{ psi}$$

$$S = 10,000 \text{ lb/in.}$$

$$\frac{1}{R_1} + \frac{1}{R_2} = \frac{P}{S} \text{ becomes}$$

$$R = -\frac{2S}{P_o}$$

$$\therefore R = -\frac{2(10,000)}{50} = -400 \text{ in.,}$$

again, as before.

Obviously, it is as simple to apply the free-body diagram approach as it is to apply the general theory, however for more complex problems, the general theory must be used in conjunction with numerical solutions on a digital computer. Appendix A presents this approach, the results of which are abstracted in the following material.

General Theory of Funicular Shells

A shell structure may be defined as a materialization of a curved surface in space. In general, the structure of a structural component so formed carries its loads primarily by direct stress. By this process, such structures make maximum use of the material from which they are formed in resisting applied loads (see Appendix B).

As stated before, among the classes of shell structures that are available for shelter application, there exists those which initially exhibit uniform direct stress characteristics under certain specified loadings. These types of shell structures possess the maximum possible structural efficiency that a two-dimensional structure is capable of providing. A structure which is of one sheet and which exhibits uniform stress characteristics under normal pressure loading is defined as a funicular shell. The particular type of such shell structures that are formed when a thin steel plate yields with "constant" stress under application of a distributed normal pressure is one such shape and is the subject at hand. The pressure need not be uniform for the funicular concept to be present.

The exact equation of curvature derived from differential geometry for a function  $z = f(x,y)$  is:

$$\frac{1}{R_1} + \frac{1}{R_2} = \frac{\left[1 + \left(\frac{\partial z}{\partial y}\right)^2\right] \frac{\partial^2 z}{\partial x^2} + \left[1 + \left(\frac{\partial z}{\partial x}\right)^2\right] \frac{\partial^2 z}{\partial y^2} - 2 \frac{\partial z}{\partial x} \frac{\partial z}{\partial y} \frac{\partial^2 z}{\partial x \partial y}}{\left[1 + \left(\frac{\partial z}{\partial x}\right)^2 + \left(\frac{\partial z}{\partial y}\right)^2\right]^{3/2}} = \frac{-P}{S}$$

## Solutions and Design Curves

This expression may be written in finite difference form and solved by iteration techniques on a digital computer for certain membrane shapes and specific edge conditions. The types considered are shown in Figure 10. The non-dimensionalized  $PD/S$  versus  $z_c/D$  curves, which are shown in Figure 11, are results from the computer study. Only the curves showing the center deflection are given, but these are the most important as far as design is concerned. These curves are based on the behavior of a rigid-plastic material. However, to use these curves with any other type of material the only additional information required is the appropriate stress-strain curve for the material.

The  $PD/S$  vs.  $z_c/D$  curves are based on the average stress and average strain across the center of the membrane. It is known that the strains are not uniform over a deflected membrane surface (2,3,4). However, as far as vertical deflections are concerned, the assumptions of uniform stresses and strains appear justified.

The only regions where this assumption leads to appreciable errors is in the corners of rectangular membranes. If reasonable care is taken during the construction to insure proper full-strength welds and if the design strain is reasonable (less than 2.5%) the yielding membrane structural element should serve quite well.

Either the circular or rectangular problems could be programmed for the computer with a non-uniform lateral pressure. Soon, it may be possible to predict the attenuation of pressure on a yielding structural element and the resulting pressure distribution. However, in working with yielding elements, they can be designed as if they were to be subjected to the full uniform lateral pressure. The yielding characteristics force the surface to take the shape it must assume.

Although certain metals, especially mild steel, have very large plastic elongation properties on uniaxial tests--sometimes greater than 30% strain--this does not mean the material will admit such large strains under biaxial conditions. In fact, most of the common yielding materials will not admit average strains greater than 9 to 10 percent even in a membrane state of stress. Since a true membrane state of stress may be difficult, if not impossible to realize in actual construction, a

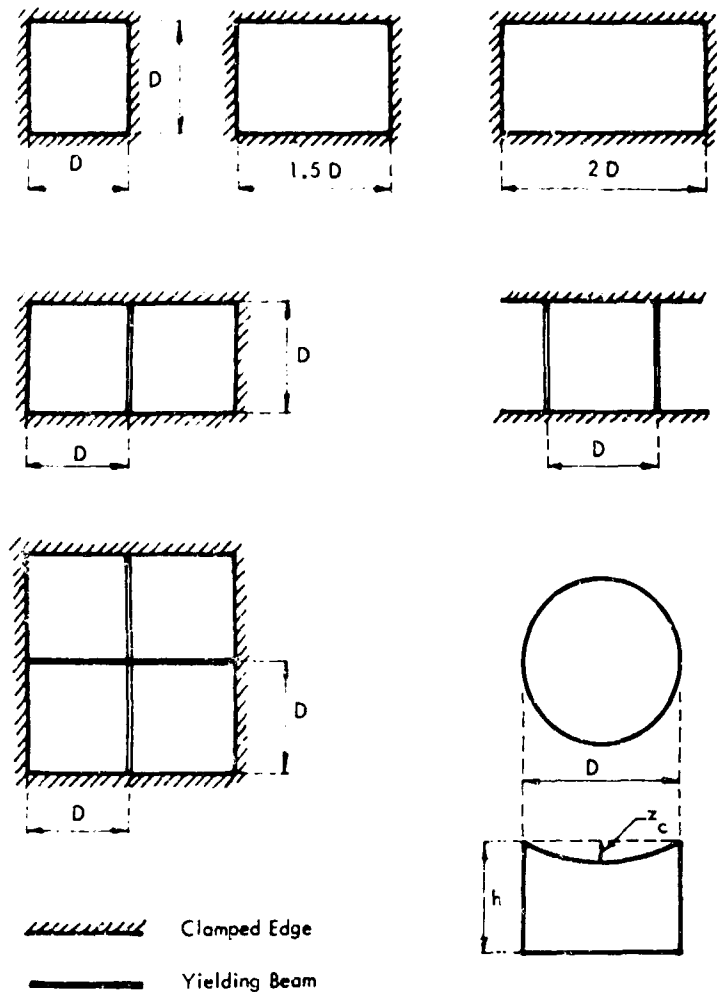


Figure 10. Plan Views of Shapes Considered

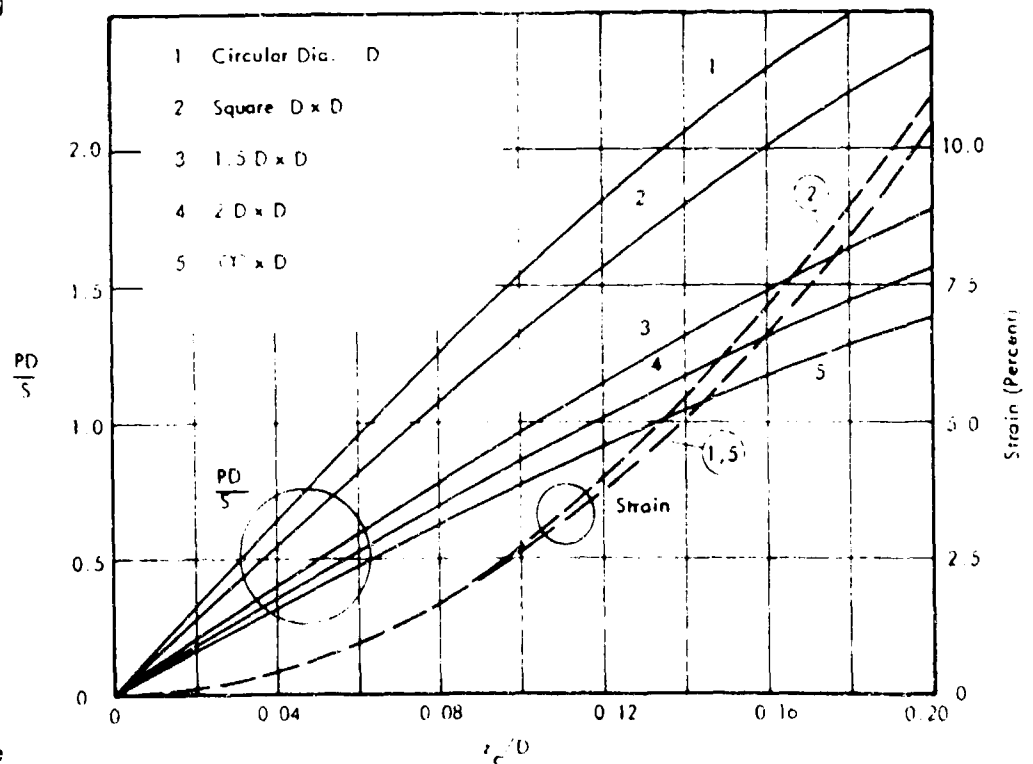


Figure 11.  $PD/S$  versus  $z_c/D$  Curves

maximum design strain of 2.5% is recommended. This strain corresponds to a  $z_c/D$  ratio of about 0.10.

To illustrate the use of these design curves, consider the circular membrane which was solved previously. In that example

$$P_{so} = P = 50 \text{ psi}$$

$$D = 15 \text{ ft} = 180 \text{ in.}$$

$$S = 10,000 \text{ lb/in.}$$

For this case

$$\frac{PD}{S} = \frac{(50)(180)}{10,000} = 0.90$$

From Figure 11;  $z_c/D = 0.057$ , which corresponds to a strain of approximately 1%. The center deflection,  $z_c$ , is then  $0.057 D$ , or 10.3 in.

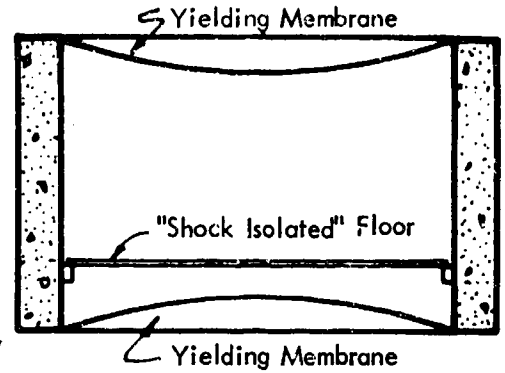


Figure 12. Yielding Membrane Shelter

The ultimate strength of this membrane may be easily determined by entering Figure 11 with a maximum biaxial strain requirement of 2.5%. For this strain  $PD/S = 1.5$  and  $z_c/D = 0.097$ . If  $PD/S = 1.5$ , then

$$P = \frac{1.5 S}{D} = \frac{1.5 (10,000)}{180} = 83 \text{ psi}$$

The center deflection,  $z_c$ , for this condition is  $z_c = 0.097 (180) = 17.5 \text{ in.}$  This example demonstrates the remarkable reserve strength of these elements.

To achieve the greatest economy and overall toughness of the shelter, it is suggested that the same type of membrane be used on the floor as on the roof. Figure 12 above, illustrates this concept.

Usually the center deflection to span ratio will be the governing design factor but, also a check should be made to insure against an excessive pressure increase in the structure which may be induced by the sudden deflection on the roof.

This "back pressure" should not be greater than 4 to 5 psi. The Lovelace Foundation indicates that this is the threshold of the eardrum damage region. The back pressure curve which is shown in Figure 13 is for a circular structure but will work well for square areas. If used for other rectangular shapes, the actual pressure would be greater than the value from the graph resulting in non-conservative answers. The whole problem of back pressure can be ignored if the membrane has an initial "dish."

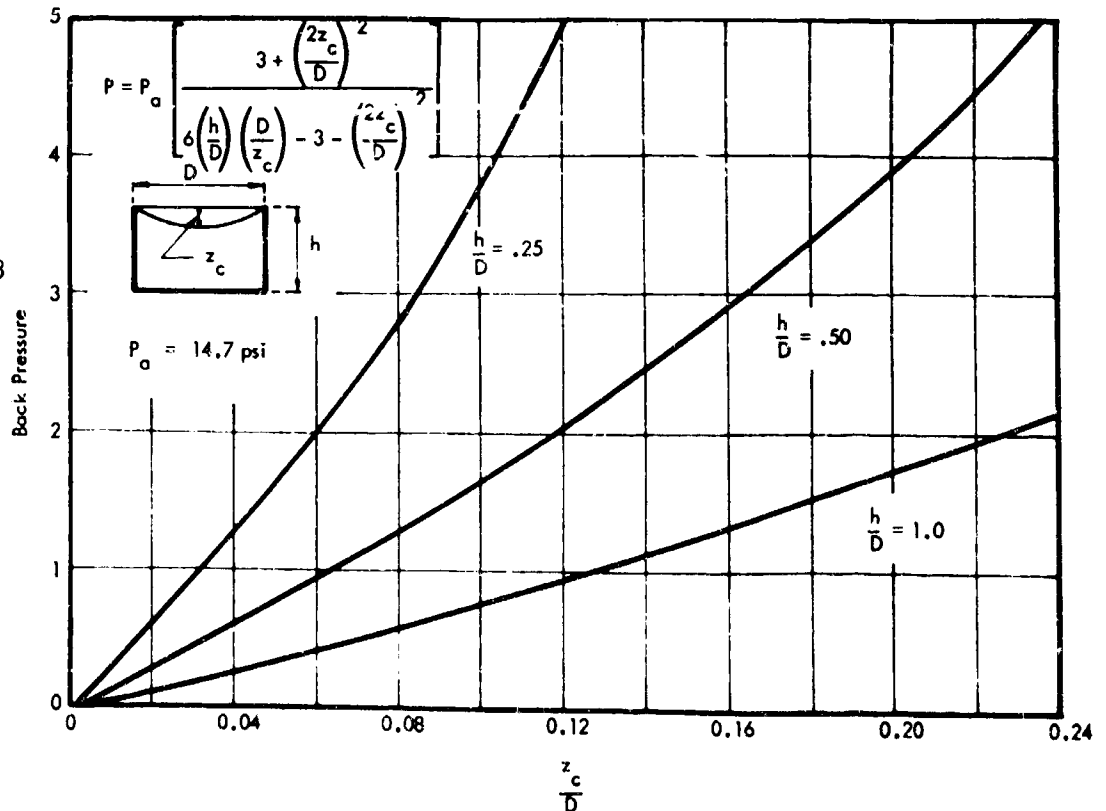


Figure 13. Peak Pressure vs. Center Deflection - Circular Membrane

## Membranes Supported by Yielding Beams

If yielding membranes were used in the design of blast shelters, it might be advantageous to use yielding beams as ribs across the membrane to decrease the maximum deflections. As with the yielding membrane itself, the force in the yielding beam would have to be resisted in some manner. In the following figures the behavior of such reinforced membranes is indicated.

The  $PD/S$  versus  $z_c/D$  curves (Figures 14, 15, and 16) are non-dimensionalized pressure versus deflection curves for the points of maximum deflection of the membrane and the center points on the beams for the conditions of edge constraint. The numbers inside the circles are values of the ratio  $F/SD$  where:

- F = strength of beam and membrane
- S = membrane strength
- D = short span distance

The subscripts refer to the locations of the point. For example,  $(1)_{9,9}$  refers to the  $PD/S$  vs.  $z/D$  curve for the center point of the membrane, when the ratio of beam strength to the product of the membrane strength and the span is one. These graphs are for symmetrical cases, i.e., it is assumed that the conditions on both sides of the supporting beams are the same (see Figures 18 and 19).

### Boundary Conditions

The yielding membrane, to be effective, must be supported by bounding structural elements which are capable of absorbing the full thrust of the material, at yield. For the type of situation shown in the first example of Chapter II, the concrete arches are well suited to provide the necessary support. For the second example shown in Chapter II, other details must be considered.

The following considers, in detail, examples of preliminary design solutions to the enumerated types of boundary support problems (Figure 17):

1. Yielding membranes supported by concrete arch rings
2. Yielding membranes supported by straight edge beams
3. Yielding membranes supported by curved edge beams
4. Yielding membranes supported by in plane beams
5. Yielding membranes supported by membrane elements

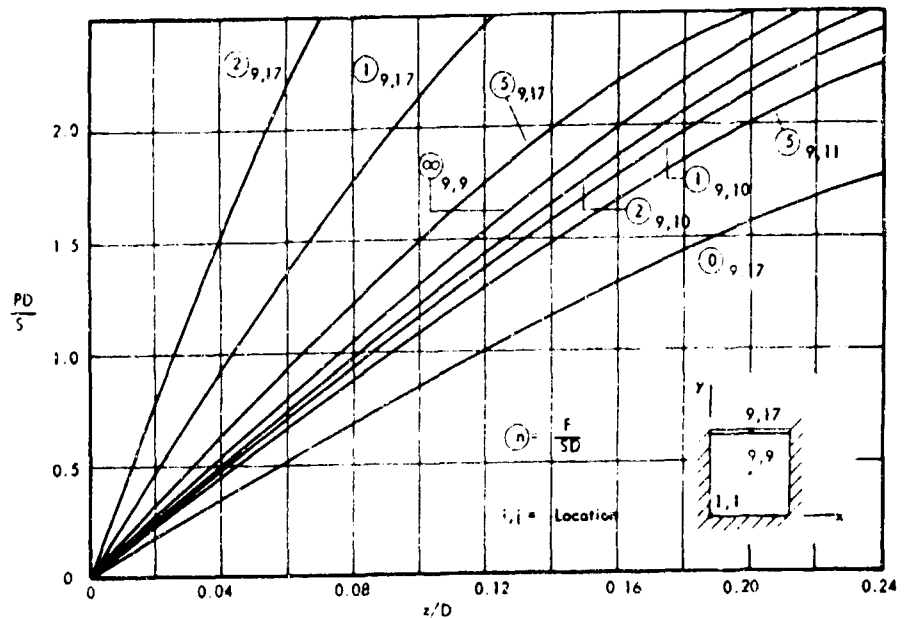


Figure 14.  $\frac{PD}{S}$  vs.  $\frac{z}{D}$ ; Square Membrane with One Edge Beam

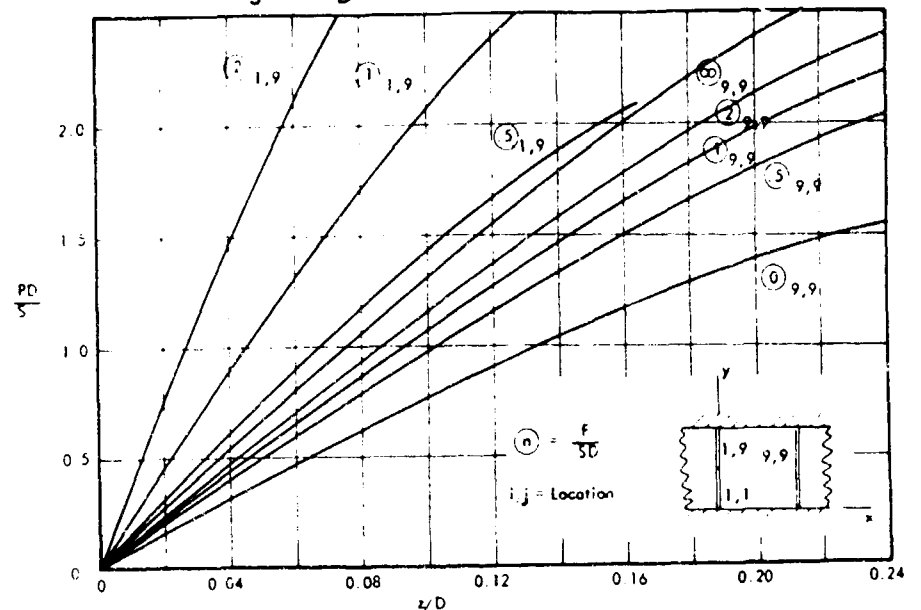


Figure 15.  $\frac{PD}{S}$  vs.  $\frac{z}{D}$ ; Square Membrane with Beams on Two Opposite Edges

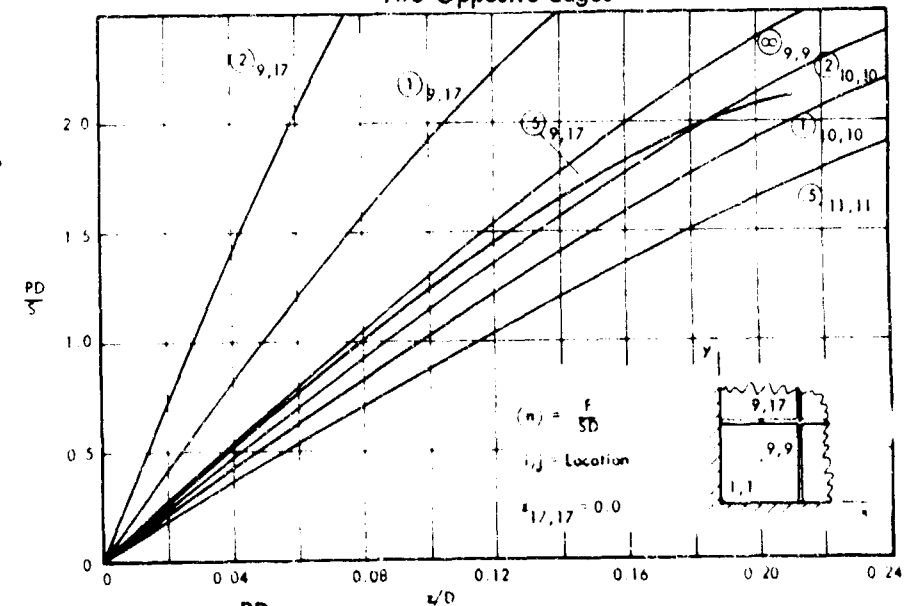
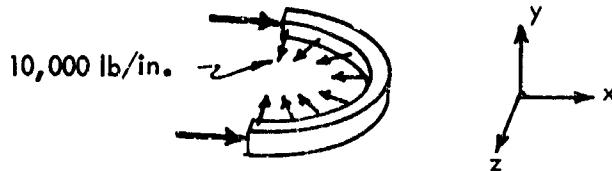
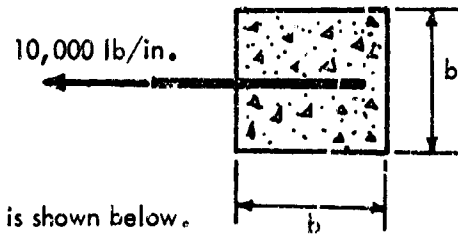


Figure 16.  $\frac{PD}{S}$  vs.  $\frac{z}{D}$ ; Square Membrane with Beams on Two Adjacent Edges

Yielding Membranes Supported by Concrete Arch Rings (Figure 17a). For an example of a supporting reinforced concrete arch ring for the circular membrane, see the design on page 19. Assume that the span,  $L$ , is 30 feet, a considerable span for a 1/4 inch roof structure which supports 50 psi. The edge ring requirement may be determined approximately as follows:

Consider the section loaded as shown by the full yield strength of the membrane. Note that at initial yield, the membrane force is horizontal.

For preliminary calculation purposes, assume a square arch of cross section  $b \times b$  and reinforced by mild steel at a percentage of 4%. A free body diagram of this arch is shown below.



$$\sum F_x = 0 \quad \text{yield:}$$

$$2P = (10,000) (30) (12)$$

$$P = 1.8 \times 10^6 \text{ lb.}$$

It is assumed that the ultimate concrete strength is 3,000 psi and that the yield strength of the reinforcing steel is 40,000 psi. Equation (19-7) of the 1963 code of the American Concrete Institute applies to this situation -- that is, a column which is under direct compression.

$$P_o = 0.85 f'_c (A_g - A_{st}) + A_{st} f_y$$

where

$P_o$  is the ultimate axial load

$f'_c$  is the ultimate concrete strength

$A_g$  is the gross section

$A_{st}$  is the area of the steel, and

$f_y$  is the yield strength of the steel.

Substituting

$$A_{st} = 0.04 b^2 \quad \text{and} \quad A_g = b^2,$$

we have

$$P_o = 0.85 f'_c (b^2 - 0.04 b^2) + 0.40 b^2 f_y$$

$$P_o = 0.799 f'_c b^2 + 0.40 f_y b^2 = b^2 [0.799 (3,000) + 0.40 (40,000)]$$

$$= 3997 b^2$$

Equating to  $P$ :

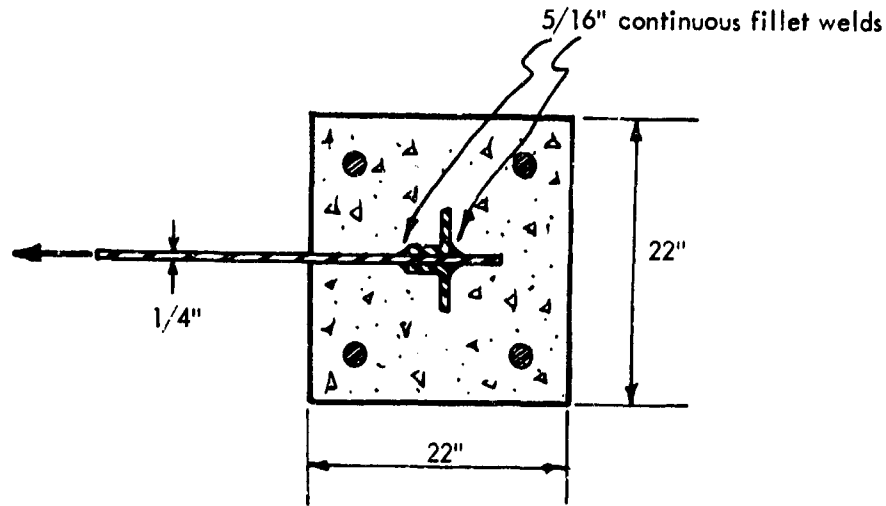
$$1.8 \times 10^6 = 3997 b^2$$

$$b^2 = 450.34$$

$$b = 21.2 \text{ in.}$$

$$A_{st} = 0.04 (b^2) = 0.04 (450.34) = 18 \text{ in.}^2$$

Use, for preliminary purposes, the following section:



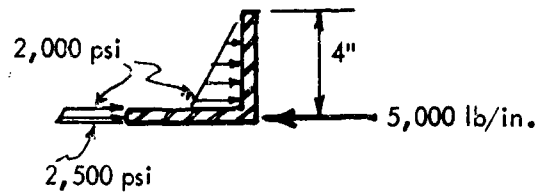
Required bearing area for angles =  $\frac{10,000 \text{ lb/in}}{1250} = 8 \text{ in.}$  Try 4 x 4 x 3/4 angles. Check bending stress in outstanding leg.

$$\sigma = \frac{Mc}{I} = \frac{\frac{2000}{2} (3.25) \left(\frac{3.25}{3}\right) 6}{t^2}$$

$$40,000 = \frac{21125}{t^2} \quad t^2 = 0.53$$

$$t = 0.73 \text{ in.}$$

Use 4 x 4 x 3/4" angles with  $t = 0.75 \text{ in.}$



Determination of area of reinforcing steel:

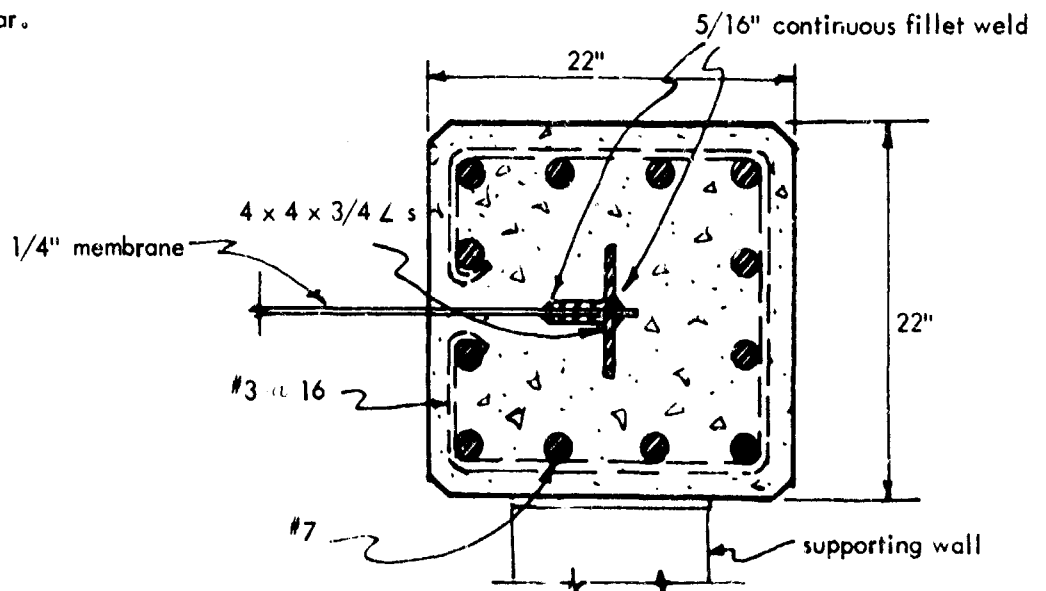
Two 4 x 4 x 3/4 angles have an area of 10.88 in<sup>2</sup>.

The required  $A_{st}$  is 18 in<sup>2</sup>, therefore 7.12 in<sup>2</sup> must be added as reinforcement.

If 12 bars are used,  $A_s$  per bar is 0.595 in<sup>2</sup>.

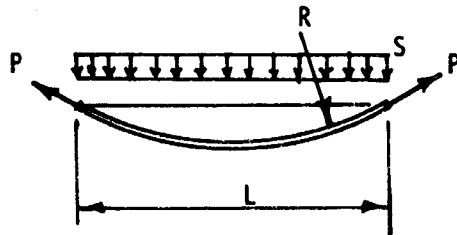
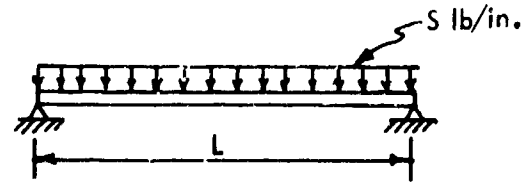
Use 12 #7 @ 0.60 in<sup>2</sup> per bar.

Use #3 ties at 16" as shown.



Yielding Membrane Supported by Straight Edge Beams (Figure 17b). It is logical to consider the method of supporting rectangular membranes at their outer edges by initially straight steel beams which, on loading, yield inward much in the same manner as the yielding stiffening ribs, discussed previously. If the design of such are considered, it becomes obvious that the amount of material required is excessive and such a support is impractical. This is demonstrated in the following development.

Consider a straight edge member which is loaded by a uniform membrane tension. Let the span be  $L$  between supports and the tension be  $S$  in lb. per in. The situation is shown at the right. Under action of force  $S$ , the beam deflects in a circular arc of radius,  $R$ , to a maximum center deflection,  $h$ . The beam in this configuration carries a maximum axial load of  $P$  lb. A free-body diagram of the deflected member is shown as follows:



$$\sum F_y = 0 \quad \text{yields}$$

$$2P \left( \frac{L/2}{R} \right) = SL$$

or

$$P = SR$$

For a given steel beam with an area,  $A$ , and a yield stress,  $f_y$ ,

$$P = f_y A$$

on substitution and simplification

$$A = \frac{SR}{f_y}$$

Thus, for a given situation, the area of edge beam that is required is only a function of the membrane tension, the yield stress, and the radius of curvature of the deflected shape. Now,  $S$  is the membrane yield tension which is  $f_y t$  where  $t$  is the thickness of the membrane. On substitution

$$A = \frac{f_y t R}{f_y} = t R$$

If limits are established for the axial strain in the edge beam, say about 10%, then  $R$  has a limit based on this strain. To determine the upper limit of  $R$ , which is actually the minimum value of  $R$ , consider the geometry shown at the right. The average % strain is

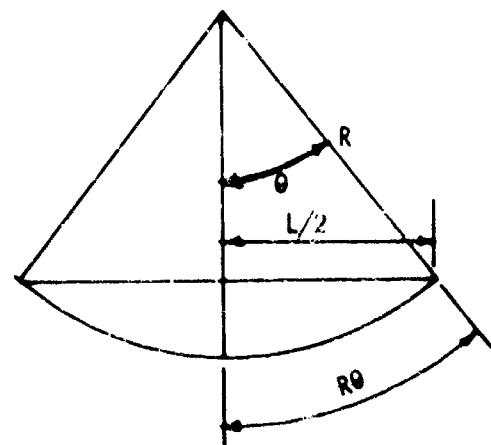
$$\frac{R\theta - L/2}{L/2} (100)$$

Now

$$\frac{R\theta - L/2}{L/2} (100) = 10$$

$$R\theta - L/2 = \frac{L}{20}$$

$$R\theta = \frac{11L}{20}$$



but

$$\theta = \arcsin \frac{L/2}{R} = \arcsin \frac{L}{2R}$$

$$R \arcsin \frac{L}{2R} = \frac{11L}{20}$$

$$\arcsin \frac{L}{2R} = \frac{11}{20} \frac{L}{R} = \frac{11}{10} \left(\frac{L}{2R}\right)$$

$$\arcsin x = \frac{11}{10} x$$

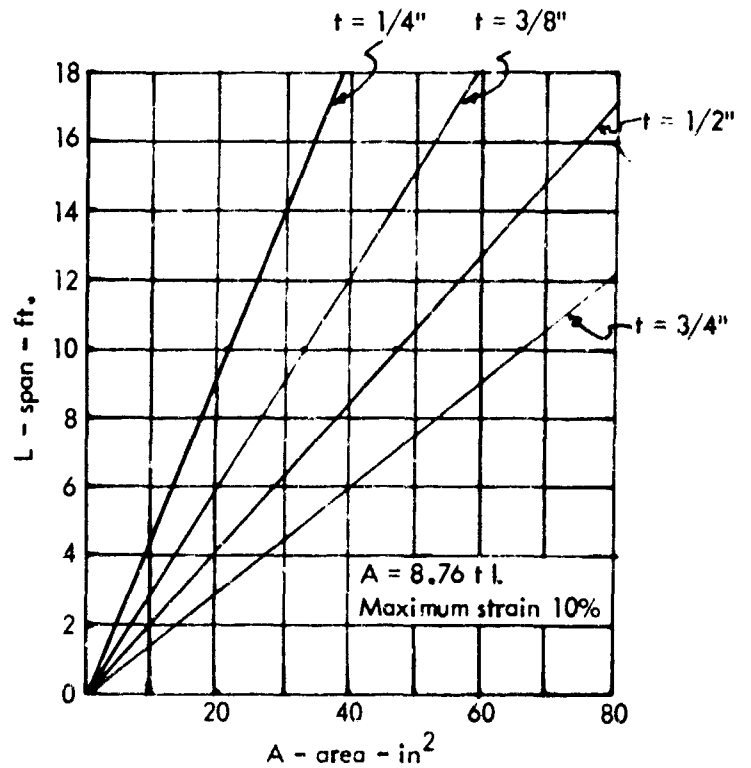
The solution to this transcendental equation is approximately  $x = 0.685$ . If  $L/2R = 0.685$  for 10% strain, then

$$R = \frac{L}{2(0.685)} = 0.73 L$$

and

$$A = tR = .73 tL$$

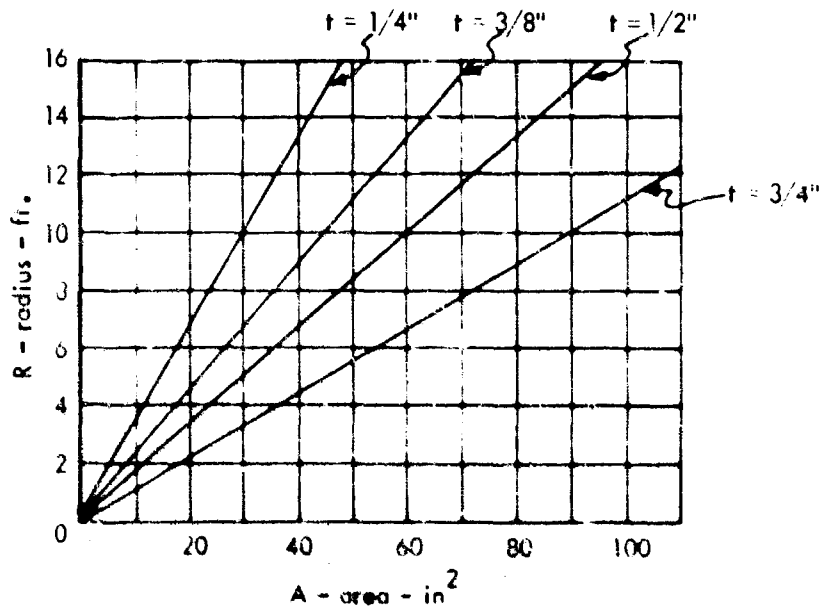
Solutions to this equation are plotted on the figure at the right.



It is seen that even for small spans of around 10 ft., a 1/4 in. membrane requires a steel edge beam of 21.5 in.<sup>2</sup> in cross section. This assumes, of course, that the beam is initially straight and that it yields to a limited maximum uniaxial strain of 10%.

Yielding Membranes Supported by Curved Edge Beams (Figure 17c). If the edge beams are initially curved to radius,  $R$ , they will act more efficiently when the membrane yields; because they are not limited to small curvatures, by strain requirements. For this case,  $A = tR$  as before. This equation, for various membrane thicknesses, may be plotted as shown below.

It is observed that a curved member of 5 ft. radius and area 15 in<sup>2</sup> would provide support for a 1/4 in. membrane. This produces a slight saving in material over the last case, but is much more difficult to construct. It is therefore concluded that such support is impractical.



Yielding Membranes Supported by Reinforced Concrete Shear Slabs (Figure 17d). One of the most practical solutions is use of reinforced concrete slabs in all outside panels and allow these slabs to resist the membrane thrust of interior elements through beam action as deep beams. In this case, membrane economies will only be achieved if large numbers of repetitive bays are used. The design of these reinforced concrete slabs (deep beams) is fairly routine and will not be presented here.

Yielding Membranes Supported by Membrane Elements (Figure 17e). A method of support that seems most likely is use of yielding membranes supported by membrane elements. At the corners of cubical structures, in which yield membranes are used as the exterior structural skin, membrane elements themselves may be used to "corner" the thrust.

For this case

$$F_x = 0 \quad t_2 f_y \cos \theta = t_1 f_y$$

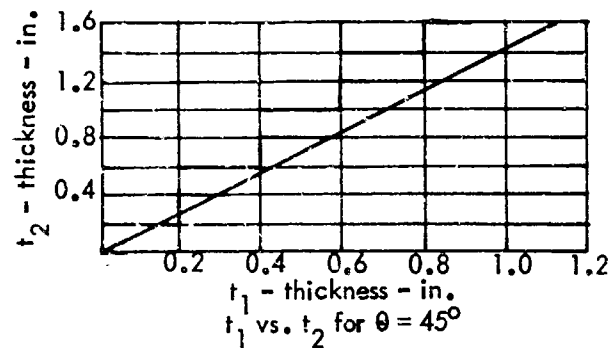
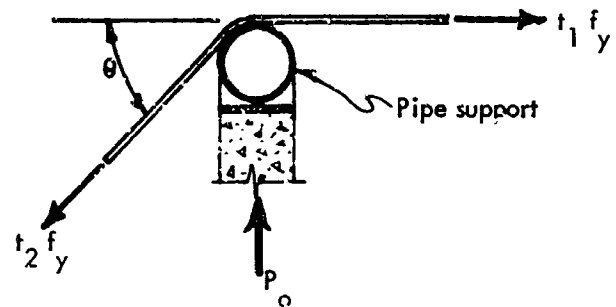
$$t_2 \cos \theta = t_1$$

if

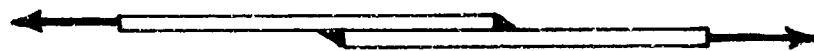
$$\theta = 45^\circ$$

$$t_2 = \frac{t_1}{.707} = 1.414 t_1$$

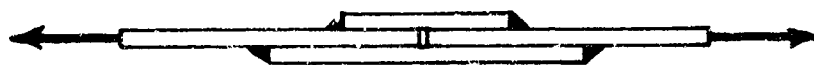
A plot of the relative thicknesses is shown above. For 1/4 in. side membranes, 0.35 in. thick corner membranes are required.



Membrane Splices. Practical construction considerations, based on limited sizes of available sheet steel, require the use of splices on membrane plates. Two types of full strength splices are recommended. They are shown as follows:



Simple lap splice



Simple butt splice

It is felt that either of these splices can be properly designed and constructed to develop the full yield strength of the membrane plates.

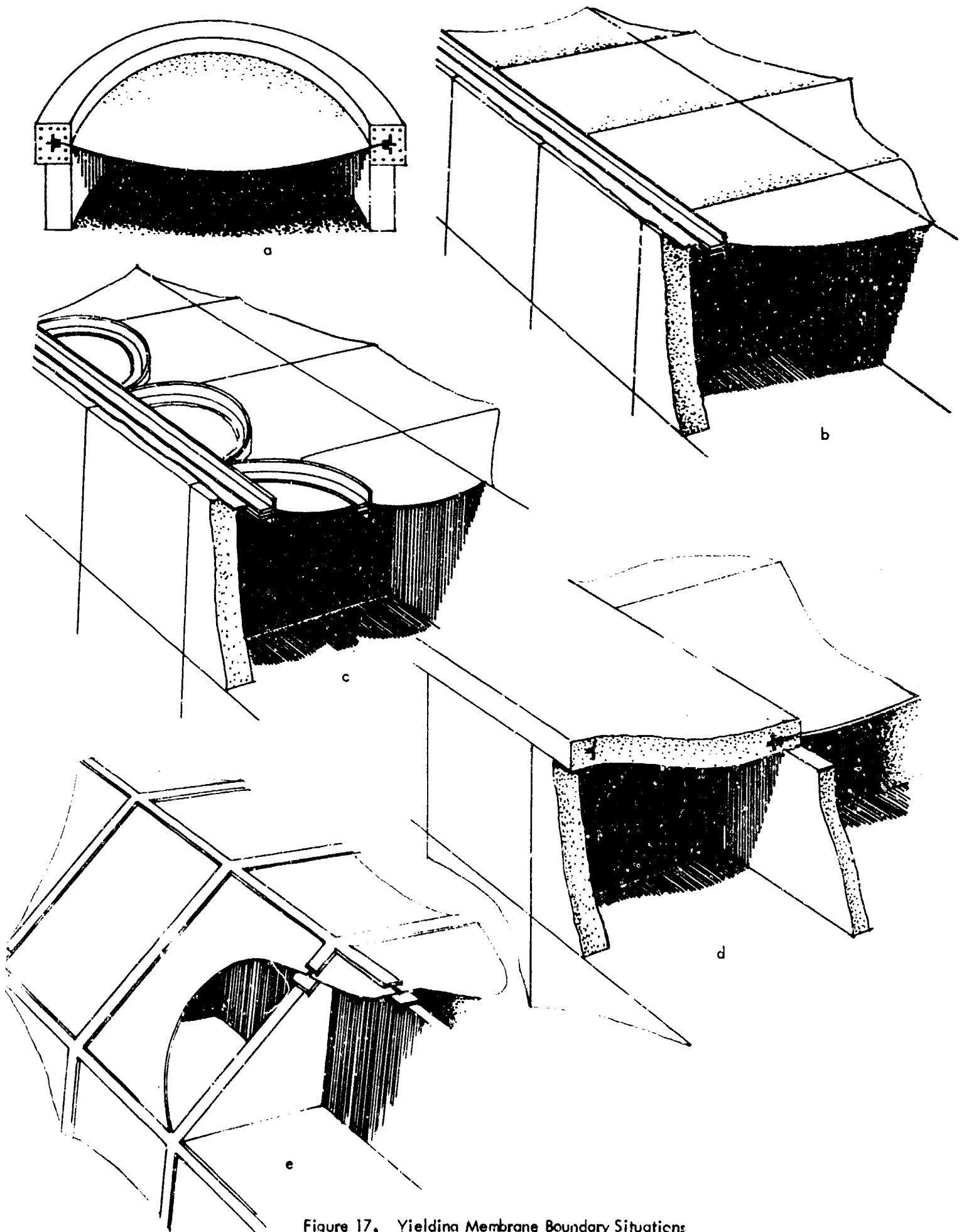


Figure 17. Yielding Membrane Boundary Situations

## Dynamic Tests

Dynamic tests were conducted in the University of Arizona blast simulator. This simulator is a plane-wave generator powered by a hydrogen-oxygen explosion. The blast chamber, shown in Figure 20, is a 300 gallon, 8 ft. by 2.5 ft diameter tank mounted vertically on rubber bushings to a heavy concrete base. Access to the chamber is achieved by unbolting the top section of the tank and swinging the bottom section and the base around a pivot. The 2.5 ft. x 2.5 ft. soil bin is then exposed for the placement of model structures, gauges, and sand. There is also a 14 in. diameter access hole in the bottom of the soil bin and two 4 in. diameter access holes and windows in the top section.

The blast wave is caused by a hydrogen-oxygen explosion detonated by an electric spark. Predetermined quantities of hydrogen, oxygen, and air are measured in the three auxiliary tanks on the side of the chamber. The air controls the rise time of the blast wave. The gases are fed into an evacuated plastic bag at the top of the tank. The explosion is detonated by an electric spark which is triggered by the same switch that starts the recording instruments. The decay time is controlled by adjustable exhaust valves and spacing washers between the chamber sections. The decay curve is exponential. The detonating spark and the gas bag are centered in the tank to minimize dynamic imbalance during tests.

The overpressure range is from 0 to 50 psi with variable rise times from less than one millisecond to over one-tenth of a second, and decay times from one-tenth of a second and up. The blast waves could be controlled to within 10 percent from test to test. The instrumentation and recording devices included two Statham pressure transducers (0 to 50 psi), two Tectronix dual beam oscillators with cameras, one six-channel Brush recorder, and one two-channel Sanborn recorder.

The blast simulator has been used to test yielding membrane models above and below ground. The test models were 3.5 to 4.0 inch cylinders which were constructed so that the edges held a membrane tightly clamped (Figure 21). The investigations were made to determine the effects of depths of burial and structural flexibility on the percentage of load carried by the yielding elements.

From the tests made in the blast chamber, some insight has been gained into the amount of attenuation of overpressure which is caused by soil cover. These tests showed that soil cover does attenuate overpressures appreciably; mainly due to an arching action in the soil as the membrane yields. Had these models been rigid they would have been subjected to pressures close to the surface overpressure. As can be seen from the test evidence, the arching



Figure 18. Square Membrane Test Yielding



Figure 19. Square Membrane with Two Yielding Beams



Figure 20. Blast Simulator

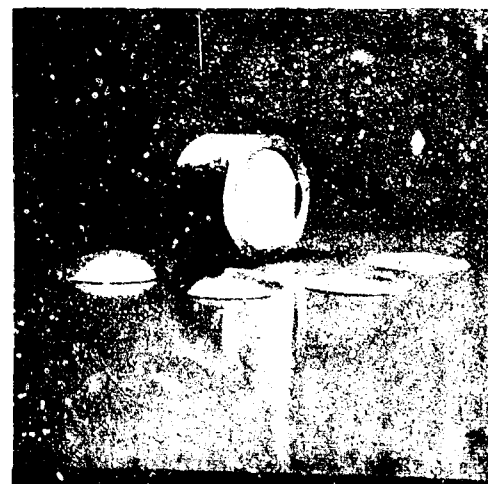


Figure 21. Model Structure and Deformed Model Shells

action was acting well before the model was buried one-half the diameter and at one diameter only one-tenth of the overpressure is felt by the buried membrane roof (Figure 22).

These results are not useable for prototype predictions because the principles of similitude are not satisfied. They do serve to illustrate the attenuation due to soil arching. The arching, in this case, has, as a point of support, the edge ring of the model structure. Had this edge ring not been present, the soil would have arched from a point outside the structure; but the arch would have been longer and flatter and thus the attenuation of overpressure would have been less.

In tests with the circular models, it was noted that the deflected shape was nearly spherical except that near the edges where the soil arch was supported by the structure the curvature was greater. The radii of curvature along a diameter was measured and by making use of the basic formula

$$\frac{1}{R_1} + \frac{1}{R_2} = -\frac{P}{S}$$

a fairly accurate distribution of the pressure across the membrane was determined (Figure 23). Note: a thin rubber sheet was placed over the surface of the sand to prevent the blast wave from permeating the pores.

Tests have shown that yielding membranes have the ability to deform dynamic overpressures. It has been noted in the test conducted at the University of Arizona that there is 10 to 20 percent increase in deflection under a dynamic load as compared to the same magnitude of overpressure applied statically.

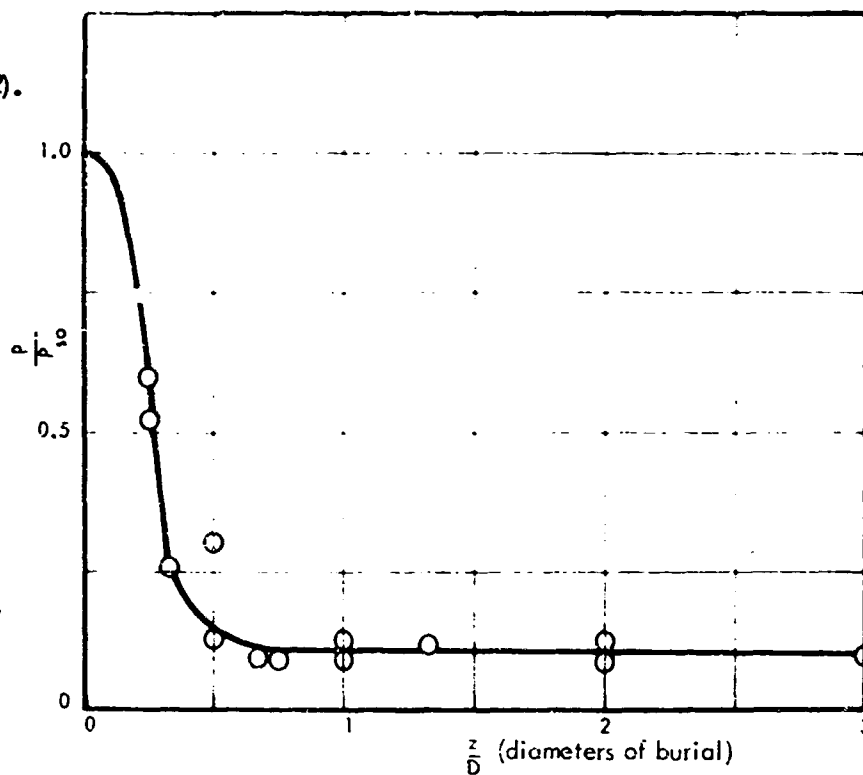


Figure 22. Attenuation of Pressure with Depth

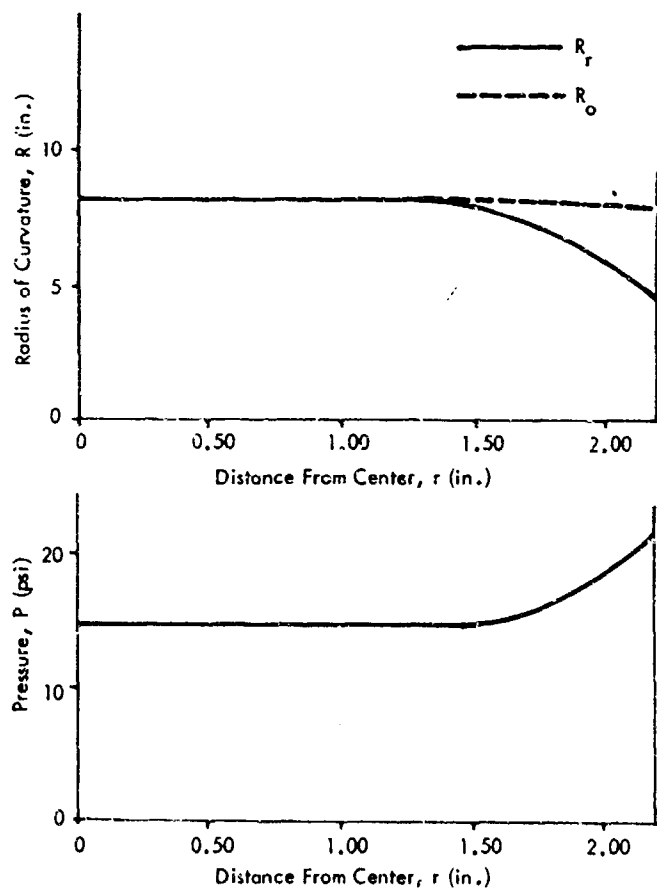


Figure 23. Radius of Curvature and Pressure Distribution across a Circular Membrane with Soil Cover

## CHAPTER IV

### SUMMARY AND CONCLUSIONS

Yielding membranes as elements of shelters to protect civilian population from overpressure effects of nuclear weapons are definitely feasible. As indicated on page 8 of this report, under certain conditions a 1/4 in. thick steel membrane will carry more load than a 19 in. thick concrete slab which is reinforced with steel at a rate of 4.08 in.<sup>2</sup>/ft. The membrane itself uses less steel than the reinforced concrete slab. Favorable soil-structure interaction effects are induced, by these elements, in all situations.

Construction difficulties, brought about by pre-dishing, may be overcome as more information is obtained on the response of flat membranes to blast overpressures. Problems associated with corrosion, and continuity of welds, may be largely overcome by using (as pseudo-membranes) thin concrete slabs which are reinforced by a closely spaced wire mesh which runs continuously in both directions. The wire mesh then acts as the membrane and the concrete as the corrosion resisting and local transfer medium.

Boundary supports and full scale testing are items that need more attention and are suggested as parts of future investigations. In addition, analytical studies on strain variations and time response functions to dynamic loads are needed.

At the present time, however, the response of these structures has been sufficiently bounded to warrant their use in civil defense situations. The methods used in this feasibility study are as valid and reliable as any that are currently being used on the design and analysis of conventional types of structures. It is recommended that the Office of Civil Defense seriously consider adding these types of solutions to the ever expanding inventory of such solutions.

## APPENDIX A

### YIELDING MEMBRANE FORCES

#### Introduction

This Appendix considers the configuration taken by yielding membranes under uniform lateral pressure loading. It deals with rectangular membranes which are rigidly supported on four sides and rectangular membranes which have one or more sides supported by yielding supports, in the form of beams which deflect as the membrane deflects. Some of the results of this effort were presented in Chapter III, but the complete details are included in this section.

The deflections of the membranes are very large, producing center deflection-to-span ratios as large as 0.20 which results in average biaxial strains as large as 10 percent. The result is that bending forces in the membrane are of little importance and membrane forces predominate.

If  $D$  is defined as the short-span distance, the types of membranes considered are: (1)  $D \times D$  with four edges clamped, (2)  $1.5 D \times D$  with four edges clamped, (3)  $2 D \times D$  with four edges clamped, (4)  $D \times D$  with a plastic edge beam on one side and clamped on the other three sides, (5)  $D \times D$  with plastic edge beams on two sides and clamped on two sides, (6)  $D \times D$  with plastic edge beams on three sides and one side clamped, and (7) plastic edge beams on all four sides. Plan views of the shapes are shown in Figure A-1.

Only membrane forces are considered. Further, the assumption is made that the same membrane stress level exists at all points on the resulting surface. The problem considered in this investigation involves uniform lateral pressure only. However, the differential equations developed can be solved for other types of lateral loadings.

#### Yielding Membrane Theory

Formulation of the Problem. To properly predict the configuration of yielding membranes under normal pressure loading, it is necessary to develop adequate theories. Few of the theories presented in Historical Review (Appendix D) are directly applicable to the problem at hand. However, minor modifications to them allow applicability. The work which follows presents these modifications.

#### NOTATION

$a$ . . . . .	Width of plate or radius of circular plate
$b$ . . . . .	Length of plate
$c, d$ . . . . .	Dimensions of membrane
$D$ . . . . .	Span of membrane or flexural rigidity of plate
$E$ . . . . .	Modulus of Elasticity
$\epsilon$ . . . . .	Strain
$F$ . . . . .	Force in yielding beam or stress function
$h$ . . . . .	Thickness of plate, $x$ direction grid size
$i$ . . . . .	Grid point in $x$ direction
$j$ . . . . .	Grid point in $y$ direction
$k$ . . . . .	$y$ direction grid size
$L$ . . . . .	Length of membrane
$N$ . . . . .	Normal force per unit length
$P$ . . . . .	Pressure
$\nu$ . . . . .	Poisson's ratio
$R$ . . . . .	Radius of curvature
$S$ . . . . .	Membrane strength

- $\sigma$  ..... Stress
- $\sigma_c$  ..... Constant stress (usually the yield stress)
- $t$  ..... Thickness of membrane
- $u, v, w$  ..... Components of displacements in  $x, y, z$  directions, respectively
- $x, y, z$  ..... Rectangular coordinates
- $z_c$  ..... Vertical deflection in center of membrane
- $z_{i,j}$  ..... Vertical deflection at grid point,  $x = i, y = j$

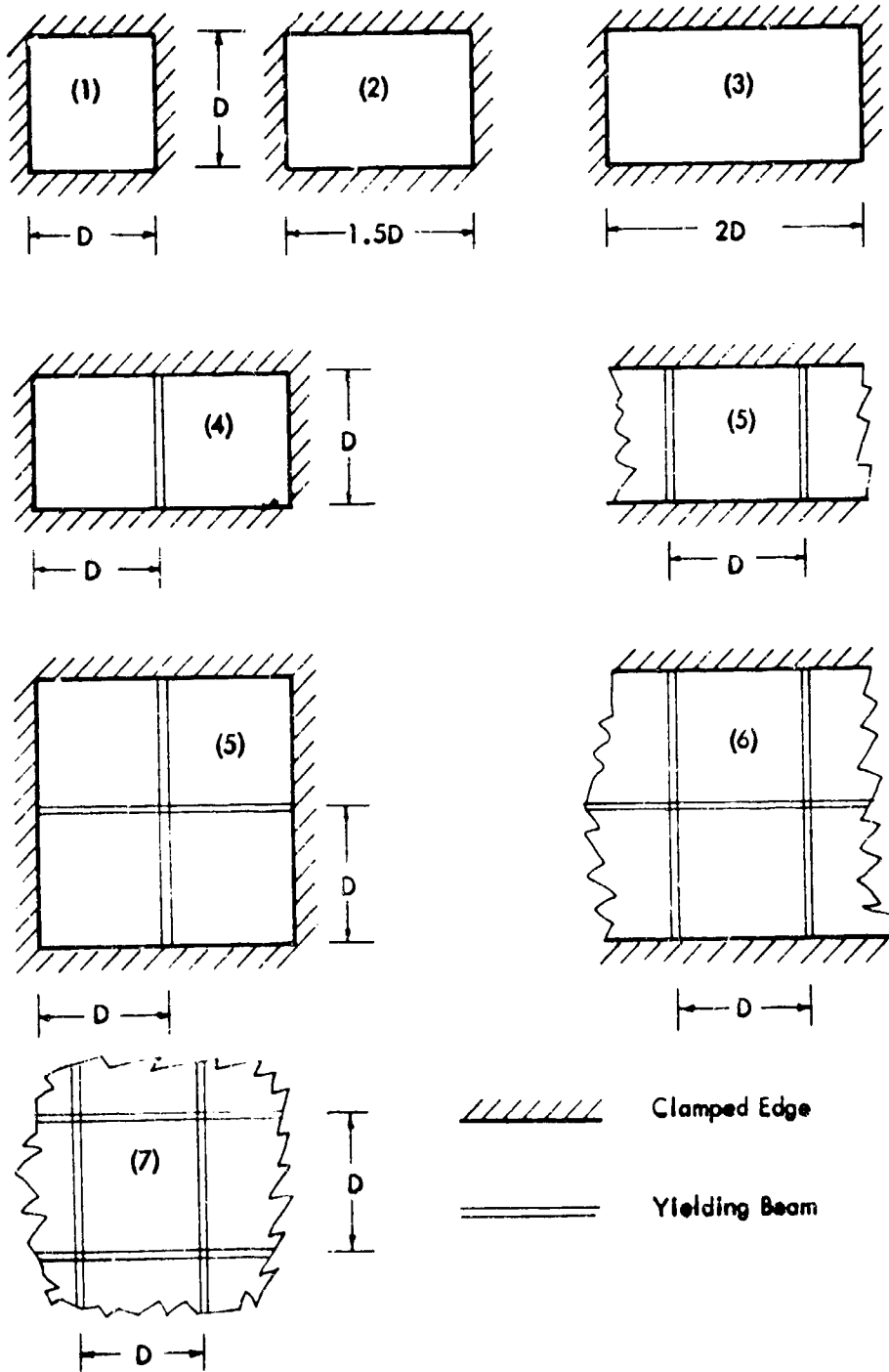


Figure A-1. Plan Views of the Shapes Considered

The formulation of the basic equation of membrane shells is well known. From the statics of a membrane shell this equation of equilibrium is obtained

$$\frac{N_1}{R_1} + \frac{N_2}{R_2} - P_3 \quad (1)$$

If it is assumed that the entire membrane is at the same stress level  $S$  such that  $N_1 = N_2 = S^*$ , this equation of equilibrium becomes

$$\frac{1}{R_1} + \frac{1}{R_2} - \frac{P_3}{S} \quad (2)$$

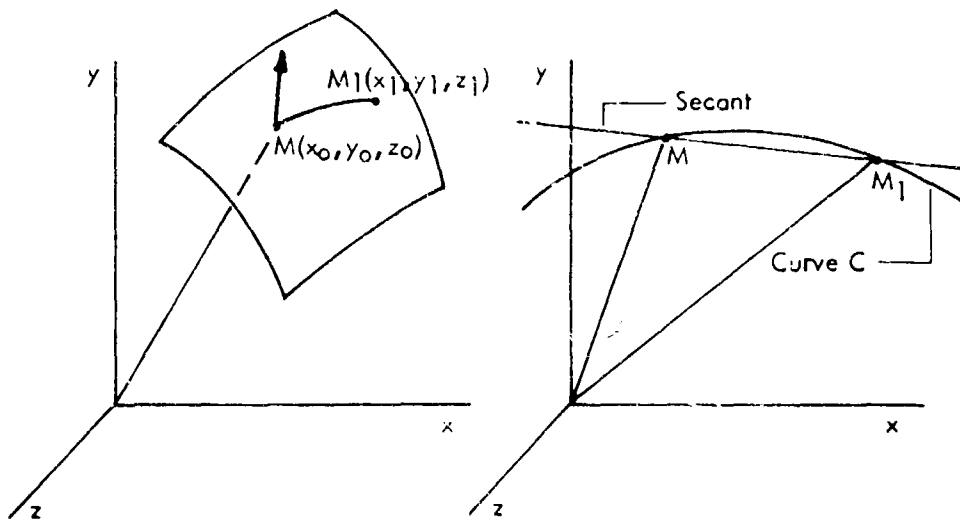
The linear theory of membrane shells uses this approximation to the curvature

$$\frac{1}{R_1} + \frac{1}{R_2} = \frac{\partial^2 z}{\partial x^2} + \frac{\partial^2 z}{\partial y^2} = -\frac{P_3}{S} \quad (3)$$

which is Poisson's equation. Von Karman's equations under the assumption of a uniform stress level in a membrane reduce to

$$\frac{\partial^2 z}{\partial x^2} - 2 \frac{\partial^2 z}{\partial x \partial y} + \frac{\partial^2 z}{\partial y^2} = -\frac{P_3}{S} \quad (4)$$

To arrive at the exact expression for the mean curvature of a surface is a problem of differential geometry.



The tangent to a curve at a point  $M$  is the limiting position of the secant through  $M$  and a point  $M_1$  of the curve  $M_1$  approaches  $M$  as a limit. The equations of the tangents through  $M$  and  $M_1$  are

$$\frac{x-x_0}{\frac{dx}{ds}} = \frac{y-y_0}{\frac{dy}{ds}} = \frac{z-z_0}{\frac{dz}{ds}} = h \quad (5)$$

where  $x$ ,  $y$ , and  $z$  are coordinates of a point on the curve, their values depending upon the parameter  $h$ .

\* H. P. Harrenstien, "Configuration of Shell Structures for Optimum Stresses," Proceedings of the Symposium on Shell Research, Delft, The Netherlands, 1961.

A tangent line to a curve upon a surface is called a "tangent line to the surface" at the point of contact. It is evident that there is an infinite number of tangent lines to a surface at any point. However, all of these lines lie in a plane called the "tangent plane" which is tangent to the surface at the point. If the equation of the curve,  $C$ , in curvilinear coordinates is  $v = f(u)$ , then the above equations may be written

$$x - x_0 = h \left( \frac{\partial x}{\partial u} + f' \frac{\partial x}{\partial v} \right) \frac{du}{ds} \quad (6)$$

$$y - y_0 = h \left( \frac{\partial y}{\partial u} + f' \frac{\partial y}{\partial v} \right) \frac{du}{ds} \quad (7)$$

$$z - z_0 = h \left( \frac{\partial z}{\partial u} + f' \frac{\partial z}{\partial v} \right) \frac{du}{ds} \quad (8)$$

where the prime indicates differentiation. In order to obtain the locus of these tangent lines, eliminate  $f'$  and  $h$  from these equations. This gives

$$\begin{vmatrix} x - x_0 & y - y_0 & z - z_0 \\ \frac{\partial x}{\partial u} & \frac{\partial y}{\partial u} & \frac{\partial z}{\partial u} \\ \frac{\partial x}{\partial v} & \frac{\partial y}{\partial v} & \frac{\partial z}{\partial v} \end{vmatrix} = 0 \quad (9)$$

which is evidently the equation of a plane through  $M$ .

The equation of the tangent plane may be written as

$$(x - x_0) X + (y - y_0) Y + (z - z_0) Z = 0 \quad (10)$$

Now define

$$E = \left( \frac{\partial x}{\partial u} \right)^2 + \left( \frac{\partial y}{\partial u} \right)^2 + \left( \frac{\partial z}{\partial u} \right)^2 \quad (11)$$

$$F = \frac{\partial x}{\partial u} \frac{\partial x}{\partial v} + \frac{\partial y}{\partial u} \frac{\partial y}{\partial v} + \frac{\partial z}{\partial u} \frac{\partial z}{\partial v}$$

$$G = \left( \frac{\partial x}{\partial v} \right)^2 + \left( \frac{\partial y}{\partial v} \right)^2 + \left( \frac{\partial z}{\partial v} \right)^2$$

$$H = \sqrt{EG - F^2}$$

$$X = \frac{1}{R} \begin{vmatrix} \frac{\partial y}{\partial u} & \frac{\partial z}{\partial u} \\ \frac{\partial y}{\partial v} & \frac{\partial z}{\partial v} \end{vmatrix}$$

$$Y = \frac{1}{R} \begin{vmatrix} \frac{\partial z}{\partial u} & \frac{\partial x}{\partial u} \\ \frac{\partial z}{\partial v} & \frac{\partial x}{\partial v} \end{vmatrix}$$

$$Z = \frac{1}{R} \begin{vmatrix} \frac{\partial x}{\partial u} & \frac{\partial y}{\partial u} \\ \frac{\partial x}{\partial v} & \frac{\partial y}{\partial v} \end{vmatrix}$$

The positive direction of the normal-to-the-tangent plane is defined to be that for which the functions  $X$ ,  $Y$  and  $Z$  are the direction cosines.

Consider any curve,  $C$ , on a surface,  $S$ , through a point,  $M$ . The direction of its tangent,  $MT$ , is determined by a value,  $dv/du$ . Let  $\theta$  denote the angle which the positive direction of the normal to the surface makes with the positive direction of the principal normal to  $C$  at  $M$ , angles being measured toward the positive binormal. Thus

$$\cos \theta = r \left( X \frac{d^2 x}{ds^2} + Y \frac{d^2 y}{ds^2} + Z \frac{d^2 z}{ds^2} \right) \quad (12)$$

where  $r$  is the radius of curvature of the arc of  $C$ . In terms of  $du/ds$  and  $dv/ds$ , the derivatives in the parenthesis have the forms

$$\begin{aligned} \frac{d^2 x}{ds^2} &= \frac{\partial^2 x}{\partial u^2} \left( \frac{du}{ds} \right)^2 + 2 \frac{\partial^2 x}{\partial u \partial v} \frac{du}{ds} \frac{dv}{ds} + \frac{\partial^2 x}{\partial v^2} \left( \frac{dv}{ds} \right)^2 \\ &\quad + \frac{\partial x}{\partial u} \frac{d^2 u}{ds^2} + \frac{\partial x}{\partial v} \frac{d^2 v}{ds^2} \end{aligned} \quad (13)$$

Now define:

$$\begin{aligned} D &= X \frac{\partial^2 x}{\partial u^2} + Y \frac{\partial^2 y}{\partial u^2} + Z \frac{\partial^2 z}{\partial u^2} \\ D' &= X \frac{\partial^2 x}{\partial u \partial v} + Y \frac{\partial^2 y}{\partial u \partial v} + Z \frac{\partial^2 z}{\partial u \partial v} \\ D'' &= X \frac{\partial^2 x}{\partial v^2} + Y \frac{\partial^2 y}{\partial v^2} + Z \frac{\partial^2 z}{\partial v^2} \end{aligned} \quad (14)$$

Making these changes

$$\frac{\cos \Theta}{r} = \frac{D du^2 - 2 D' du dv + D'' dv^2}{E du^2 + 2 F du dv + G dv^2} \quad (15)$$

Consider the tangent curve in which the surface is cut by the plane determined by MT and the normal to the surface at M, called the "normal section" tangent to MT, and let  $r_n$  denote its radius. Since the right-hand member of the above equation is the same for C and the normal section tangent to it,

$$\frac{\cos \Theta}{r} = \frac{e}{r_n} \quad (16)$$

where  $e$  is  $+1$  or  $-1$ , depending on whether  $\theta$  is less than or greater than a right angle. The radii  $r$  and  $r_n$  are positive.

Now, let us introduce a new function  $R$  which is equal to  $r_n$  when  $0 \leq \theta \leq \pi/2$ , and equal to  $-r_n$  when  $\pi/2 \leq \theta \leq \pi$ , and call it the "radius of normal curvature" of the surface for the given direction MT. As defined:

$$\frac{1}{R} = \frac{D du^2 + 2 D' du dv + D'' dv^2}{E du^2 + 2 F du dv + G dv^2} \quad (17)$$

or on substituting  $t = dv/du$

$$\frac{1}{R} = \frac{D + 2 D' t + D'' t^2}{E + 2 F t + G t^2} \quad (18)$$

To obtain the values of  $t$  for which  $R$  is a maximum or minimum, differentiate this expression with respect to  $t$  and set the result equal to zero. This gives

$$0 = (D' + D''t)(E + 2 Ft + Gt^2) - (F + Gt)(D + 2 D't + D''t^2) \quad (19)$$

This is a quadratic in  $t$ . It can be shown that at every ordinary point of a surface there is a direction for which the radius of normal curvature is a maximum and a direction for which it is a minimum, and they are at right angles to one another.

Thus the two values of  $R$  become

$$\frac{1}{R} = \frac{D' + D''t}{F + Gt} \quad \text{and} \quad \frac{1}{R} = \frac{D + D't}{E + Ft} \quad (20)$$

and the following relations hold between the principle radii and the corresponding values of  $t$

$$\begin{aligned} E + Ft - R(D + D't) &= 0 \\ F + Gt - R(D' + D''t) &= 0 \end{aligned} \quad (21)$$

Eliminating  $t$  from these equations

$$0 = (D D'' - D'^2) R^2 - (E D'' + G D - 2 F D') R + (E G - F^2) \quad (22)$$

The roots of this equation are the principal radii. These principal radii are denoted by  $R_1$  and  $R_2$  and thus:

$$\frac{1}{R_1} + \frac{1}{R_2} = \frac{ED'' + GD - 2FD'}{H^2} \quad (23)$$

$$\frac{1}{R_1 R_2} = \frac{DD'' - D'^2}{H^2}$$

Now, for the case of a surface defined by  $z = f(x, y)$ , the following values are obtained:

$$\begin{aligned} X &= \frac{-P}{(1 + p^2 + q^2)^{1/2}} & D &= \frac{r}{(1 + p^2 + q^2)^{1/2}} \\ Y &= \frac{-q}{(1 + p^2 + q^2)^{1/2}} & D' &= \frac{s}{(1 + p^2 + q^2)^{1/2}} \\ Z &= \frac{1}{(1 + p^2 + q^2)^{1/2}} & D'' &= \frac{t}{(1 + p^2 + q^2)^{1/2}} \end{aligned} \quad (24)$$

where

$$\begin{aligned} p &= \frac{\partial z}{\partial x}, & q &= -\frac{\partial z}{\partial y} \\ r &= \frac{\partial^2 z}{\partial x^2}, & s &= \frac{\partial^2 z}{\partial x \partial y}, & t &= \frac{\partial^2 z}{\partial y^2} \end{aligned}$$

and thus

$$\frac{1}{R_1} + \frac{1}{R_2} = \frac{(1 + p^2)t - 2pqs + (1 + q^2)r}{(1 + p^2 + q^2)^{3/2}} \quad (25)$$

also

$$\frac{1}{R_1} - \frac{1}{R_2} = \text{constant.}$$

Using this exact expression for the normal curvatures the equation of equilibrium becomes:

$$\frac{(1 + q^2)r - 2pqs + (1 + p^2)t}{(1 + p^2 + q^2)^{3/2}} = \frac{-P}{S} \quad (26)$$

where  $P$  is the uniform lateral pressure denoted by  $P_3$  previously.

This equation, which governs the shape of a membrane that is loaded by pressures large enough to cause deformations in excess of the "large" deflection theory, generally may not be solved by means usually employed for equations of this type. The equation is distinctively non-linear, involving products and powers of partial derivatives. The method presented here consists of defining the partial derivatives in the equation in terms of finite differences and iterating the resulting equations by the Newton-Raphson technique to obtain a description of the surface.

An over-relaxation procedure was used to speed the iterative process. This iteration procedure was too involved to attempt by desk calculator so a high-speed digital computer was used. The procedure was programmed in basic Fortran computer language for the IBM 709 computer at the University of Arizona. The computer program is presented in Appendix B.

Yielding Edge Beams. In situations where the boundaries are fixed,  $z = 0$  on the boundary is a sufficient condition to admit a unique solution. However, in cases where these boundaries yield, as in the case of an edge beam which yields normal to the initial plane of the surface, this condition is not valid.

In this case the differential equation governing the behavior of this plastic beam across the membrane is

$$\frac{F \frac{\partial^2 z}{\partial y^2}}{\left[1 + \left(\frac{\partial z}{\partial y}\right)^2\right]^{3/2}} + \frac{2S \frac{\partial z}{\partial x}}{\left[1 + \left(\frac{\partial z}{\partial x}\right)^2\right]^{1/2}} + PW = 0 \quad (27)$$

where  $F$  is the plastic strength of beam plus membrane strength and  $W$  is the beam width. The second term is a load term giving the contribution of the pull of the membrane to the shape of the plastic beam. The 2 in the numerator arises because the membrane is considered symmetrical about the beam.

This equation assumes that the coordinates extend to the edge of the beam. Thus  $F$  is actually the strength of the beam and the membrane combined, which must be taken into account with wide beams. However, in the computer study, the coordinates were taken from the center of the beam, the beam width was assumed zero, and  $F$  became the strength of the beam alone. This assumption results in less than two percent error in most cases.

Finite Difference Equations. The equations presented for the membrane and the yielding edge beams were written in finite difference form in order to reduce the differential equations to more easily handled algebraic equations. The computer programs were written using the finite difference forms of equations. In the programs involving the yielding edge beams the two sets of equations were solved simultaneously.

The membrane equation written in terms of finite differences about a point involves nine points as shown in Figure A-2. In this case there is no need to write a special finite difference equation to handle points along the boundaries because the boundary points are either zero along the clamped edges or a point on a yielding beam. The points on the yielding beams are obtained by solutions of the beam equation.

The partial derivatives written in finite difference form are

$$\begin{aligned} 2h \left. \frac{\partial z}{\partial x} \right|_i &= 2h D_x z_i = z_r - z_l + (0) h^2 \\ 2k D_y z_i &= z_u - z_b + (0) k^2 \\ h^2 D_{xx} z_i &= z_r - 2z_i + z_l + (0) h^2 \\ k^2 D_{yy} z_i &= z_u - 2z_i + z_b + (0) k^2 \\ 4hk D_{xy} z_i &= z_{ar} - z_{al} - z_{br} + z_{bl} + (0) hk \end{aligned} \quad (28)$$

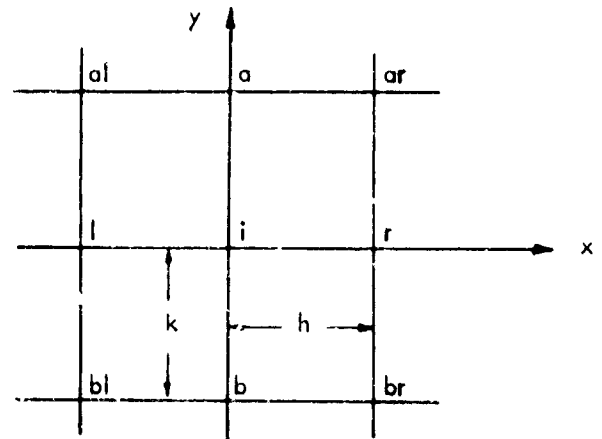


Figure A-2. Finite Difference Grid Arrangement

In finite difference form the membrane equilibrium equation becomes

$$\begin{aligned} & \left[ 4k^2 + (z_a - z_b)^2 \right] \left[ z_r - 2z_i + z_l \right] + \left[ 4h^2 + (z_r - z_l)^2 \right] \left[ z_a - 2z_i + z_b \right] \\ & - \frac{1}{2} (z_r - z_l) (z_a - z_b) (z_{ar} - z_{al} - z_{br} + z_{bl}) \\ & + \frac{P}{2hks} \left[ 4h^2 k^2 + k^2 (z_r - z_l)^2 + (z_a - z_b)^2 \right]^{3/2} = 0 \end{aligned} \quad (29)$$

For a square mesh,  $h = k$ ;

$$\begin{aligned} & \left[ 4h^2 + (z_a - z_b)^2 \right] \left[ z_r - 2z_i + z_l \right] + \left[ 4h^2 + (z_r - z_l)^2 \right] \left[ z_a - 2z_i + z_b \right] \\ & - \frac{1}{2} (z_r - z_l) (z_a - z_b) (z_{ar} - z_{al} - z_{br} + z_{bl}) \\ & + \frac{P}{S} \frac{h}{2} \left[ 4h^2 + (z_r - z_l)^2 + (z_a - z_b)^2 \right]^{3/2} = 0 \end{aligned} \quad (30)$$

If  $k = (d/c)h$ , i.e., if there are an equal number of divisions in each direction, then

$$\begin{aligned} & \left[ 4 \left( \frac{d}{c} \right)^2 h^2 + (z_a - z_b)^2 \right] \left[ z_r - 2z_i + z_l \right] \\ & + \left[ 4h^2 + (z_r - z_l)^2 \right] \left[ z_a - 2z_i + z_b \right] \\ & - \frac{1}{2} (z_r - z_l) (z_a - z_b) (z_{ar} - z_{al} - z_{br} + z_{bl}) \\ & + \frac{P h (c)}{S^2 d} \left[ 4 \left( \frac{d}{c} \right)^2 h^2 + \left( \frac{d}{c} \right)^2 (z_r - z_l)^2 + (z_a - z_b)^2 \right]^{2/3} = 0 \end{aligned} \quad (31)$$

Note that  $c$  is the  $x$ -dimension of the membrane and  $d$  is the  $y$ -dimension.

In finite difference form the yielding beam equation is

$$\frac{8 F k (z_a - 2z_i - z_b)}{\left[ 4k^2 + (z_a - z_b)^2 \right]^{3/2}} + \frac{2 S (z_l - z_i)}{\left[ h^2 + (z_l - z_i)^2 \right]^{1/2}} + PW = 0 \quad (32)$$

Where

$F$  = Strength in beam and membrane

$S$  = Strength in membrane

$P$  = Lateral pressure

$W$  = Width of beam

$h$  = Grid size in  $x$  direction

$k$  = Grid size in  $y$  direction

$z_i$  = Deflection at point  $i$

**Computer Results.** The membrane equation in finite difference form (Equation 29) was solved by the computer using a modified Newton-Raphson technique. Pressure-to-membrane strength ratios of from zero to three were used in the computer programs. In the cases of membranes supported by yielding edge beams, Equations 29 and 32 were solved simultaneously. Values of the ratio of beam strength to the product of the membrane strength and span of 0.5, 1.0 and 2.0 were used in the programs.

The illustrations in this section are the result of the computer study. Curves are computed for a uniform stress distribution over the entire surface. However, this assumption does not noticeably affect the center deflection values as will be shown in the comparison of results section. In fact, the only areas this assumption affects, to any degree, is the corners.

These curves of  $PD/S$  versus  $z_0/D$  are general curves and may be used for any ductile material if the biaxial stress-strain curve for the material is available. Only in the case of a rigid-plastic material can the  $S$  value be considered a constant.

Figure A-3 shows the standard grid layout used in all of the following graphs, tables and discussions. It was found that a  $16 \times 16$  grid gave results within the desired degree of accuracy. In the following  $z_{i,j}$  means  $z_{x,y}$ . The  $PD/S$  versus  $z_0/D$  curves (Figures A-4 through A-9) are non-dimensionalized pressure versus center deflection curves for membranes with clamped edges. The  $PD/S$  versus  $z_0/D$  curves (Figures A-10 through A-16) are non-dimensionalized pressure versus deflection curves for the points of maximum deflection of the membrane and center points on the beams for various conditions of edge constraint. The numbers inside the circles are values of the ratio  $F/SD$ , where

$F$  = Strength of beam and membrane

$S$  = Membrane strength

$D$  = Short span distance

The subscripts on the circles refer to the location of the point (see Figure A-3). For example,  $\textcircled{1}_{9,9}$  refers to the  $PD/S$  versus  $z_0/D$  curve for the center point of the membrane, when the ratio of edge beam strength to the product of the membrane strength and the span is one.

The graphs and tables, shown relating to membranes supported by various yielding edge beam arrangements, are for symmetrical cases. That is, it is assumed that the conditions on both sides of the yielding beams are the same. These tables and graphs are useful in preliminary design. The actual values of membrane strength and beam strengths involved in a design should be fed into a computer program to determine the

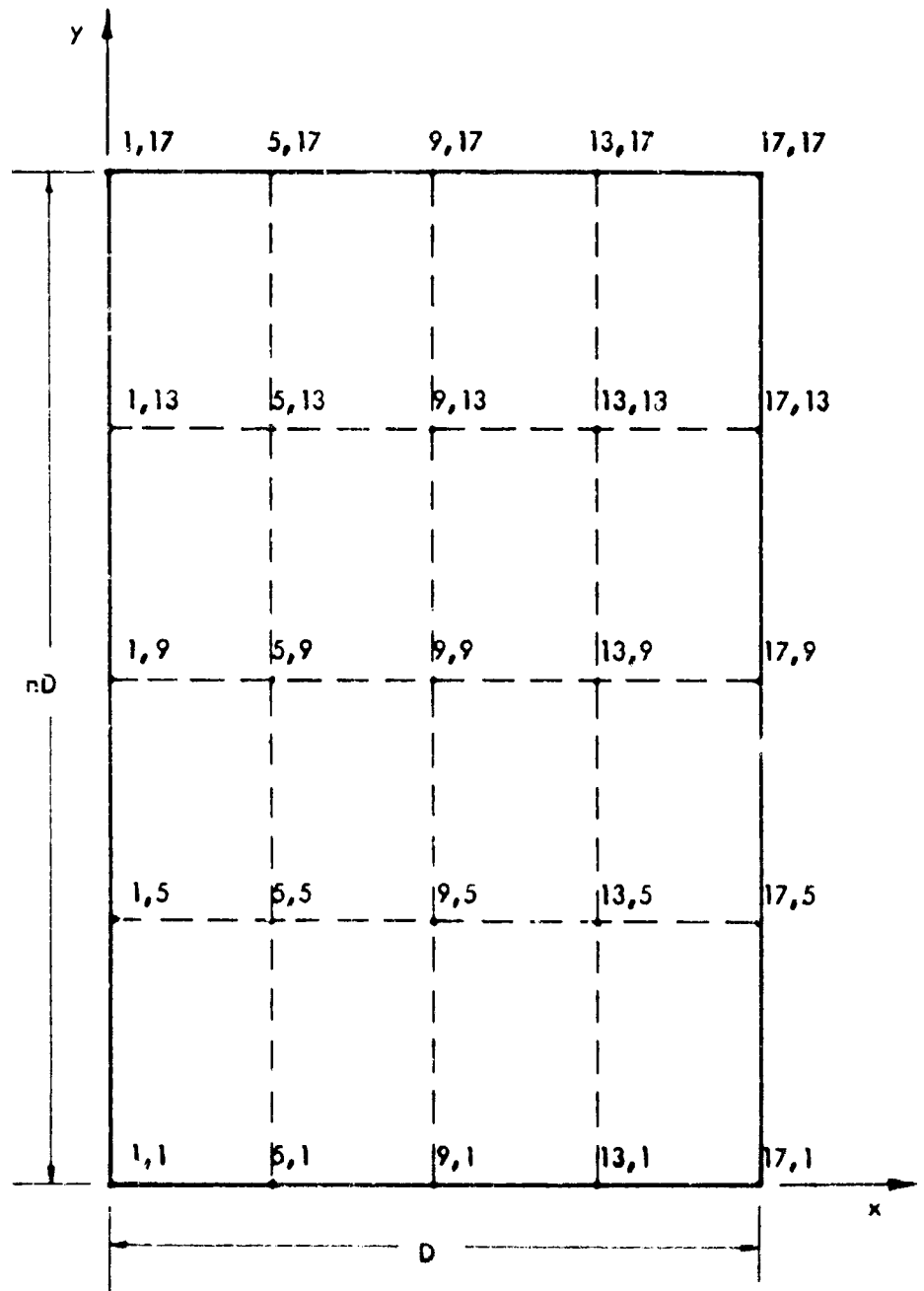


Figure A-3. Standard Grid Layout

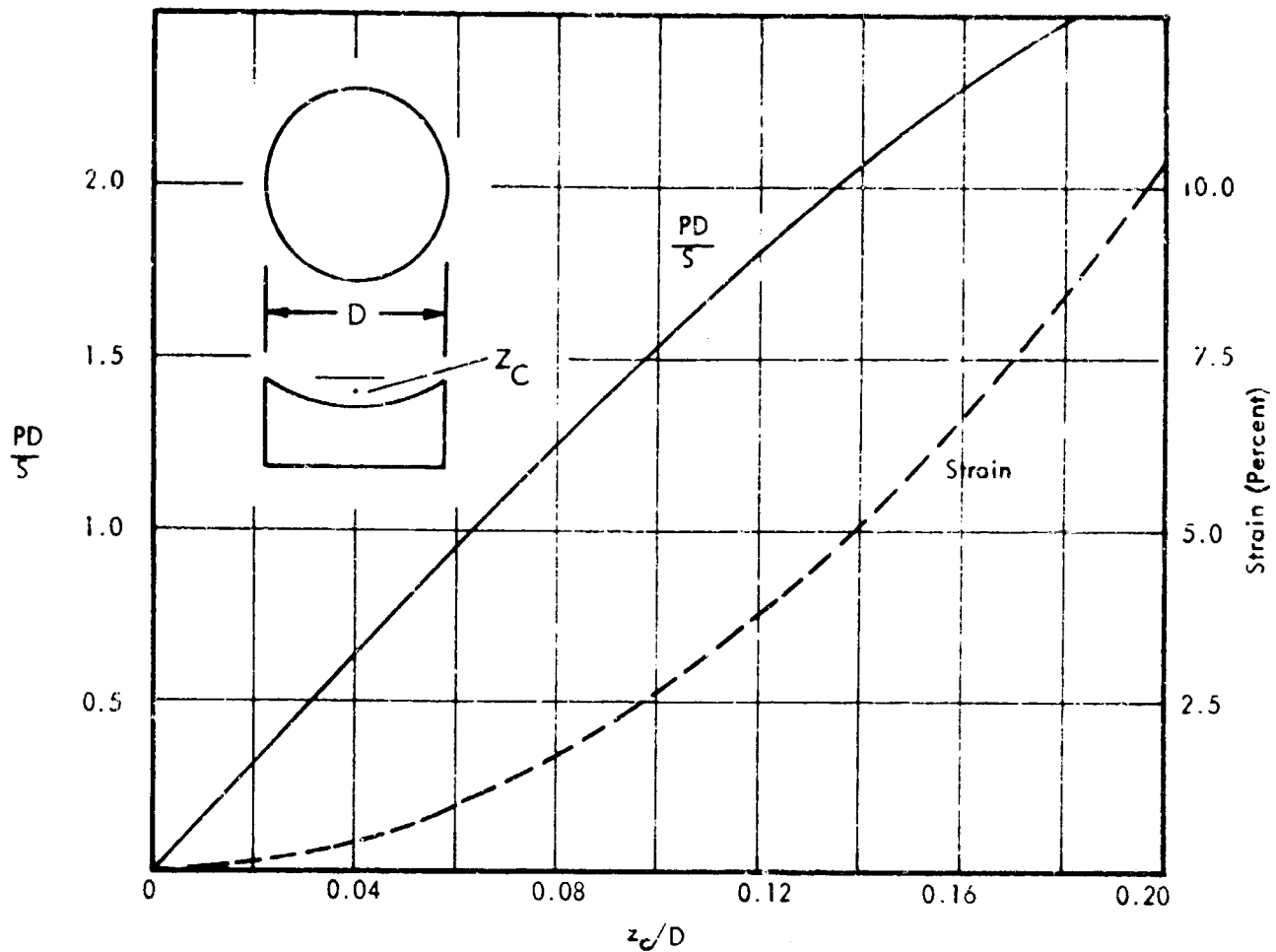


Figure A-4.  $PD/S$  versus  $z_c/D$  Curve for a Circular Membrane

TABLE 1

Summary of Computer Results; Membranes with Clamped Edges

$\frac{PD}{S}$	Circular		1 x 1		1.5 x 1		2 x 1		3 x 1		$\infty$ x 1	
	$z_c/D$	Strain	$z_c/D$	Strain	$z_c/D$	Strain	$z_c/D$	Strain	$z_c/D$	Strain	$z_c/D$	Strain
0.25	.018	0.08	.018	0.10	.025	0.17	.028	0.22	.031	0.25	.031	0.26
0.50	.031	0.25	.037	0.38	.051	0.70	.057	0.88	.062	1.02	.064	1.07
0.75	.044	0.52	.055	0.88	.077	1.59	.087	2.03	.095	2.38	.097	2.49
1.00	.064	1.07	.075	1.58	.104	2.90	.119	3.74	.130	4.44	.134	4.68
1.25	.080	1.65	.095	2.52	.132	4.69	.152	6.13	.169	7.43	.175	7.93
1.50	.098	2.55	.115	3.75	.163	7.05	.190	9.43	.214	11.78	.225	12.88
1.75	.115	3.40	.137	5.24	.196	10.16	.233	14.00	.269	18.33	.293	21.36
2.00	.134	4.70	.160	7.12	.233	14.27	.284	20.49	.347	29.55	.420	41.45
2.25	.155	6.30	.186	9.47	.277	19.87	.352	30.69	-	-	-	-
2.50	.175	8.00	.213	12.42	.332	27.99	-	-	-	-	-	-

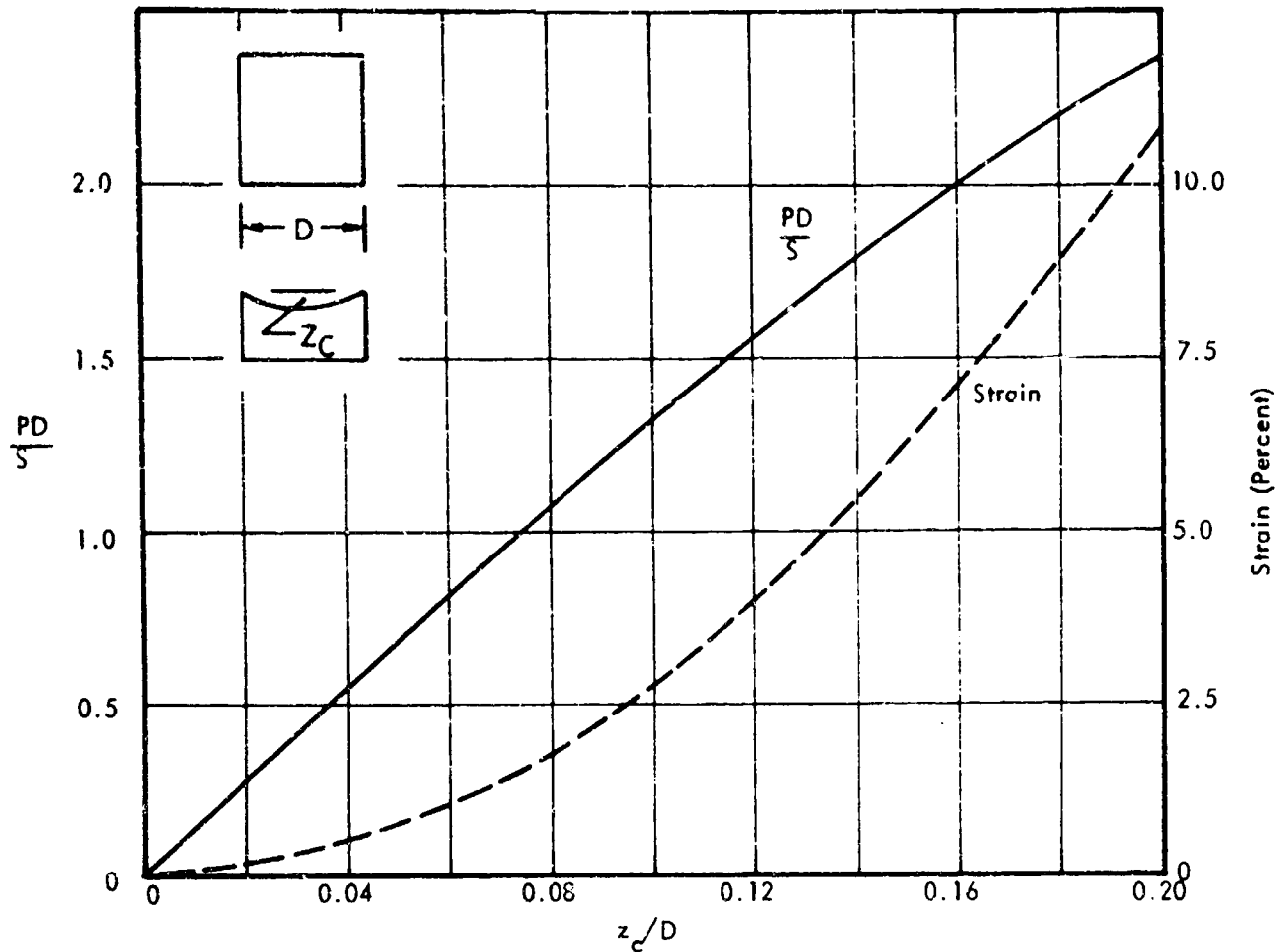


Figure A-5.  $PD/S$  versus  $z_c/D$  Curve for a Square Membrane

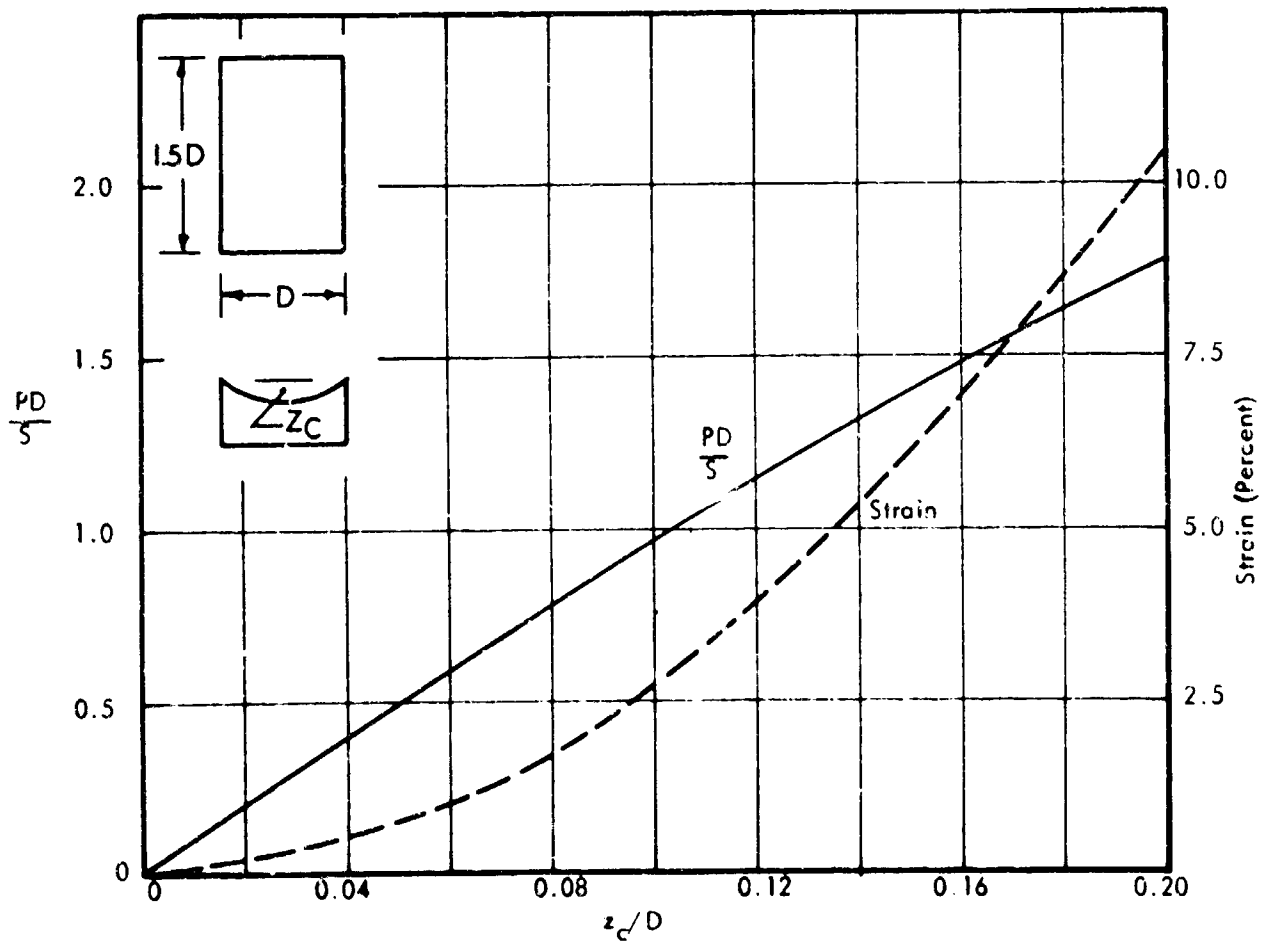


Figure A-6.  $PD/S$  versus  $z_c/D$  Curve for a  $1.5 \times 1$  Membrane

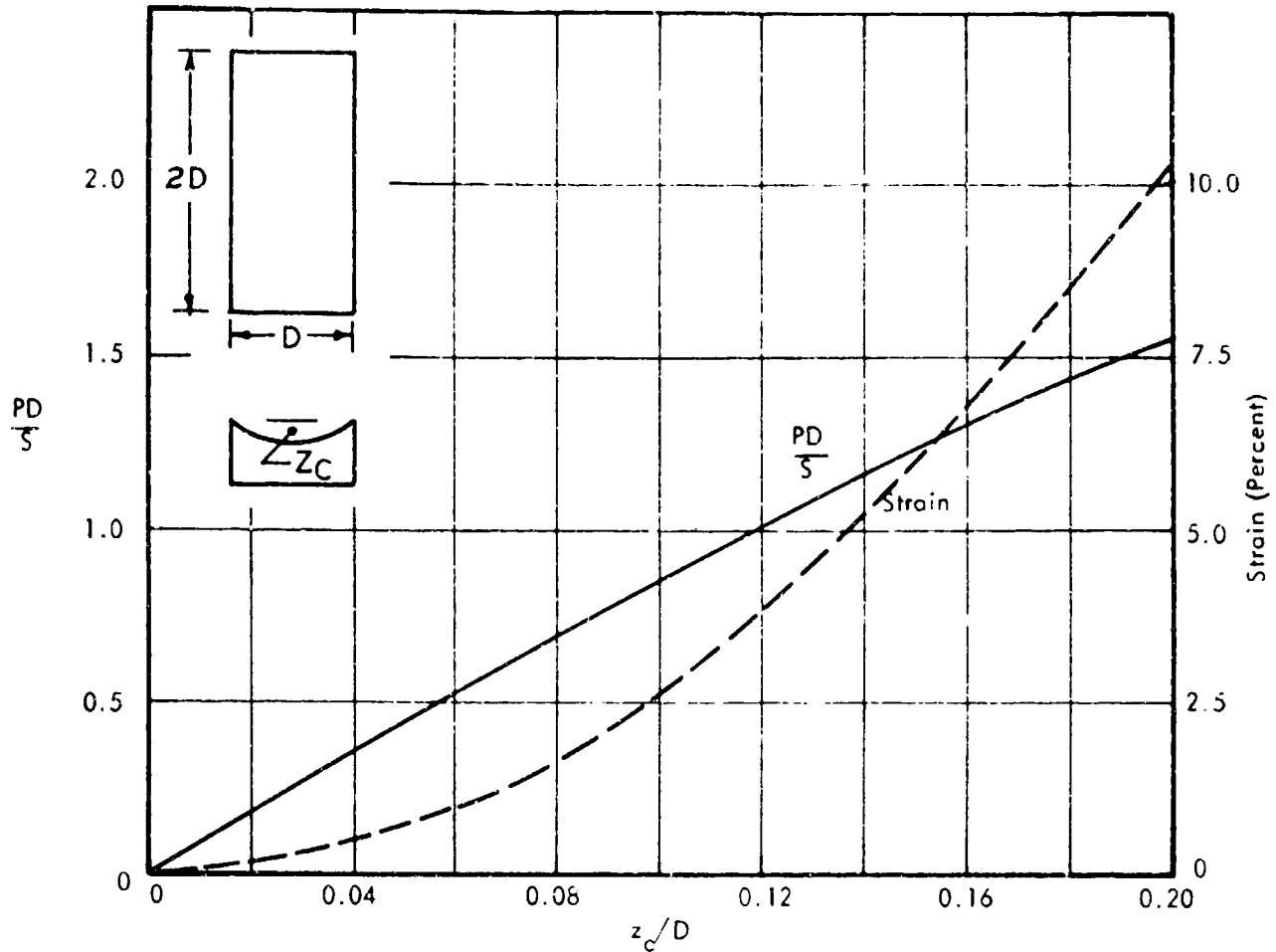


Figure A-7.  $PD/S$  versus  $z_c/D$  Curve for a 2.0 x 1 Membrane

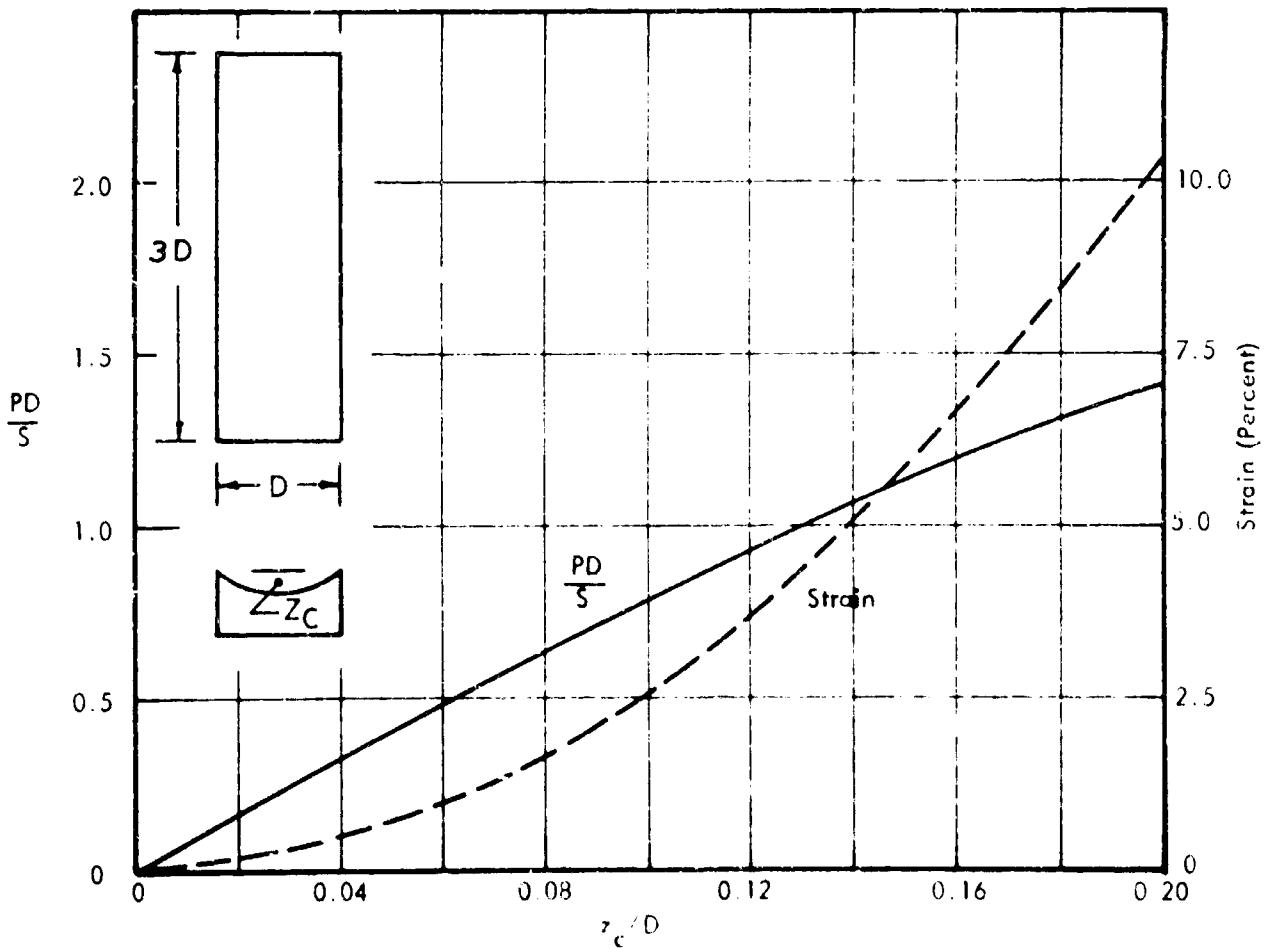


Figure A-8.  $PD/S$  versus  $z_c/D$  Curve for a 3.0 x 1 Membrane

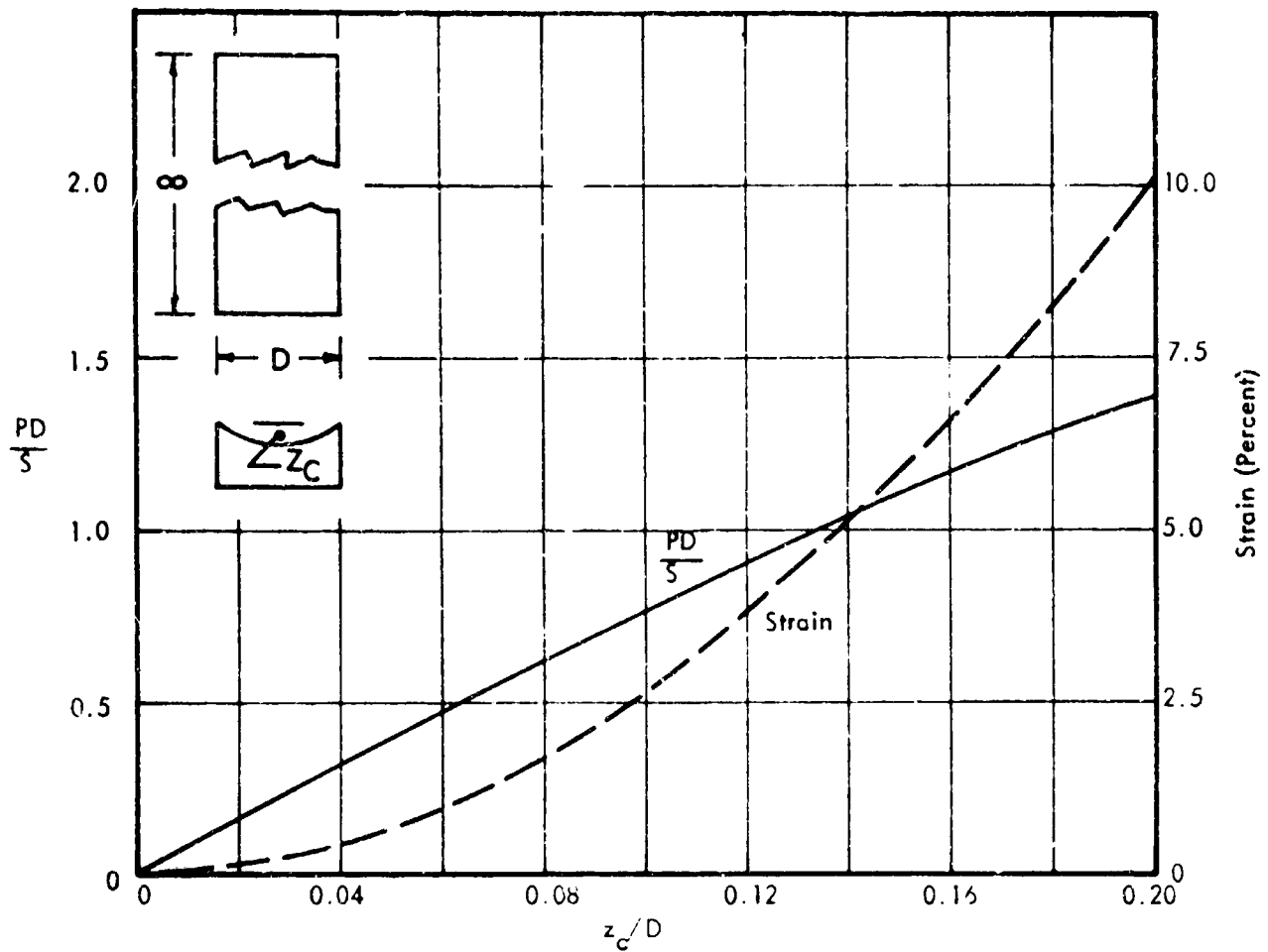


Figure A-9.  $PD/S$  versus  $z_c/D$  Curve for an  $\infty \times 1$  Membrane

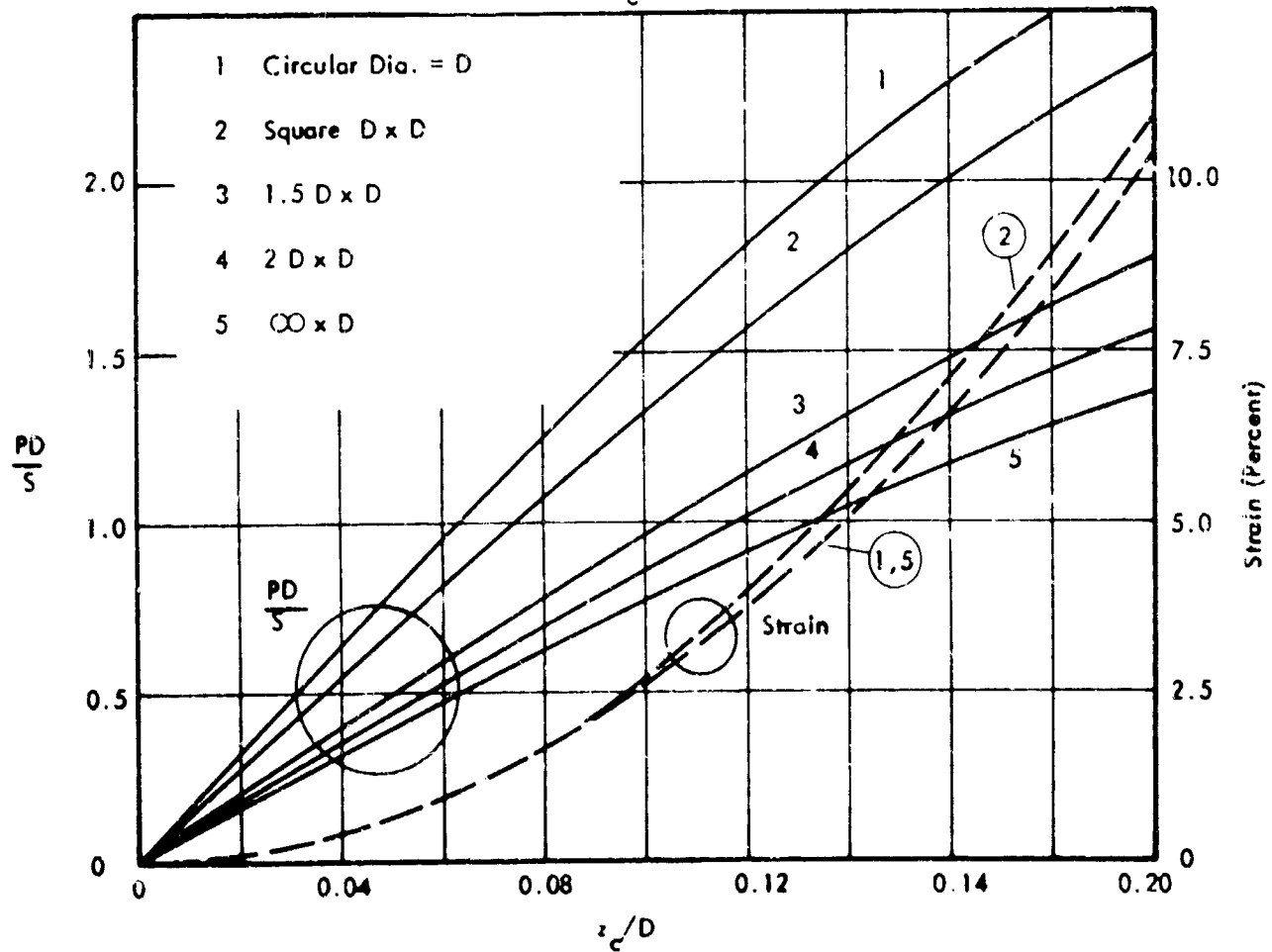


Figure A-10.  $PD/S$  versus  $z_c/D$  Composite Curve

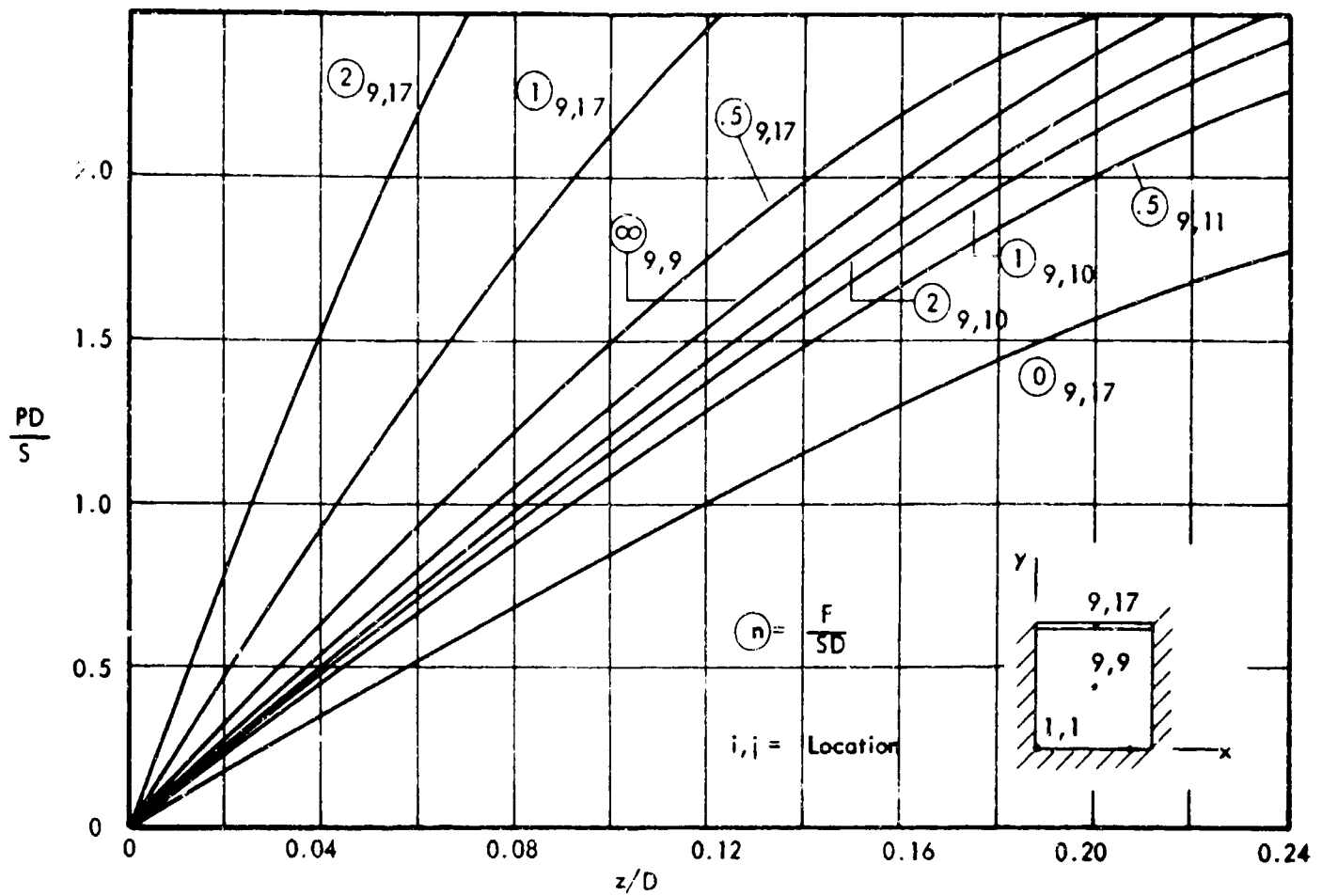


Figure A-11. PD/S versus z/D Curves for a Square Membrane with One Yielding Beam

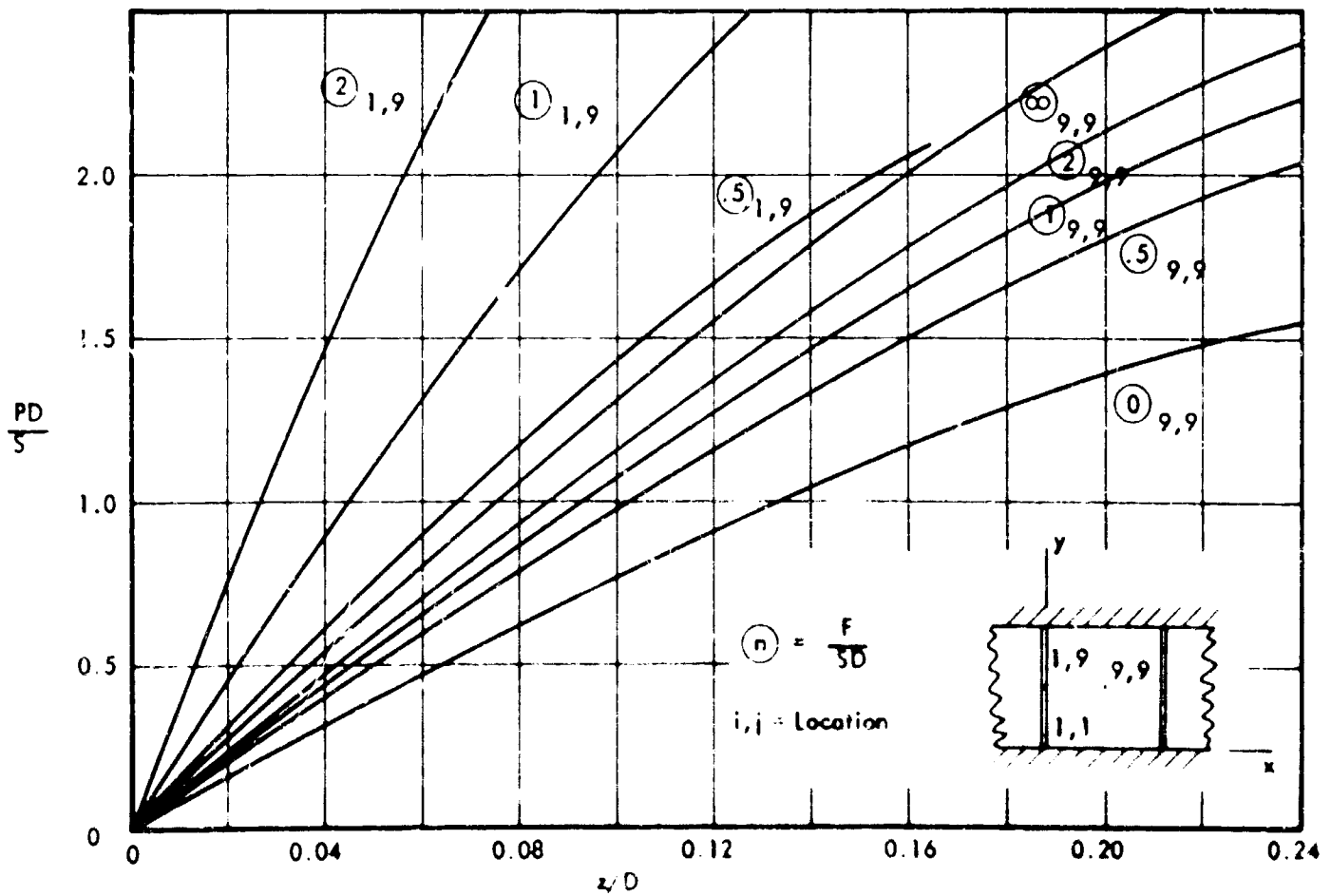
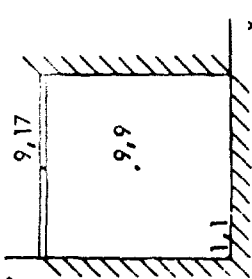


Figure A-12. PD/S versus z/D Curves for a Square Membrane with Beams on Two Opposite Edges

Summary of Computer Results - Square Membrane with One Yielding beam

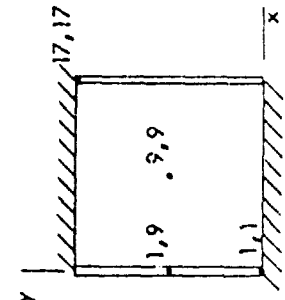
Beam Width = 0.0



$\frac{F}{SD}$	$\frac{PD}{S}$	$\frac{z_{max}}{D}$	$\frac{z_{9,9}}{D}$	$\frac{z_{9,17}}{D}$	Strain in Beam (%)
		$z_{9,11}/D$			
0.5	0.5	0.0444	0.0431	0.0310	0.245
	1.0	0.0506	0.0680	0.0633	1.021
	1.5	0.1405	0.1367	0.0988	2.477
	2.0	0.1980	0.1927	0.1403	4.977
		$z_{9,10}/D$			
1.0	0.5	0.0416	0.0411	0.0212	0.114
	1.0	0.0847	0.0837	0.0430	0.468
	1.5	0.1307	0.1292	0.0662	1.107
	2.0	0.1822	0.1804	0.0917	2.127
2.0	0.5	0.0396	0.0394	0.0130	0.042
	1.0	0.0804	0.0802	0.0262	0.173
	1.5	0.1238	0.1235	0.0398	0.399
	2.0	0.1718	0.1716	0.0541	0.740
		$z_{9,9}/D$			
3.0	0.5	0.0387	0.0387	0.0093	0.022
	1.0	0.0786	0.0786	0.0188	0.089
	1.5	0.1211	0.1211	0.0284	0.204
	2.0	0.1682	0.1682	0.0384	0.372

Summary of Computer Results - Square Membrane with Yielding Beams on Two Opposite Edges

Beam Width = 0.0  
 $z_{max} = z_{9,9}$



$\frac{F}{SD}$	$\frac{PD}{S}$	$\frac{z_{9,9}}{D}$	% Strain along $l = 9$	$\frac{z_{1,9}}{D}$
0.5	0.5	.0501	0.677	.0325
	1.0	.1028	2.840	.0670
	1.5	.1613	6.927	.1057
	2.0	.2317	14.037	.1534
1.0	0.5	.0456	0.569	.0218
	1.0	.0931	2.359	.0445
	1.5	.1443	5.626	.0688
	2.0	.2022	10.911	.0960
2.0	0.5	.0421	0.489	.0131
	1.0	.0857	2.021	.0266
	1.5	.1320	4.768	.0405
	2.0	.1840	9.423	.0562

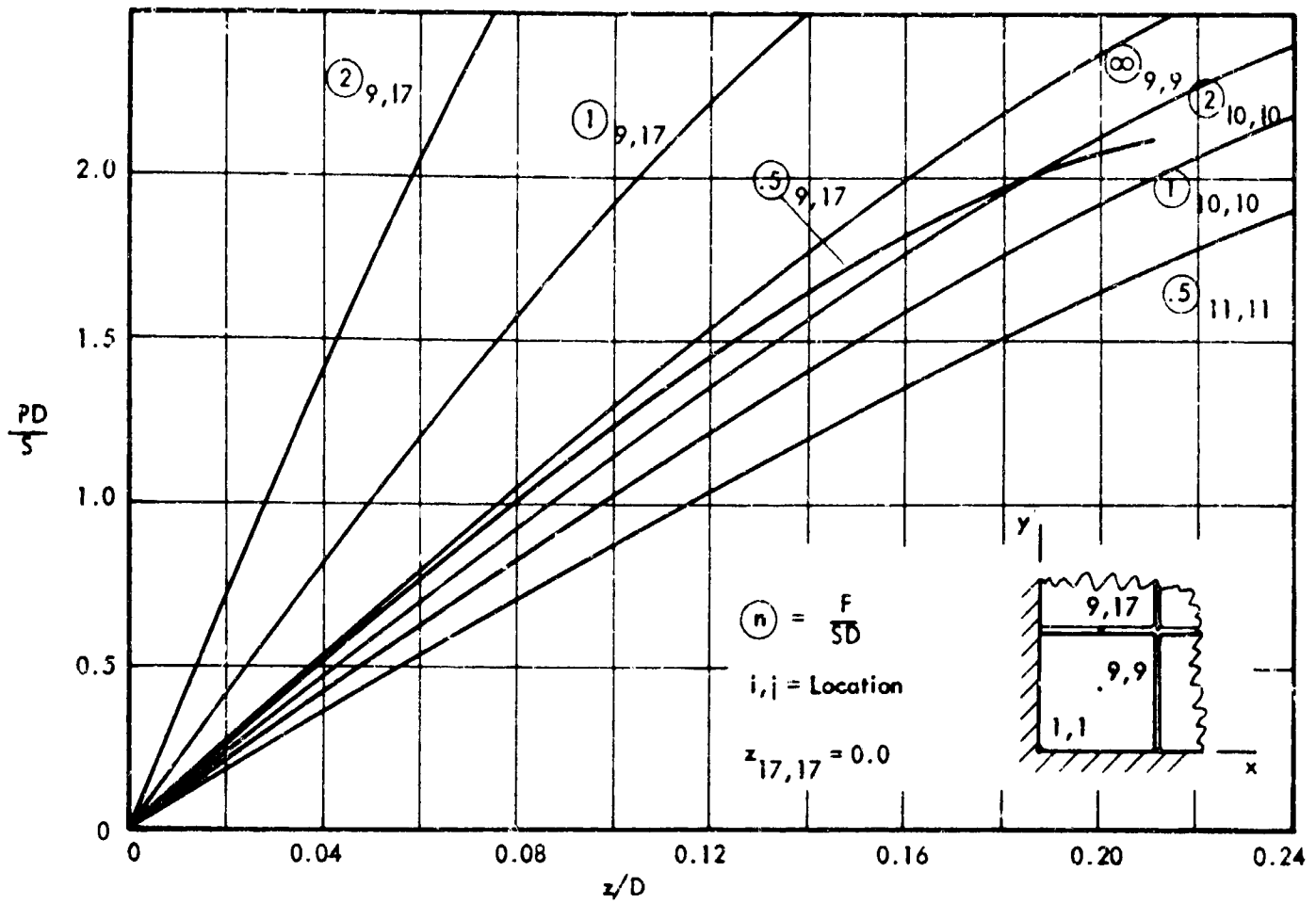


Figure A-13. PD/S versus z/D Curves for a Square Membrane with Beams on Two Adjacent Edges

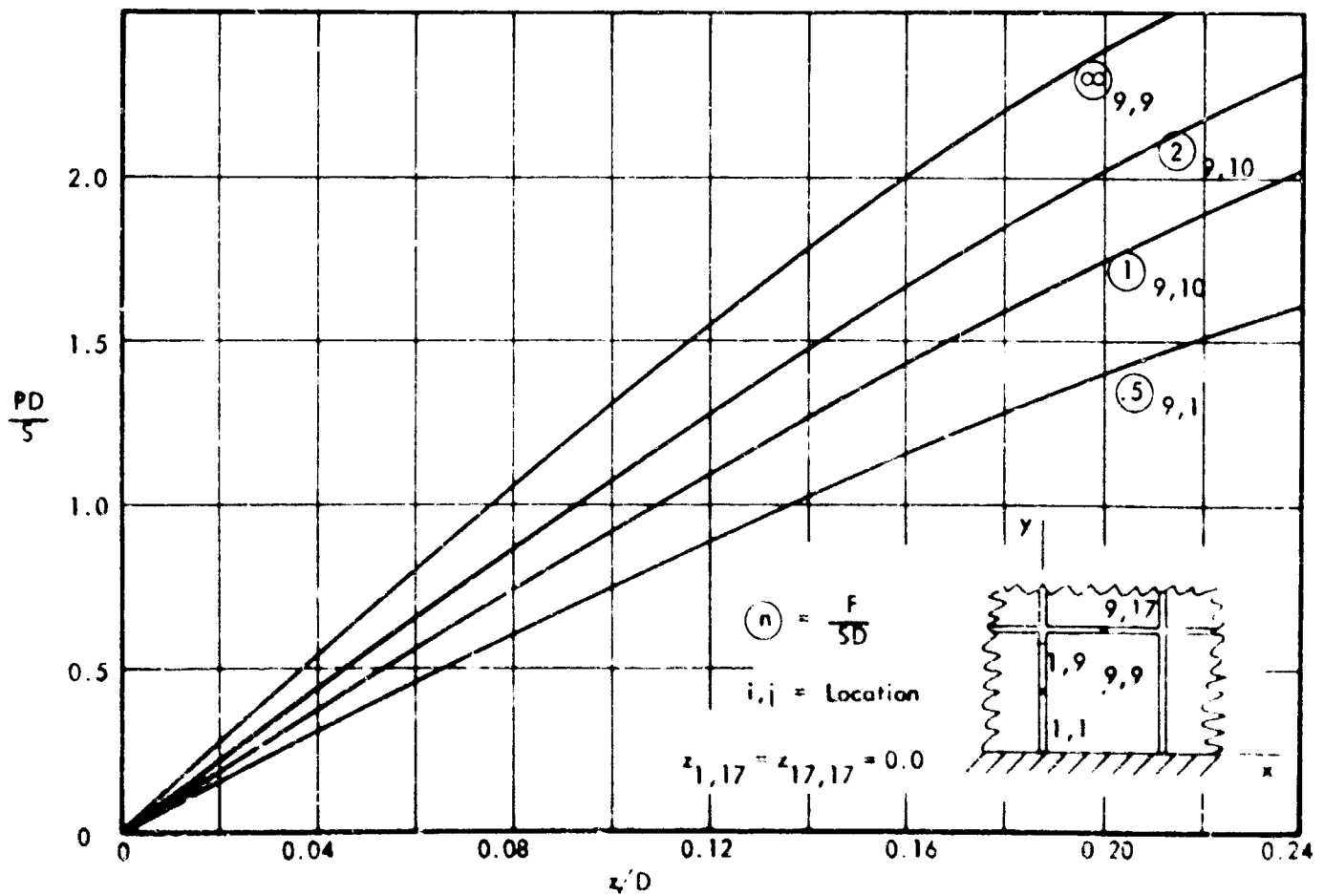
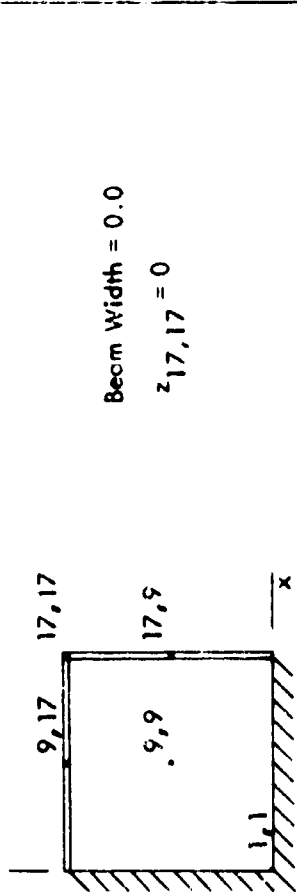


Figure A-14. PD/S versus z/D Curves for a Square Membrane with Beams on Three Edges (Membrane)

TABLE 4

Summary of Computer Results - Square Membrane with Yielding Beams on Two Adjacent Edges

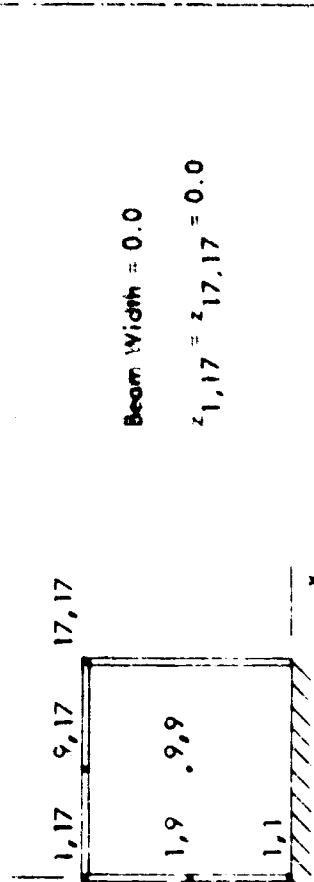


Beam Width = 0.0  
 $z_{17,17} = 0$

F SD	PD S	$\frac{z_{max}}{D}$ $z_{11,11}/D$	Percent Strain Along J=11	$\frac{z_{9,17}}{D}$	Percent Strain Along J=17	$\frac{z_{9,9}}{D}$
0.5	0.5	.0555	0.416	.0382	0.398	.0527
	1.0	.1139	1.734	.0789	1.686	.1082
	1.5	.1786	4.199	.1251	4.225	.1700
	2.0	.2573	8.464	.1838	9.053	.2458
1.0	0.5	.0479	0.374	.0243	0.153	.0468
	1.0	.0974	1.541	.0492	0.631	.0952
	1.5	.1504	3.661	.0759	1.493	.1473
	2.0	.2096	7.063	.1053	2.866	.2058
2.0	0.5	.0423	0.365	.0140	0.050	.0425
	1.0	.0869	1.507	.0283	0.204	.0864
	1.5	.1335	3.561	.0427	0.470	.1331
	2.0	.1847	6.814	.0581	0.863	.1845

TABLE 5

Summary of Computer Results - Square Membrane with Yielding Beams on Three Edges



Beam Width = 0.0  
 $z_{1,17} = z_{17,17} = 0$

F SD	PD S	$\frac{z_{max}}{D}$ $z_{9,11}/D$	% Strain Along J=11	% Strain f=9	$\frac{z_{1,9}}{D}$	% Strain f=1	$\frac{z_{9,17}}{D}$	% Strain J=17
0.5	0.50	.0661	.163	.554	.0421	.481	.0470	.615
	1.00	.1366	.676	2.344	.0875	2.079	.0981	2.673
	1.50	.2179	1.604	5.833	.1420	5.451	.1596	7.027
	2.00	.3287	3.112	-	.2217	13.154	.2505	17.082
1.0	0.50	.0537	.217	.457	.0256	.170	.0277	.202
	1.00	.1092	.896	1.886	.0520	.702	.0561	.829
	1.50	.1687	2.134	4.484	.0803	1.671	.0865	1.965
	2.00	.2354	4.144	8.686	.1120	3.239	.1201	3.772
2.0	0.50	.0459	.278	.414	.0144	.053	.0152	.059
	1.00	.0931	1.148	1.705	.0290	.214	.0304	.239
	1.50	.1429	2.722	4.021	.0440	.494	.0460	.546
	2.00	.1975	5.248	7.684	.0596	.907	.0621	.993

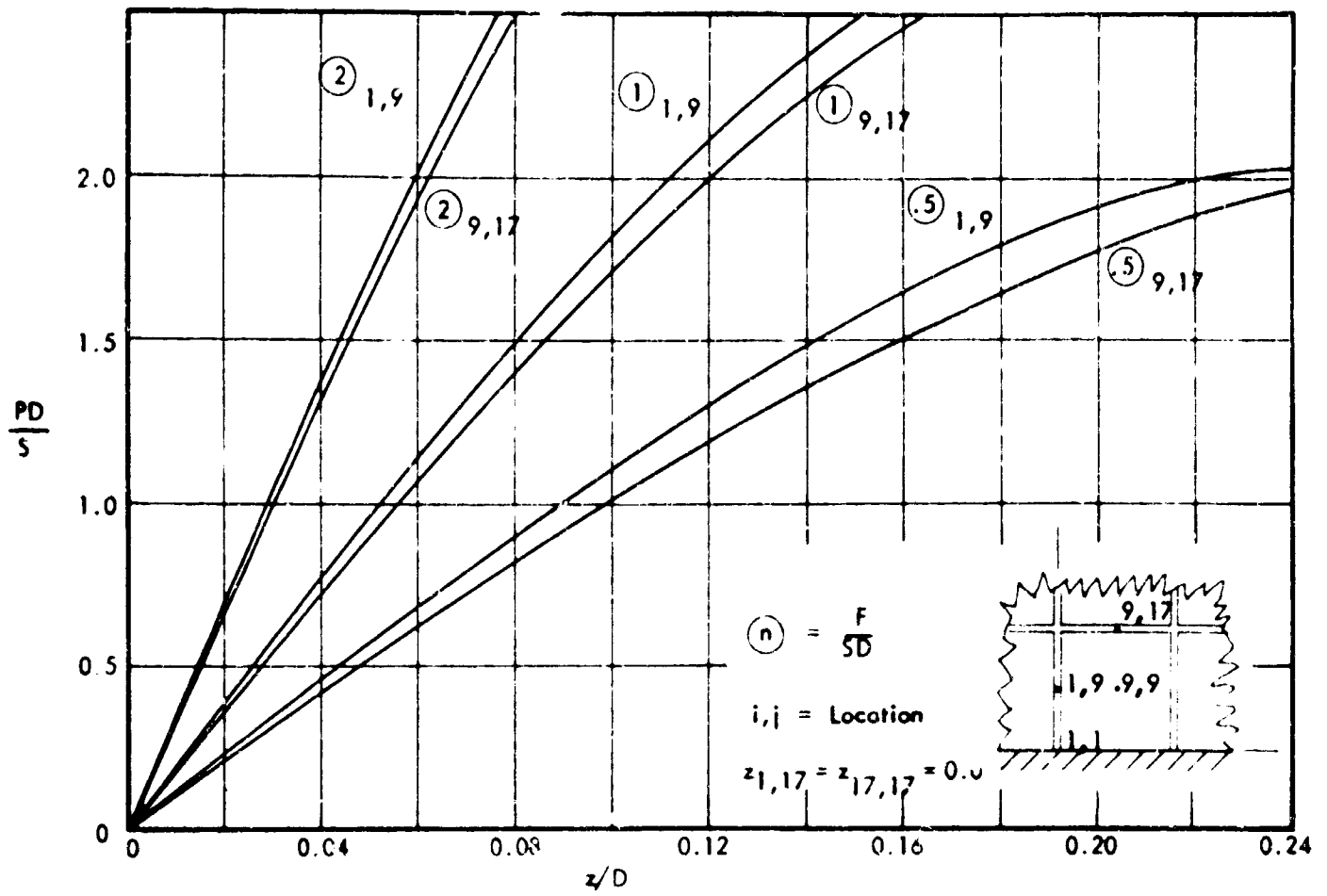


Figure A-15. PD/S versus z/D Curves for a Square Membrane with Beams on Three Edges (Beams)

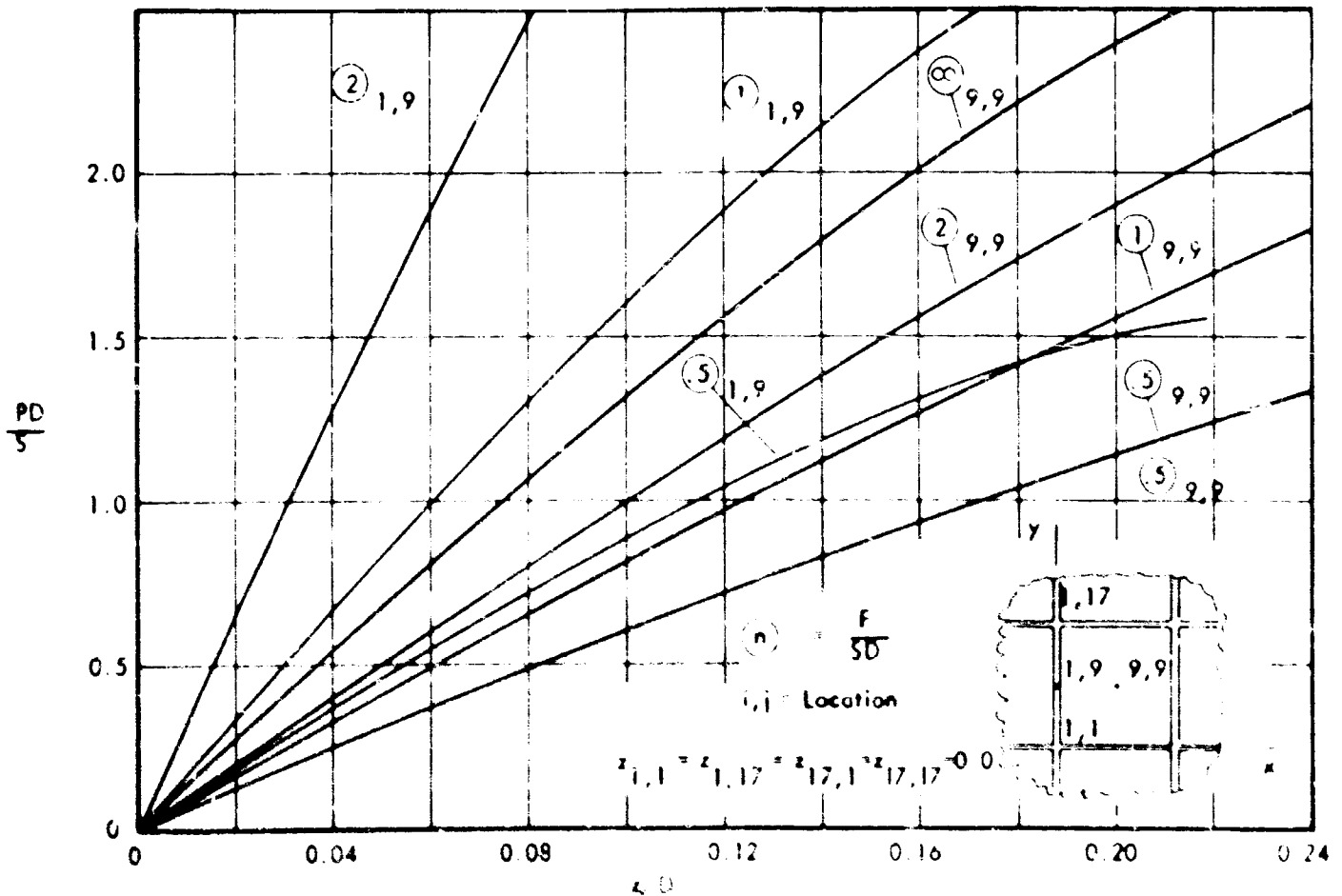


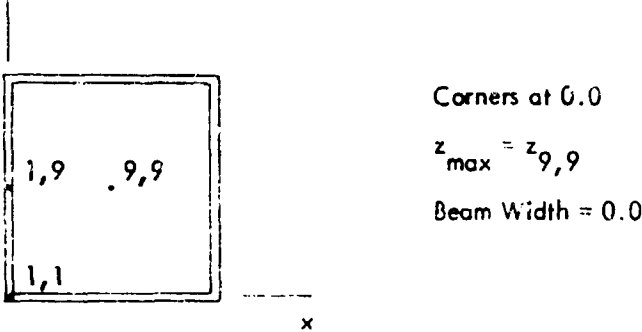
Figure A-16. PD/S versus z/D Curves for a Square Membrane with Beams on Four Edges

actual deflections of the surface. However, although the edge conditions and strengths and loadings of one panel affect the adjacent panels, it is not likely that they will affect panels farther away to any significant extent. Conservative use of the information given here will allow membrane structures to be designed within the desired degree of accuracy.

**Equivalent Curves for Other Materials.** The  $PD/S$  versus  $z/D$  curves are completely general and may be used with any type of ductile material. For a rigid-plastic material the  $S$  value is a constant which simplifies the use of the graphs. If these curves are used a number of times with a certain material, it may be advantageous to choose some constant  $S$  value (such as the yield strength) and draw a new "equivalent rigid-plastic" design curve. This eliminates unnecessary reference back to the biaxial stress-strain curve, for the material, to obtain an  $S$  value at various strain levels.

To construct this "equivalent rigid-plastic" curve, a stress value,  $\sigma_c$ , is chosen at which the general  $PD/S$  versus  $z/D$  curve is to coincide with that of the given material (point A of Figure A-17). A table with the following headings is then constructed (Table 7). Columns 1, 2, and 3 are obtained by choosing a number of points from the general  $PD/S$  versus  $z/D$  versus strain curve. At least three or four points should be used in the portion below  $PD/S = 0.25$ . From the biaxial stress-strain curve, stress values are found which coincide with the strains in column 3. The values of column 1 are multiplied by the values of column 4 and divided by the "constant" stress  $\sigma_c$ . A plot of column 2 versus column 5 will result in an "equivalent rigid-plastic"  $PD/S$  versus  $z/D$  curve for the given material. The new constant  $S$  value is  $\sigma_c t$ .

TABLE 6  
Summary of Computer Results - Square Membrane with Yielding Beams on Four Edges



$F/SD$	$PD/S$	$\frac{z_{max}}{D}$	% Strain along $l=9$	$\frac{z_{1,9}}{D}$	% Strain along $l=1$
0.5	0.5	.0819	0.20	.0538	0.804
	1.0	.1719	0.83	.1148	3.652
	1.5	.2855	1.96	.1976	10.741
	2.0	-	-	-	-
1.0	0.5	.0611	0.27	.0295	0.229
	1.0	.1244	1.10	.0601	0.951
	1.5	.1918	2.60	.0928	2.259
	2.0	.2666	5.00	.1290	4.342
2.0	0.5	.0497	0.32	.0156	0.063
	1.0	.1005	1.30	.0315	0.254
	1.5	.1539	3.08	.0475	0.580
	2.0	.2117	5.90	.0639	1.048

TABLE 7  
Column Headings for "Equivalent-Rigid-Plastic" Curves

Column No.	1	2	3	4	5
Heading	$\frac{PD}{S}$	$\frac{z_c}{D}$	strain	biaxial stress	$\frac{\sigma_n PD}{\sigma_c S}$

## Experimental Analysis

**Introduction.** Tests were conducted on various membrane shapes. These tests were designed to obtain membrane deflection data which could be used to check the accuracy of the computer results and compare with the predicted deflections. Tests were run on 1 x 1, 1.5 x 1 and 2 x 1 clamped edge membranes. Tests on membranes with yielding beams included a 1 x 1 membrane with 2 beams, 1.5 x 1 membrane with 2 and 3 beams and 2 x 1 membranes with 1, 3 and 4 beams.

**Test Equipment.** A testing device was constructed to test the membranes. The test bed was a 25 x 15 x 3/4 in. high strength aluminum plate. Edge beams 2-1/2 x 3/4 in. thick were bolted to the test bed by 1/2 in. cap screws spaced 1 in. apart. These edge beams were used to clamp the membrane in place. Fluid pressure was applied to the membrane through a hole in the test bed. One edge beam could be moved so that membranes of 10 x 10 in., 10 x 15 in., and 10 x 20 in. could be tested (see Chapter III).

Two tracks ran parallel to the long side the test bed. A framework was fabricated to span from one side to the other over the membrane. This framework held a sliding bar to which was fastened a 2 in. dial gage which measured within 0.001 in.

The dial gage was positioned crosswise on the membrane by means of a calibrated screw thread which moved the sliding bar. The entire framework was positioned lengthwise on the membrane by means of another calibrated screw thread. Great care was taken to ensure that the tracks were level, the sliding bar was parallel to the test bed, and the gage was dead center on the test bed when the screw threads were positioned. This arrangement permitted test results accurate within 0.002 in. in the vertical direction, and within 0.005 in. in the horizontal direction.

Water pressure was applied to the membrane as the loading medium. This reduced the danger to personnel which could have been present with air pressure only. Air under pressure stores energy which would have been suddenly released when the shell burst and could have caused some shell fragments to be thrown about. A surplus oxygen tank

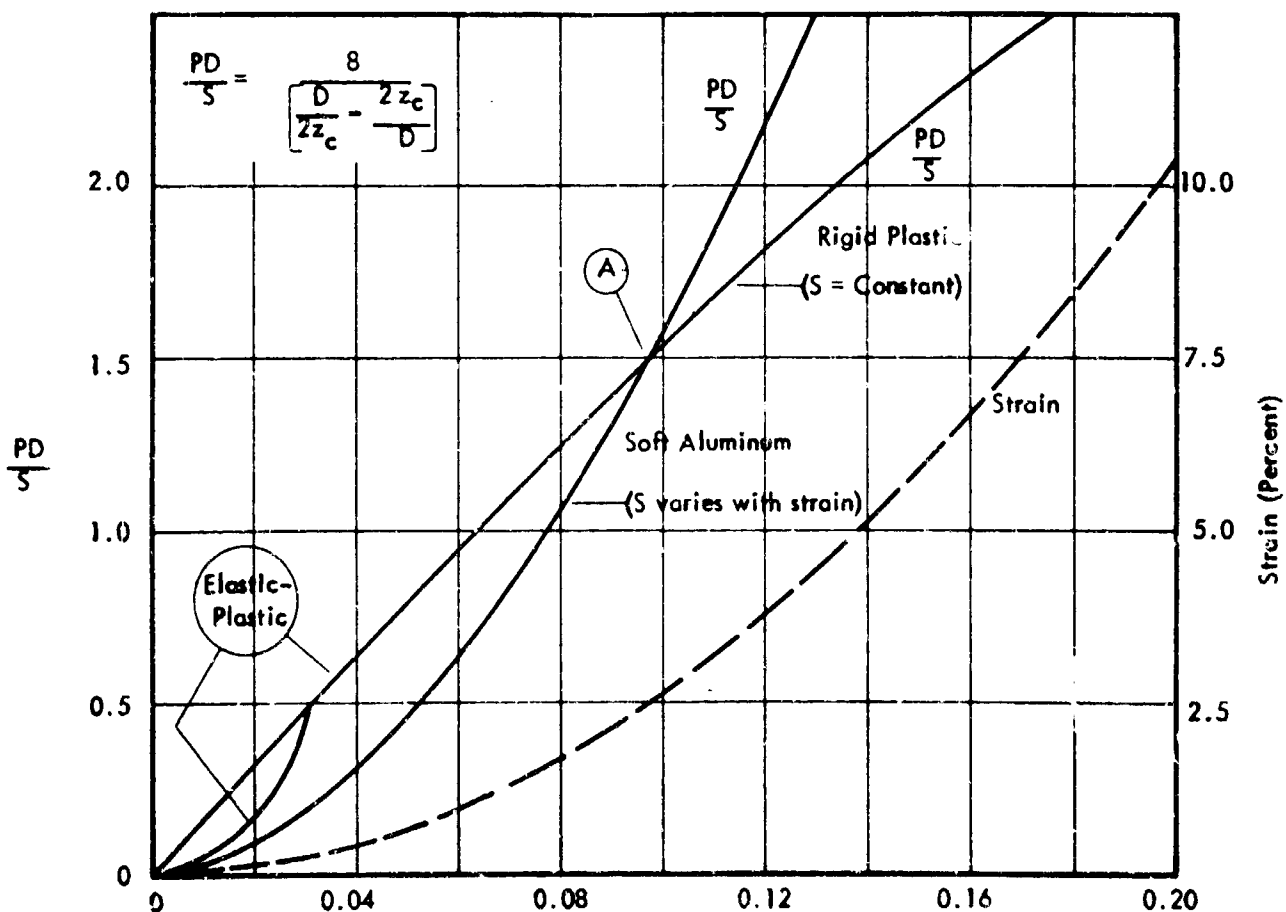


Figure A-17. "Equivalent Rigid-Plastic"  $PD/S$  versus  $z_c/D$  Curve for a Circular Membrane

was used as a reservoir and air pressure to water pressure conversion unit. A sensitive pressure test gage was attached to the tank. Also a 60 psi pressure cell, in conjunction with a strain box, was used to record the pressure. The pressure was measured to within 0.015 psi.

Test Procedure. Test membranes were held flat by a styrofoam block as the edge beams were attached. The water level in the reservoir tank was at the level of the test bed at the start of each test. At this point all gages and screw threads were checked to be certain they were zeroed. Deflection measurements were taken at set grid points. (Each membrane was divided into 16 grids each direction and measurements were made on 1/4 or 1/2 of the membrane depending upon the symmetry involved.) As a result, either 64 or 128 deflection readings were taken at each pressure level. There were usually five or six pressure levels in each test. Test results were reproducible and so, in the latter tests, only one test was made on each membrane shape.

Yielding beams were simulated by No. 8 soft steel wire. They were stretched by means of a simple jacking device to assure that they were well into the plastic range before the test was started. In this manner the load-displacement curve for the beam was essentially horizontal, and the load in the beam was relatively independent of the strain and could be more closely approximated. All the initial strain during testing was assumed to take place across the width of the shell because the edge beams clamped down on the wire as well as the membrane. This strain was obtained from the  $\sigma/D$  versus strain curves. At points where the wires crossed, a small device bent one wire over the other so that the wires themselves were in the same plane. The added strain, caused by bending the one wire, was taken into account.

The yielding beam tests were all of a type in which sag was permitted at points where the beams crossed. The apparatus would have been unnecessarily cluttered if a heavy bar had been used to hold those points at zero deflection.

Experimental Observations. It was noted that as the membrane deformed the material seemed to stretch quite unevenly -- even though, at the same time, the deflections were very regular and predictable. It could be explained by the nature of the thin metal membranes -- copper, aluminum, and steel all acted the same way -- in that the membranes seemed to thin out along irregular paths leaving thicker areas surrounded by thinner areas. As the material was stretched, the thicker areas gradually decreased in size and finally, just before failure, most of the earlier thick areas had thinned. It seemed that this thinning of the material occurred at first where the strains were greater (at the center and about half way toward the center from each edge. As the material was stretched the thinner regions were strained into the strain-hardening region and thus reached a point where the membrane force in the thinner portions became equal to the force in the thicker, less strained, portions; in effect equalizing the membrane force in almost the entire membrane. The areas in the corners of the rectangular shapes were the last to be strained into the plastic region. Also, it was noted that the circular tests (used to obtain the biaxial stress-strain curve) the straining was regular and more uniform.

In an attempt to measure the strain distribution over the shell surface, a photo grid of 20 lines to the inch was fixed on the surface of the clamped edge membranes. Near the edge, the strain becomes more uniaxial than biaxial; therefore, in order to maintain the uniform stress level, the membrane must strain more near the edges (see Figure A-18).

As is shown in Figure A-18, the stress does not vary much even though the strain does vary considerably. The points in the square symbol are the stresses taken from the uniaxial stress-strain curve. As can be observed, the uniaxial stress at the edge is the same value as the biaxial stress at the center. This is another point in favor of the uniform-stress-distribution assumption. The significance of this graph is also considered later with material on comparison of Computer and Test Results.

Because of the irregular strain distribution and the apparent ability of the material to equalize the membrane forces, it seems that the assumption of a uniform stress distribution may be applicable. This assumption obviously results in some error in the values of the displacement in the corners of a rectangular membrane. The amount of error and the region it involves becomes apparent in Computer and Test Results comparison.

The yielding beams strained fairly uniformly across the span. When the center deflection of the beam became larger than one inch, straining began to localize near the edges. Failure did occur in the wire during one of the tests and, as anticipated, it failed near the edge due to a combination of tensile and bending strains.

The stress-strain curves for the membrane material are shown in Figures A-19 and A-20. The material used was annealed steel sheet 0.004 in. thick. The load-strain curve for the yielding beam material (No. 8 soft, drawn,

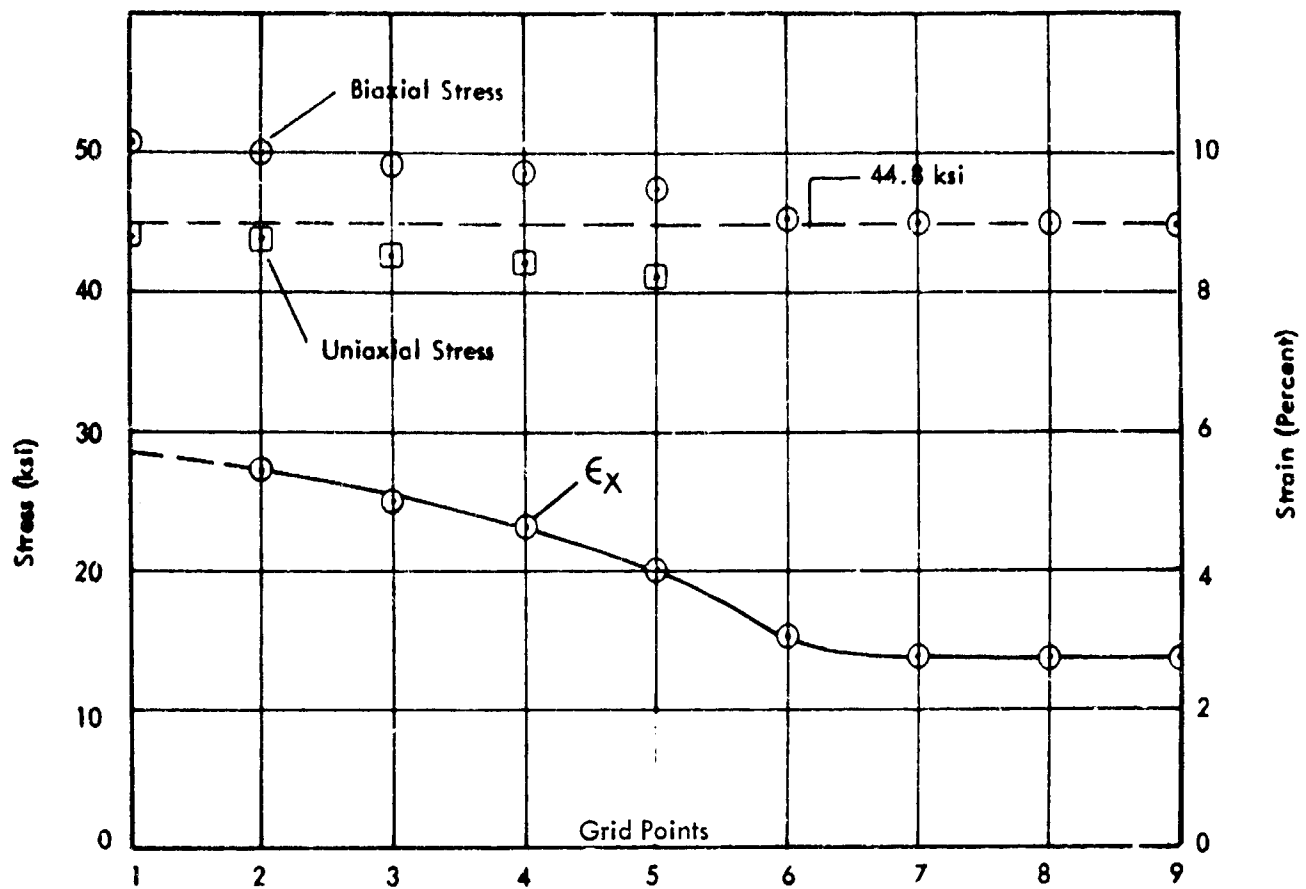


Figure A-18. Characteristic Stress and Strain Distributions across Center of 2 x 1 Membrane (Points along  $z_{9,i}; z_c/D = 0.125$ )

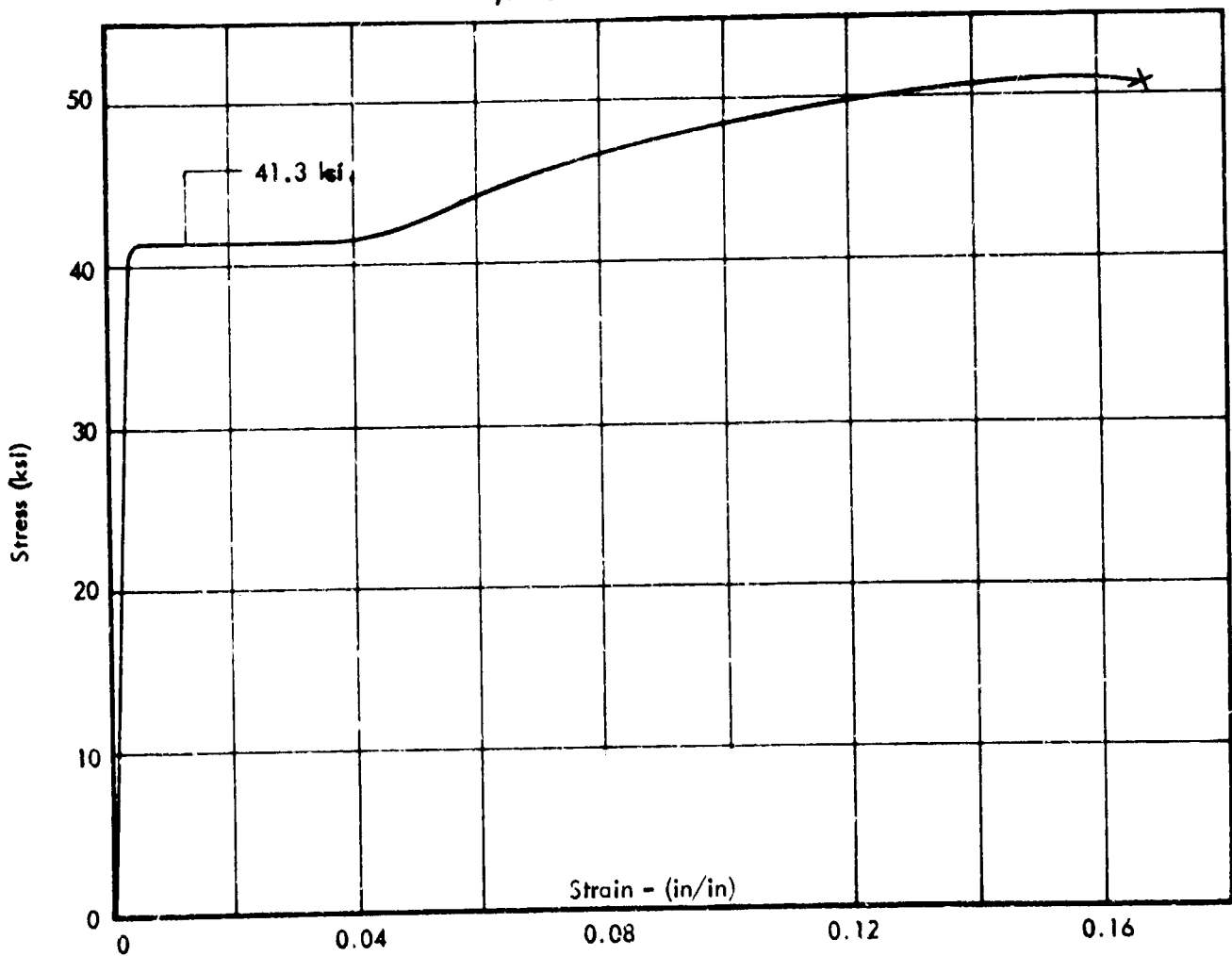


Figure A-19. Uniaxial Stress-Strain Curve for Membrane Test Material

fencing wire) is shown in Figure A-21. The biaxial stress-strain curve is an average stress, average strain curve computed by assuming spherical deformation over a circular membrane. This results in the following equations:

$$\text{Strain} = \left( \frac{r}{z_c} + \frac{z_c}{r} \right) \arctan \frac{z_c}{r} - 1 \quad (33)$$

$$\text{Radius of Curvature} = \frac{r}{2} \left( \frac{r}{z_c} + \frac{z_c}{r} \right) \quad (34)$$

$$\text{Membrane Strength} = \frac{Pr}{4} \left( \frac{r}{z_c} + \frac{z_c}{r} \right) \quad (35)$$

The deformation was spherical -- at least to within the least count of the measuring system which was 0.001 in. Although the strains may not be uniform, they were assumed to be for the computation of the biaxial stress-strain curve because this was to be the assumption used in the rectangular membranes.

The stress-strain curves and the membrane tests were run at the same strain rates -- zero strain rate. At each load level the deflections were allowed to stabilize before readings were taken. In this way, the discrepancies, which may have arisen due to unequal strain rates, were minimized.

The deflection readings on the membranes were taken with the pressure held constant so the deflections, and thus the strains, included both the elastic and plastic portions. This is what was intended since a normal stress-strain

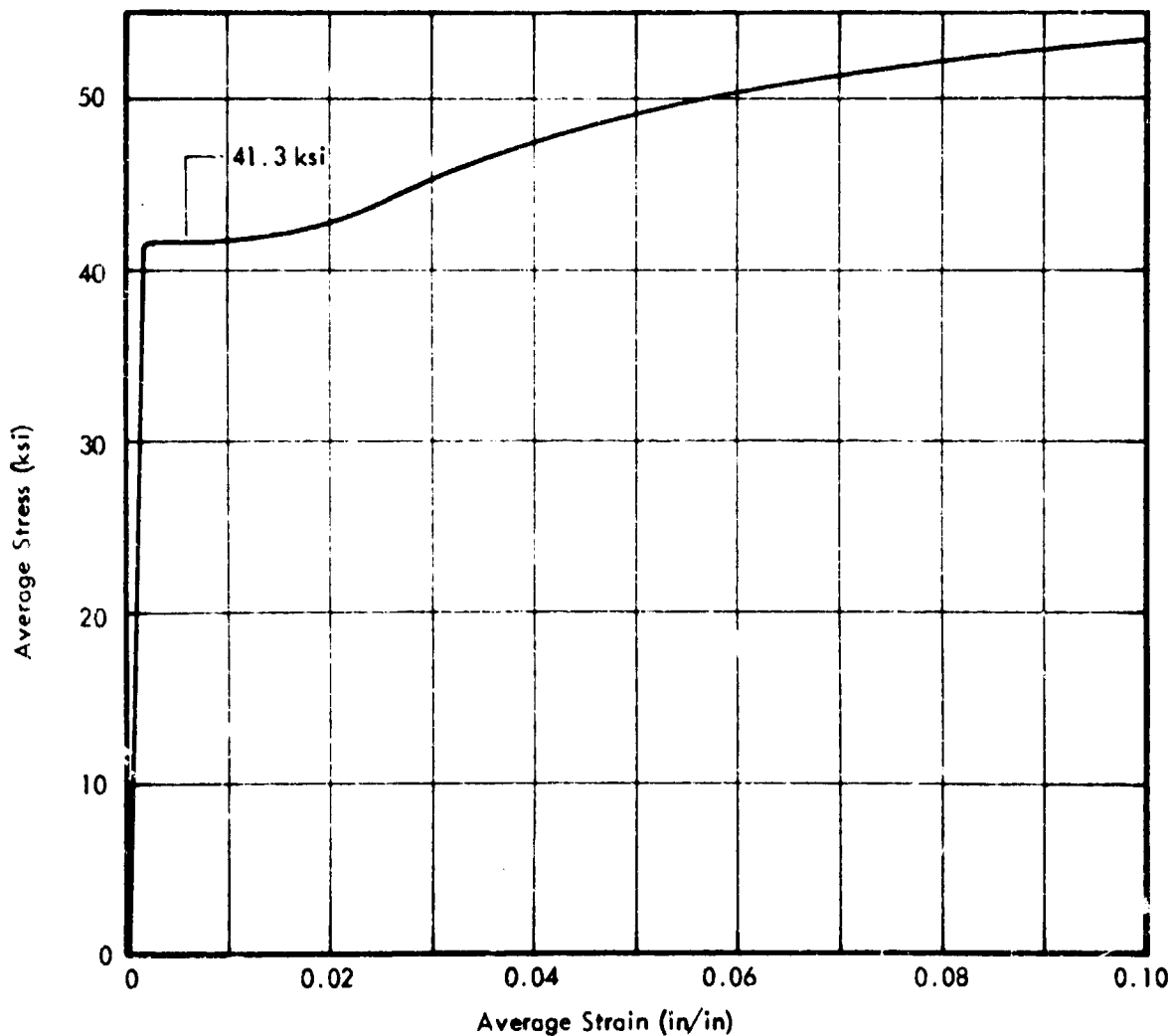


Figure A-20. Biaxial Stress-Strain Curve for Membrane Test Material

curve includes both portions. However, as a note of interest, the pressure was relieved a number of times during various tests to get an indication as to the effect of the elastic strains on the deflections. When the pressure was relieved the decrease in the amount of deflection was 100 percent up to  $z_c/D = 0.023$ , 50 percent at  $z_c/D = 0.030$ , 10 percent at  $z_c/D = 0.073$ , 5 percent at  $z_c/D = 0.103$ , and 2 percent at  $z_c/D = 0.163$ . These can also be obtained by using the biaxial yield strain of 0.0015 in/in and the strain versus  $z_c/D$  curves.

Membrane Boundary Conditions. The membrane forces are independent of bending and are wholly defined by the conditions of static equilibrium. However, the reactive forces and deformation obtained by the use of the membrane theory at the shell's boundary usually become incompatible with the actual boundary conditions.

As will be shown, there is no doubt about the membrane state of stress existing in the main portion of the shell. However, very near the boundary the clamped edge causes a narrow band in which the curvature is of the opposite sign from that of the main portion of the membrane. In this region, then, there are large bending and shearing stresses. Fortunately, this region is of the order of thickness of the membrane, which in the tests was only 0.004 in.; or more accurately, the boundary layer would be  $\sqrt{Rt}$ , which in the tests would only be  $\sqrt{.03(.004)}$  in.<sup>2</sup>, or 0.01 in. Because, in this edge region, bending stresses and shear stresses exist as well as the membrane stresses; it is very likely that this is where failure will occur first.

If the strain present in the membrane is broken into two parts,  $\epsilon_1$  due to tension and  $\epsilon_2$  due to bending, then the relative amounts of each can be determined from the deflected shape. If a circular deflected shape is assumed for this purpose it will be a simple matter to determine  $\epsilon_1$  and  $\epsilon_2$ . Choosing  $z_c$  = center deflection,  $D$  = span,  $R$  = radius of curvature,  $t$  = thickness of the membrane, then it can be shown that

$$\epsilon_1 = \frac{2R}{D} \arcsin \frac{D}{2R} - 1 \quad (36)$$

and

$$\epsilon_2 = \frac{t}{2R} \quad (37)$$

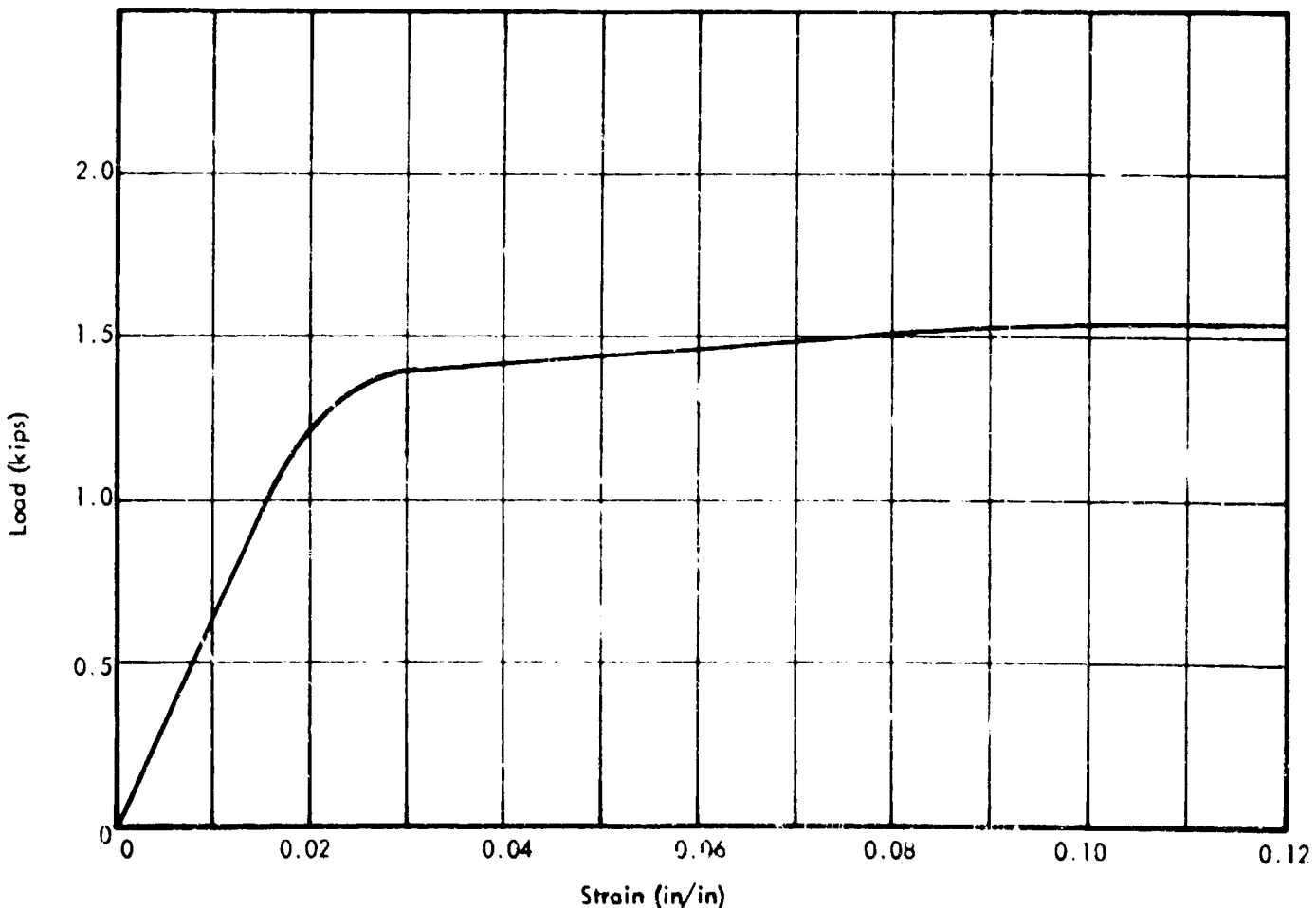


Figure A-21. Tensile Load-Strain Curve for Yielding Beam Test Material

For the tests  $D = 10$  in. and  $t = 0.004$  in. Table 8 is presented for the center portion of the membrane shell.

TABLE 8  
Strains in Center Portion of Membrane

$z_c/D$	$R$ (in)	$\epsilon_1$ (membrane)	$\epsilon_2$ (bending)
.05	2500	.006	.0000008
.10	1250	.027	.0000016
.15	833	.059	.0000024
.20	626	.101	.0000032
.25	500	.158	.0000040

This shows the insignificance of the bending strain over the major portion of the shell area. Also if  $R_1, R_2 \leq 0$  bending stresses are not restricted to the edge zone of the shell. In this case, however,  $R_1$  and  $R_2$  are both of the same sign; thus  $R_1, R_2 > 0$  and the bending stresses are restricted to the edge zone. Just at the edge of the membrane the curvatures measured in the deformed shells were as small as 0.03 in. This occurred at the midpoint of the longer edge. From Figure A-22

$$l_c = (R + \frac{t}{2})\Theta, \quad l_o = (R + t)\Theta$$

$$t = 0.004'' \quad (39)$$

$$R = 0.03''$$

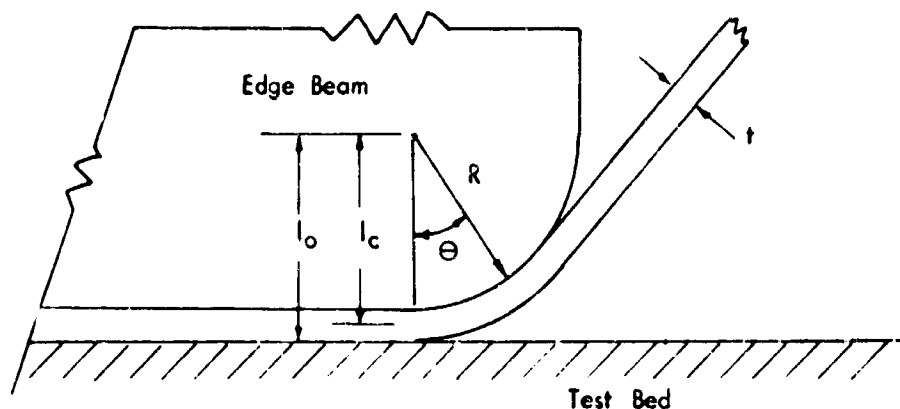


Figure A-22. Edge Conditions

and

$$\epsilon_b = \frac{l_o - l_c}{l_c} = \frac{t/2}{R + t/2} = \frac{0.002}{0.03 + 0.002} = 0.0625 \text{ in/in.}$$

This results in an  $\epsilon_2$  at the center of the clamped edges on the order of 0.0625 in/in. just before failure. The shells usually failed along the edge when the  $z_c/D$  ratio was somewhat over 0.20. At failure, then, the total strain at the edge was  $\epsilon_1 + \epsilon_2 = 0.1635$ .

This rough calculation of the strain existing at the clamped edge at failure indicates only that the strain would be increased by the flexure occurring at the boundary. However, using a Poisson's ratio of 1/2, which would be valid in the plastic range, it can be shown that the maximum biaxial strain should be only two-thirds of the maximum uniaxial strain. This explains why the circular membrane tests failed at strains of about 10 percent; whereas the uniaxial test specimens failed at strains of 16 to 17 percent. The circular membranes did not fail at the edges but rather at some point of weakness in the material. This indicates that, although the rectangular membranes failed at the edges, they were near failure due to biaxial strains in the center portion of the membrane.

To prevent premature failure at the edges of a membrane, a rounded edge of some type must be provided. In the tests, the edge beams were purposely rounded to retard failure at the edges and, yet, the rounding was not great enough to effect the deflection readings or the dimension of the span.

### Analytical and Experimental Comparisons

Updating Previous Work. From published results of tests conducted on circular membranes and analytical studies on circular membranes an accurate check of the PD/S versus  $z_c/D$  curve for a circular membrane may be obtained. This is shown in Figure A-23 and Tables 9 and 10. Both of these studies attempted to acquire stress and strain distributions over the membrane surface. In order to correlate with the present results the average stress in the membrane was used. Note that the results correspond very well in the region below a PD/S value of 1.5; above this point the membranes are approaching the "instability strain" or the strain at which a secondary bulge forms at the crown. The greater error is found in this upper region because at the time this secondary bulge forms a noticeable leveling off occurs in the pressure

versus deflection curve. The  $PD/S$  versus  $z_c/D$  curves are not meant to account for this loss in membrane strength -- similar to the decrease in stress just before failure on a stress-strain curve for ductile materials. Failure follows soon after this "instability strain" is reached.

Test results for the deflection of square clamped plates under uniform lateral load included one test in which the center deflection to plate thickness ratio was 12:2. The tests were made with aluminum specimens with the following specifications:  $D = 7.5$  in.,  $t = 0.0158$  in.,  $E = 10,300$  ksi,  $\sigma = 37.5$  ksi at 0.002 in/in offset. The stress-strain curve for the material was also given. Using this data, the 5, 8, 10 and 12  $w_c/h$  ratios were converted to  $z_c/D$  values and the  $Pa^4/Et^4$  ratios were converted to  $PD/S$  values. The results are shown in Figure A-24 and Table 11. This gives some indication of the point at which the bending forces can be taken as having a negligible effect on the deflections. If the bending forces were affecting the load-carrying capacity of the plate, the points plotted should be above the curve. The reason the points are below the curve may be in the difference in strain rates between the stress-strain curves and the test. If all the values were increased so that the largest value coincided with the curve, then it can be seen that somewhere between the  $w_c/h$  values of five and eight the bending forces begin to exert a negligible effect. In fact, at a  $w_c/h$  of 5.1 the bending forces carry only about 12 percent of the load.

Results of failure tests on 1.55 x 1 rectangular membranes with clamped edges subjected to uniform lateral pressure are shown in Figure A-25 and Table 12. There is substantial scatter in the data. The ultimate stresses of the materials tested were obtained by uniaxial tests on coupons of the materials. The scatter of data may be due partly to the difference in the rate of strain between the coupon tests and the membrane tests. It is not known if any attempt was made to run the tests at similar rates of strain.

Greenspan considered the problem of large deflections of a plate under uniform pressure loading. He used the Poisson Equation approximation

$$\frac{\partial^2 z}{\partial x^2} + \frac{\partial^2 z}{\partial y^2} = \frac{-P}{S} \quad (40)$$

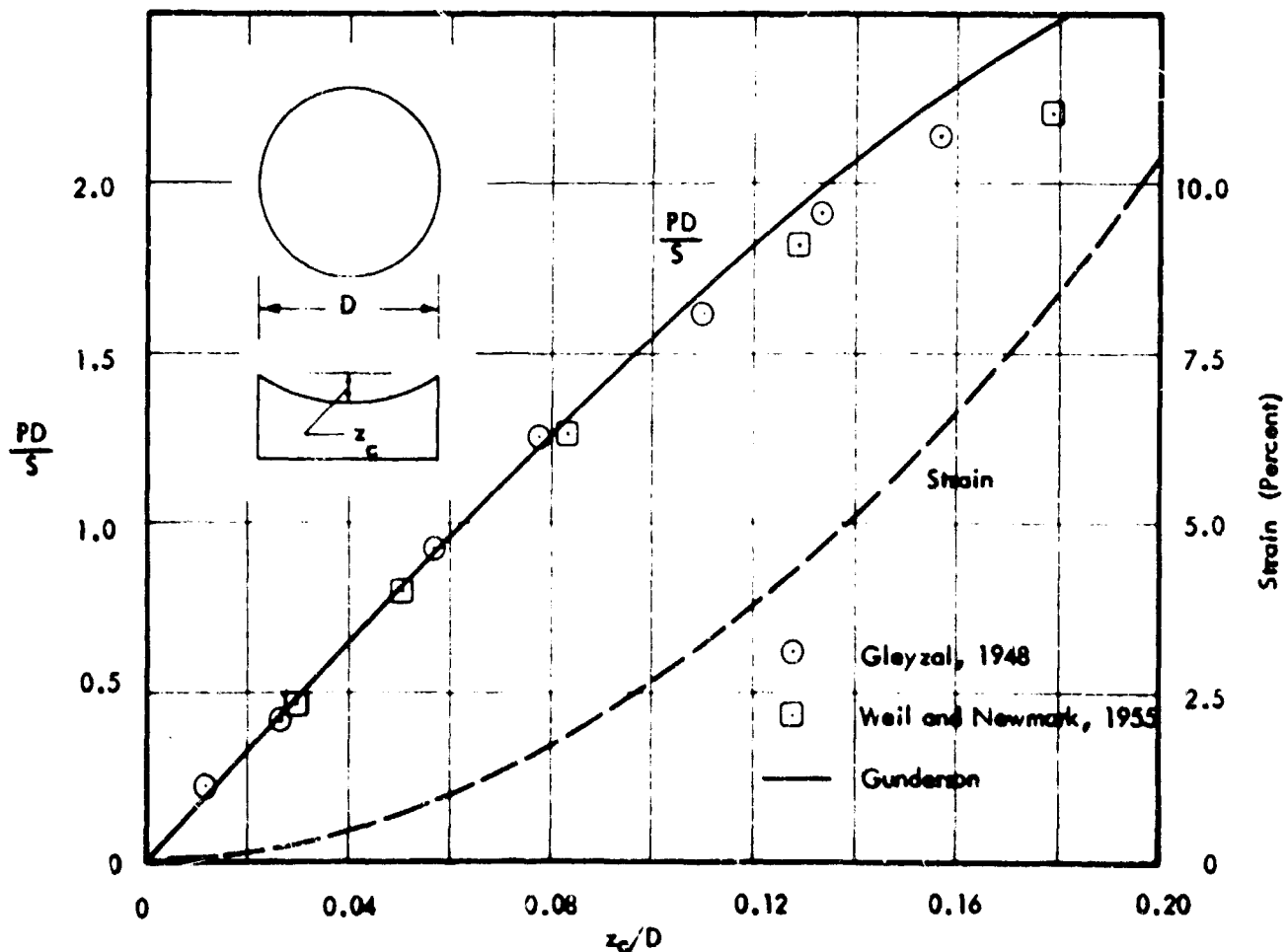


Figure A-23. Comparison with Gleyzal (1948) and Weil and Newmark (1955), Circular Membrane

TABLE 9  
Results of Circular Diaphragm Tests (Gleyzal, 1948)

$\frac{Pa}{h}$ (ksi)	Ave. Radial Strain (%)	Ave. Radial Stress (ksi)	$\frac{w_c}{a}$	$\frac{PD}{S}$	$\frac{z_c}{D}$
2.09	0.035	24.0	0.024	0.174	0.012
7.83	0.190	36.5	0.054	0.430	0.027
21.37	0.875	47.0	0.113	0.908	0.057
35.28	1.580	58.5	0.156	1.208	0.078
55.92	3.200	70.0	0.221	1.595	0.110
71.68	4.700	74.5	0.267	1.925	0.133
84.76	6.400	78.5	0.314	2.160	0.157

TABLE 10  
Results of Circular Membrane Tests (Weil and Newmark, 1955)

$\frac{Po}{h}$ (ksi)	Ave. Radial Strain (%)	Ave. Radial Stress (ksi)	$w_c$	$\frac{PD}{S}$	$\frac{z_c}{D}$
2.76	0.225	11.75	0.342	0.47	0.030
5.51	0.675	13.85	0.582	0.80	0.051
11.02	1.775	17.50	0.954	1.26	0.083
22.04	4.400	24.20	1.484	1.82	0.129
35.82	8.300	32.50	2.056	2.20	0.179
51.80	16.300	43.70	3.052	2.37	0.266

TABLE 11  
Results of Square Membrane Tests (Ramberg, et. al., 1942)

$\frac{w_c}{h}$	$\frac{Pa^4}{4Eh}$	Strain (%)	Stress (ksi)	p (psi)	$\frac{PD}{S}$	$\frac{z_c}{D}$
5.1	320	0.040	3.75	1.03	0.131	0.011
7.67	900	0.075	7.50	2.91	0.184	0.016
10.05	2200	0.125	12.50	7.11	0.270	0.021
12.20	3700	0.180	18.00	11.96	0.315	0.026

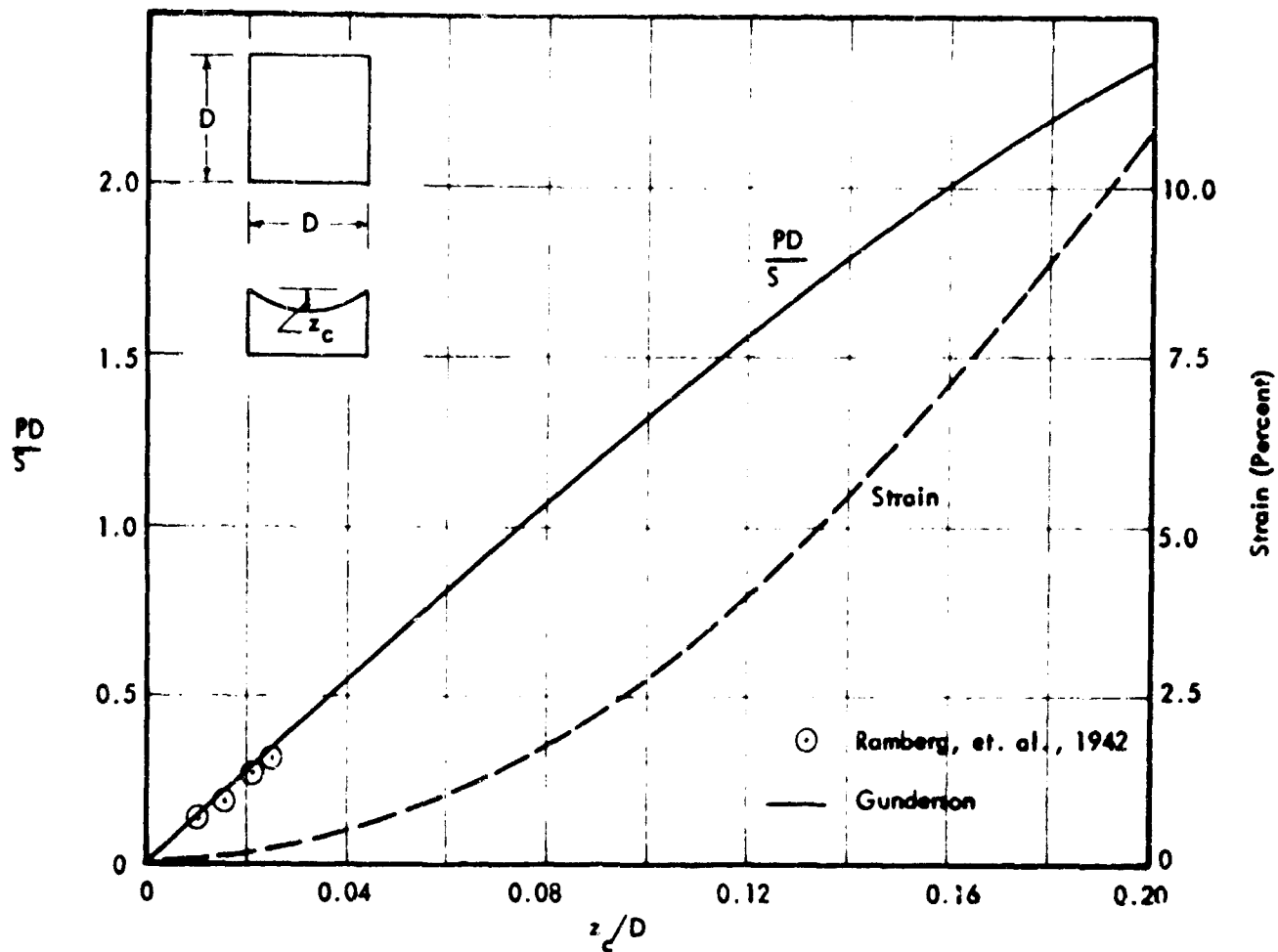


Figure A-24. Comparison with Ramberg, et al (1942), Square Membrane

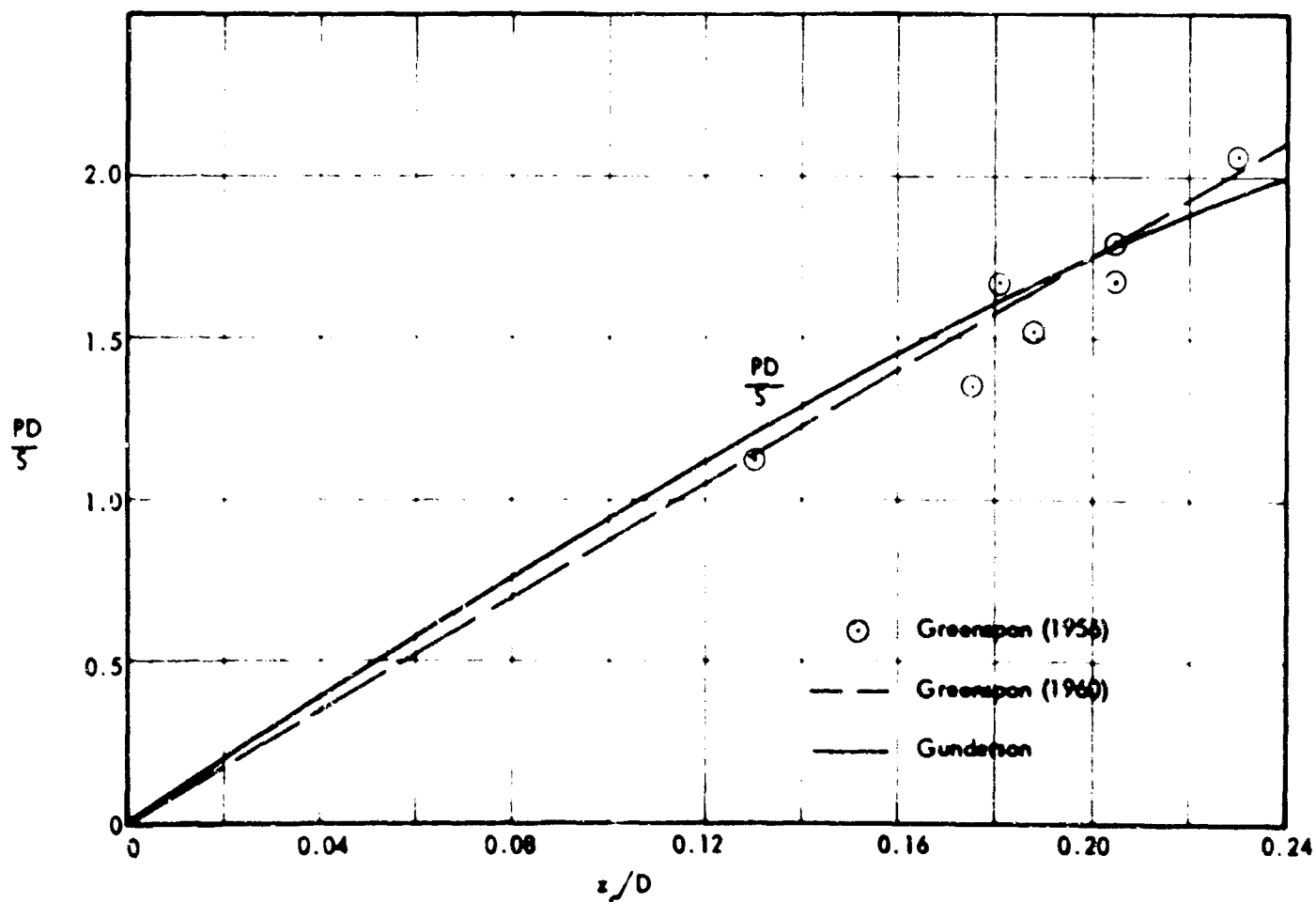


Figure A-25. Comparison with Greenspan (1956); Failure Tests on 1.55 to 1 Membrane

and obtained a general solution to the problem

$$w_{\max} = \frac{0.164 Pa^2}{S \left[ 1 + \left( \frac{a}{b} \right)^2 \right]} \quad (41)$$

This equation may be rewritten, in terms used here, as follows:

$$\frac{z_c}{D} = \frac{0.164 PD}{S \left[ 1 + \left( \frac{a}{b} \right)^2 \right]} \quad (42)$$

Thus if

$$D = L, \quad z_c/D = 0.082 \frac{PD}{S}$$

$$1.5 D = L, \quad z_c/D = 0.1135 \frac{PD}{S}$$

and

$$3 D = L, \quad z_c/D = 0.1476 \frac{PD}{S}$$

TABLE 12

Results of Failure Tests on Rectangular Membranes (Greenspon, 1956)

$\sigma_u$ (ksi)	$h$ (in.)	$a$ (in.)	$P_u$ (psi)	$w_c$ (in.)	$\frac{PD}{S}$	$\frac{z_c}{D}$
61.0	0.113	13.5	920	2.77	1.80	0.205
70.7	0.119	13.5	950	2.54	1.52	0.188
41.8	0.134	13.5	700	2.44	1.69	0.181
46.1	0.104	13.5	600	2.76	1.69	0.205
41.8	0.068	13.5	435	3.12	2.07	0.231
72.3	0.125	54.0	226	9.47	1.35	0.175
65.0	0.182	54.0	245	7.06	1.12	0.131

The comparison of this Poisson Equation approximation and the more exact equation presented here, is shown in Figure A-26.

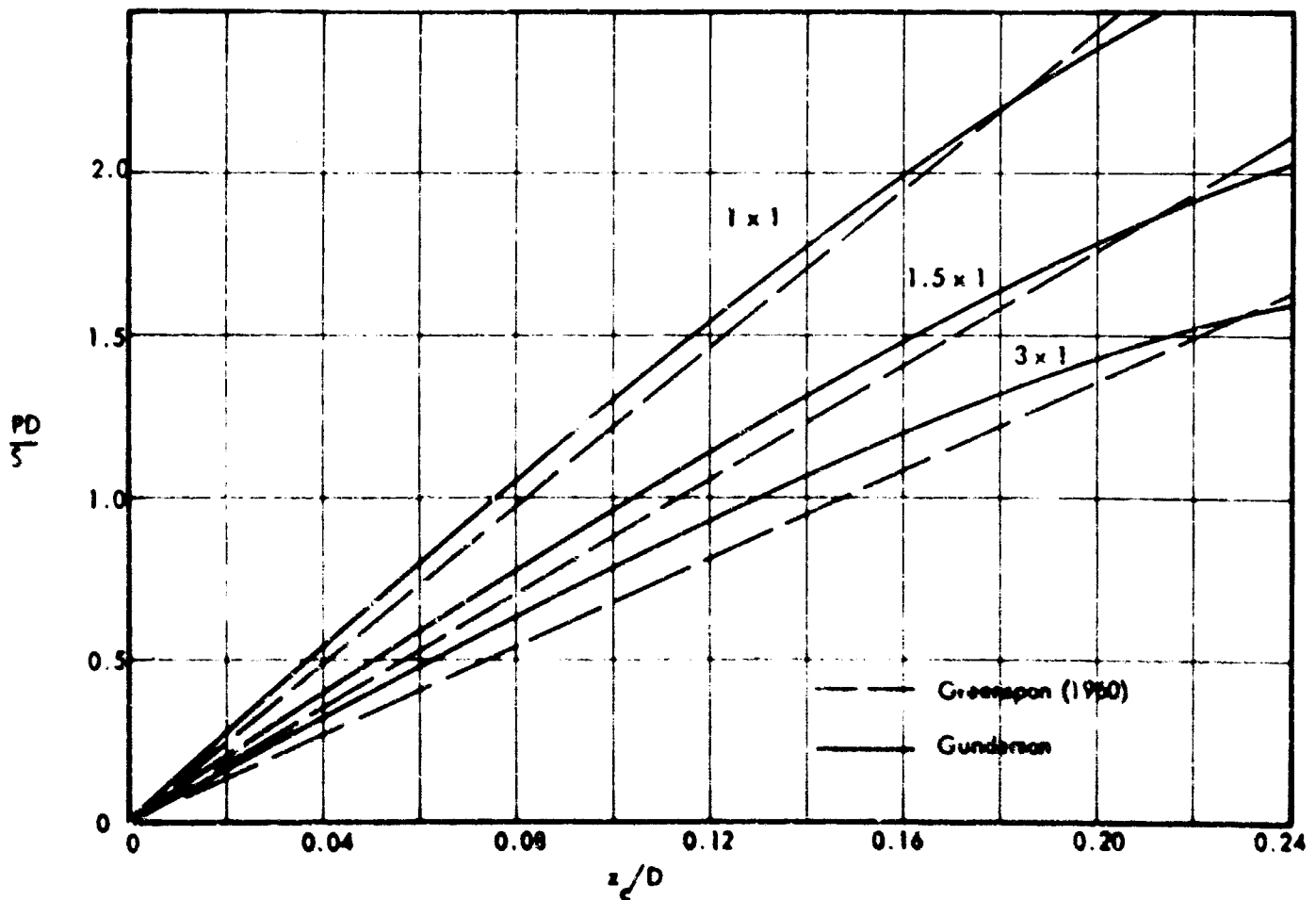


Figure A-26. Comparison with Greenspon (1960); Poisson Equation Curves

Comparison of Test Results and Computer Results. All of the comparisons of the PD/S versus  $z/D$  curves made in this section are based on the "equivalent rigid-plastic" curves. Thus, to make a comparison or determine the magnitude of the errors the "equivalent rigid-plastic" curve (a dotted line) and the test points (a dot in a circle) should be used. Use of the "equivalent rigid-plastic" curve is one way to make the non-linear behavior of the material more apparent (see Figure A-27 and Table 13).

It will be noted that, for all the shapes tested, the points in a band about one-half the span of the membrane in either direction across the center of the membrane show negligible error between the test results and computer results. In fact, the only region in which errors appear is in the corners in an area with a radius of about one-fourth the span with the center at the corner. The error in the corners, as shown in Figure A-28, is very large at low pressure levels, and about 20 percent at high pressure levels. This is to be expected because the computer program assumes a uniform stress distribution which does not exist in the corners of a rectangular membrane. However, in Figure A-29, for a point a little further away from the corners, the error is much less (less than 10 percent for most of the curve).

In Figure A-30, for a point away from the corners but along the edge, the errors are less than 5 percent. This same trend is evident in all of the shapes considered and also in the membrane supported by yielding beams (see Figures A-31 through A-40).

In the illustrations titled "Comparison of Results -  $z/z_{max}$ ...", beginning with Figure A-41, the amount of error and the location is readily apparent. From these illustrations a few characteristic cross-sections have been plotted.

The results for the square membrane with one yielding beam show excellent correlation between computer and test results. The results for the square membrane with two yielding beams show an error of about eight percent in the main portion of the membrane. To construct these charts, first the stress-strain curves were made for the materials used in the membrane and in the beams; then the tests were conducted. The yielding beams were stretched to about three percent strain before pressure was applied. The average strain across the point of maximum deflection was computed. Going to the biaxial stress-strain curve, the stress in the material was found. Thus, the values of pressure and membrane strength which were fed into the computer program were determined from the test results. In this way, if the computer program gave results very nearly the same as the test results the conclusion could be made that the assumptions used in the theory were justified (see Figures A-41 through A-53).

It can be observed from the results on the square membrane with clamped edges, and the square membrane with one yielding beam, that the results of the tests correspond very closely with those of the computer study. The strains were easily measured in both of these cases, so accurate values of the membrane strength could be obtained. The errors in the square membrane with two yielding beams were due mainly to the errors in the membrane strengths which were fed into the computer. It was difficult to obtain a high degree of accuracy in computing the strains in the membrane, and thus the membrane strength. The program is very sensitive to this value of membrane strength.

The greatest errors between the test results and the computer results occur in the corners. Here the membrane is not strained as much. Because the strain is at a low level, the stress in the corner is also at a lower level than in the main portion of the membrane, and in fact the stresses in the corners approach zero. Thus, because the strength in the corners of the test membrane has not reached the same strength as in the rest of the membrane, the deflections in the corners of the test membrane are greater than the computer values which are based on a uniform stress distribution.

As can be seen from the comparison of results tables, the two sets of results always agree well in the main portion of the shell; yet have errors as high as 30 percent in the corners in some cases. Note also that the error in the corners decreases as the total deflection increases. This is because the stress in the main portion of the membrane has been increasing rapidly in the elastic range of the stress-strain curve (see Tables 14 and 15).

The membranes yield to a very nearly circular deformation pattern in the short span direction, even near the clamped edges. The greatest deviation from a circular shape occurs at a distance of about  $1/8$  the span from the edges. A circular deformation pattern is evident from the strain versus center deflection curves which show that the strain varies very little for the different rectangular plans and the circular plan. The circular membrane and the strip membrane both deflect to a circular deformation pattern under uniform lateral load.

The stress and strain distribution curve (Figure A-19) shows that the average stress is about 44.8 ksi. If the strain versus  $z/D$  curve is entered with  $z/D = 0.125$ , the value of strain is 4.4 percent. From the biaxial stress-strain curve (Figure A-10) a stress value of 48.5 ksi is obtained. This is the value of stress used to obtain the  $S$  value used for

comparison purposes in Figure A-36. Had the true average stress value of 44.8 ksi been used the correlation would have been even better.

If an attempt is made to use a stress function which has a maximum value at the center of the membrane and approaches zero in the corners, the discrepancies between computer results and test results will decrease.

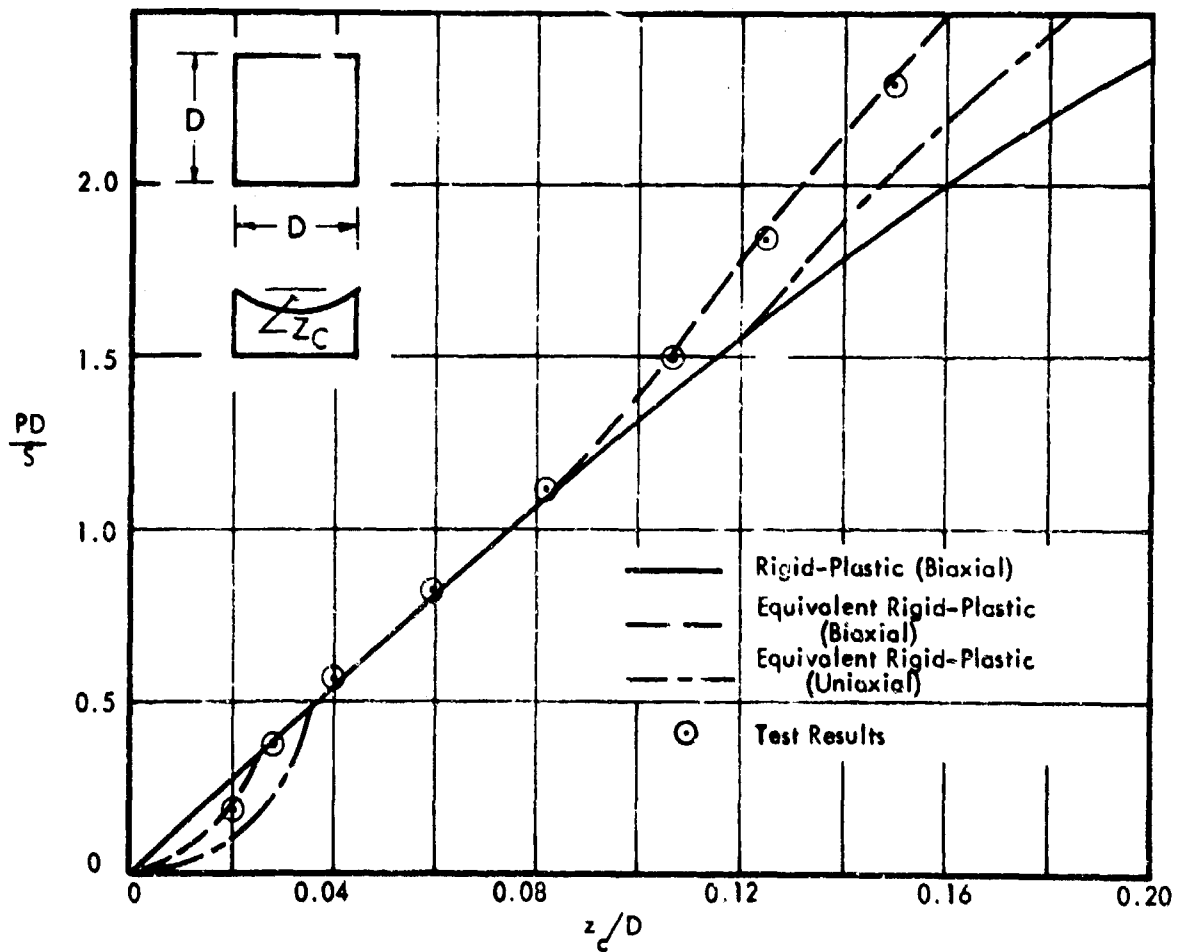


Figure A-27. Comparison of Computer and Test Results - Square Membrane,  $z_c, 9$

TABLE 13  
 Computer Results and Test Results - Square Membrane  
 (Points  $z_{9,9}$ ,  $z_{5,9}$ ,  $z_{5,5}$ )

Computer Results							Test Results			
$\frac{PD}{S}$	$\frac{z_{9,9}}{D}$	$\frac{z_{5,9}}{D}$	$\frac{z_{5,5}}{D}$	% Strain Across Center	Biaxial Stress $\sigma_n$	$\frac{\sigma_n}{\sigma_c} \frac{PD}{S}$	$\frac{PD}{S_c}$	$\frac{z_{9,9}}{D}$	$\frac{z_{5,9}}{D}$	$\frac{z_{5,5}}{D}$
0.25	.0184	.0143	.0112	0.0956	25.5	0.15	0.20	.0207	.0173	.0142
0.50	.0369	.0288	.0227	0.3853	41.3	0.50	0.37	.0278	.0229	.0194
0.75	.0558	.0435	.0343	0.8769	41.4	0.75	0.56	.0414	.0330	.0264
1.00	.0750	.0586	.0463	1.5829	42.8	1.03	0.81	.0594	.0470	.0384
1.25	.0948	.0744	.0587	2.5235	44.4	1.34	1.14	.0828	.0660	.0532
1.50	.1155	.0909	.0718	3.7278	47.0	1.71	1.49	.1060	.0842	.0674
1.75	.1372	.1085	.0858	5.2413	49.5	2.10	1.85	.1265	.1010	.0804
2.00	.1604	.1275	.1010	7.1248	51.5	2.49	2.23	.1480	.1190	.0936
2.25	.1856	.1485	.1178	9.4662	52.8	2.88				
2.50	.2135	.1722	.1370	12.4226	-	-				

$\sigma_c = 41.3 \text{ ksi} = \text{Equivalent Plastic Stress}$

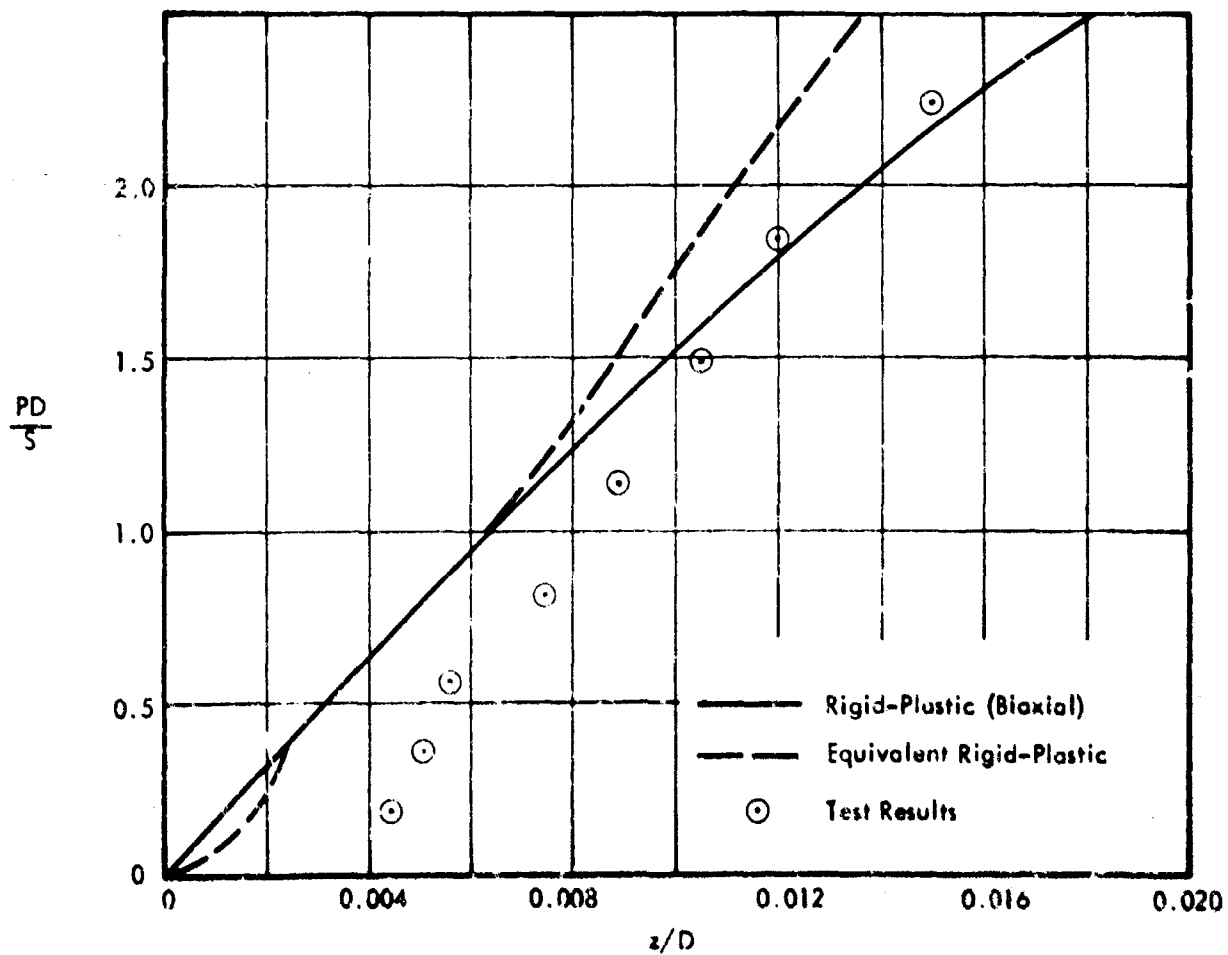


Figure A-28. Comparison of Computer and Test Results - Square Membrane,  $z_{7,2}$

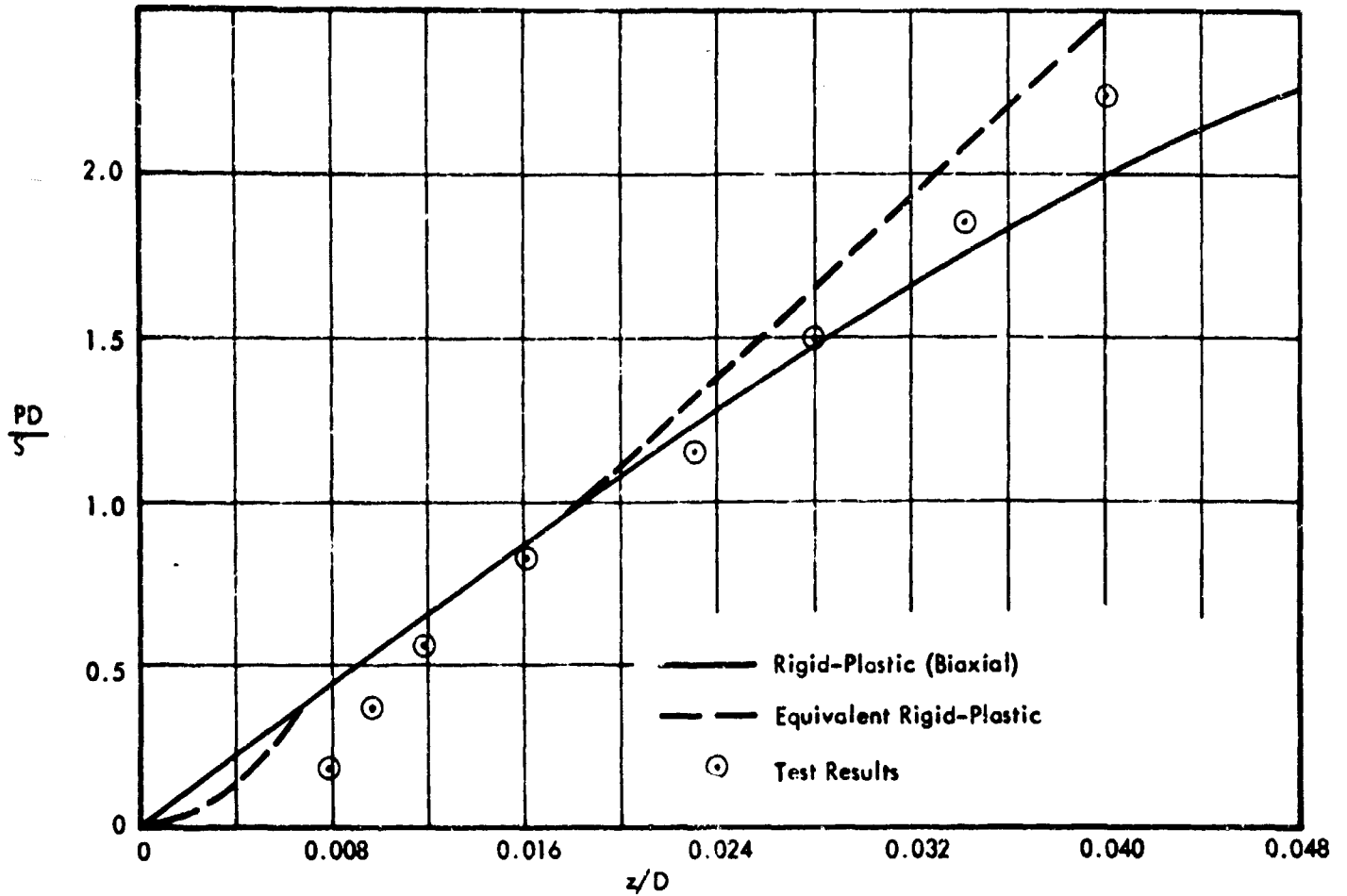


Figure A-29. Comparison of Computer and Test Results - Square Membrane,  $z_{3,3}$

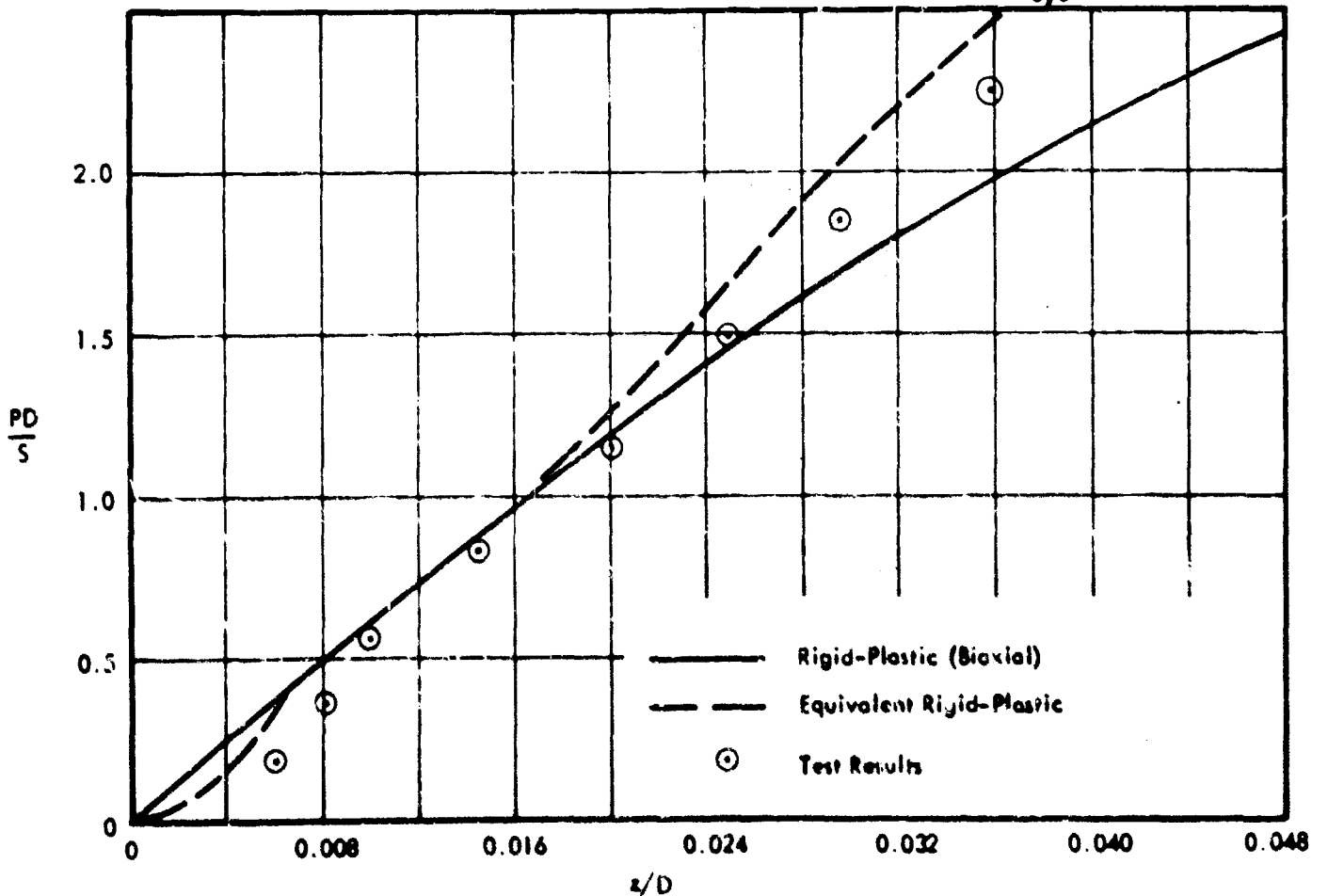


Figure A-30. Comparison of Computer and Test Results - Square Membrane,  $z_{5,2}$

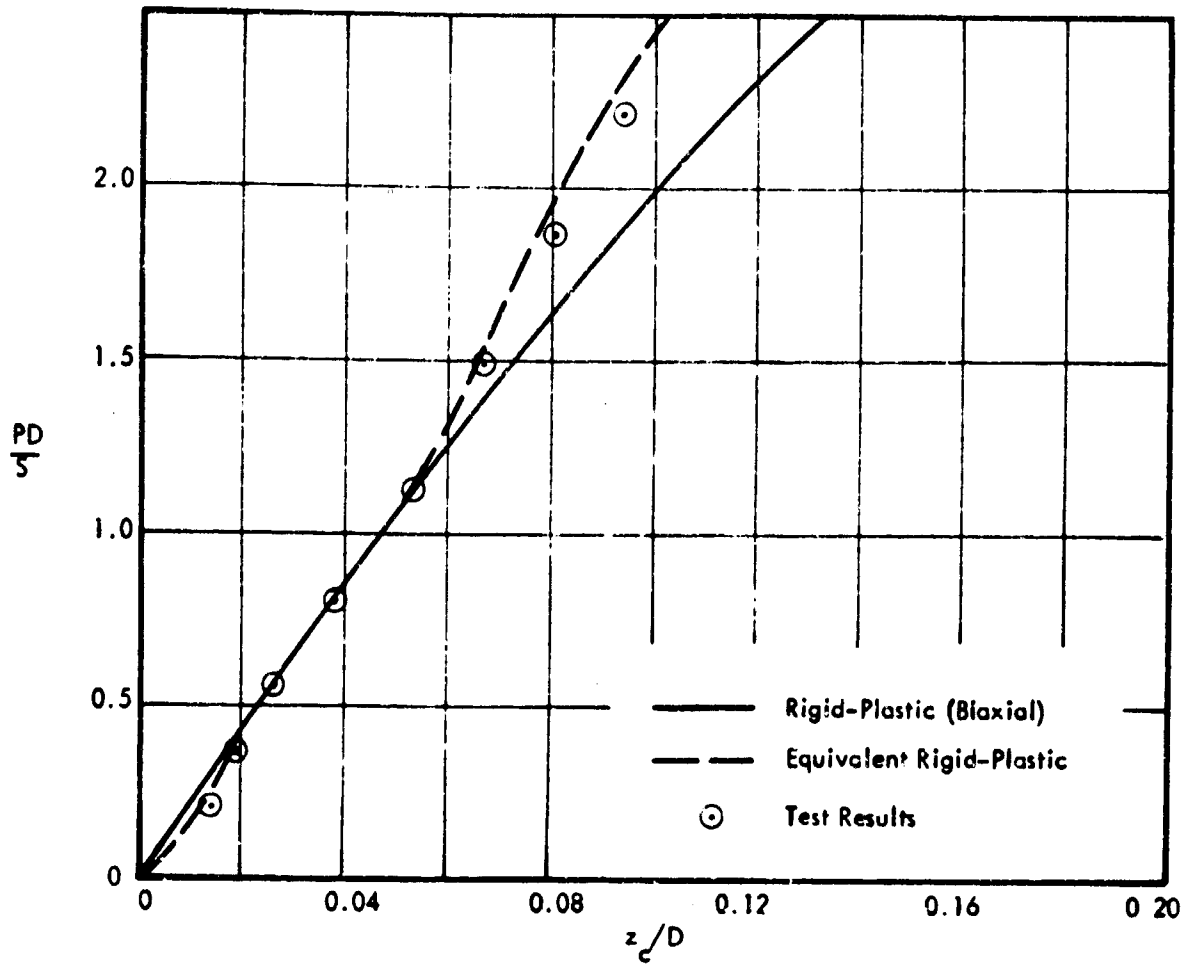


Figure A-31. Comparison of Computer and Test Results - Square Membrane,  $z_{5,5}$

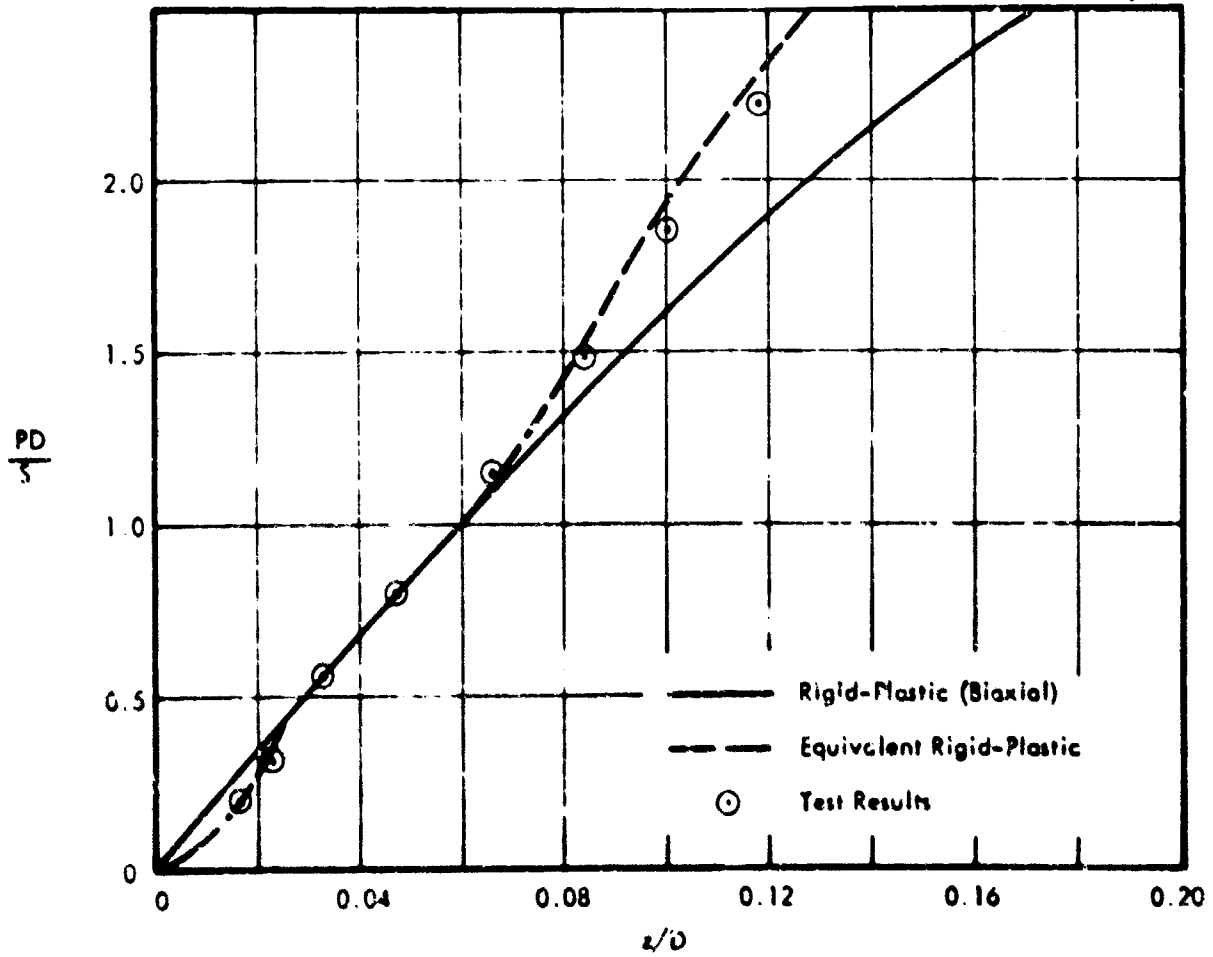


Figure A-32. Comparison of Computer and Test Results - Square Membrane,  $z_{5,9}$

TABLE 14  
 Computer Results and Test Results (Points  $z_{9,9}$ ,  $z_{5,9}$ ,  
 $z_{9,5}$  and  $z_{5,5}$ ) - 1.5 x 1 Membrane

Computer Results								Test Results				
$\frac{PD}{S}$	$\frac{z_{9,9}}{D}$	$\frac{z_{5,9}}{D}$	$\frac{z_{9,5}}{D}$	$\frac{z_{5,5}}{D}$	% Strain Across Center	Biaxial Stress $\sigma_n$	$\frac{\sigma_n}{\sigma_c} \frac{PD}{S}$	$\frac{PD}{S_c}$	$\frac{z_{9,9}}{D}$	$\frac{z_{5,9}}{D}$	$\frac{z_{9,5}}{D}$	$\frac{z_{5,5}}{D}$
0.25	.0252	.0192	.0205	.0157	0.172	41.3	0.25	0.067	.0158	.0115	.0130	.0102
0.50	.0507	.0386	.0412	.0317	0.696	41.3	0.50	0.249	.0253	.0199	.0222	.0180
0.75	.0767	.0587	.0625	.0482	1.593	42.8	0.78	0.410	.0390	.0308	.0322	.0252
1.00	.1033	.0798	.0845	.0653	2.902	45.0	1.09	0.619	.0592	.0450	.0489	.0378
1.25	.1322	.1022	.1077	.0836	4.686	48.8	1.48	0.911	.0878	.0684	.0724	.0560
1.50	.1627	.1269	.1327	.1034	7.054	51.4	1.87	1.240	.1163	.0907	.0967	.0758
1.75	.1940	.1545	.1600	.1255	10.161	53.0	2.24	1.568	.1400	.1090	.1158	.097
2.00	.2335	.1864	.1910	.1509	14.272	-	-	1.845	.1596	.1250	.1335	.1050
2.25	.2774	.2252	.2275	.1815	19.872	-	-					
2.50	.3324	.2756	.2737	.2214	27.993							

$\sigma_c = 41.3 \text{ ksi} = \text{Equivalent Plastic Stress}$

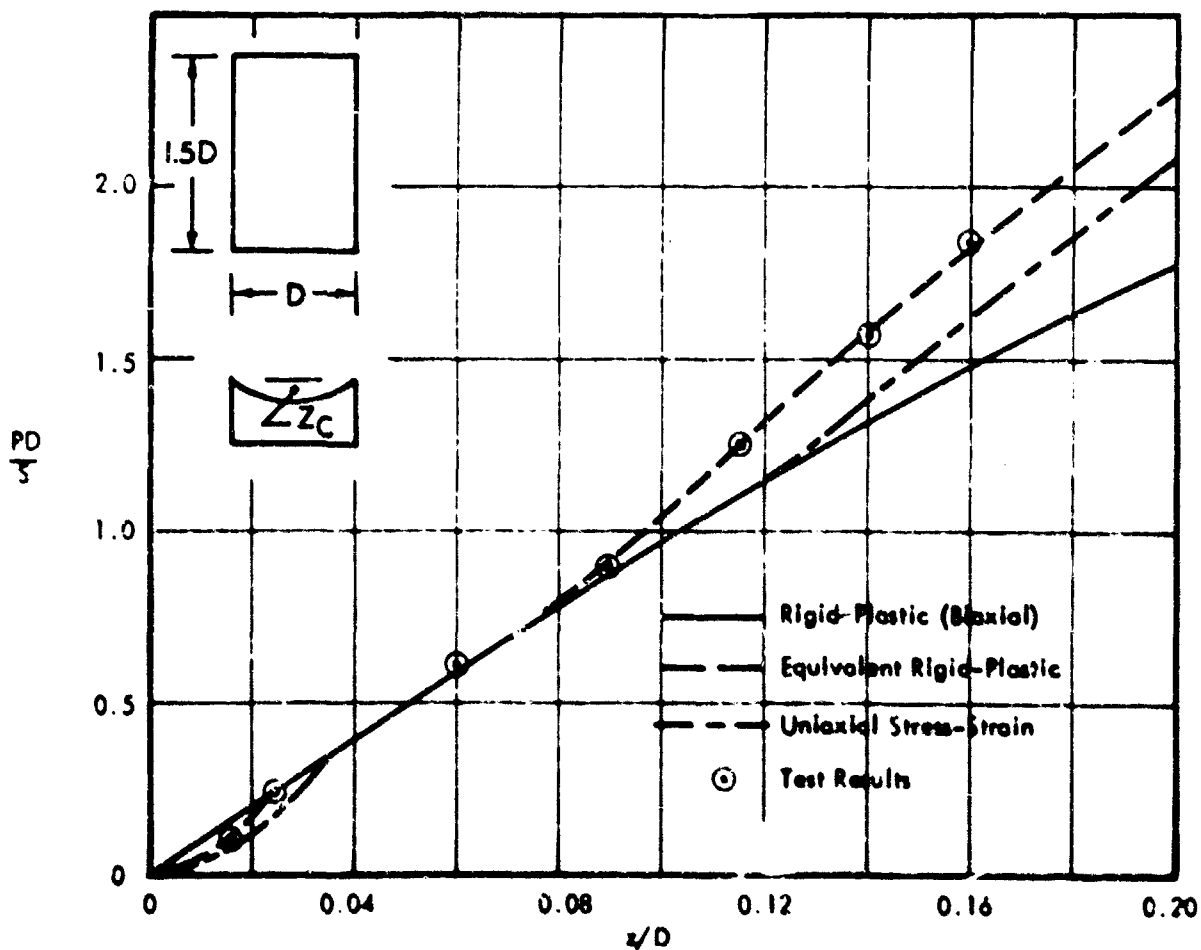


Figure A-33. Comparison of Computer and Test Results - 1.5 x 1 Membrane,  $z_{9,9}$

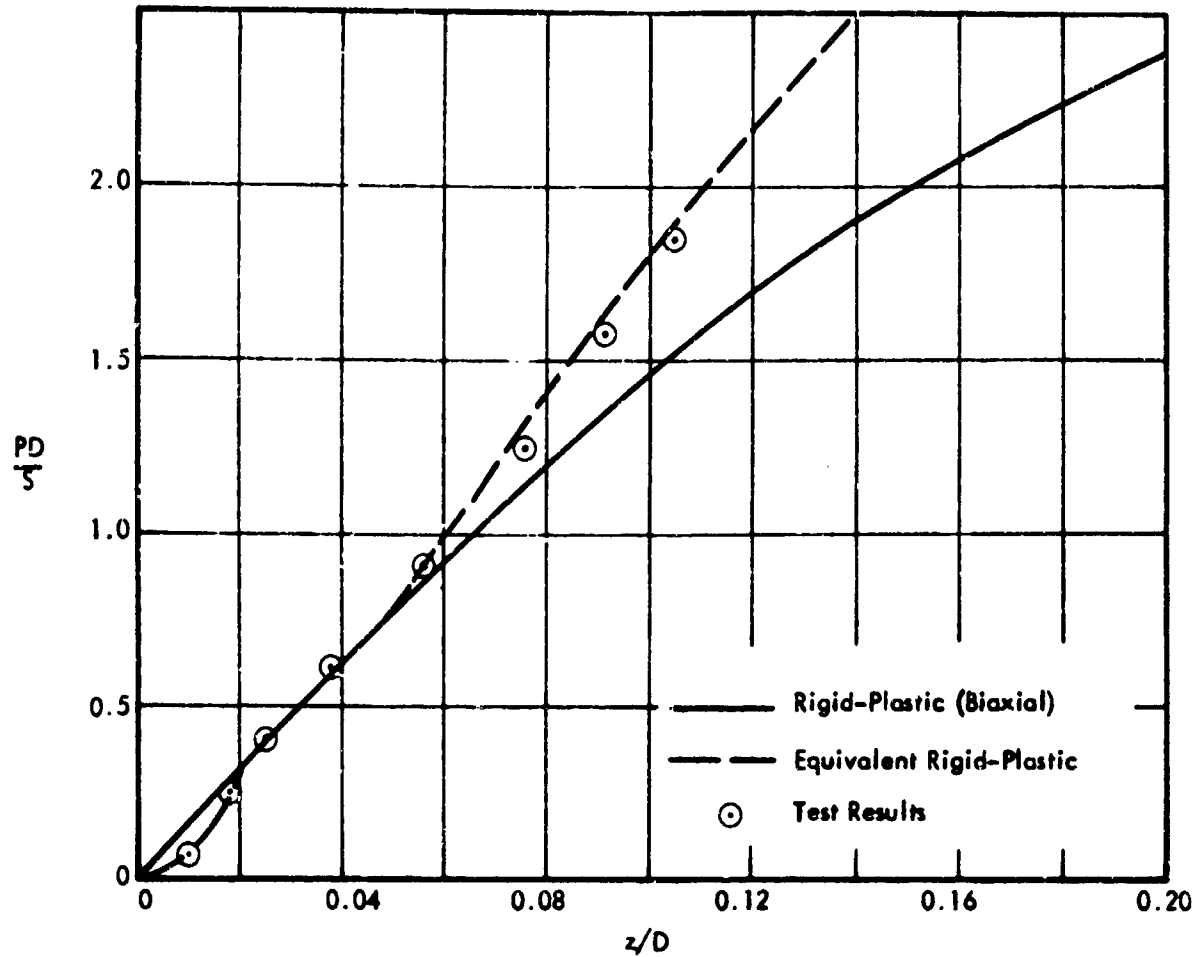


Figure A-34. Comparison of Computer and Test Results - 1.5 x 1 Membrane,  $z_{5,5}$

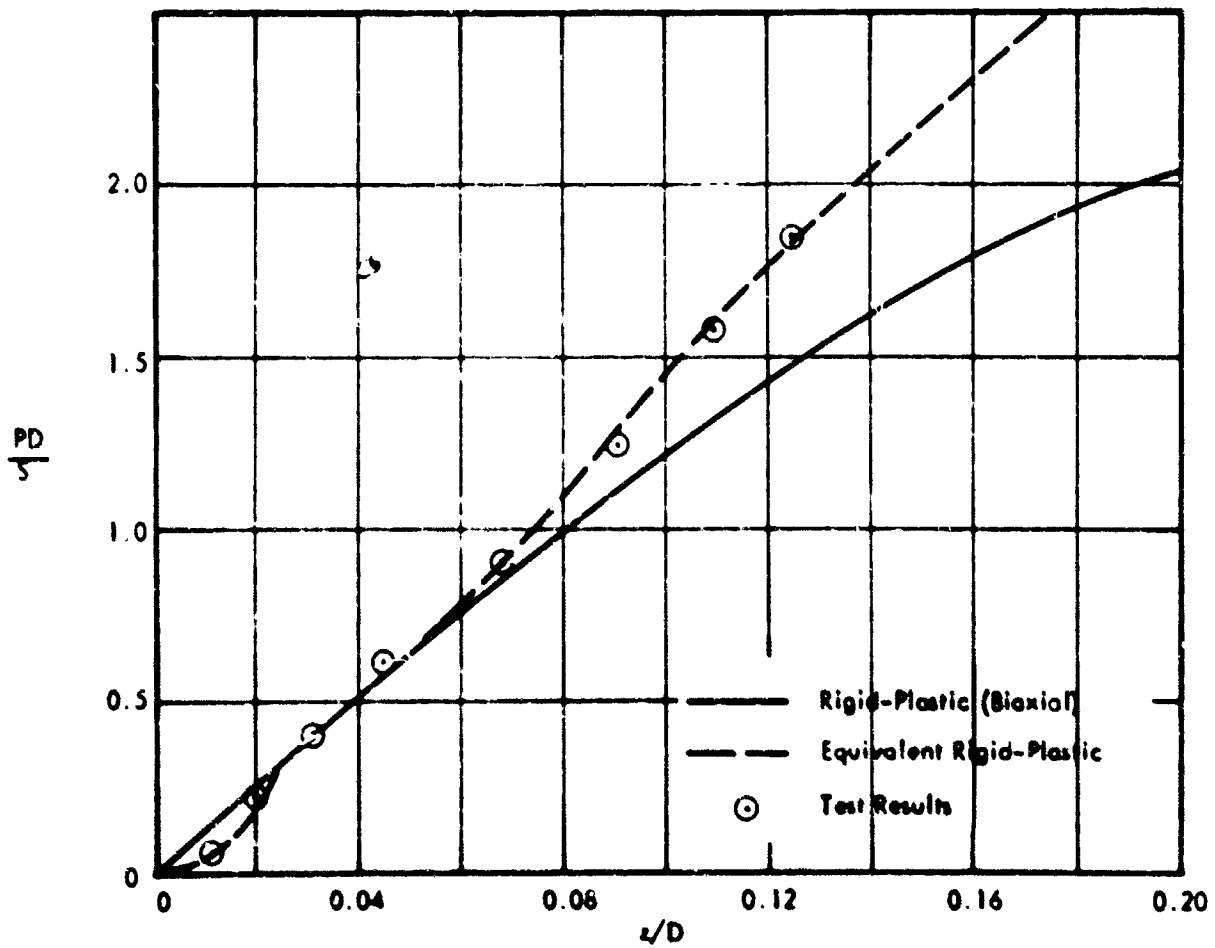


Figure A-35. Comparison of Computer and Test Results - 1.5 x 1 Membrane,  $z_{5,9}$

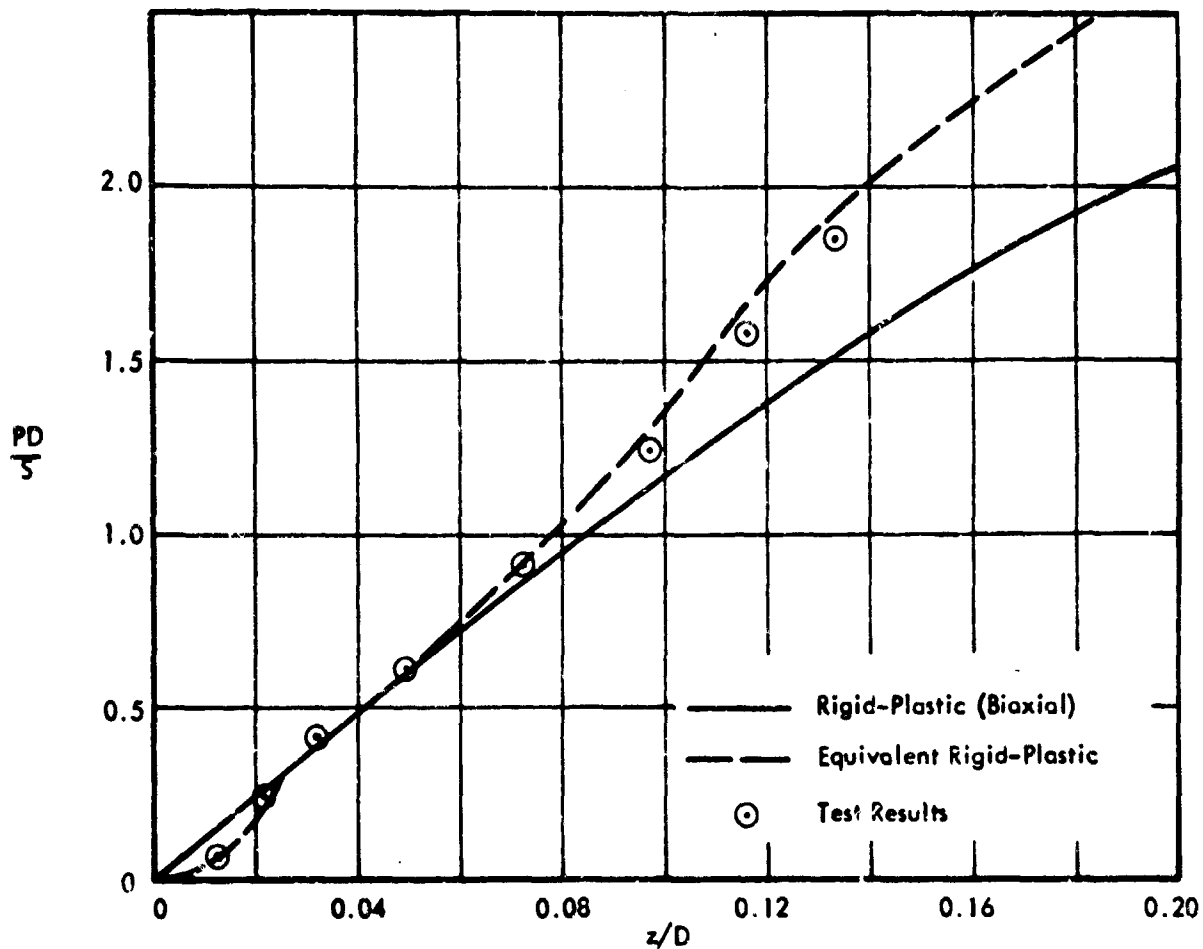


Figure A-36. Comparison of Computer and Test Results - 1.5 x 1 Membrane,  $z_{9,5}$

TABLE 15  
Computer Results and Test Results (Points  $z_{9,9}$ ,  $z_{5,9}$ ,  
 $z_{9,5}$ , and  $z_{5,5}$ ) - 2 x 1 Membrane

Computer Results								Test Results				
$\frac{PD}{S}$	$\frac{z_{9,9}}{D}$	$\frac{z_{5,9}}{D}$	$\frac{z_{9,5}}{D}$	$\frac{z_{5,5}}{D}$	% Strain Across Center	Biaxial Stress $\sigma_n$	$\frac{\sigma_n}{\sigma_c} \frac{PD}{S}$	$\frac{PD}{S_c}$	$\frac{z_{9,9}}{D}$	$\frac{z_{5,9}}{D}$	$\frac{z_{9,5}}{D}$	$\frac{z_{5,5}}{D}$
0.25	.0285	.0216	.0243	.0816	0.218	41.3	0.25	0.062	.0181	.0137	.0172	.0129
0.50	.0573	.0434	.0488	.0373	0.880	41.4	0.50	0.126	.0220	.0174	.0208	.0167
0.75	.0872	.0663	.0741	.0568	2.028	43.4	0.79	0.250	.0304	.0235	.0273	.0219
1.00	.1187	.0909	.1007	.0775	3.739	47.0	1.14	0.522	.0604	.0462	.0515	.0397
1.25	.1525	.1177	.1290	.0998	6.135	50.5	1.53	0.868	.0909	.0757	.0853	.0662
1.50	.1899	.1483	.1602	.1240	9.431	52.7	1.91	1.150	.1250	.0953	.1085	.0838
1.75	.2327	.1845	.1954	.1538	13.997	-	-	1.555	.1565	.1200	.1395	.1069
2.00	.2840	.2295	.2372	.1889	20.493	-	-	-	-	-	-	-
2.25	.3517	.2919	.2919	.2368	30.688	-	-	-	-	-	-	-
2.50	-	-	-	-	-	-	-	-	-	-	-	-

$\sigma_c = 41.3 \text{ ksi} = \text{Equivalent Plastic Stress}$

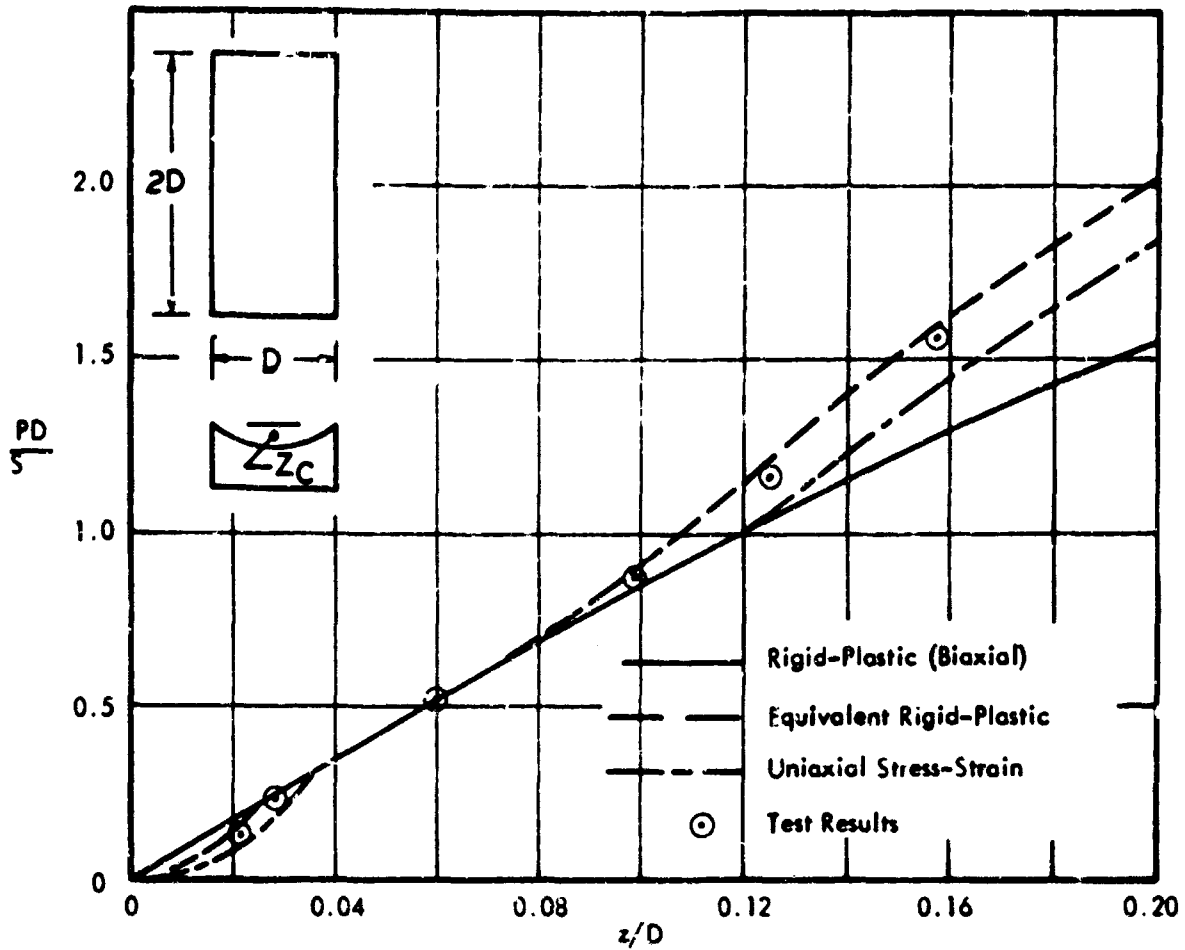


Figure A-37. Comparison of Computer and Test Results - 2 x 1 Membrane,  $z_{9,9}$

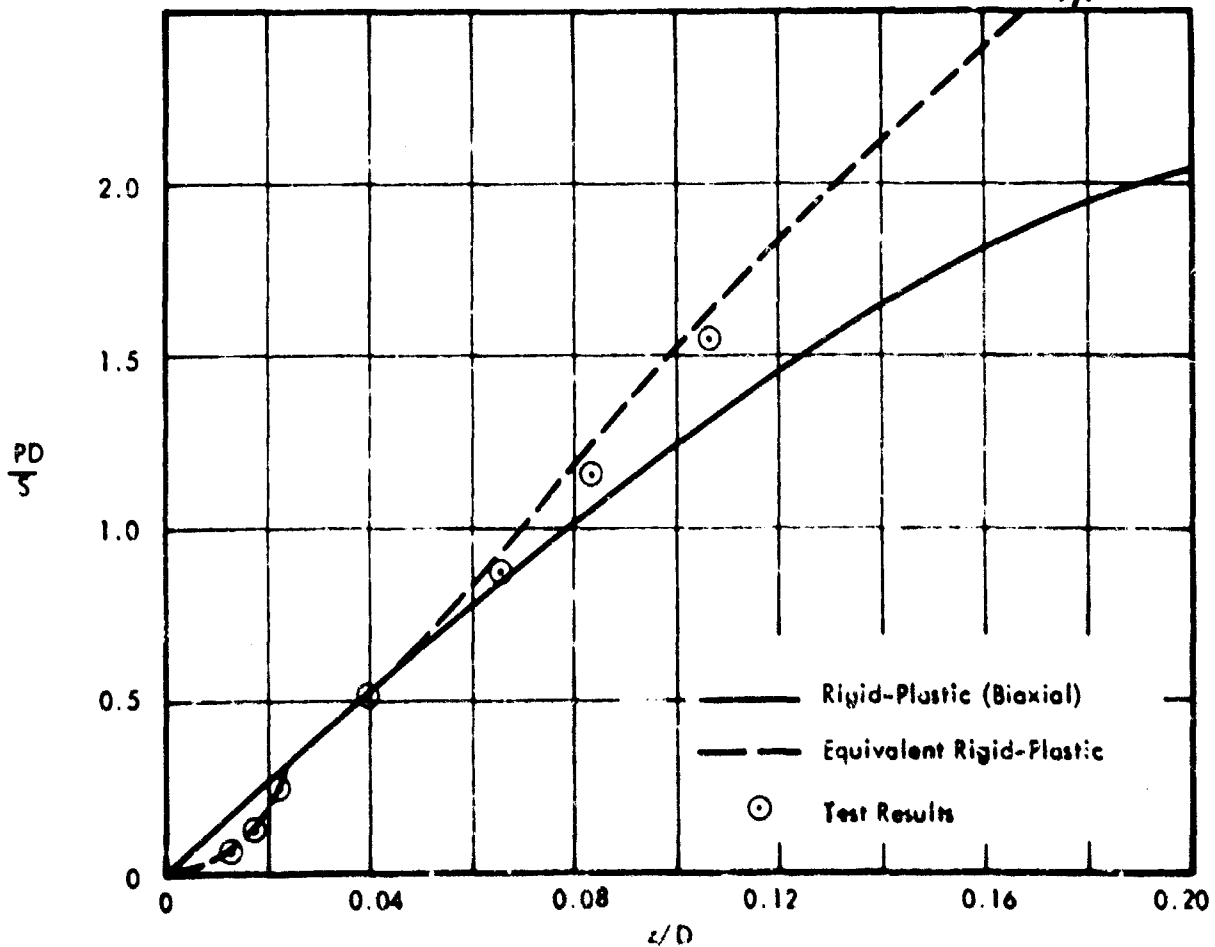


Figure A-38. Comparison of Computer and Test Results - 2 x 1 Membrane,  $z_{5,5}$

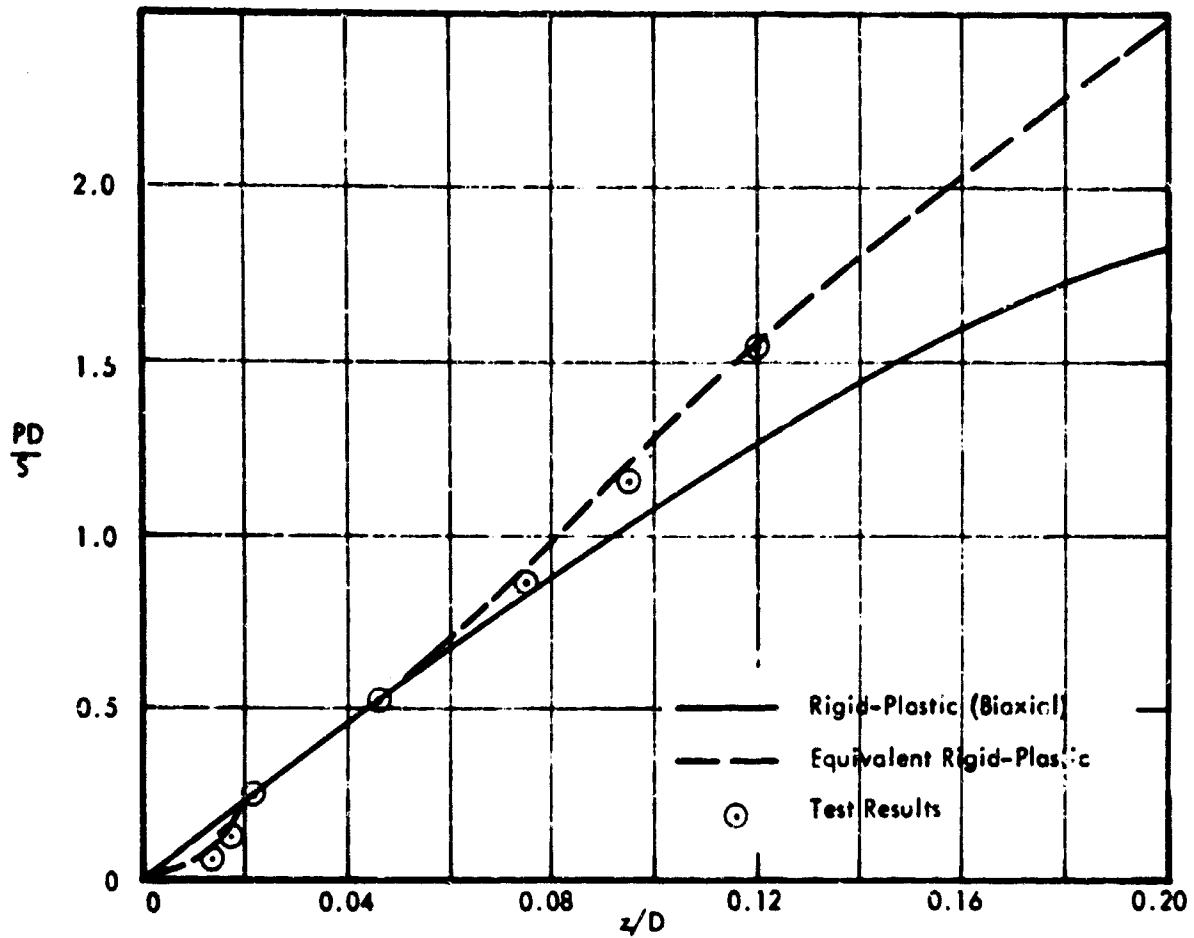


Figure A-39. Comparison of Computer and Test Results - 2 x 1 Membrane,  $z_{5,9}$

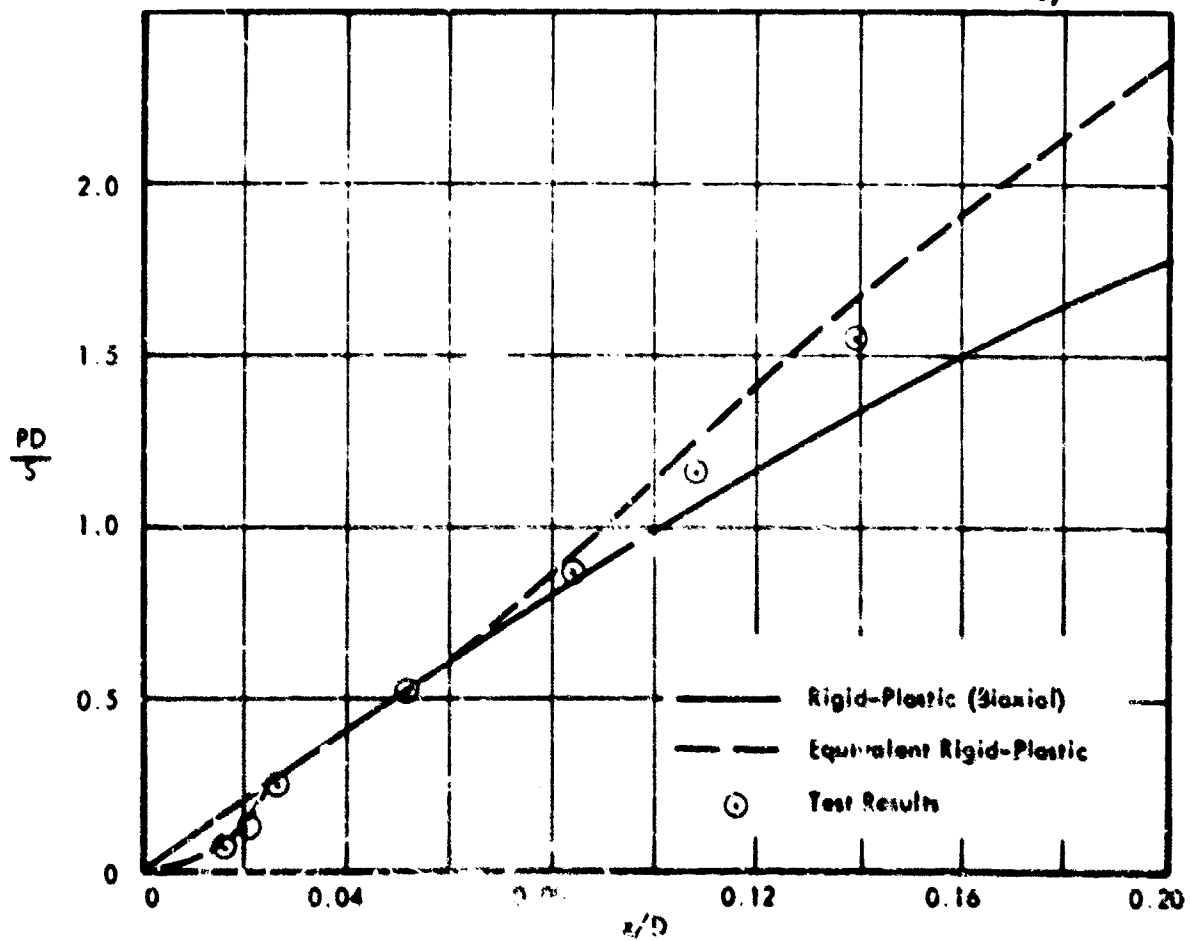


Figure A-40. Comparison of Computer and Test Results - 2 x 1 Membrane,  $z_{9,5}$

Test = Upper  
Computer = Lower

$$\frac{z_{\max}}{D} = 0.1265 \quad \frac{PD}{S} = 1.5777 \quad P = 30.6 \text{ psi}$$

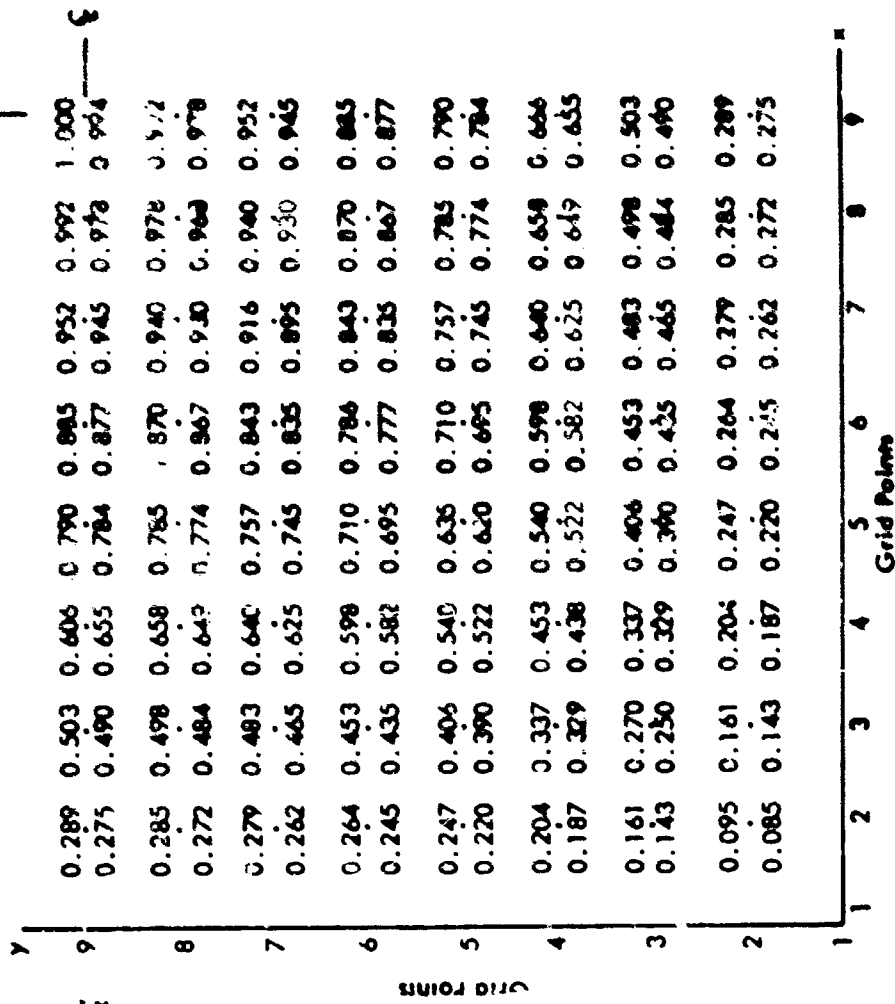


Figure A-42. Comparison of Results -  $z/z_{\max}$  for Square Membrane with Clamped Edges,  $z_{\max}/D = 0.1265$

Test = Upper  
Computer = Lower

$$\frac{z_{\max}}{D} = 0.0594 \quad \frac{PD}{S} = 0.805 \quad P = 13.37 \text{ psi}$$

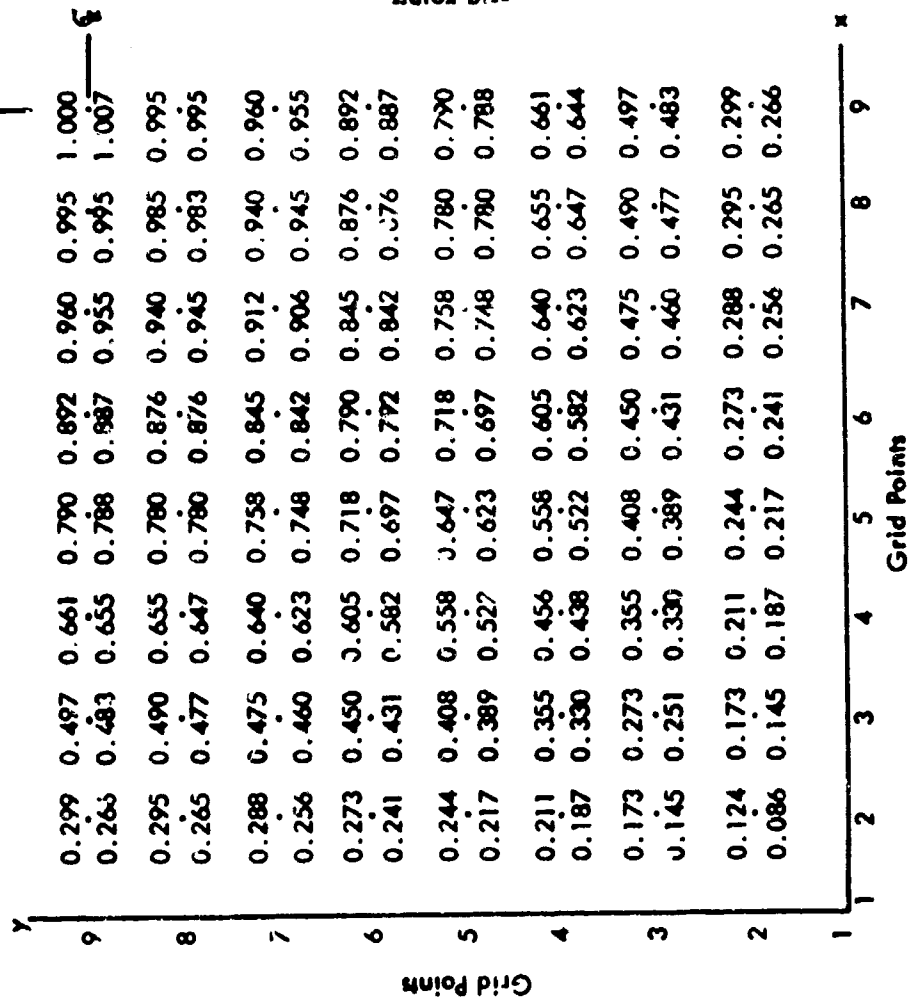


Figure A-41. Comparison of Results -  $z/z_{\max}$  for Square Membrane with Clamped Edges,  $z_{\max}/D = 0.0594$

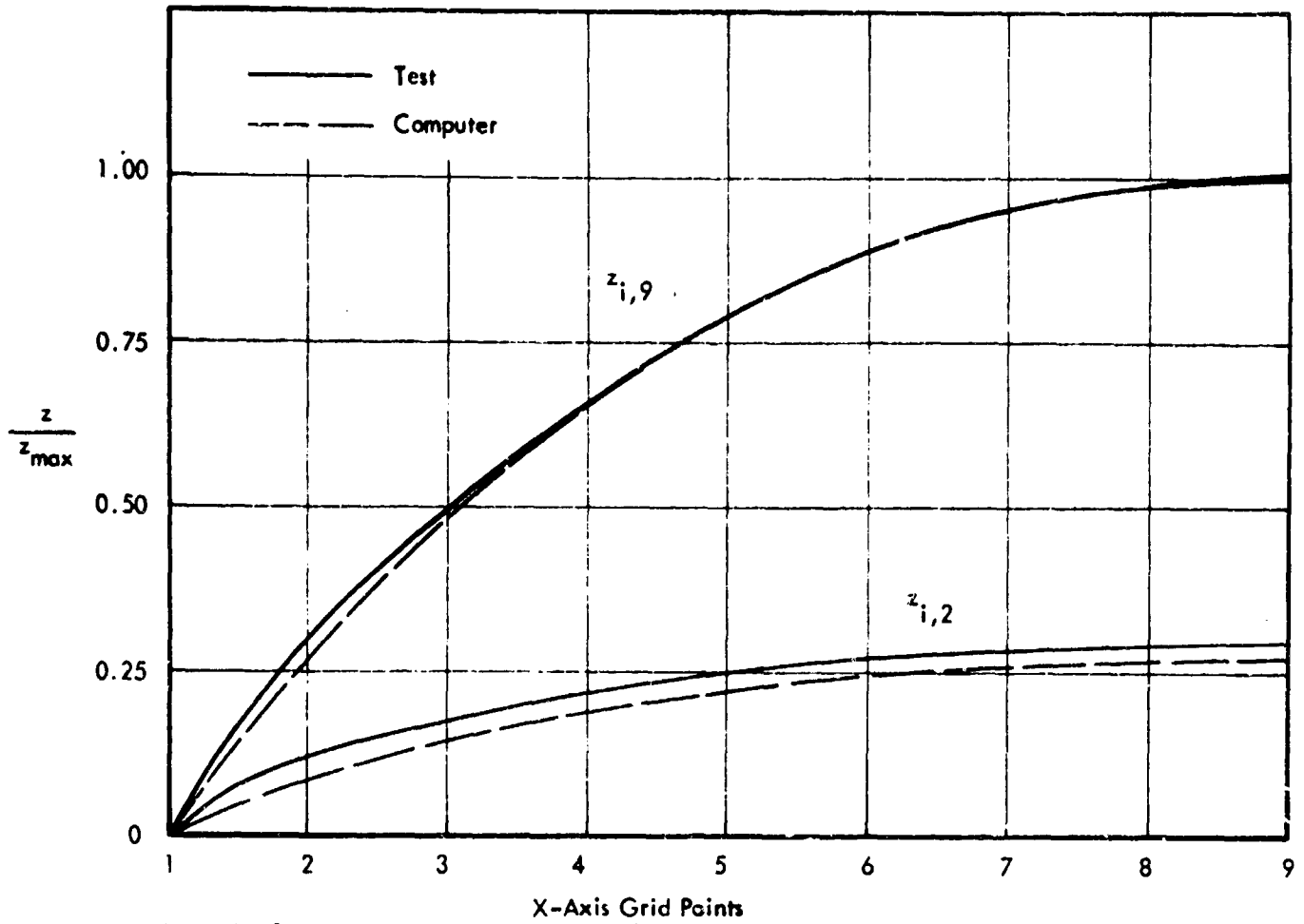


Figure A-43. Cross-Sections - Square Membrane with Clamped Edges,  $z_{\max}/D = 0.0594$

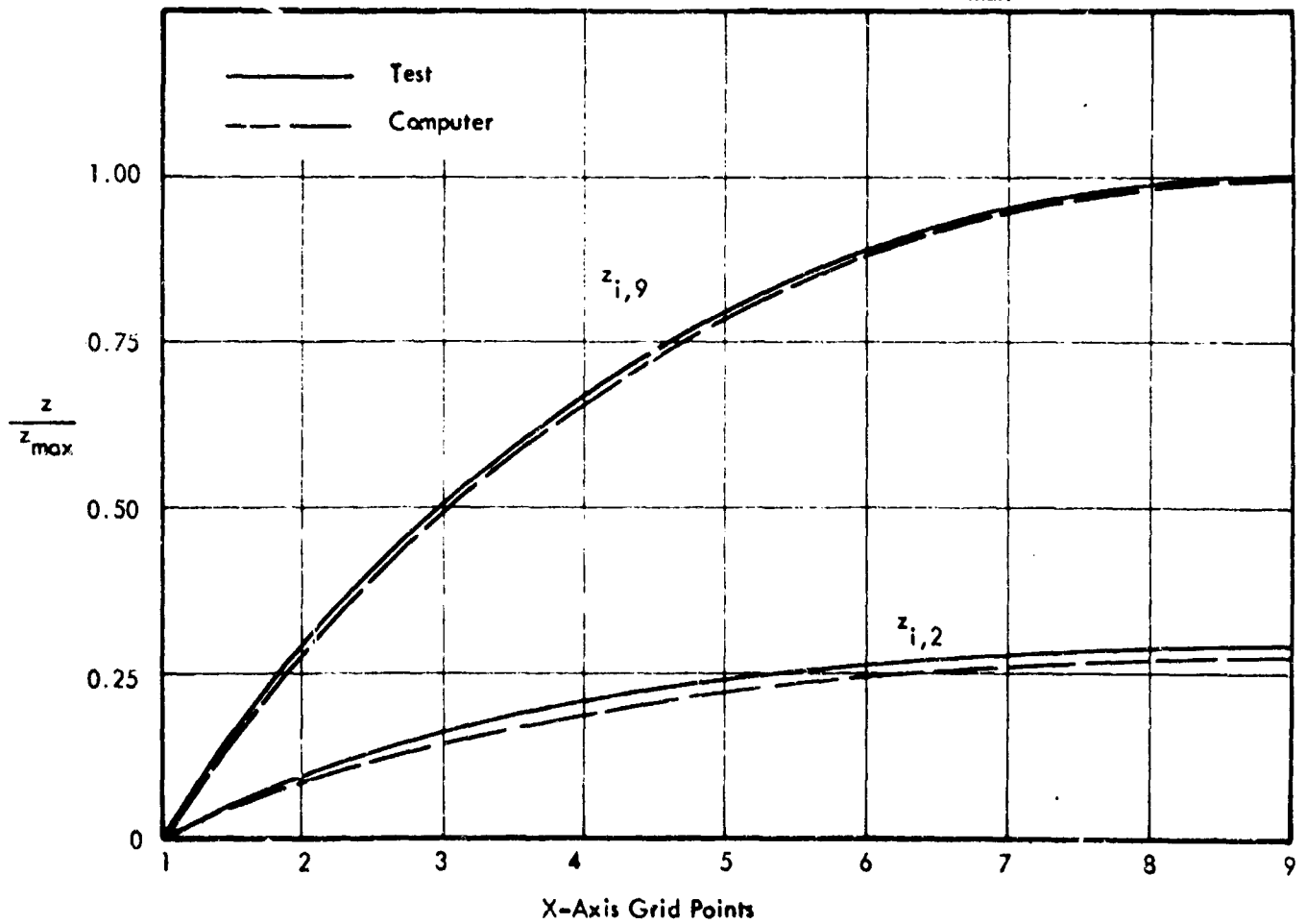


Figure A-44. Cross-Sections - Square Membrane with Clamped Edges,  $z_{\max}/D = 0.1265$

Test = Upper  
Computer = Lower

$$\frac{F}{SD} = 0.86$$

$$\frac{z_{max}}{D} = 0.0575$$

$$\frac{PD}{S} = 0.691$$

$$P = 11.5 \text{ psi}$$

$$\epsilon$$

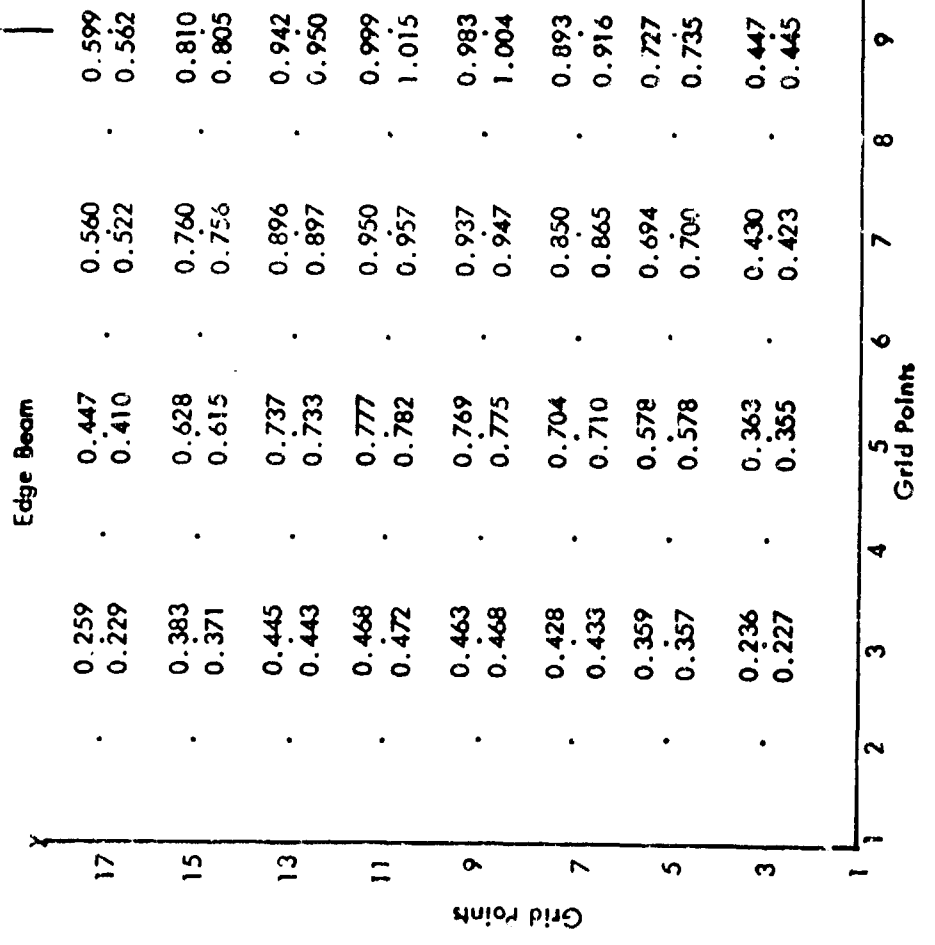


Figure A-45. Comparison of Results -  $z/z_{max}$  for Square Membrane with One Yielding Beam,  $z_{max}/D = 0.0575$

Test = Upper  
Computer = Lower

$$\frac{F}{SD} = 0.852$$

$$\frac{z_{max}}{D} = 0.0937$$

$$\frac{PD}{S} = 1.10$$

$$P = 18.60 \text{ psi}$$

$$\epsilon$$

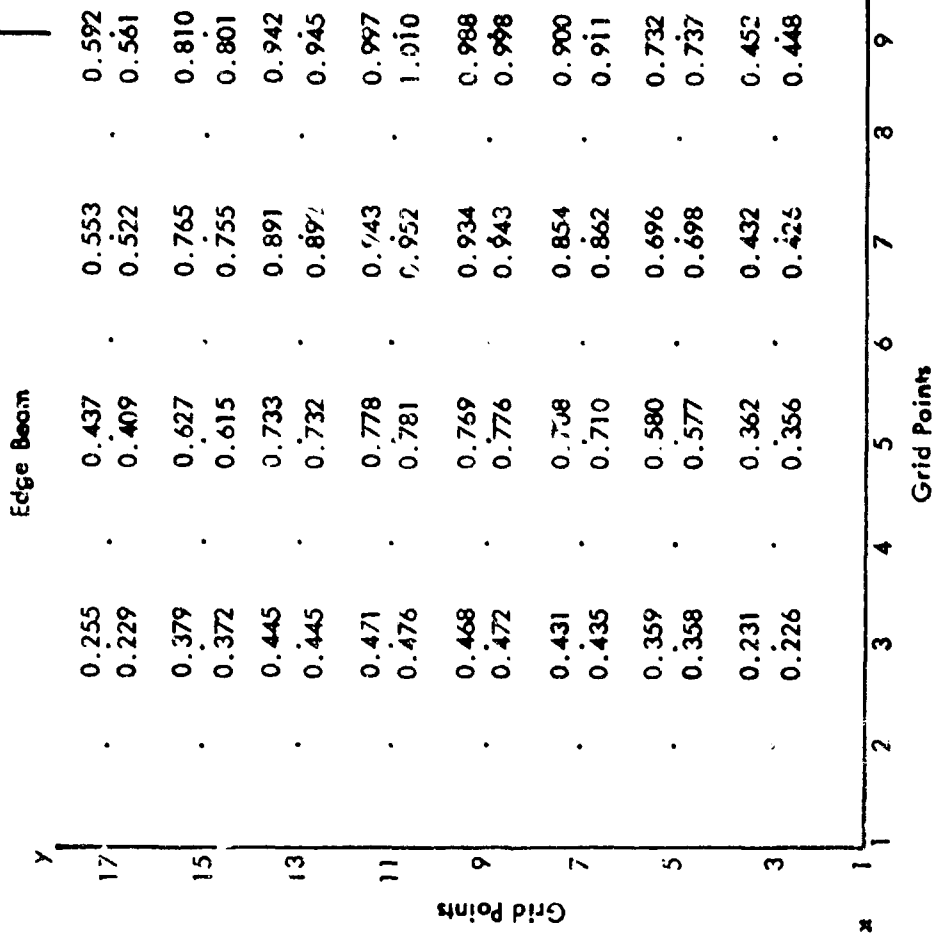


Figure A-46. Comparison of Results -  $z/z_{max}$  for Square Membrane with One Yielding Beam,  $z_{max}/D = 0.0937$

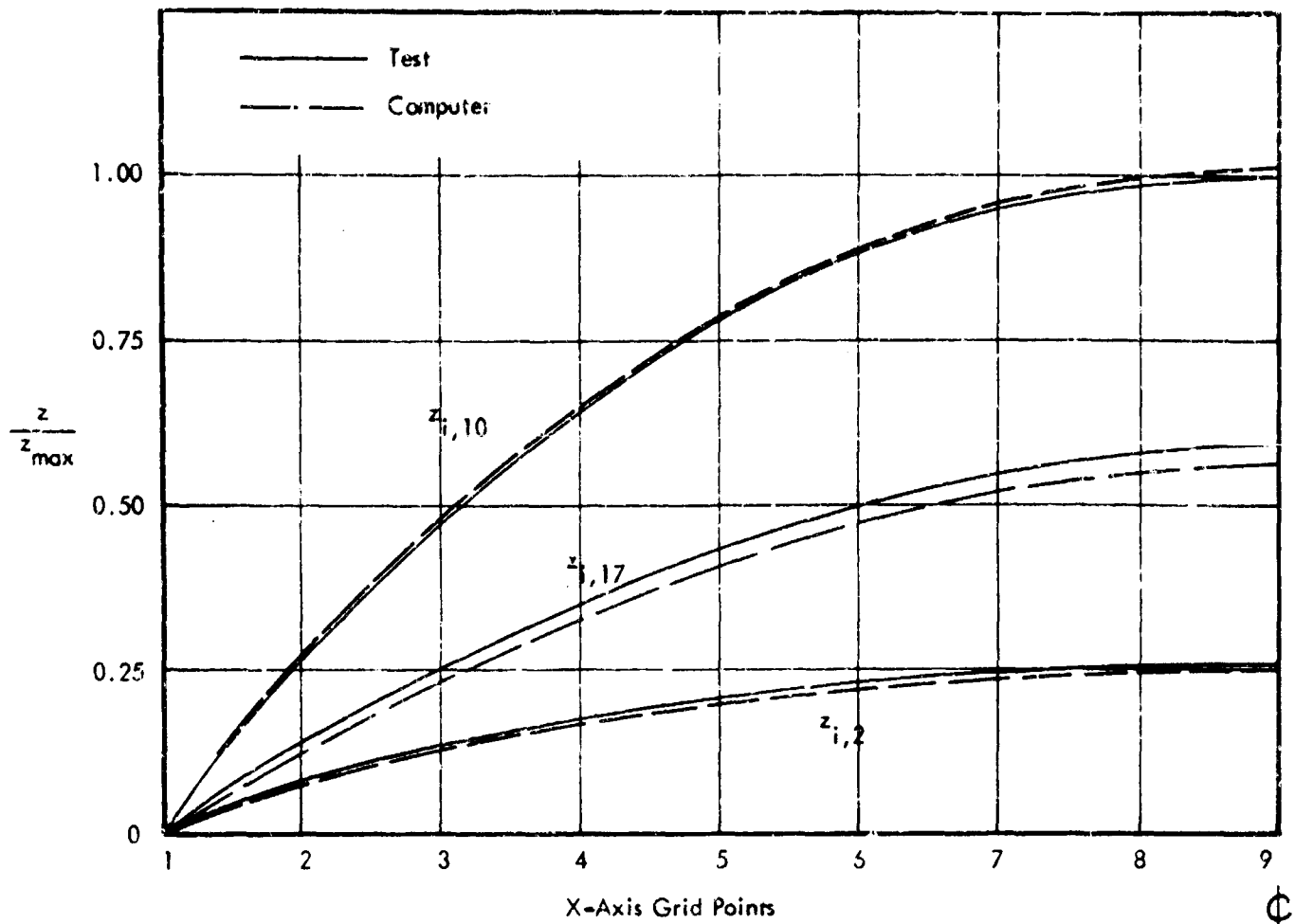


Figure A-47. Cross-Sections - Square Membrane with One Yielding Beam,  $z_{\max}/D = 0.0937$  (Parallel to X-Axis)

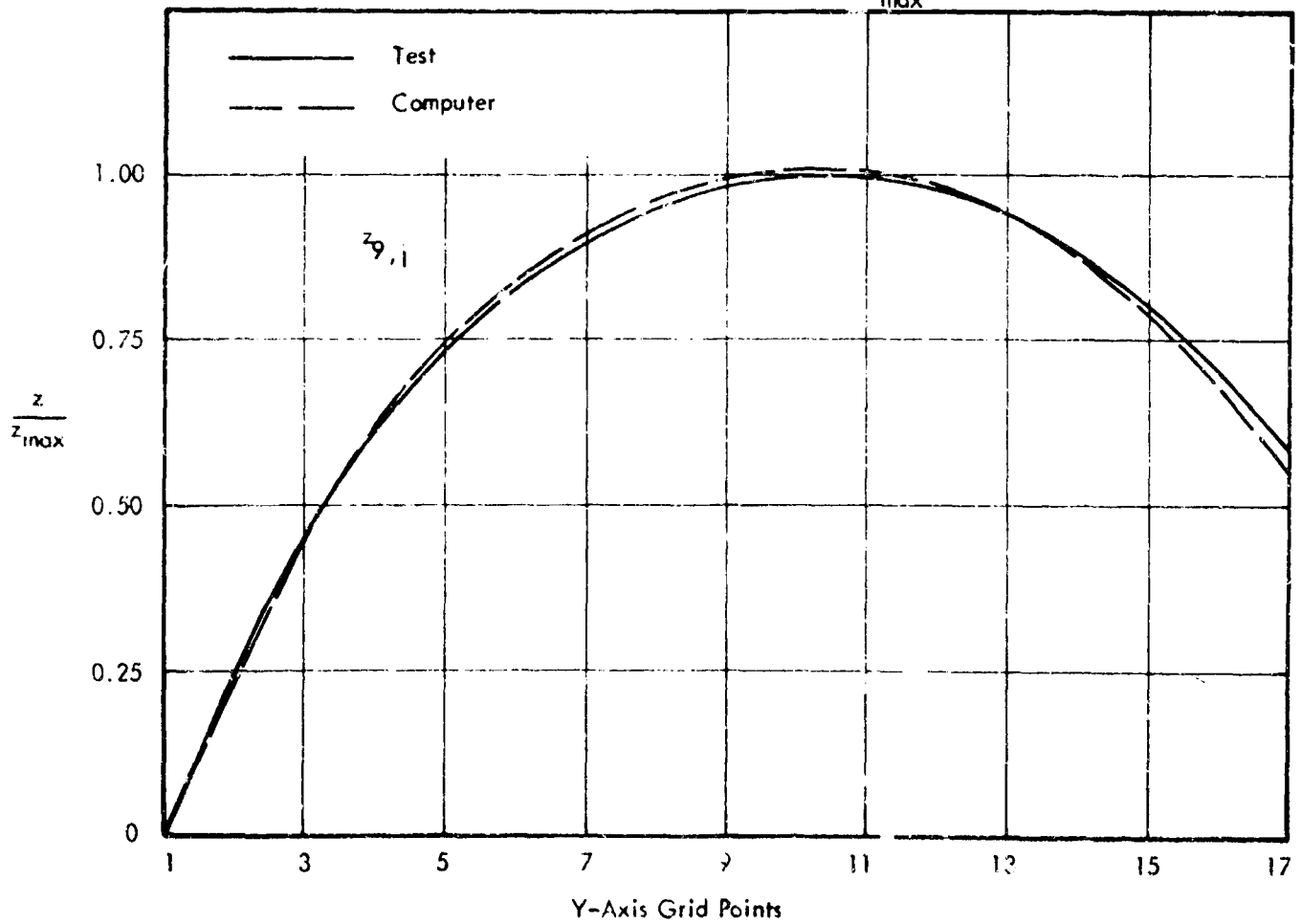


Figure A-48. Cross-Sections - Square Membrane with One Yielding Beam,  $z_{\max}/D = 0.0937$  (Parallel to Y-Axis)

Test = Upper

Computer = Lower

$$\frac{F}{SD} = 0.837$$

$$\frac{z_{\max}}{D} = 0.1243$$

$$\frac{PD}{S} = 1.483$$

$$P = 25.80 \text{ psi}$$

Grid Points	Y	Edge Beam	z
17	0.256	0.445	0.597
	0.242	0.432	0.590
15	0.389	0.635	0.816
	0.393	0.645	0.836
13	0.452	0.740	0.948
	0.473	0.767	0.986
11	0.474	0.781	0.995
	0.506	0.823	1.050
9	0.469	0.771	0.967
	0.502	0.813	0.985
7	0.437	0.712	0.907
	0.460	0.745	0.950
5	0.363	0.585	0.740
	0.378	0.607	0.771
3	0.232	0.367	0.454
	0.238	0.375	0.473

Test = Upper

Computer = Lower

$$\frac{F}{SD} = 1.70$$

$$\frac{z_{\max}}{D} = 0.065$$

$$\frac{PD}{S} = 2.075$$

$$P = 17.12 \text{ psi}$$

Grid Points	Y	Edge Beam	z
17	0.228	0.402	0.555
	0.176	0.335	0.467
15	0.358	0.545	0.710
	0.285	0.494	0.647
13	0.380	0.626	0.803
	0.338	0.580	0.748
11	0.398	0.660	0.840
	0.357	0.612	0.782
9	0.395	0.653	0.814
	0.350	0.597	0.762
7	0.360	0.592	0.735
	0.319	0.538	0.681
5	0.303	0.488	0.592
	0.260	0.431	0.538
3	0.210	0.303	0.360
	0.161	0.260	0.319

Figure A-49. Comparison of Results -  $z/z_{\max}$  for Square Membrane with One Yielding Beam,  $z_{\max}/D = 0.1243$

Figure A-50. Comparison of Results - Square Membrane with Yielding Beams on Two Adjacent Edges,  $z_{\max}/D = 0.065$



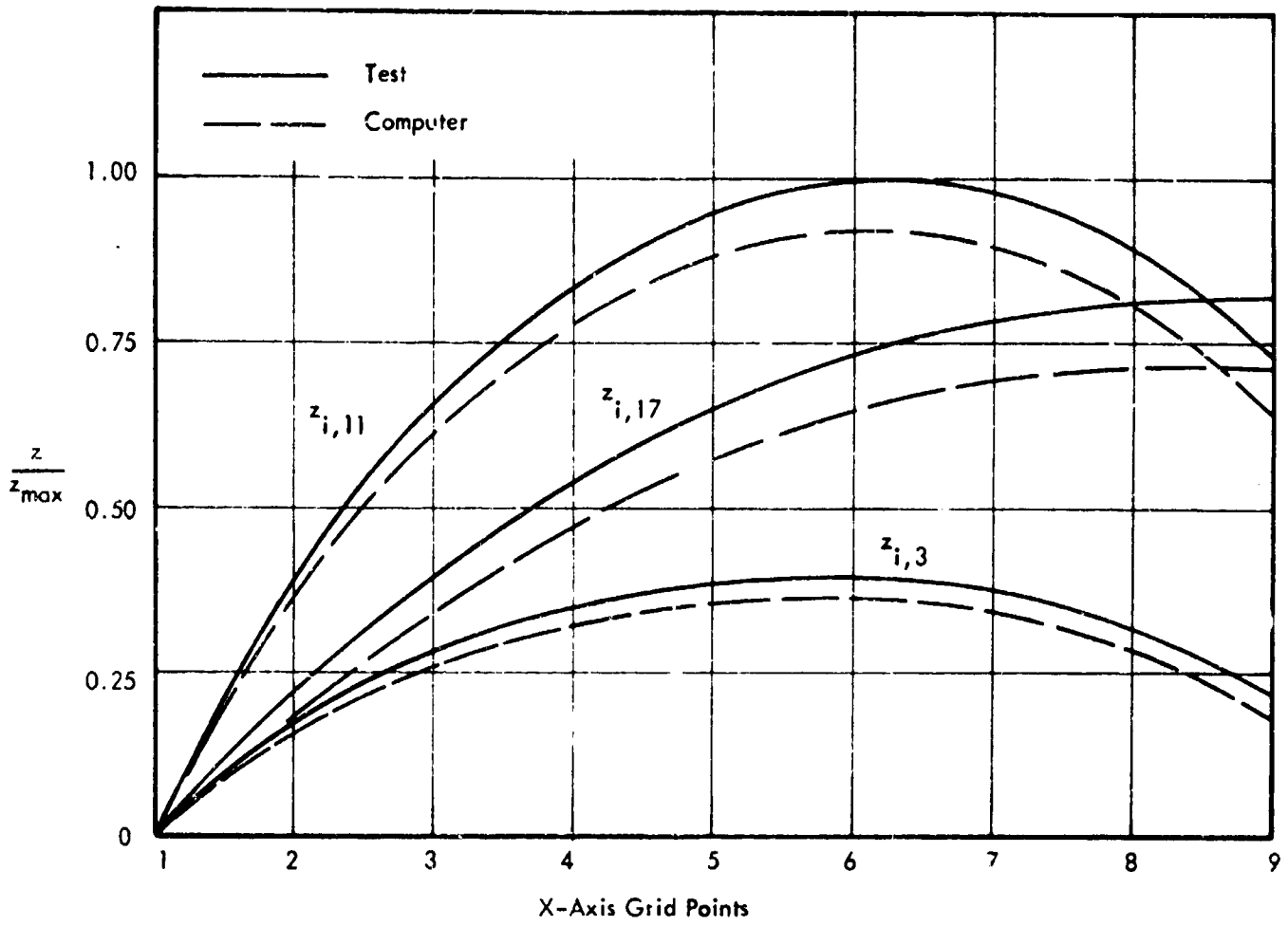


Figure A-53. Cross-Sections - Square Membrane with Yielding Beams on Two Adjacent Edges,  $\frac{z_{\max}}{D} = 0.1522$

## APPENDIX B

### YIELDING MEMBRANE PROGRAM

#### Abstract

This Appendix presents a computer program for iterative solution of the large deflection membrane equation using finite differences. An investigation of relaxation factors at various  $P_3/S$  ratios and grid sizes is included. Graphs are given showing the relationship between strain in the membrane,  $P_3/S$  ratios and center deflections.

Modifications of the basic program are given which allow variation of pressure across the entire membrane, use of Poisson's Equation, inclusion of plastic beams across the membrane along the center lines, and creating free edges with or without plastic beams.

#### Introduction

The equation defining the shape a membrane takes when loaded with pressures large enough to cause deformations, in excess of those allowed by small deflection theory, defies solution by means usually employed for equations of this type. The equation is distinctively nonlinear, involving products and powers of partial derivatives. The method of solution presented here consists of defining the partial derivatives in the equation in terms of finite differences, and iterating the resulting equation to obtain a description of the surface. An over-relaxation procedure is used to speed the iterative process. The iteration procedure involves a long and tedious process and may be accomplished only through use of high speed digital computers. Therefore, the procedure presented here is programmed in basic Fortran computer language.

#### Mathematical Formulation of the Problem

Consider a typical element of surface (Figure B-1).  $\xi_1$  and  $\xi_2$  are general curvilinear coordinates, which, when combined with the position vector,  $\bar{r}$ , describe the surface completely.  $n$  is the normal to the surface at the point. Then the general equation for the principal curvatures  $k_n$  of the surface as developed by Wang\* is:

$$H^2 k_n^2 - (EN - 2FM + GL)k_n + (LN - M^2) = 0 \quad (1)$$

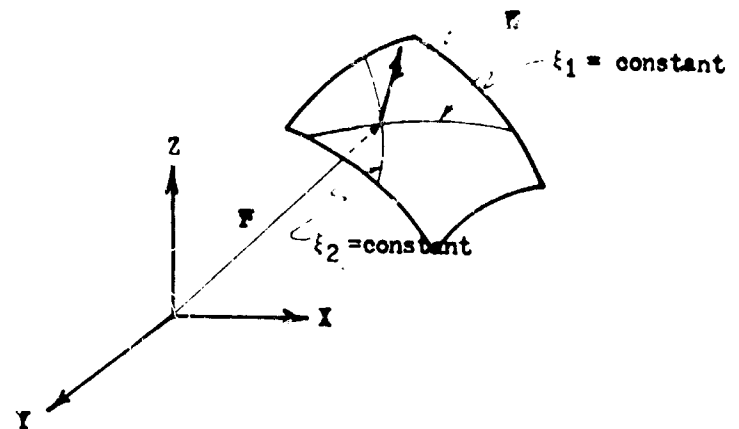


Figure B-1. Typical Element of Surface

Solving this equation for  $k_1$  and  $k_2$  by the quadratic formula:

$$k_{1,2} = \frac{EN - 2FM + GL + \sqrt{(EN - 2FM + GL)^2 - 4H(LN - M^2)}}{2H^2} \quad (2)$$

Where:

$$E = \left( \frac{\partial x}{\partial \xi_1} \right)^2 + \left( \frac{\partial y}{\partial \xi_1} \right)^2 + \left( \frac{\partial z}{\partial \xi_1} \right)^2 \quad (3-a)$$

$$F = \frac{\partial x}{\partial \xi_1} \frac{\partial x}{\partial \xi_2} + \frac{\partial y}{\partial \xi_1} \frac{\partial y}{\partial \xi_2} + \frac{\partial z}{\partial \xi_1} \frac{\partial z}{\partial \xi_2} \quad (3-b)$$

$$G = \left( \frac{\partial x}{\partial \xi_2} \right)^2 + \left( \frac{\partial y}{\partial \xi_2} \right)^2 + \left( \frac{\partial z}{\partial \xi_2} \right)^2 \quad (3-c)$$

$$H = \sqrt{EG - F^2} \quad (3-d)$$

\* C. T. Wang, Applied Elasticity, McGraw-Hill, New York, 1953.

$$L = \bar{n} \cdot \frac{\partial^2 \bar{F}}{\partial \xi_1^2} \quad (3-e)$$

$$M = \bar{n} \cdot \frac{\partial^2 \bar{F}}{\partial \xi_1 \partial \xi_2} \quad (3-f)$$

$$N = \bar{n} \cdot \frac{\partial^2 \bar{F}}{\partial \xi_2^2} \quad (3-g)$$

If we choose for our generalized coordinates  $\xi_1 = x$  and  $\xi_2 = y$ , equations (3) become:

$$E = 1 + \left( \frac{\partial z}{\partial x} \right)^2 \quad (4-a)$$

$$F = \frac{\partial z}{\partial x} \frac{\partial z}{\partial y} \quad (4-b)$$

$$G = 1 + \left( \frac{\partial z}{\partial y} \right)^2 \quad (4-c)$$

$$H = \sqrt{1 + \left( \frac{\partial z}{\partial x} \right)^2 + \left( \frac{\partial z}{\partial y} \right)^2} \quad (4-d)$$

$$L = \frac{\frac{\partial^2 z}{\partial x^2}}{H} \quad (4-e)$$

$$M = \frac{\frac{\partial^2 z}{\partial x \partial y}}{H} \quad (4-f)$$

$$N = \frac{\frac{\partial^2 z}{\partial y^2}}{H} \quad (4-g)$$

The five equations developed by Wang defining the equilibrium of the element in Figure B-1 reduce to a single equation if all of the stress resultants except  $N_1$  and  $N_2$  are assumed zero. For this stress condition to exist only normal loads may be considered as shown in Figure B-2. Let  $R_1$  and  $R_2$  be the principal radii of curvature, then the equation of equilibrium of the element is:

$$\frac{N_1}{R_1} + \frac{N_2}{R_2} = 0$$

If we let  $N_1 = N_2 = S = \text{a constant}$ , this equation becomes:

$$\frac{1}{R_1} + \frac{1}{R_2} = - \frac{p_3}{S}$$

In terms of principal curvatures this becomes:

$$k_1 + k_2 = - \frac{p_3}{S}$$

From equation (2) we see that:

$$k_1 + k_2 = \frac{\Delta N - 2FM + GL}{H^2}$$

Substituting equations (4) in this equation:

$$k_1 + k_2 = \frac{\left[ 1 + \left( \frac{\partial z}{\partial x} \right)^2 \right] \frac{\partial^2 z}{\partial x^2} - 2 \left( \frac{\partial z}{\partial x} \right) \left( \frac{\partial z}{\partial y} \right) \frac{\partial^2 z}{\partial x \partial y} + \left[ 1 + \left( \frac{\partial z}{\partial y} \right)^2 \right] \frac{\partial^2 z}{\partial y^2}}{\left[ \left( \frac{\partial z}{\partial x} \right)^2 + \left( \frac{\partial z}{\partial y} \right)^2 + 1 \right]^{3/2}}$$

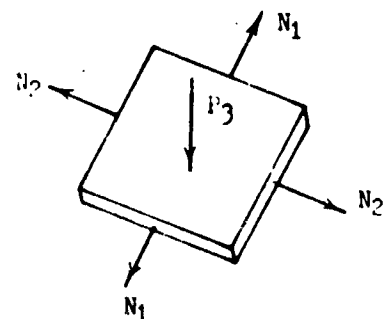


Figure B-2. Element Under Stress

Substituting this expression into equation (5) we arrive at the final equations describing the surface of a membrane under a pressure loading  $p_3$ .

$$\left[1 + \left(\frac{\partial z}{\partial y}\right)^2\right] \frac{\partial^2 z}{\partial x^2} - 2 \frac{\partial z}{\partial x} \frac{\partial z}{\partial y} \frac{\partial^2 z}{\partial x \partial y} + \left[1 + \left(\frac{\partial z}{\partial x}\right)^2\right] \frac{\partial^2 z}{\partial y^2} = - \frac{p_3}{s} \left[1 + \left(\frac{\partial z}{\partial x}\right)^2 + \left(\frac{\partial z}{\partial y}\right)^2\right]^{3/2} \quad (6)$$

The finite difference expressions for the partial derivatives in equation (6) are:

$$\frac{\partial z}{\partial x} = \frac{z_{1,j+1} - z_{1,j-1}}{2\lambda_x} \quad (7-a)$$

$$\frac{\partial z}{\partial y} = \frac{z_{1+1,j} - z_{1-1,j}}{2\lambda_y} \quad (7-b)$$

$$\frac{\partial^2 z}{\partial x^2} = \frac{z_{1,j+1} - z_{1,j} + z_{1,j-1}}{\lambda_x^2} \quad (7-c)$$

$$\frac{\partial^2 z}{\partial x \partial y} = \frac{z_{1+1,j+1} - z_{1-1,j+1} - z_{1+1,j-1} + z_{1-1,j-1}}{4\lambda_x \lambda_y} \quad (7-d)$$

$$\frac{\partial^2 z}{\partial y^2} = \frac{z_{1+1,j} - z_{1,j} + z_{1-1,j}}{\lambda_y^2} \quad (7-e)$$

Substituting these in equation (6) and reducing we find:

$$(4\lambda_x^2 + A^2)C - \frac{1}{2} ABE + (4\lambda_y^2 + B^2)D + \frac{p_3}{s} \frac{1}{2\lambda_x \lambda_y} (4\lambda_x^2 \lambda_y^2 + \lambda_x^2 B^2 + \lambda_y^2 A^2)^{3/2} = 0 \quad (8)$$

Where:

$$A = (z_{1,j+1} - z_{1,j-1}) \quad (9-a)$$

$$B = (z_{1+1,j} - z_{1-1,j}) \quad (9-b)$$

$$C = (z_{1+1,j} - z_{1,j} + z_{1-1,j}) \quad (9-c)$$

$$D = (z_{1,j+1} - z_{1,j} + z_{1,j-1}) \quad (9-d)$$

$$E = (z_{1+1,j+1} - z_{1-1,j+1} - z_{1+1,j-1} + z_{1-1,j-1}) \quad (9-e)$$

$\lambda_x$  = grid size parallel to the X axis

$\lambda_y$  = grid size parallel to the Y axis

If equation (8) is satisfied by the correct value of  $Z_{i,j}$ , the identity will hold. However, through the iterative process the correct value of  $Z_{i,j}$  are not known and equation (8) is not equal to zero but rather to some value  $f$  which approaches zero as the values of  $Z_{i,j}$  approach their correct values.

This suggests the following relaxation scheme:

$$Z_{i,j} \text{ (new)} = Z_{i,j} \text{ (old)} - \Phi \frac{f \text{ (old)}}{\frac{\partial f \text{ (old)}}{\partial Z_{i,j}}} \quad (10)$$

Where:

$\Phi$  = over-relaxation factor

$$\frac{\partial f \text{ (old)}}{\partial Z_{i,j}} = -2(4\lambda_x^2 + A^2 + 4\lambda_y^2 + B^2)$$

### Discussion of the Computer Program

Figure B-3 defined the various parameters used in this program to describe the physical dimensions of the membrane. Because the pressure is assumed constant over the surface, symmetry can be used and only one-quarter of the membrane need be computed.

A series of trials was made to determine the optimum relaxation factors that would give convergence in the least number of iterations. The trials were made at PD/S ratios of one and two (Figures B-4 and B-5). It should be noted that the relaxation factor is not critical for large grid spacing and low PD/S values but becomes increasingly critical as either PD/S rises or grid spacing decreases. There is little change in the relaxation factor with respect to the convergence limit CONVL; however, the number of iterations increase as the convergence limit decreases.

Figures B-6 and B-7 indicate that the error decreases sharply as the grid size decreases. Less than one percent error may be achieved with an 8 x 8 grid. These curves are for a square membrane and the "exact" values shown are from a 32 x 32 grid size with a convergence limit of CONVL = 0.0001. This was considered to be exact enough for the purposes of an error analysis. A 16 x 16 grid size with CONVL = 0.001 was used to obtain the computer PD/S versus  $x/D$  curves. It was found that minus signs appearing in the output column giving maximum change for each iteration indicate the relaxation factor is too high. The ideal relaxation factor was found to produce only one or two minus signs in this column.

The programs had numerous comment statements to aid in identification of the program components and the variables involved. It also had many additional features such as: initial values could be read in as data; all points could begin as zero; a limit on the number of iterations; a convergence limit (usually CONVL = 0.001 in.); a stop on the iterations if the center deflection became larger than one-half the span; and strain computed across the point of maximum deflection and along the yielding beams.

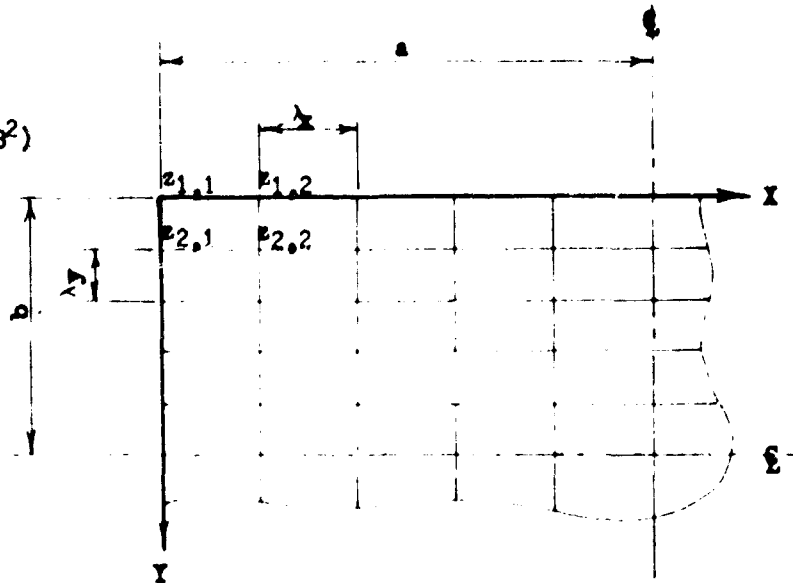


Figure B-3. One-quarter of the Membrane

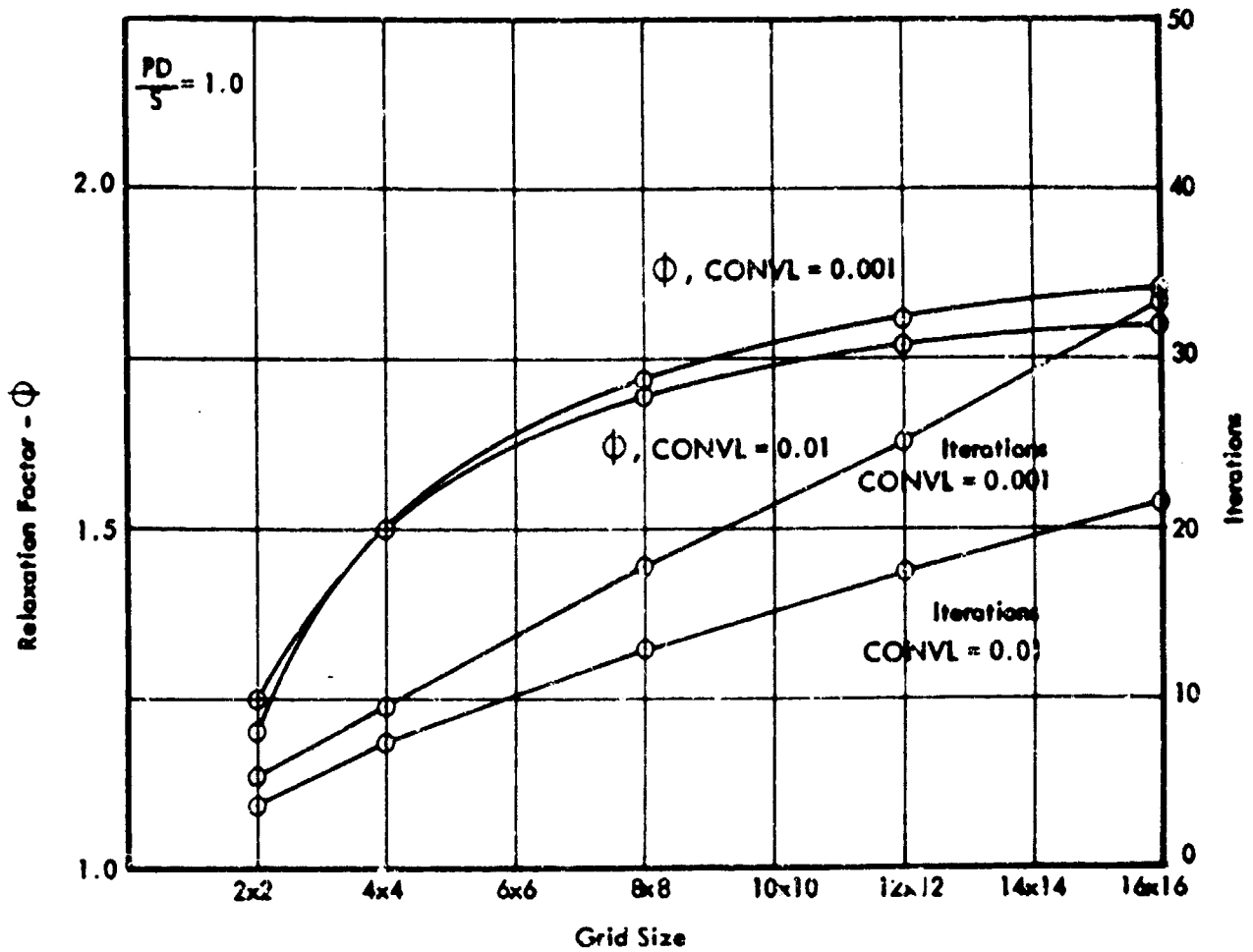


Figure B-4. Relaxation Factor versus Grid Size, PD/S = 1.0

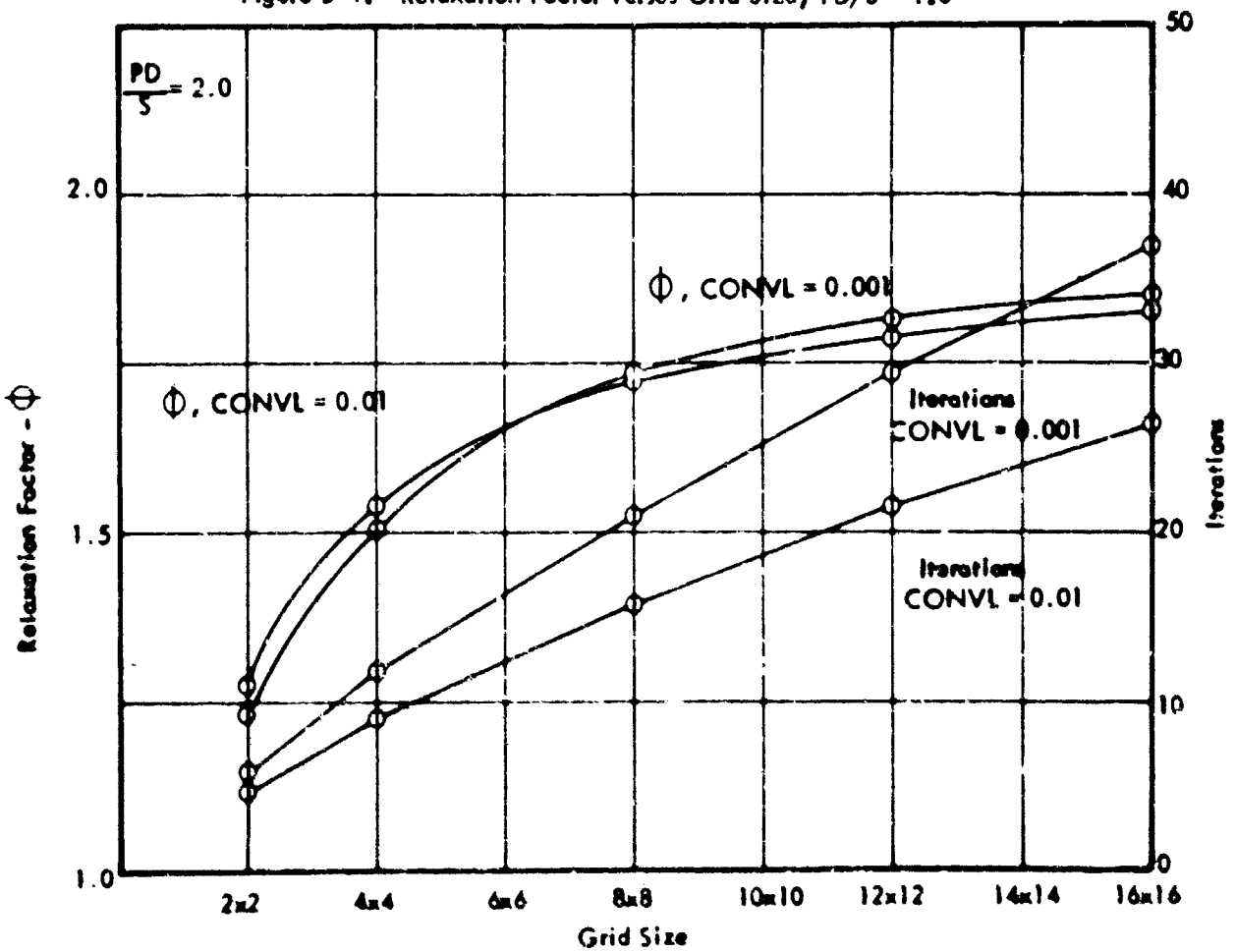


Figure B-5. Relaxation Factor versus Grid Size, PD/S = 2.0

**Capacity.** The program will handle a finite-difference grid 64 by 64 on one-quarter of the membrane. The capacity of the program may be altered by replacing the parameters of the DIMENSION statement, appearing at the beginning of the program, with new parameters; and replacing the limiting values of the two DO statements, immediately following the DIMENSION statement, with the new parameters. The parameters to be entered must be the desired maximum size of grid plus two. This requirement arises because the program includes the boundary points and one line of points past each centerline. Thus, the altered statements would read as follows:

```

DIMENSION Z(XXX,XXX)
C ZERO Z(I, J) BAND
1 DO2I = 1,XXX
  DO2J = 1,XXX
2 Z(I, J)=0.
  
```

where the new array size would appear in place of the X's.

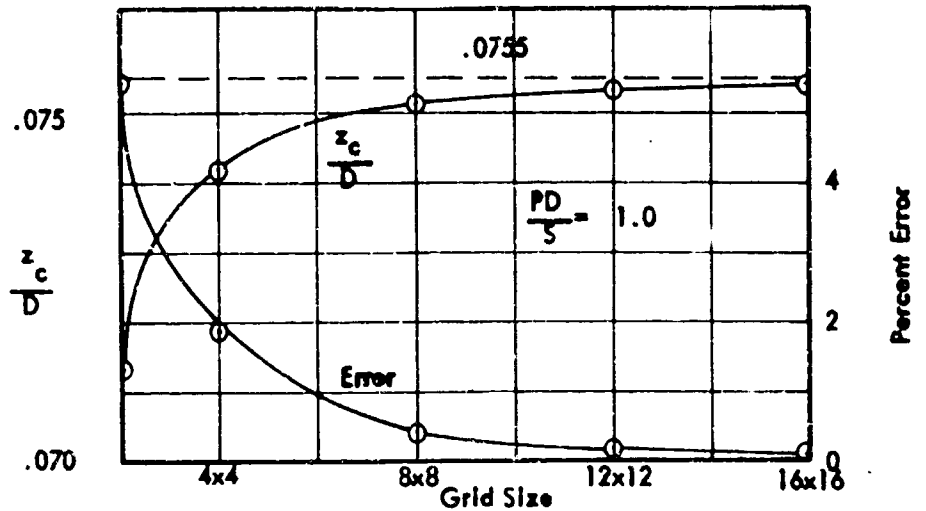


Figure B-6. Percent Error versus Grid Size, PD/S = 1.0

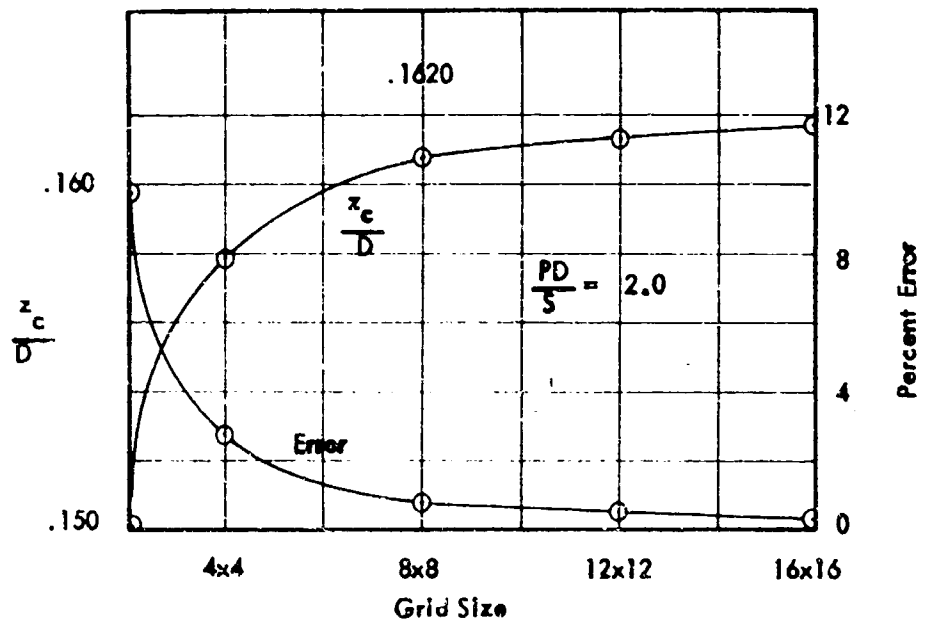


Figure B-7. Percent Error versus Grid Size, PD/S = 2.0

**Detailed Procedure.** Before each set of data cards is read, the storage spaces for Z(I, J) are set to zero.

Input: Necessary data is read into the computer on two data cards.

Card 1: IDENT . . . . . Data identification. May be any three digit number. It will be printed out with the results as:

IDENTIFICATION. . .XXX

ICODZ . . . . . This parameter tells the computer whether or not initial values of Z(I, J) are to be read in from data cards. Punch column 10, 1 if initial Z(I, J) are given, 2 if not given.

- IX . . . . . The number of finite divisions on one-quarter of the membrane parallel to DIMA. Max. = 64
- IY . . . . . The number of finite divisions on one-quarter of the membrane parallel to DIMB. Max. = 64
- ITERL . . . . . The maximum number of iterations allowed.
- CONVL . . . . . The maximum change between iterations to be allowed at any point. The membrane will converge approximately to an accuracy one place less than the convergence limit set. Thus, if CONVL = .001 the results will be accurate to .01.
- PHI . . . . . Over-relaxation factor
- Card 2: DIMA . . . . . Dimension of one-quarter of the plate parallel to the X axis.
- DIMB . . . . . Dimension of one-quarter of the plate parallel to the Y axis.
- STRES . . . . . The membrane stress. The stress usually used here is the plastic strength of the material to be used per unit length. Thus, if steel with a yield point of 36,000 psi and a thickness of .125 inches is to be used, we would compute:  
 $STRES = 36,000 \times .125 = 4500 \text{ lbs/in.}$
- PRES3 . . . . . Pressure acting normal to the membrane surface.

It is possible to read initial values of deflections into the computer through use of ICODZ. If ICODZ is punched 1 in column 10 of card 1, the computer will read in initial values for deflections. If ICODZ is punched 2 in the same column, the computer will bypass reading of initial deflection values and initial deflections will be assumed zero. If initial deflections are to be read in, the following procedure must be followed. The machine will read the first word of the first card as  $Z_{11}$ , the second as  $Z_{12}$ , etc., until the first row has been read in. The machine finds the number of pieces of data to place in the first row by interpreting the parameters given it on Cards 1 and 2. If more than one card is required to fill the first row, the machine will read a second card and continue placing numbers in the first row until the first row has been completed. The first number of the second row will then be read, i.e.,  $Z_{21}$ , as the number immediately following the last number of the first row. A new card must not be started for each new row unless the first value for that row begins a new card as a natural part of the sequence. The data must be placed on the cards in the 10 column fields, with decimal points included, continuously beginning with the first deflection of the first row and ending with the center point of the membrane. All boundary points must be included but only one-quarter of the membrane may be read in. The following example demonstrates this procedure. Suppose we have the plate, given in Figure B-8, with initial deflections as shown at the grid points. Then suppose we wish to determine the deflected shape of the plate under pressure of 20 psi. The plastic strength of the plate is 100 lbs./in. The information would be entered on the data cards as follows:

Card 1:

<u>ITEM</u>	<u>CARD COL.</u>	<u>EXAMPLE</u>
IDENT	8-10	xx xxxx x125
ICODZ	20	xx xxxx xx1
IX	29-30	xx xxxx x.04
IY	39-40	xx xxxx xx04
ITERL	41-50	xx xxxx xx50
CONVL	51-60	xx xxxx .001
PHI	61-70	xx xxxx 1.50

Card 2:

DIMA	1-10	xx xxxxx xx5.
DIMB	11-20	xx xxxxx xx5.
STRES	21-30	xx xxxxx 100.
PRES3	31-40	xx xxxxx x20.

CARD	CARD COL.	POINT	EXAMPLE
3	1-10	Z <sub>1,1</sub>	00 0000 0000
3	11-20	Z <sub>1,2</sub>	00 0000 0000
3	21-30	Z <sub>1,3</sub>	00 0000 0000
3	31-40	Z <sub>1,4</sub>	00 0000 0000
3	41-50	Z <sub>1,5</sub>	00 0000 0000
3	51-60	Z <sub>2,1</sub>	00 0000 0000
3	61-70	Z <sub>2,2</sub>	00 0000 00.2
3	71-80	Z <sub>2,3</sub>	00 0000 00.3
4	1-10	Z <sub>2,4</sub>	00 0000 00.3
4	11-20	Z <sub>2,5</sub>	00 0000 00.4
4	21-30	Z <sub>3,1</sub>	00 0000 0000
etc.			

Where x's are shown the card columns may be left blank. Decimals may not be included where not shown. Where decimals are shown the data may be placed anywhere within the ten column field designated, provided the decimal is supplied. If the decimal is not supplied, it will be automatically placed after the last column in the field regardless of where the data is placed. Preceding zeros need not be punched.

After reading in all data cards, the machine computes necessary parameters and sets up checks for use later in the program. The first value computed is Z<sub>2,2</sub>. Equations (9) are evaluated, using the initial values given, then substituted into equation (8). The value of f, thus found, is substituted into equation (10) and a new value of Z<sub>2,2</sub> is found. This value is checked against the old value of Z<sub>2,2</sub> to see if convergence has been obtained. The old value is then replaced by the new value and the program moves to point 2,3 where the process is repeated.

At each point, the new value is subtracted from the old value and the difference is compared with the largest difference yet found. If the new difference is larger, it replaces the old largest difference. At the completion of an iteration the largest difference anywhere in the plate, together with its coordinates, is printed out. If this difference is smaller than the convergence limit set, the program goes to print; if not, the program returns to 2,2 and the process is repeated.

At the center-lines the program makes use of symmetry to obtain values of points outside the quarter-plate being computed. At the completion of each iteration the number of iterations completed is checked against the iteration limit given in the input data. If the limit is reached, before convergence is reached, the program prints out all the data obtained to that point and goes on to read the next data cards. Each point is computed consecutively, row by row, beginning with point 2,2 and ending with the center point of the plate.

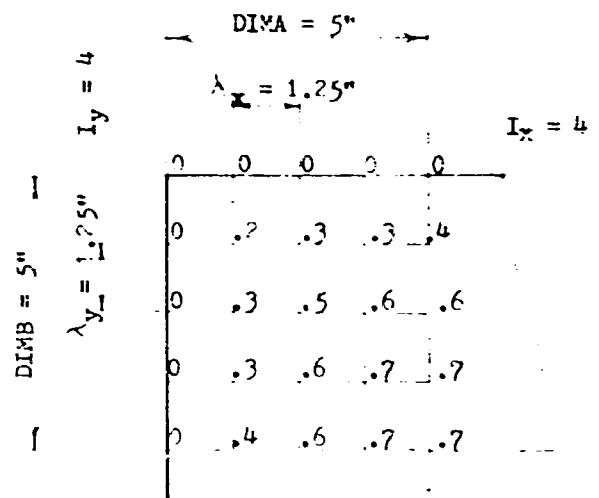


Figure B-8. Example

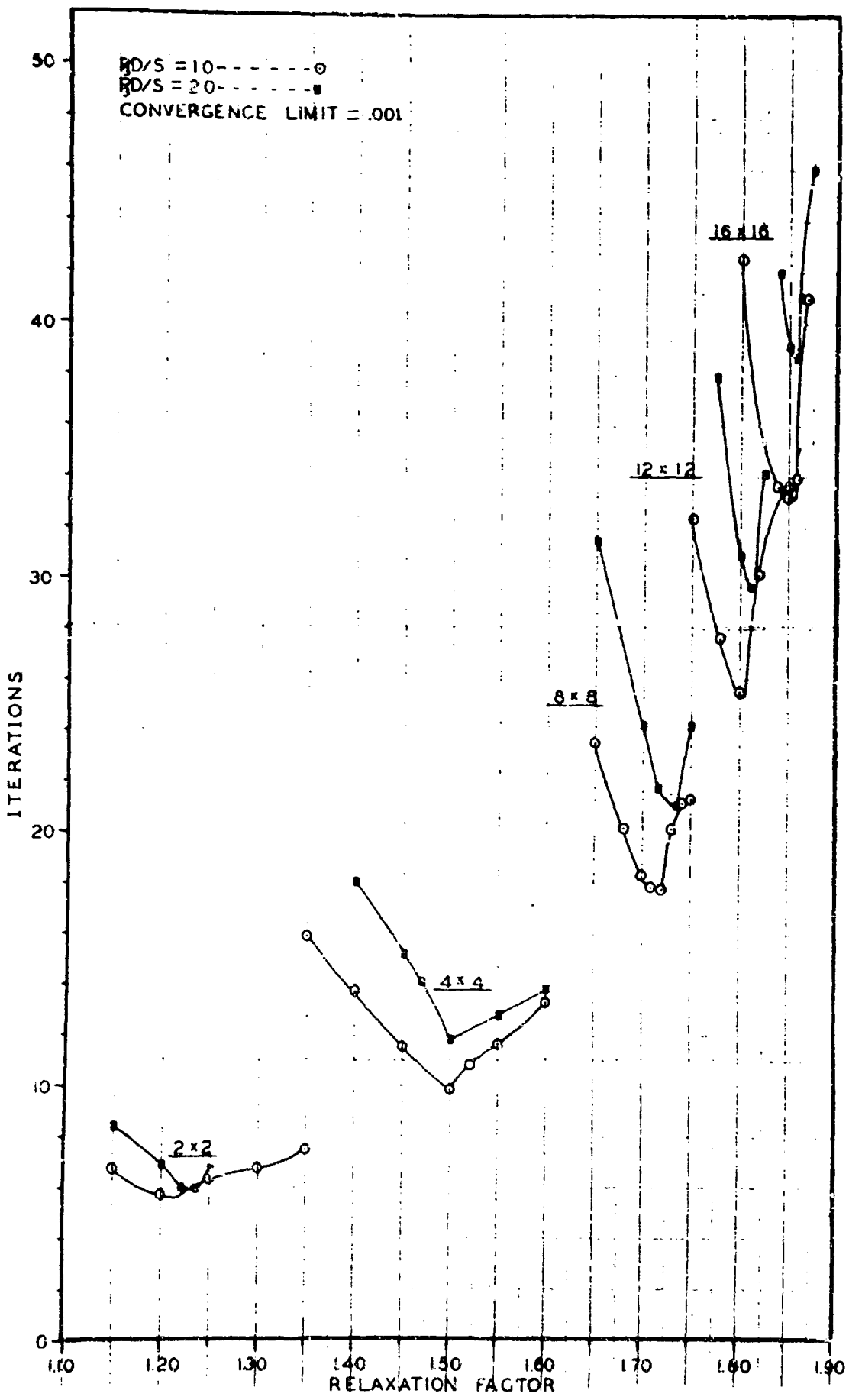


Figure B-9

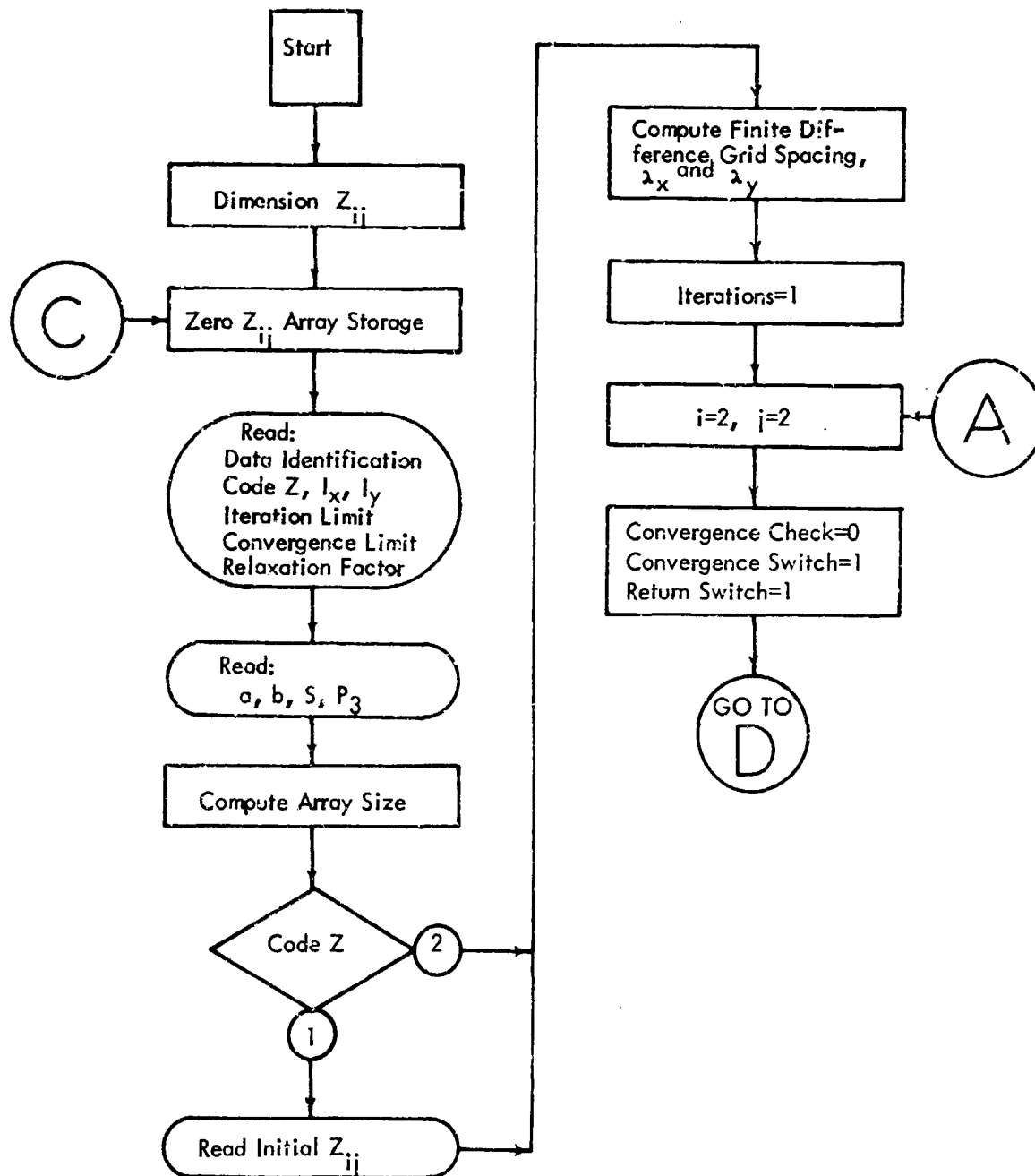
After the equations have converged or the limit set on iterations has been reached, the program computes the average strain along the centerline parallel to DIMB and along the centerline parallel to DIMA. To find this strain the computer sums the chord distances between grid points along the centerline and subtracts the plan projection of the centerline from it. This gives the elongation. To find the average percent strain, the elongation is divided by the plan projection of the centerline and multiplied by 100.

It was found that the equations diverge after the average slope (computed as the center deflection divided by the shortest side) exceeds 1:1. The computer computes the slope along both centerlines. The program will automatically stop iterating, when this slope is reached, and print out all available data plus the following statement:

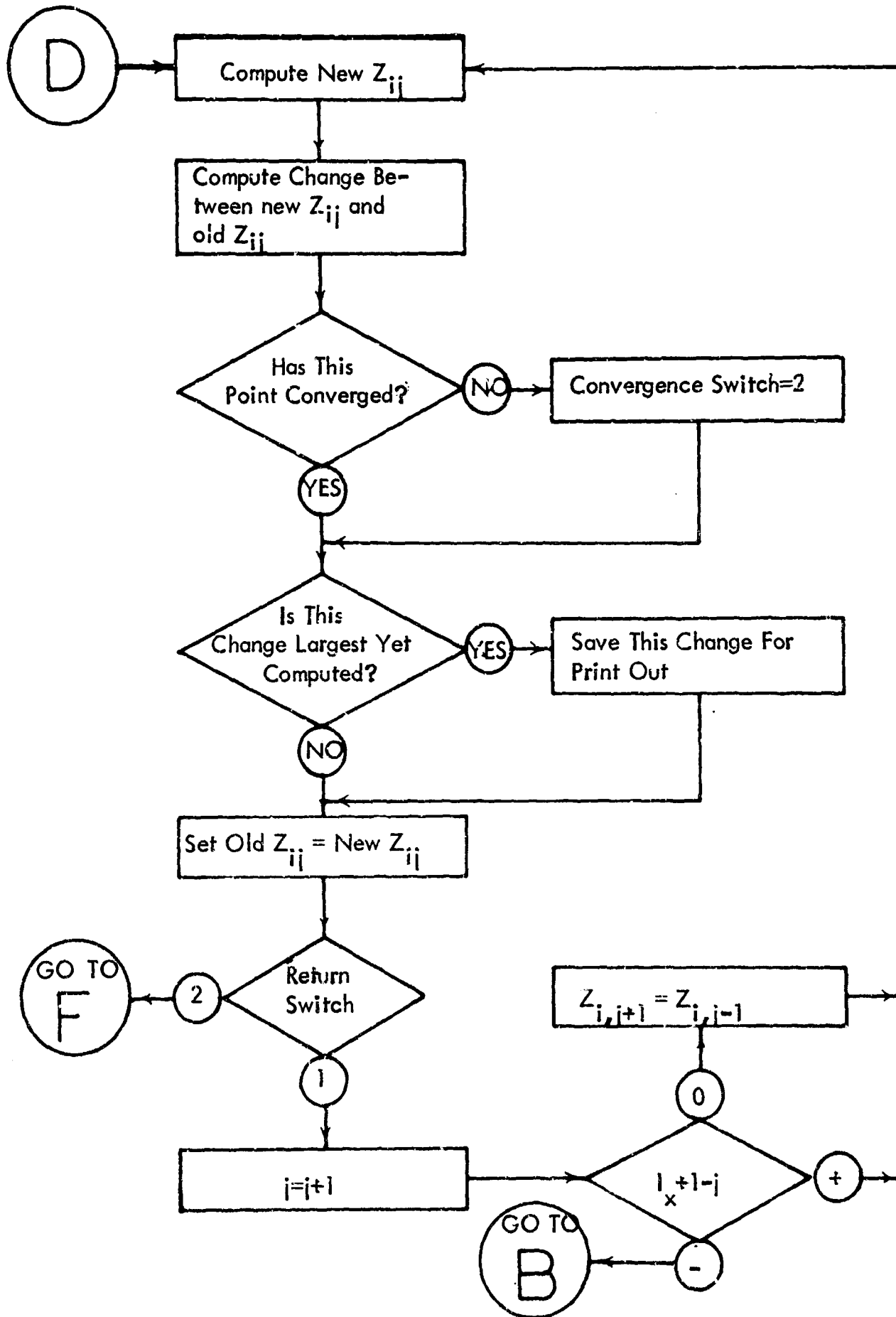
AVERAGE SLOPE EXCEEDS 1:1, EQUATIONS DIVERGE BEYOND THIS POINT

Output. A flow diagram and a print of the computer program follows. The program is supplemented with comment statements to facilitate coordination with the flow diagram. The first four cards of the program (the fourth card is blank)

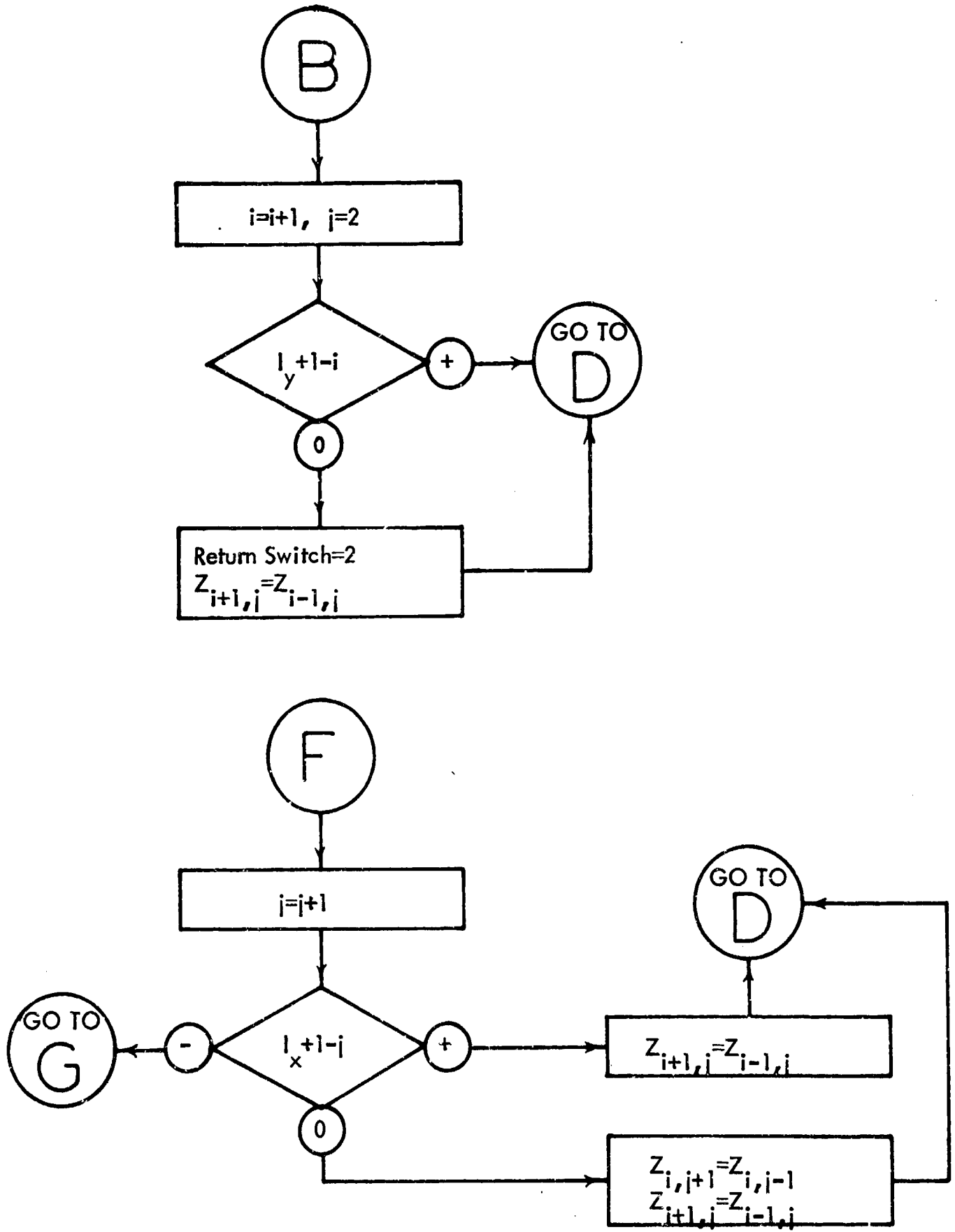
Flow Diagram, Funicular Shell



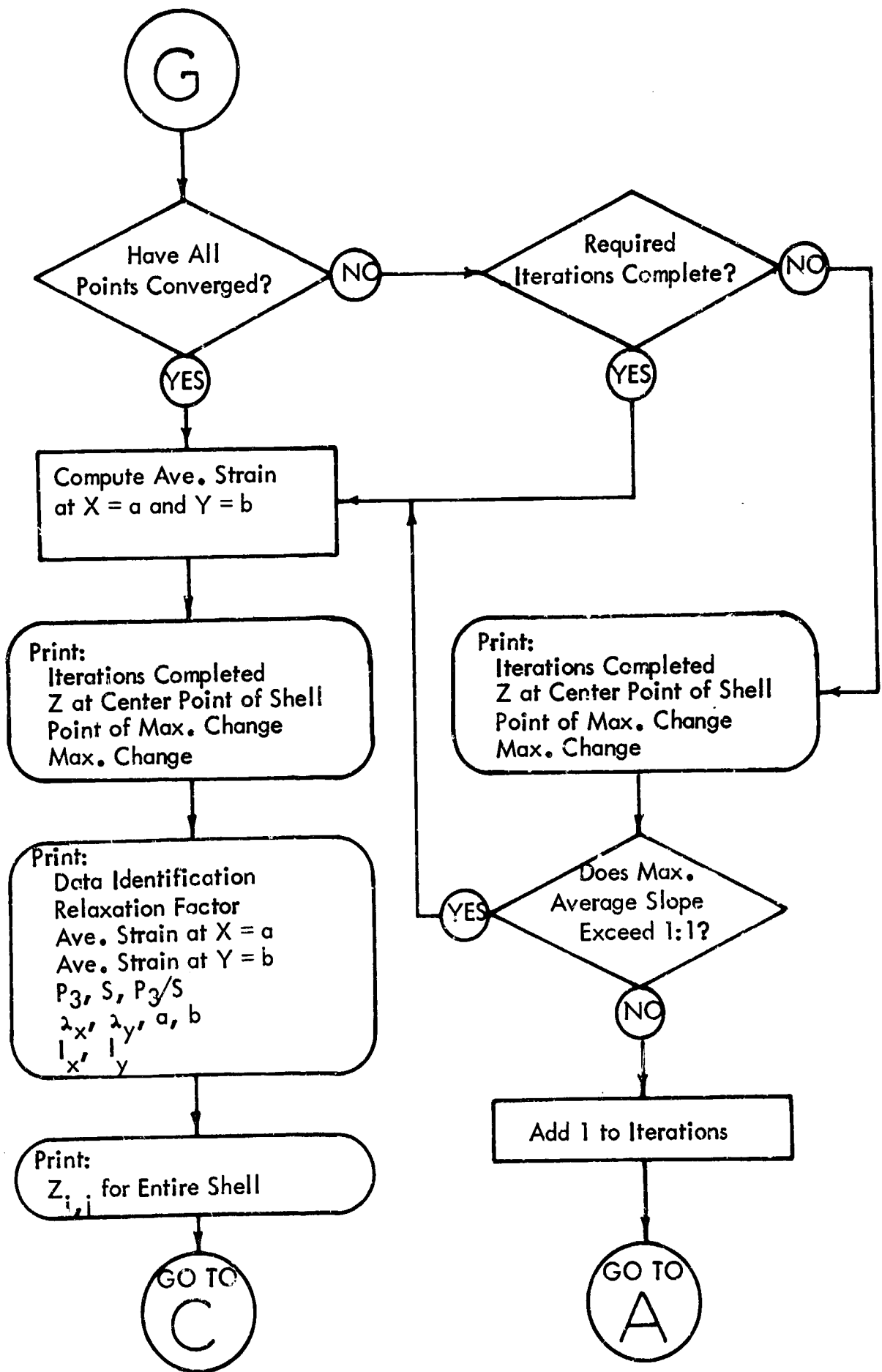
Flow Diagram, Funicular Shell



Flow Diagram, Funicular Shell



Flow Diagram, Funicular Shell



```

*** HANSEN
** PROGRAM IS ITERATIVE
* COMPILE FORTRAN,EXECUTE FORTRAN

```

2R

```

C FUNICULAR SHELL, PRESSURE CONSTANT
C RESTRAINING BANDS ACROSS X=0 AND X=2*DIMA
C DIMENSION Z(66,66)
C ZERO Z(I,J) BAND
1 DO2I=1,66
  DO2J=1,66
2 Z(I,J)=0.
C MAX IX = MAX IY = 64
C ICODZ.....PUNCH COL 10, 1 IF Z(I,J) GIVEN, 2 IF NOT GIVEN
C IX.....NUMBER OF DIVISIONS ALONG DIMA
C IY.....NUMBER OF DIVISIONS ALONG DIMB
C ITERL....MAXIMUM ITERATIONS ALLOWED
C CONVL....CONVERGENCE LIMIT..MAX CHANGE BETWEEN ITERATIONS
C DIMA.....HORIZONTAL DIMENSION OF 1/4 SHELL
C DIMB.....VERTICAL DIMENSION OF 1/4 SHELL
C STRES....STRESS PER LINEAR DISTANCE
C PRES3....PRESSURE PER UNIT AREA
C PHI.....RELAXATION FACTOR...USE 1.7 FOR AN 8 BY 8 GRID
C STRNB....YIELD FORCE OF BEAM, POUNDS
C ITER.....ITERATIONS COMPLETED
C Z(I,J)....RIZE AT POINT I,J
C TCON2....MAX CHANGE BETWEEN THIS ITER AND LAST
C IP,JP....POINT OF MAX CHANGE
C PS.....PRESSURE OVER STRESS RATIO
C STNBX....AVERAGE STRAIN OF RESTRAINING BAND (BEAM) AT X=0
C STNSX....AVERAGE STRAIN OF MIDDLE LINE AT X=DIMA
C          COMPUTED AS 100 TIMES (ARC LENGTH - DIMB)/DIMB
C XLAM.....MESH SIZE ALONG DIMA
C YLAM.....MESH SIZE ALONG DIMB
C INPUT
  READ 500,IDENT,ICODZ,IX,IY,ITERL,CONVL,PHI
500 FORMAT(5I10,2F10.0)
  READ 501,DIMA,DIMB,STRES,PRES3,STRNB,WIDTH
501 FORMAT(6F10.0)
  PRINT 599
599 FORMAT(54HIFUNICULAR SHELL,RESTRAINING BANDS ACROSS X=0, X=2DIMA/
118H IDENTIFICATION...I3)
600 FORMAT(75H ITER CENTER DEFLECTION MAX CHANGE IN SHELL
1 MAX CHANGE IN BEAM/)
C COMPUTE ARRAY SIZE
  M=IX+1
  N=IY+1
C CHECK TO SEE IF INITIAL Z(I,J) ARE GIVEN
  IF(ICODZ-1)999,3,4
3 READ 502,((Z(I,J),J=1,M),I=1,N)
502 FORMAT (8F10.0)
4 XI=IX
  YI=IY
  XLAM=DIMA/XI
  YLAM=DIMB/YI
  ITER=1
10 I=2
  J=2
  TCON2=0
  TCON4=0.
  ICSWH=1
  ISWCH=1

```

```

      GO TO 100
101 J=J+1
      IF(M-J)11,12,100
12 Z(I,J+1)=Z(I,J-1)
      GO TO 100
11 I=I+1
      J=2
      IF(N-I)999,15,100
15 ISWCH=2
      Z(I+1,J)=Z(I-1,J)
      GO TO 100
102 J=J+1
      IF(M-J)150,20,21
20 Z(I,J+1)=Z(I,J-1)
      Z(I+1,J)=Z(I-1,J)
      GO TO 100
21 Z(I+1,J)=Z(I-1,J)
      GO TO 100
C      COMPUTATION PHASE
C      COMPUTE NEW Z(I,J)
100 A=Z(I,J+1)-Z(I,J-1)
      B=Z(I+1,J)-Z(I-1,J)
      C=Z(I+1,J)-2.*Z(I,J)+Z(I-1,J)
      D=Z(I,J+1)-2.*Z(I,J)+Z(I,J-1)
      E=Z(I+1,J+1)-Z(I-1,J+1)-Z(I+1,J-1)+Z(I-1,J-1)
      F=(4.*XLAM**2+A**2)*C-5*A*P*E+(4.*YLAM**2+B**2)*D
      G=PRES3/(STRES*2.*XLAM*YLAM)*(4.*XLAM**2*YLAM**2+XLAM**2*B**2
1+YLAM**2*A**2)**1.5
      H=2.*(4.*XLAM**2+AF*2+4.*YLAM**2+B**2)
      T=Z(I,J)+PHI*(F+G)/H
      PS=PRES3/STRES
C      SET UP CONVERGENCE CHECK
      TCON1=T-Z(I,J)
      IF(ABS(TCON1)-CONVL)111,111,107
107 ICSWH=2
111 IF(ABS(TCON1)-ABS(TCON2))106,106,108
108 TCON2=TCON1
      IP=I
      JP=J
106 Z(I,J)=T
C      FIND RETURN STATEMENT
109 GO TO (IC1,102),ISWCH
C      COMPUTE BEAM
150 I=2
      J=1
155 AB=Z(I,J+1)-Z(I,J)
      SB=Z(I+1,J)-Z(I-1,J)
      CS=Z(I+1,J)-2.*Z(I,J)+Z(I-1,J)
      DB=(4.*YLAM**2+BB**2)**1.5
      FB=2.*STRES*AB/SQRT(XLAM**2+AB**2)
      GB=8.*STRNB*YLAM*CB/DB
      GDB=PRES3*WIDTH
      HB=16.*STRNB*YLAM/DB
      TB=Z(I,J)+(FB+GB+GDB)/HB*PHI
C      SET UP CONVERGENCE CHECK
      TCON3=TB-Z(I,J)
      IF(ABS(TCON3)-CONVL)151,151,152
152 ICSWH=2
151 IF(ABS(TCON3)-ABS(TCON4))153,153,154
154 TCON4=TCON3
      IPB=I

```

```

      JPB=J
153  Z(I,J)=TB
      I=I+1
      IF(N-I)200,156,155
156  Z(I+1,J)=Z(I-1,J)
      GO TO 155
C    CHECK CONVERGENCE
200  GO TO (203,202),ICSWH
C    CHECK ITERATIONS
202  IF(ITERL-ITER)203,204,204
C    DATA TO BE PRINTED OUT EACH ITERATION
204  PRINT610,ITER,Z(N,M),IP,JP,TCO2,IPB,JPB,TCO4
610  FORMAT(I5,F18.5, 10H          Z( I2, 1H, I2, 2H)= F9.5,
      1          10H          Z( I2, 1H, I2, 2H)= F9.5)
C    CHECK AVERAGE SLOPE
      IF(1.-Z(N,M)/DIMB)29,29,30
29  PRINT611
611  FORMAT(64H AVERAGE SLOPE EXCEEDS 1 TO 1, EQUATIONS DIVERGE PAST TH
      1 IS POINT)
      GO TO 203
C    ITERATE AGAIN
30  ITER=ITER+1
      GO TO 10
C    COMPUTE STRAIN IN BEAM AT X=0
203  I=1
      J=1
      ARC=0.
41  ARC1=SORF(YLAM**2+(Z(I+1,J)-Z(I,J))**2)
      ARC=ARC+ARC1
      I=I+1
      IF(N-I)999,42,41
42  STNBX=(ARC-DIMB)/DIMB*100.
C    COMPUTE STRAIN IN SHELL AT X=A
      I=1
      J=M
      ARC=0.
31  ARC1=SORF(YLAM**2+(Z(I+1,J)-Z(I,J))**2)
      ARC=ARC+ARC1
      I=I+1
      IF(N-I)999,32,31
32  STNSX=(ARC-DIMB)/DIMB*100.
      PRINT610,ITER,Z(N,M),IP,JP,TCO2,IPB,JPB,TCO4
      PRINT599,ICUN7
      PRINT 600,PHI
600  FORMAT(17H RELAX. FACTOR...F10.5)
      PRINT 612,M,STNSX
612  FORMAT(16H STRAIN ALONG J=12,4H IS F5.2)
      PRINT 601,PRESB,STNBX
601  FORMAT(17H PRESSURE.....F10.5,20H STRAIN IN BEAM...F10.5)
      PRINT 602,STRES,STNMB
602  FORMAT(17H SHELL STRENGTH..F10.5,20H BEAM STRENGTH....F10.5)
      PRINT 603,PS,WIDTH
603  FORMAT(17H P/S.....F10.5,20H BEAM WIDTH .....F10.5)
      PRINT 604,XLAM,DIVA
604  FORMAT(17H LAMDA X.....F10.5,20H A.....F10.5)
      PRINT605,YLAM,DIMB
605  FORMAT(17H LAMDA Y.....F10.5,20H B.....F10.5)
      PRINT 606,IX,IY
606  FORMAT(17H GRID SIZE.....I3,4H BYI3)
      PRINT 607
607  FORMAT(26HCZ DISTANCES FOR 1/4 SHELL/)

      PRINT 608, (I,J,Z(I,J),J-1,M),I=1,M)
608  FORMAT(5H          Z(I2,1H,I2,2H)=F9.5,5H          Z(I2,1H,I2,2H)=F8.5,
      1          5H          Z(I2,1H,I2,2H)=F8.5,5H          Z(I2,1H,I2,2H)=F8.5,
      2          5H          Z(I2,1H,I2,2H)=F8.5,5H          Z(I2,1H,I2,2H)=F8.5)
C    READ NEXT DATA
      GO TO 1
END

```

are instructions for the computer necessary for correct handling of the program and for time charges. These cards will, of course, vary with the individual system. A print of the sample data follows the program. This data was run on the computer for both cases wherein initial values were given and not given. It is interesting to note that the same number of iterations was required for convergence in both cases. Closer investigation of the output for each iteration revealed that initial rise of the membrane is very rapid. Indeed, by the end of the sixth iteration, the center deflection for both cases was almost identical. This property makes the method even more desirable because initial values are not necessary in order to reach convergence within a reasonable computation time.

The first page of output gives storage locations of the parameters used in the program. This information expedites modifications in the program because all statement numbers and all variable names are given. The second page of output gives the center deflections at each iteration and the point of maximum change and the value of the maximum change for that iteration. The third page of output gives all of the final data.

### Relaxation Factors

A series of trials was made to determine relaxation factors that would give convergence in the least number of iterations. These trials were all made on a 10 x 10 inch plate with a yield strength of 100 lbs./in. The trials were made with pressure of 10 and 20 psi. Figure B-9 gives a comparison of the two pressures. It should be noted that the relaxation factor is not critical for low grid sizes and low pressures but becomes increasingly critical as either the  $P_3D/S$  ratio rises or the grid size increases. For a 16 x 16 grid at a  $P_3/S$  ratio of 2.0 the graph is extremely shape and slight error in the relaxation factor will mean a sharp increase in iterations required for convergence. Although error in the relaxation factor becomes important as the  $P_3D/S$  ratio increases, there is little change in the factor itself. A comparison of Figures B-10 and B-11 reveal that both give almost identical relaxation factors for a particular grid size; however, as expected, a larger number of iterations is required for the higher  $P_3D/S$  ratio. These two figures also indicate that there is little change of relaxation factor with respect to the convergence limit  $\beta$ ; however, the number of iterations increase as the convergence limit decreases. Figures B-12 and B-13 indicate that the error decreases very sharply as the grid size decreases. Indeed, less than 1% error may be achieved with an 8 x 8 grid. In developing these curves, it was found that minus signs appearing in the output column, giving maximum change for each iteration, indicate the relaxation factor is too high. The ideal relaxation factor was found to produce only 1 or 2 minus signs in this column. This feature became a guide in arriving at the best relaxation factor. An example of too large a relaxation factor may be found in the paragraph on modifications, to follow. Modifications to the physical conditions of the basic program may alter the "best" relaxation factor slightly; however, the curves in Figures B-10 and B-11 have been shown in use to be excellent guides.

### Strain

A series of trials determined the strain relationships at various pressures and length-to-width ratios. The trials were all made with a base width of 10 inches. The length was varied from 10 to 30 inches, with an additional series of infinite length. The strain was calculated as the average strain of the centerline parallel to the narrowest side. The length of centerline, used in this calculation, was the sum of the chord distances between grid points. Figure B-14 gives the results of this series. It should be noted that the curves relating per cent strain and  $d_c/D$  ratios for the case of the square membrane, and the case of the semi-infinite membrane, are very close. This indicates that the strain along the centerline of the membrane is very close to that of the semi-infinite case of the same width and  $d_c/D$  ratio; and therefore, for all practicable cases, independent of the length-to-width ratio. This, of course, would not be true for other lines across the membrane. The curves relating  $P_3D/S$  and  $d_c/D$  ratios indicate that the center deflection becomes almost independent of the length-to-width ratio above a length-to-width ratio of approximately 3:1.

### Modifications to the Program

The program for the membrane has, as its boundary conditions, fixed edges lying in the same plane. Variations may be obtained by altering these boundary conditions. The boundary may be given an arbitrary form by reading in initial values other than zero. However, the boundary must remain symmetrical about both axes because only one-quarter of the plate is considered in the program. Further alteration may be had by allowing the boundaries to be supported by plastic beams which take their shape by responding to the force of the pressure and the pull of the supported membrane. These beams may also be placed across the interior of the plate. Edges of the membrane may be freed by reducing the plastic strength of these beams to zero. The pressure need not be a constant over the surface of the membrane. The pressure may be made a variable by introducing, into the program, a routine that computes the pressure at each point; or by reading in a given set of pressures defined at every point in the grid. If it is necessary to consider the

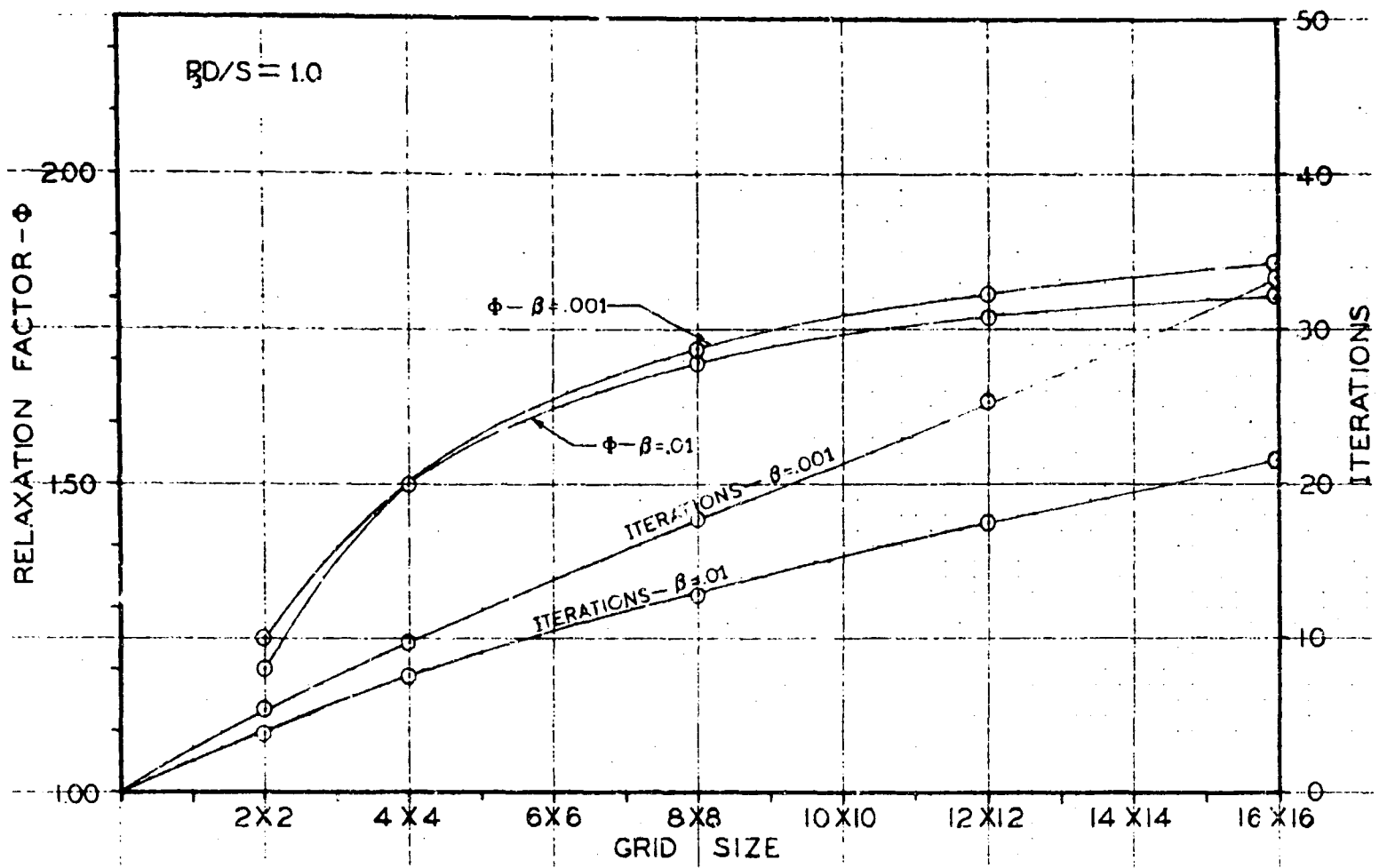


Figure B-10

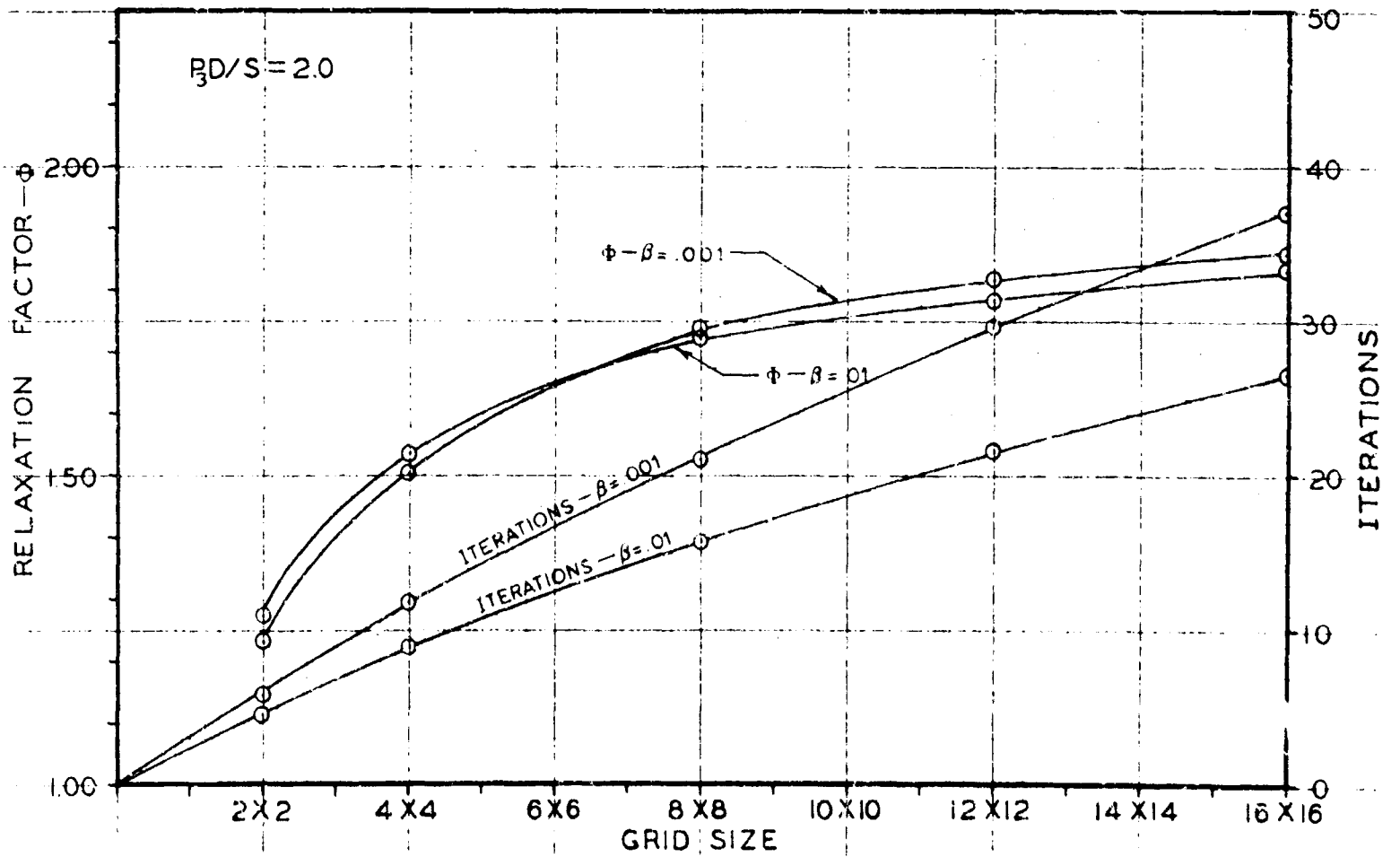


Figure B-11

entire plate, rather than just the quarter plate heretofore considered, the parameters M and N following statement 600 should be changed to read:

$$M = 2 * X + 1$$

$$N = 2 * Y + 1$$

This changes the indexing so that the iteration process covers the entire plate. By using combinations of these conditions, a wide variety of boundary and loading conditions are possible. The equations have been isolated from the iteration process. They are listed from statement 155 to the beginning of the convergence check. Poisson's equation, or any other suitable equation, may be inserted provided the same parameters are used to identify information either given to or required by other parts of the program. Several of these variations will be discussed in the following paragraphs.

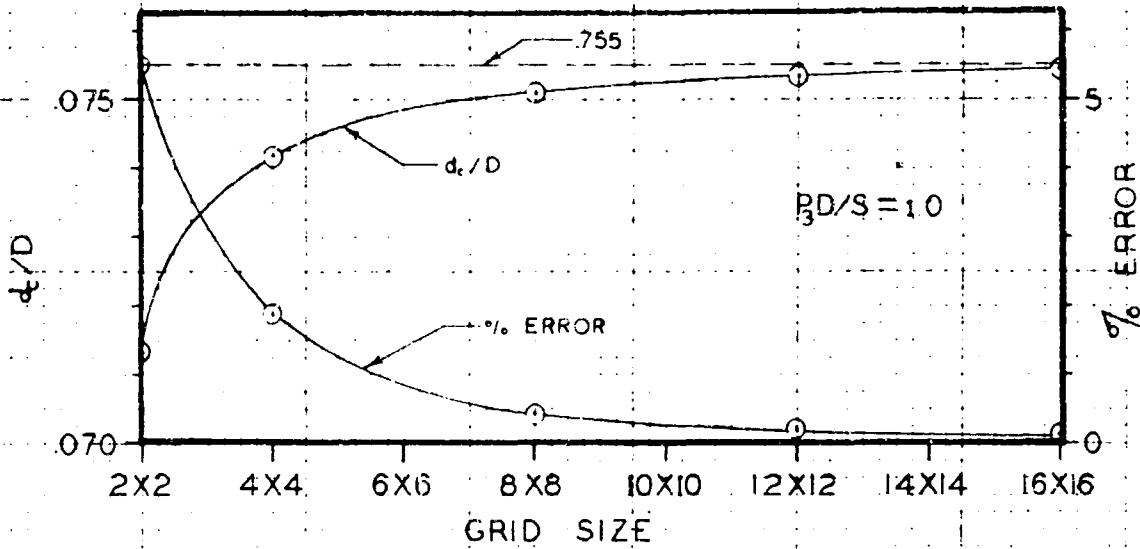


Figure B-12

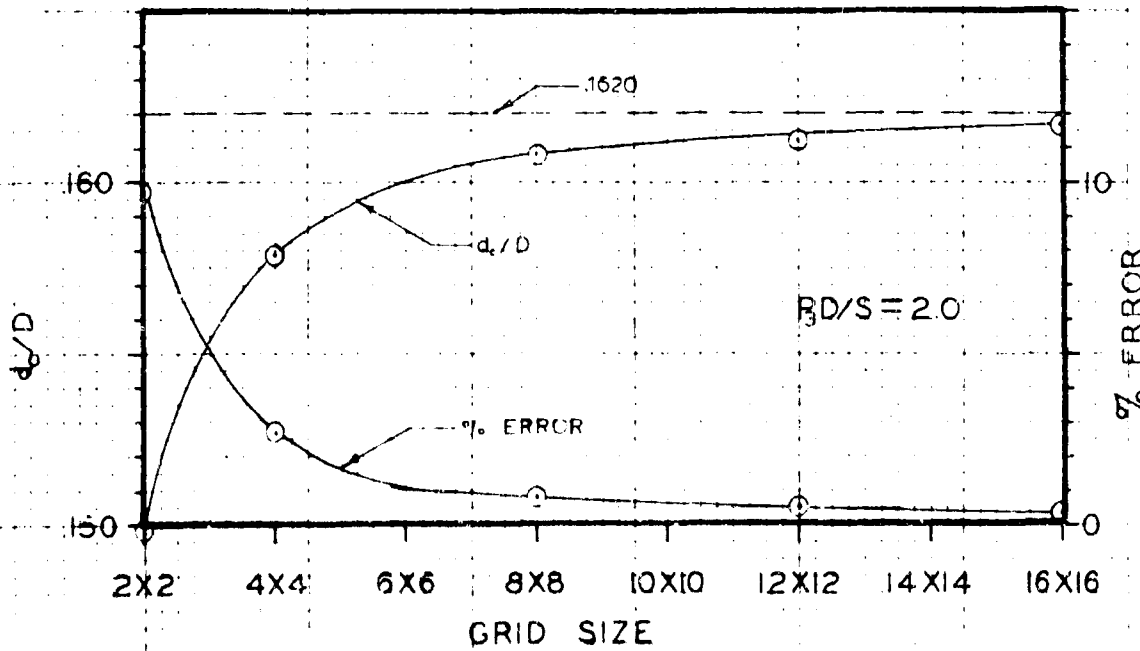


Figure B-13

**Two Parallel Edges Free.** Under a constant pressure loading the membrane with two parallel edges free, takes on a cylindrical shape that is independent of the coordinate perpendicular to the free edges. For this condition the governing equation is:

$$\frac{\frac{d^2 z}{dy^2}}{\left[1 + \left(\frac{dz}{dy}\right)^2\right]^{3/2}} + \frac{P_3}{S} = 0$$

In terms of finite differences:

$$\frac{8\lambda(z_{i+1} - 2z_i + z_{i-1}))}{\left[4\lambda^2 + (z_{i+1} - z_{i-1})^2\right]^{3/2}} + \frac{P_3}{S} = 0$$

The parameters of this program are the same as those previously discussed, where applicable. They are individually identified in the comment statements at the beginning of the program. Input requirements are those dictated by READ 500 immediately following the comment statements. Output is similar for all of the programs.

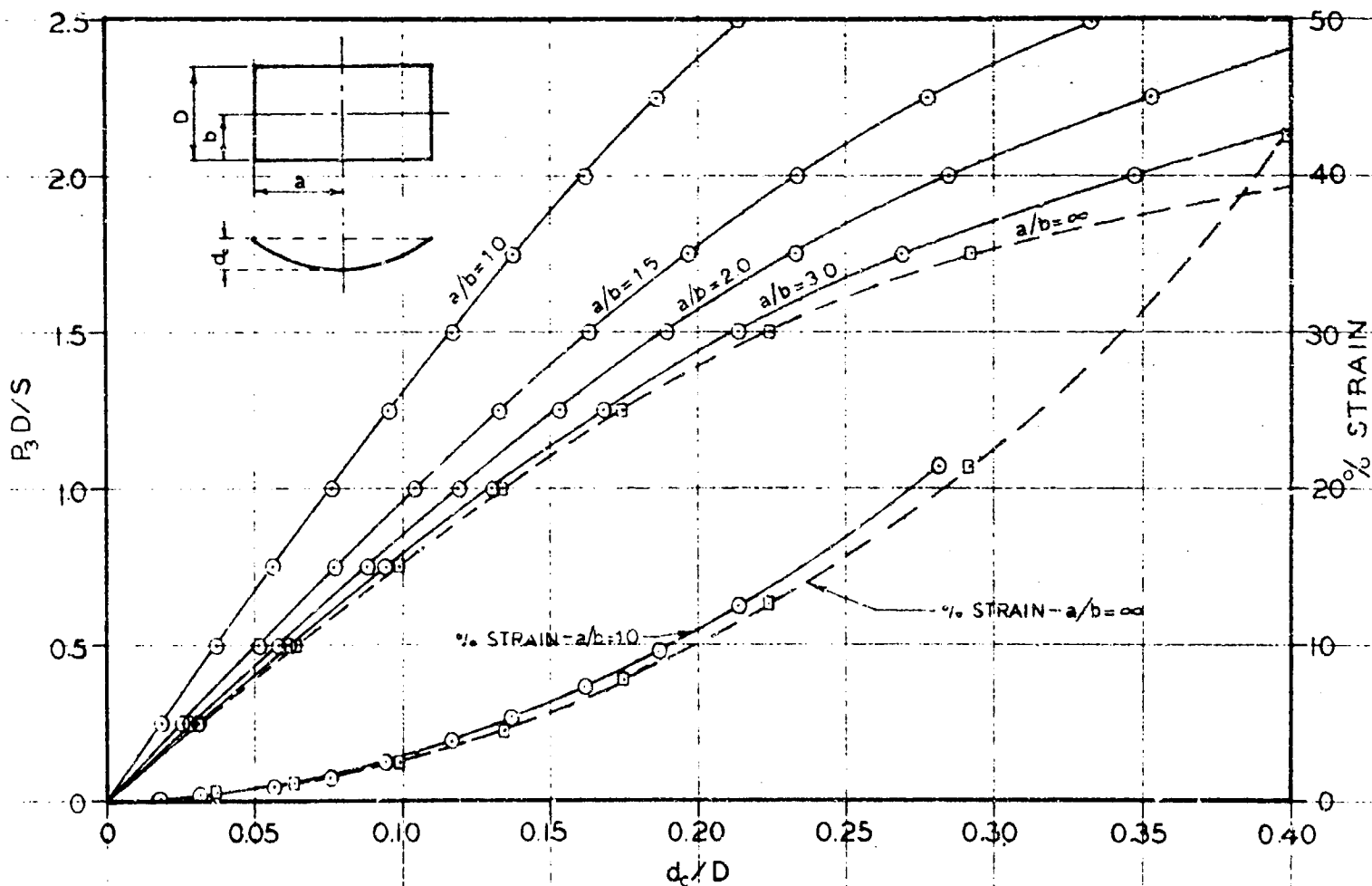


Figure B-14

```

*** HANSEN
*   COMPILE FORTRAN,EXECUTE FORTRAN

C   FUNICULAR SHELL, PRESSURE CONSTANT
C   TWO EDGES FREE, CYLINDRICAL SHAPE
C   DIMENSION Z(66)
C   ZERO Z(1) BAND
1   DO21=1,66
2   Z(1)=0.
C   MAX IY=64
C   IY.....NUMBER OF DIVISIONS ALONG DIMB
C   ITEPL....MAXIMUM ITERATIONS ALLOWED
C   CONVL....CONVERGENCE LIMIT...MAX CHANGE BETWEEN ITERATIONS
C   DIMB.....VERTICAL DIMENSION OF 1/2 SHELL
C   STRES.....STRESS PER LINEAR DISTANCE
C   PRES3....PRESSURE PER UNIT AREA
C   OMEGA....RELAXATION FACTOR
C   ITER.....ITERATIONS COMPLETED
C   Z(1).....RISE AT POINT 1
C   TCON2....MAX CHANGE BETWEEN THIS ITER AND LAST
C   IP.....POINT OF MAX CHANGE
C   PS.....PRESSURE OVER STRESS RATIO
C   STRN.....AVERAGE STRAIN
C   YLAM.....MESH SIZE ALONG DIMB
C   INPUT
      READ 500,IDENT,IY,ITERL,CONVL,DIMB,STRES,PRES3,OMEGA
500  FORMAT(3I10,5F10,0)
      PRINT 600,IDENT
600  FORMAT(26H1FUNICULAR SHELL, CYLINDER/18H IDENTIFICATION...I3/)
      PRINT 612
612  FORMAT(51H ITER      CENTER DEFLECTION      MAX CHANGE IN SHELL/)
C   COMPUTE ARRAY SIZE
      N=IY+1
      YI=IY
      YLAM=DIMB/YI
      ITER=1
4   TCON2=0.
      ICSWH=1
      I=2
3   A=Z(I+1)-2.*Z(I)+Z(I-1)
      B=Z(I+1)-Z(I-1)
      C=(4.*YLAM**2+B**2)**1.5
      D=A*8.*YLAM/C+PRES3/STRES
      E=16.*YLAM/C
      T=Z(I)+D/E*OMEGA
      PS=PRES3/STRES
C   SET UP CONVERGENCE CHECK
      TCON1=T-Z(I)
      IF(ABSF(TCON1)-CONVL)10,10,11
11  ICSWH=2
10  IF(ABSF(TCON1)-ABSF(TCON2))12,12,13
13  TCON2=TCON1
      IP=I
12  Z(I)=T
      I=I+1
      IF(N-I)100,14,3
14  Z(I+1)=Z(I-1)
      GO TO 3
C   CHECK CONVERGENCE
100 GO TO (101,102),ICSWH
C   CHECK ITERATIONS

```

```

102 IF(ITER-ITER)101,103,103
C   DATA TO BE PRINTED OUT EACH ITERATION
103 I=N
    PRINT 610,ITER,Z(1),IP,TCON2
610 FORMAT(15,F18.5,13H          Z(12,2H)=F9.5)
C   CHECK AVERAGE SLOPE
    IF(.9-Z(1)/DIMB)104,104,105
104 PRINT 611
611 FORMAT(66H AVERAGE SLOPE EXCEEDS 0.9 TO 1, EQUATIONS DIVERGE PAST
    THIS POINT)
    GO TO 101
C   ITERATE AGAIN
105 ITER=ITER+1
    GO TO 4
C   COMPUTE STRAIN IN SHELL
101 I=1
    ARC=0.
106 ARC1=SQRT(YLAM**2+(Z(I+1)-Z(I))**2)
    ARC=ARC+ARC1
    I=I+1
    IF(N-I)999,107,106
107 STRN=(ARC-DIMS)/DIMB*100.
    PRINT 610,ITER,Z(1),IP,TCON2
    PRINT 600,IDENT
    PRINT 609,OMEGA
609 FORMAT(17H RELAX. FACTOR...F10.5)
    PRINT 601,PRES3
601 FORMAT(17H PRESSURE.....F10.5)
    PRINT 602,STRES
602 FORMAT(17H SHELL STRENGTH..F10.5)
    PRINT 603,PS
603 FORMAT(17H P/S.....F10.5)
    PRINT 605,YLAM,DIMB
605 FORMAT(17H LAMDA Y.....F10.5,20H   E.....F10.5)
    PRINT 606,IY,STRN
606 FORMAT(17H GRID SIZE.....13,27H          STRAIN IN SHELL:;F10.5)
    PRINT 607
607 FORMAT(26HZ DISTANCES FOR 1/2 SHELL/)
    PRINT 608,(I,Z(I),I=1,N)
608 FORMAT(5H   Z(12,2H)=F8.5,5H   Z(12,2H)=F8.5,5H   Z(12,2H)=F8.5,
    1   5H   Z(12,2H)=F8.5,5H   Z(12,2H)=F8.5)
C   READ NEXT DATA
    GO TO 1
999 END

```

The general shape of the membrane derived from this equation is given in Figure B-15.

The same simple problem used previously was reused here. For this shell, the deflections became too large and the equations began to diverge. Experience has shown that divergence begins for this shell at an average slope of about 0.9:1.

Plastic Beam Across Center of Membrane. The differential equation governing the plastic beams is:

$$\frac{P_1 \frac{\partial^2 z}{\partial y^2}}{\left[1 + \frac{\partial z}{\partial y}\right]^2}]^{3/2} + \frac{2S \frac{\partial z}{\partial x}}{\left[1 + \frac{\partial z}{\partial x}\right]^2}]^{1/2} + P_3 W = 0$$

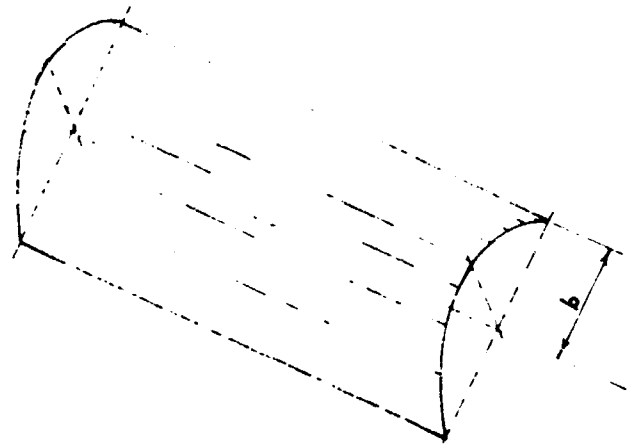


Figure B-15. Two Parallel Edges Free

The second term is a load term giving the contribution of the pull of the membrane to the shape of the plastic beam. The 2 in the numerator arises because the membrane is considered symmetrical about the beam. If the plastic beam is placed at the edge of the membrane, without an adjoining membrane to create symmetry, the number 2 should be dropped.

In terms of finite differences:

$$\frac{8P_1 \lambda_y (z_{i+1,j} - 2z_{i,j} + z_{i-1,j})}{\left[\lambda_y^2 + (z_{i+1,j} - z_{i-1,j})^2\right]^{3/2}} + \frac{2S(z_{i,j-1} - z_{i,j})}{\left[\lambda_x^2 + (z_{i,j-1} - z_{i,j})^2\right]^{1/2}} + P_3 W = 0$$

Where:

$P_1$  = plastic strength of the beam, lbs.

$W$  = width of the beam, inches.

The input requirements are given by READ 500 and READ 501. These are identical to the previous requirements except the second data card must now include the strength of the beam and the width of the beam. Initial values of the surface may be read in, as before. Because the point of maximum rise is no longer at the center of the plate, the program saves the point of maximum rise by comparing each point, as it is iterated, and saves the coordinates of the point with the largest Z value. Strains are then computed through this point and average slopes are considered between this point and the edges parallel to both coordinate axis. The point of maximum rise is identified in the output. Average strain in the plastic beam is also given. The large number of minus signs in the maximum change columns indicate the relaxation factor was too high and the program was "overshooting." The shape of membrane derived from this program is shown in Figure B-16.

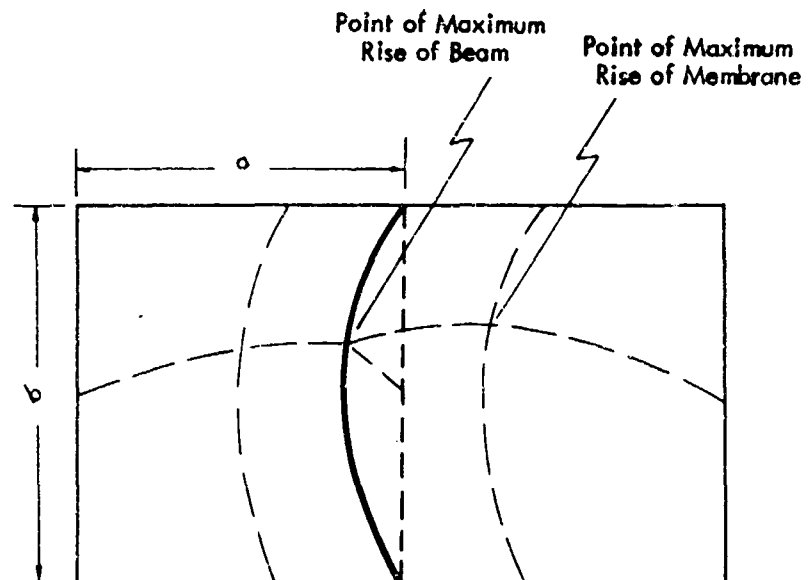


Figure B-16. Plastic Beam Across Center of Membrane

```

*** HANSEN
** PROGRAM IS ITERATIVE
* COMPILE FORTRAN,EXECUTE FORTRAN

C FUNICULAR SHELL. PRESSURE CONSTANT
C DIMENSION Z(66,66)
C ZERO Z(I,J) BAND
1 DO2I=1,66
  DO2J=1,66
2 Z(I,J)=0.

C MAX IX = MAX IY = 64
C ICODZ....PUNCH COL 10, 1 IF Z(I,J) GIVEN, 2 IF NOT GIVEN
C IX.....NUMBER OF DIVISIONS ALONG DIMA
C IY.....NUMBER OF DIVISIONS ALONG DIMB
C ITERL....MAXIMUM ITERATIONS ALLOWED
C CONVL....CONVERGENCE LIMIT...MAX CHANGE BETWEEN ITERATIONS
C DIMA.....HORIZONTAL DIMENSION OF 1/4 SHELL
C DIMB.....VERTICAL DIMENSION OF 1/4 SHELL
C STRES....STRESS PER LINEAR DISTANCE
C PRES3....PRESSURE PER UNIT AREA
C PHI.....RELAXATION FACTOR...USE 1.7 FOR AN 8 BY 8 GRID
C ITER.....ITERATIONS COMPLETED
C Z(I,J)...RISE AT POINT I,J
C TCON2....MAX CHANGE BETWEEN THIS ITER AND LAST
C IP,JP....POINT OF MAX CHANGE
C PS.....PRESSURE OVER STRESS RATIO
C STNSX....AVE. PERCENT STRAIN OF SHELL THROUGH POINT OF MAX RISE
C          AT X=J, COMPUTED AS 100 TIMES (ARC LENGTH - DIMB)/DIMB
C STNSY....AVE. PERCENT STRAIN OF SHELL THROUGH POINT OF MAX RISE
C          AT Y=I, COMPUTED AS 100 TIMES (ARC LENGTH - DIMA)/DIMA
C XLAM.....MESH SIZE ALONG DIMA
C YLAM.....MESH SIZE ALONG DIMB
C INPUT
  READ500,IDENT,ICODZ,IX,IY,ITERL,CONVL,PHI
500 FORMAT(5I10,2F10.0)
  READ 501,DIMA,DIMB,STRES,PRES3
501 FORMAT(4F10.0)
  PRINT 599,IDENT
599 FORMAT(16H1FUNICULAR SHELL/18H IDENTIFICATION...I3/)
  PRINT 600
600 FORMAT(49H ITER CENTER DEFLECTION MAX CHANGE IN SHELL/)
C COMPUTE ARRAY SIZE
  M=IX+1
  N=IY+1
C CHECK TO SEE IF INITIAL Z(I,J) ARE GIVEN
  IF(ICODZ-1)999,3,4
3 READ 502,((Z(I,J),J=1,M),I=1,N)
502 FORMAT (8F10.0)
4 XI=IX
  YI=IY
  XLAM=DIMA/XI
  YLAM=DIMB/YI
  ITER=1
10 I=2
  J=2
  TCON2=0
  ICSWH=1
  ISWCH=1
  GO TO 100
101 J=J+1
  IF(M-J)11,12,100

```

```

12 Z(I,J+1)=Z(I,J-1)
   GO TO 100
11 I=I+1
   J=2
   IF(N-I)999,15,100
15 ISWCH=2
   Z(I+1,J)=Z(I-1,J)
   GO TO 100
102 J=J+1
   IF(M-J)200,20,21
20 Z(I,J+1)=Z(I,J-1)
   Z(I+1,J)=Z(I-1,J)
   GO TO 100
21 Z(I+1,J)=Z(I-1,J)
   GO TO 100
C   COMPUTATION PHASE
C   COMPUTE NEW Z(I,J)
100 A=Z(I,J+1)-Z(I,J-1)
   B=Z(I+1,J)-Z(I-1,J)
   C=Z(I+1,J)-2.*Z(I,J)+Z(I-1,J)
   D=Z(I,J+1)-2.*Z(I,J)+Z(I,J-1)
   E=Z(I+1,J+1)-Z(I-1,J+1)-Z(I+1,J-1)+Z(I-1,J-1)
   F=(4.*XLAM**2+A**2)*C-.5*A**2*E+(4.*YLAM**2+B**2)*D
   G=PRES3/(STRES*2.*XLAM*YLAM)*(4.*XLAM**2*YLAM**2+XLAM**2*B**2
   +YLAM**2*A**2)**1.5
   H=2.*(4.*XLAM**2+A**2+4.*YLAM**2*B**2)
   T=Z(I,J)+PHI*(F+G)/H
   PS=PRES3/STRES
C   SET UP CONVERGENCE CHECK
   TCON1=T-Z(I,J)
   IF(ABSF(TCON1)-CONVL)111,111,107
107 ICSWH=2
111 IF(ABSF(TCON1)-ABSF(TCON2))106,106,108
108 TCON2=TCON1
   IP=I
   JP=J
106 Z(I,J)=T
C   FIND RETURN STATEMENT
109 GO TO (101,102),ISWCH
C   CHECK CONVERGENCE
200 GO TO (203,202),ICSWH
C   CHECK ITERATIONS
202 IF(ITERL-ITLR)203,204,204
C   DATA TO BE PRINTED OUT EACH ITERATION
204 PRINT610,ITER,Z(N,M),IP,JP,TCON2
610 FORMAT(I5,F18.5,10H          Z(I2,1H,I2,2H)=F9.5)
C   CHECK AVERAGE SLOPE AT POINT OF MAX RISE
   IF(1.-Z(N,M)/DIMB)29,29,35
35 IF(1.-Z(N,M)/DIMB)29,29,30
29 PRINT 611
611 FORMAT(64H AVERAGE SLOPE EXCEEDS 1 TO 1, EQUATIONS DIVERGE PAST TH
   11S POINT)
   GO TO 203
C   ITERATE AGAIN
30 ITER=ITER+1
   GO TO 10
C   COMPUTE STRAIN AT X=A
203 I=1
   J=M
   ARC=0.
31 ARC1=SQRTF(YLAM**2+(Z(I+1,J)-Z(I,J))**2)

```

```

ARC=ARC+ARC1
I=I+1
IF(N-I)999,32,31
32 STNSX=(ARC-DIMB)/DIMB*100.
C COMPUTE STRAIN AT Y=B
I=N
J=1
ARC=0.
33 ARC1=SQRTF(XLAM**2+(Z(I,J+1)-Z(I,J))**2)
ARC=ARC+ARC1
J=J+1
IF(M-J)999,34,33
34 STNSY=(ARC-DIMA)/DIMA*100.
PRINT 610,ITER,Z(N,M),IP,JP,TCON2
PRINT 599,IDENT
PRINT 609,PHI
609 FORMAT(17H RELAX. FACTOR...F10.5)
PRINT 612,N,STNSY,M,STNSX
612 FORMAT(16H STRAIN ALONG I=12,4H IS F5.2,18H STRAIN ALONG J=12,
14H IS F5.2)
PRINT 601,PKES3
601 FORMAT(17H PRESSURE.....F10.5)
PRINT 602,STRES
602 FORMAT(17H SHELL STRENGTH..F10.5)
PRINT 603,PS
603 FORMAT(17H P/S.....F10.5)
PRINT 604,XLAM,DIMA
604 FORMAT(17H LAMDA X.....F10.5,20H A.....F10.5)
PRINT 605,YLAM,DIMB
605 FORMAT(17H LAMDA Y.....F10.5,20H B.....F10.5)
PRINT 606,IX,IY
606 FORMAT(17H GRID SIZE.....I3,4H BYI3)
PRINT 607
607 FORMAT(26H QZ DISTANCES FOR 1/4 SHLLL/)
PRINT 608, ((I,J,Z(I,J),J=1,N),I=1,N)
608 FORMAT(5H Z(I2,1H,I2,2H)=F8.5,5H Z(I2,1H,I2,2H)=F8.5,
1 5H Z(I2,1H,I2,2H)=F8.5,5H Z(I2,1H,I2,2H)=F8.5,
2 5H Z(I2,1H,I2,2H)=F8.5,5H Z(I2,1H,I2,2H)=F8.5)
C READ NEXT DATA
GO TO 1
999 END

```

Plastic Beams Across Two Parallel Edges. The same differential equation governs these beams. It should be noted that the differential equation considers only a symmetrical case about the beam. Thus, in this instance, the membrane is computed as though there were an infinite set of such membranes set end-to-end, each contributing one-half of the force carried by the plastic beam.

Input requirements are identical to the case of a plastic beam across the center of the membrane. The shape derived by this program is given in Figure B-17.

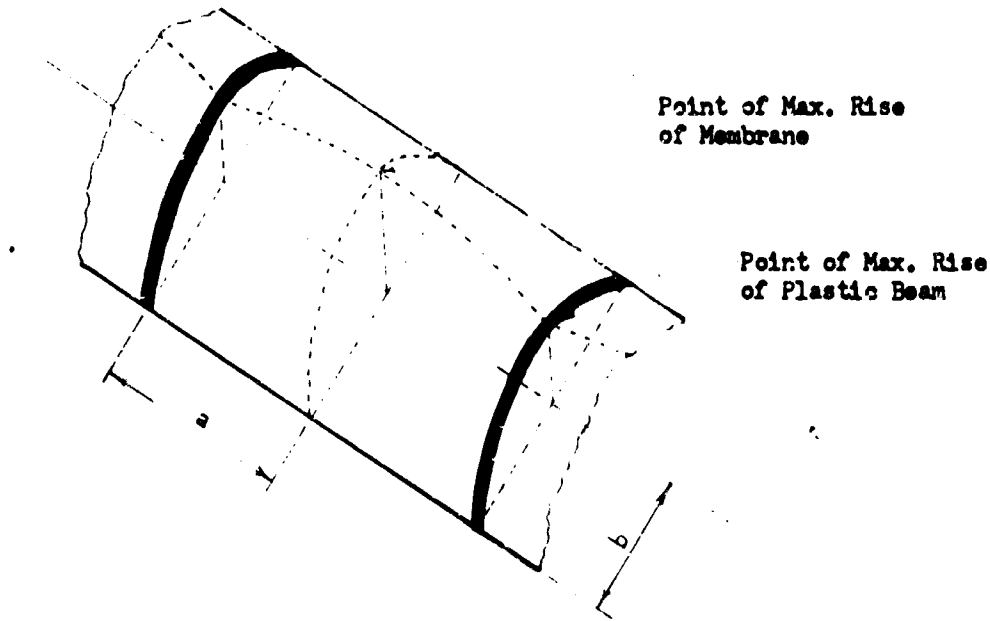


Figure B-17. Plastic Beams Across Two Parallel Edges

```

*** HANSEN
** PROGRAM IS ITERATIVE
* COMPILER FORTRAN, EXECUTE FORTRAN

C FUNICULAR SHELL, PRESSURE CONSTANT
C RESTRAINING BAND ACROSS X=DIMA
C DIMENSION Z(66,66)
C ZERO Z(I,J) BAND
1 DO2I=1,66
  DO2J=1,66
2 Z(I,J)=0.
C MAX IX = MAX IY = 64
C ICODZ....PUNCH COL 10, 1 IF Z(I,J) GIVEN, 2 IF NOT GIVEN
C IX.....NUMBER OF DIVISIONS ALONG DIMA
C IY.....NUMBER OF DIVISIONS ALONG DIMB
C ITERL....MAXIMUM ITERATIONS ALLOWED
C CONVL....CONVERGENCE LIMIT...MAX CHANGE BETWEEN ITERATIONS
C DIMA.....HORIZONTAL DIMENSION OF 1/4 SHELL
C DIMB.....VERTICAL DIMENSION OF 1/4 SHELL
C STRES....STRESS PER LINEAR DISTANCE
C PRES3....PRESSURE PER UNIT AREA
C PHI.....RELAXATION FACTOR...USE 1.7 FOR AN 8 BY 8 GRID
C STRNB....YIELD FORCE OF BEAM, POUNDS
C ITER.....ITERATIONS COMPLETED
C Z(I,J)...RISE AT POINT I,J
C TCON2....MAX CHANGE BETWEEN THIS ITER AND LAST
C IP,JP....POINT OF MAX CHANGE
C PS.....PRESSURE OVER STRESS RATIO
C STRBX....AVE. PERCENT STRAIN OF RESTRAINING BAND (BEAM) AT X=DIMA
C          COMPUTED AS 100 TIMES (ARC LENGTH - DIMB)/DIMB
C STRSX....AVE. PERCENT STRAIN OF SHELL THROUGH POINT OF MAX RISE
C          AT X=J, COMPUTED AS 100 TIMES (ARC LENGTH - DIMB)/DIMB
C STRBY....AVE. PERCENT STRAIN OF SHELL THROUGH POINT OF MAX RISE
C          AT Y=I, COMPUTED AS 100 TIMES (ARC LENGTH - DIMA)/DIMA
C XLAM....MESH SIZE ALONG DIMA
C YLAM....MESH SIZE ALONG DIMB
C INPUT
  READ 500,IDENT,ICODZ,IX,IY,ITERL,CONVL,PHI
500 FORMAT(5I10,2F10.0)
  READ 501,DIMA,DIMB,STRES,PRES3,STRNB,WIDTH
501 FORMAT(6F10.0)
  PRINT 599,IDENT
599 FORMAT(4PHIFUNICULAR SHELL, RESTRAINING BAND ACROSS X=DIMA/18H IDENTIFICATION...I3/)
  PRINT 600
600 FORMAT(75H ITER    CENTER DEFLECTION    MAX CHANGE IN SHELL
1 MAX CHANGE IN BEAM/)
C COMPUTE ARRAY SIZE
  M=IX+1
  N=IY+1
C CHECK TO SEE IF INITIAL Z(I,J) ARE GIVEN
  IF(ICODZ-1)999,3,4
3 READ 502,((Z(I,J),J=1,M),I=1,N)
502 FORMAT(3F10.0)
4 XI=IX
  YI=IY
  XLAM=DIMA/XI
  YLAM=DIMB/YI
  ITER=1
10 I=2
  J=2

```

```

TCON2=0
TCON4=0.
RISE2=0.
ICSWH=1
ISWCH=1
GO TO 100
101 J=J+1
    IF(IX-J)11,100,100
11 I=I+1
    J=2
    IF(N-I)999,15,100
15 ISWCH=2
    Z(I+1,J)=Z(I-1,J)
    GO TO 100
102 J=J+1
    IF(IX-J)150,21,21
21 Z(I+1,J)=Z(I-1,J)
    GO TO 100
C   COMPUTATION PHASE
C   COMPUTE NEW Z(I,J)
100 A=Z(I,J+1)-Z(I,J-1)
    B=Z(I+1,J)-Z(I-1,J)
    C=Z(I+1,J)-2.*Z(I,J)+Z(I-1,J)
    D=Z(I,J+1)-2.*Z(I,J)+Z(I,J-1)
    E=Z(I+1,J+1)-Z(I-1,J+1)-Z(I+1,J-1)+Z(I-1,J-1)
    F=(4.*XLAM**2+A**2)*C-.5*A*B*E+(4.*YLAM**2+B**2)*D
    G=PRES3/(STRES**2.*XLAM*YLAM)*(4.*XLAM**2*YLAM**2+XLAM**2*B**2
1+YLAM**2*A**2)**1.5
    H=2.*(4.*XLAM**2+A**2+4.*YLAM**2+B**2)
    T=Z(I,J)+PHI*(F+G)/H
    PS=PRES3/STRES
C   SAVE POINT OF MAX RISE
    IF(T-RISE2)23,23,22
22 RISE2=T
    IPS=I
    JPS=J
C   SET UP CONVERGENCE CHECK
23 TCON1=T-Z(I,J)
    IF(ABSF(TCON1)-CONVL)111,111,107
107 ICSWH=2
111 IF(ABSF(TCON1)-ABSF(TCON2))106,106,108
108 TCON2=TCON1
    IP=I
    JP=J
106 Z(I,J)=T
C   FIND RETURN STATEMENT
109 GO TO (101,102),ISWCH
C   COMPUTE BEAM
150 I=2
    J=M
155 AB=Z(I,J-1)-Z(I,J)
    CB=Z(I+1,J)-2.*Z(I,J)+Z(I-1,J)
    BB=Z(I+1,J)-Z(I-1,J)
    DB=(4.*YLAM**2+BB**2)**1.5
    FB=2.*STRES*AB/SQRT(XLAM**2+AB**2)
    GB=8.*STRES*YLAM*CB/DB
    GBB=PRES3*W1/DB
    HB=16.*STRES*YLAM/DB
    TB=Z(I,J)+(FB*CB+GBB)/PHI*PHI
C   SET UP CONVERGENCE CHECK
    TCON3=T-Z(I,J)

```

```

      IF (ABS(F(TCON3)-CONVL))151,151,152
152 ICSWH=2
151 IF (ABS(F(TCON3)-ABS(F(TCON4)))153,153,154
154 TCON4=TCON3
      IPB=I
      JPB=J
153 Z(I,J)=TB
      I=I+1
      IF(N-I)200,156,155
156 Z(I+1,J)=Z(I-1,J)
      GO TO 155
C      CHECK CONVERGENCE
200 GO TO (203,202),ICSWH
C      CHECK ITERATIONS
202 IF(ITERL-ITER)203,204,204
C      DATA TO BE PRINTED OUT EACH ITERATION
204 PRINT610,ITER,Z(N,M),IP,JP,TCON2,IPB,JPB,TCON4
610 FORMAT(I5,F18.5, 10H          Z( I2, 1H, I2, 2H)= F9.5,
      1          10H          Z( I2, 1H, I2, 2H)= F9.5)
C      CHECK AVERAGE SLOPE AT POINT OF MAX RISE
      I=IPS
      J=JPS
      XJ=J-1
      IF(1.-Z(I,J)/(XJ*YLAM))29,29,35
35 XI=I-1
      IF(1.-Z(I,J)/(XI*XLAM))29,29,30
29 PRINT611
611 FORMAT(64H AVERAGE SLOPE EXCEEDS 1 TO 1, EQUATIONS DIVERGE PAST TH
      1 IS POINT)
      GO TO 203
C      ITERATE AGAIN
30 ITER=ITER+1
      GO TO 10
C      COMPUTE STRAIN IN BEAM
203 I=1
      J=M
      ARC=0.
31 ARC1=SQRTF(YLAM**2+(Z(I+1,J)-Z(I,J))**2)
      ARC=ARC+ARC1
      I=I+1
      IF(N-I)299,32,31
32 STNBX=(ARC-DIMB)/DIMB*100.
C      COMPUTE MAX STRAIN IN SHELL AT X= CONSTANT
      I=1
      J=JPS
      ARC=0.
33 ARC1=SQRTF(YLAM**2+(Z(I+1,J)-Z(I,J))**2)
      ARC=ARC+ARC1
      I=I+1
      IF(N-I)299,34,33
34 STNSX=(ARC-DIMB)/DIMB*100.
C      COMPUTE MAX STRAIN IN SHELL AT Y=CONSTANT
      I=IPS
      J=1
      ARC=0.
35 ARC1=SQRTF(XLAM**2+(Z(I,J+1)-Z(I,J))**2)
      ARC=ARC+ARC1
      J=J+1
      IF(M-J)299,37,36
37 STNSY=(ARC-DIMA)/DIMA*100.
      PRINT610,ITER,Z(N,M),IP,JP,TCON2,IPB,JPB,TCON4

```

```

PRINT599,IDENT
PRINT 609,PHI
609 FORMAT(17H RELAX. FACTOR...F10.5)
PRINT 612,IPS,STNSY,JPS,STNSX
612 FORMAT(16H STRAIN ALONG I=I2,4H IS F5.2,18H STRAIN ALONG J=I2,
14H IS F5.2)
PRINT 601,PRES3,STNBX
601 FORMAT(17H PRESSURE.....F10.5,20H STRAIN IN BEAM...F10.5)
PRINT 602,STRES,STRNB
602 FORMAT(17H SHELL STRENGTH..F10.5,20H BEAM STRENGTH....F10.5)
PRINT 603,PS,WIDTH
603 FORMAT(17H P/S.....F10.5,20H BEAM WIDTH .....F10.5)
PRINT 604,XLAM,DIMA
604 FORMAT(17H LAMDA X.....F10.5,20H A.....F10.5)
PRINT605,YLAM,DIMB
605 FORMAT(17H LAMDA Y.....F10.5,20H B.....F10.5)
PRINT 606,IX,IY
606 FORMAT(17H GRID SIZE.....I3,4H BYI3)
PRINT 607
607 FORMAT(26H0Z DISTANCES FOR 1/4 SHELL/)
PRINT 608, ((I,J,Z(I,J),J=1,M),I=1,N)
608 FORMAT(5H Z(I2,1H,I2,2H)=F8.5,5H Z(I2,1H,I2,2H)=F8.5,
1 5H Z(I2,1H,I2,2H)=F8.5,5H Z(I2,1H,I2,2H)=F8.5,
2 5H Z(I2,1H,I2,2H)=F8.5,5H Z(I2,1H,I2,2H)=F8.5)
C READ NEXT DATA
GO TO 1
999 END

```

## APPENDIX C

### SOIL STRUCTURE INTERACTION

#### Introduction

The yielding membrane elements, in addition to being efficient structural diaphragms in themselves, bring about favorable soil-structure interaction behavior. This Appendix presents background into the qualitative aspects of this behavior and suggests probable magnitudes of ultimate attenuation of blast overpressures that could result from these interactions.

#### Soil-Structure Interaction Forces

Soil-structure interaction forces are those forces which act at the interface between a buried structure and the surrounding soil medium. These are generally considered to be normal pressures but, to be sure, shearing forces also exist at this interfacial junction.

Normal forces result from pressures which act normally to the interfacial surface are generally in the same order of magnitude as the surface overpressures in the air medium above the ground surface. Shearing forces are those forces which act tangential to the interfacial surface and generally are in the same order of magnitude as the respective shearing forces in the soil under these conditions. In general, the normal forces produce the greater effect or response in the structure; because of this fact, discussion will be limited to the action of structures under this interaction component only.

#### Effective Soil-Structure Interaction Pressures

The effective soil-structure interaction pressure is defined as that normal pressure distribution which at a given instant will produce a static free-field deformation in the structure equal to the deformation of the structure in the soil medium at the same instant. It follows then, if we can neglect the shearing components of interaction forces, that the moments and stresses under this effective pressure will equal those in the confined structure at the same instant.

Effective soil-structure interaction pressures depend upon the characteristics and homogeneity of the soil, the nature of the loading, and the stiffness and geometry of the buried structure with relation to the surrounding soil.

#### Types of Buried Structures

Because the type of buried structure has so much effect on the nature of magnification or attenuation of the passing overpressure, it is appropriate to consider these types in some detail. The three basic types, into which categories most buried structures fall, are the rigid, rigid-flexible, and flexible types. Figure C-1 shows examples of these types of structures.

Rigid Buried Structures. Rigid buried structures are those buried structures which by definition undergo negligible deformation upon loading. As a result of their rigidity, they have certain peculiarities of interaction behavior which will be discussed in more detail later.

Rigid-Flexible Buried Structures. A rigid-flexible structure is one which by definition exhibits rigid characteristics until some time in its rising loading cycle at which point it yields or flexes in such a manner so as to reduce its volume or alter its shape considerably.

Flexible Buried Structures. Flexible buried structures are those structures which by definition exhibit yielding or other noticeable structural deformation immediately on the first sign of an overload. They continue this yielding or reduction in volume behavior throughout the rising loading cycle.

#### Settlement Ratios

To fully realize the nature of soil-structure interaction phenomena, it is appropriate to consider three basic types of settlement ratios. These are positive, negative, and zero ratios.

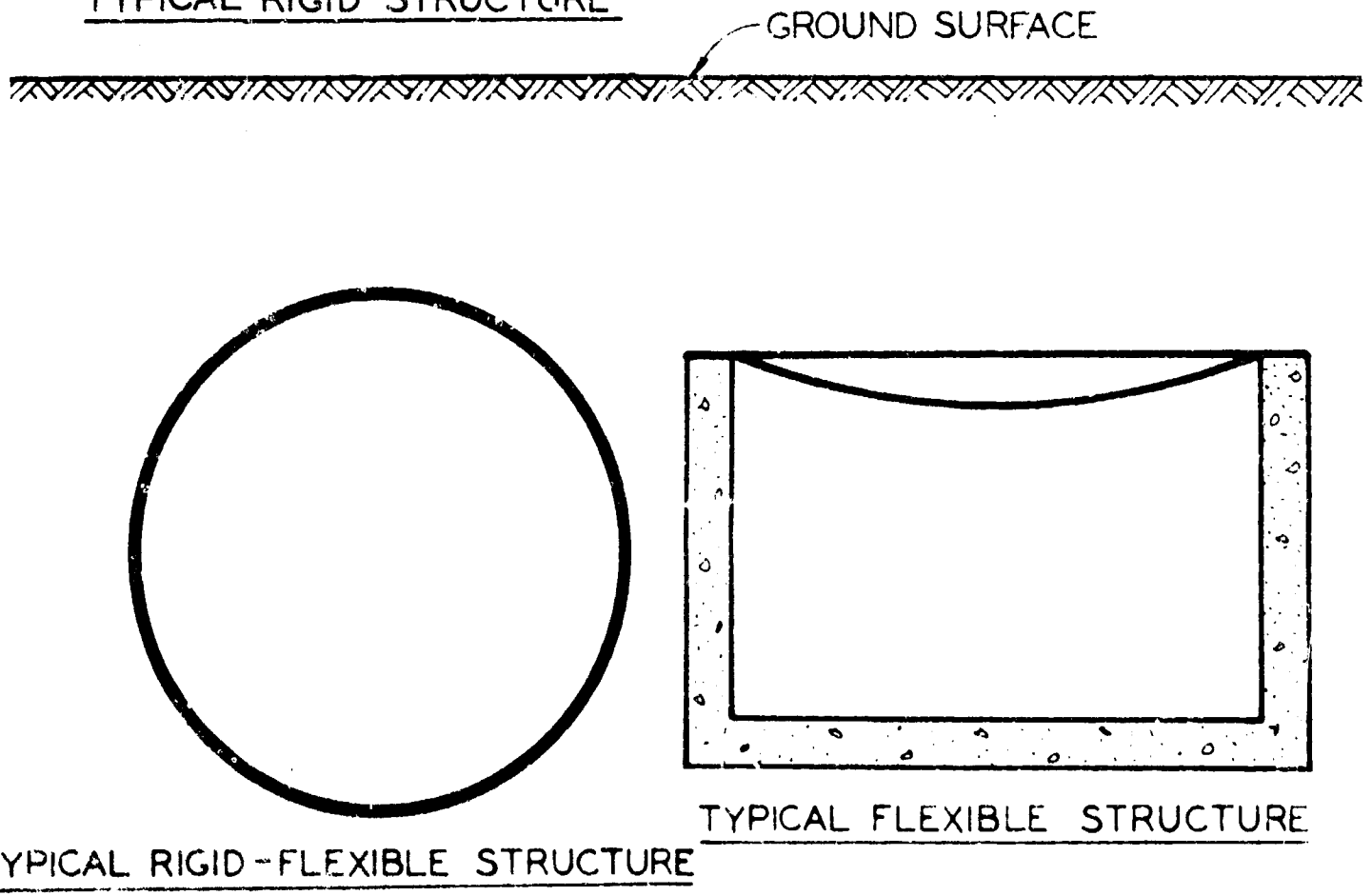
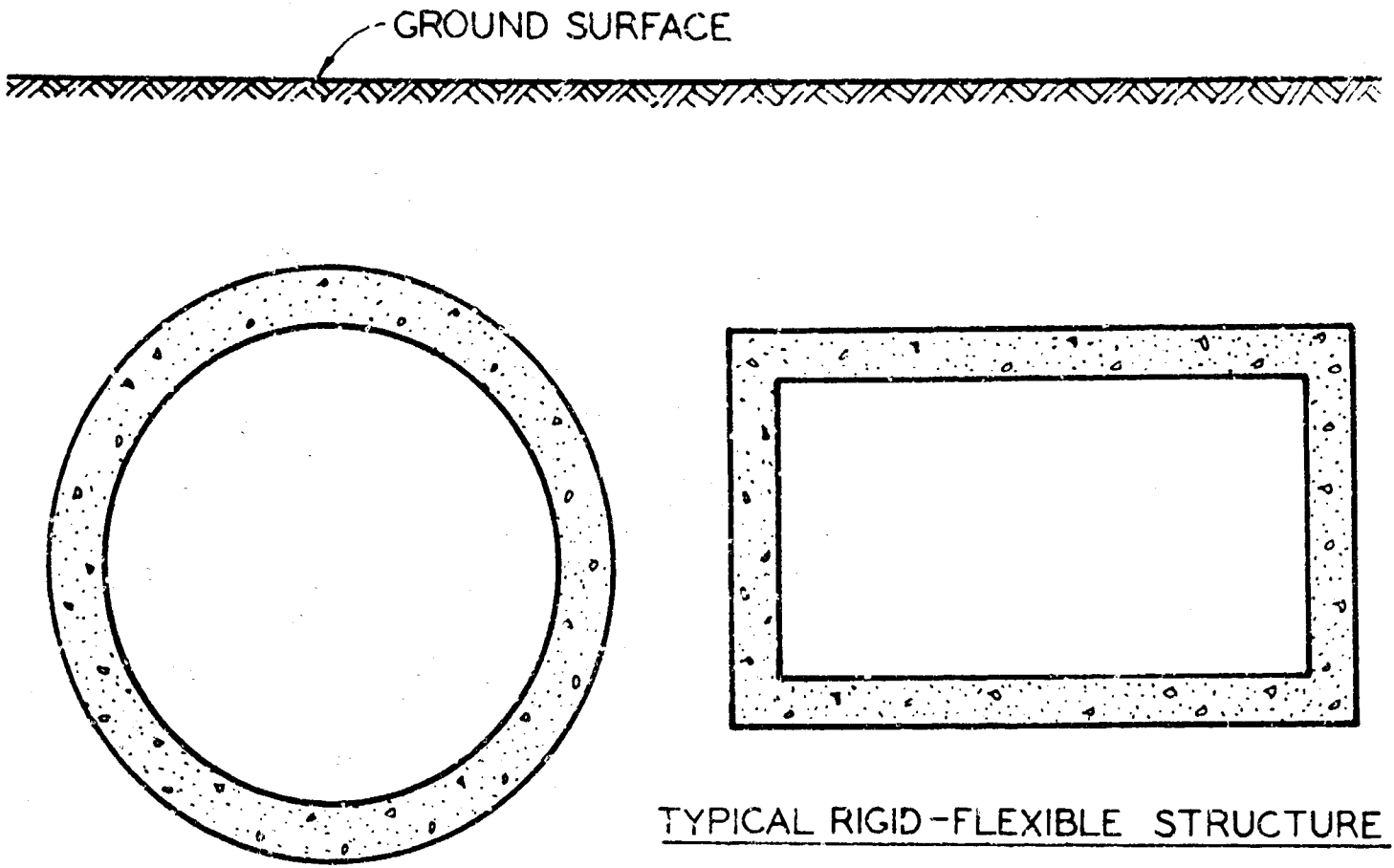


Figure C-1. Typical Buried Structures

The Positive Settlement Ratio. The positive settlement ratio by definition is associated with the change in geometry of the soil mass surrounding a buried structure such that the structure feels a vertical load in excess of the resultant of the dead and live loads immediately overhead.

The concept of positive settlement ratio may be described visually by the idealized drawing in Figure C-2. It will be observed that the soil mass surrounding the structure deflects more than the vertical column of soil in which the structure is contained. As a result of this idealized geometrical discontinuity, vertical shearing forces are produced which add to the load that is normally experienced. The effective soil structure interaction pressure for this situation is then larger than that existing in an undisturbed soil at this same depth. To be sure, this sudden discontinuity does not usually exist and more corbeling action may be observed, however, the overall effect is the same.

Systems which produce positive settlement ratios are generally those which contain rigid structures. These rigid structures increase the overall stiffness of the vertical column of soil in which they are contained. A simplified version of this result is shown in Figure C-3. If we assume a stress-strain relationship such as Hooke's Law to be valid, the left column of soil will deflect an amount  $\Delta L_1$ , where  $\Delta L_1 = pL/E$ . The column of soil on the right, which contains the rigid structure, will deflect an amount  $\Delta L_2 = p(L-D)/E$ , where  $D$  is the height of the rigid structure. These two displacements differ by an amount  $pD/E$ . The first is always greater than the second, all other things being equal. The magnitude of this difference to some extent determines the amount to which the pressure reaching the structure is increased by this geometrical action.

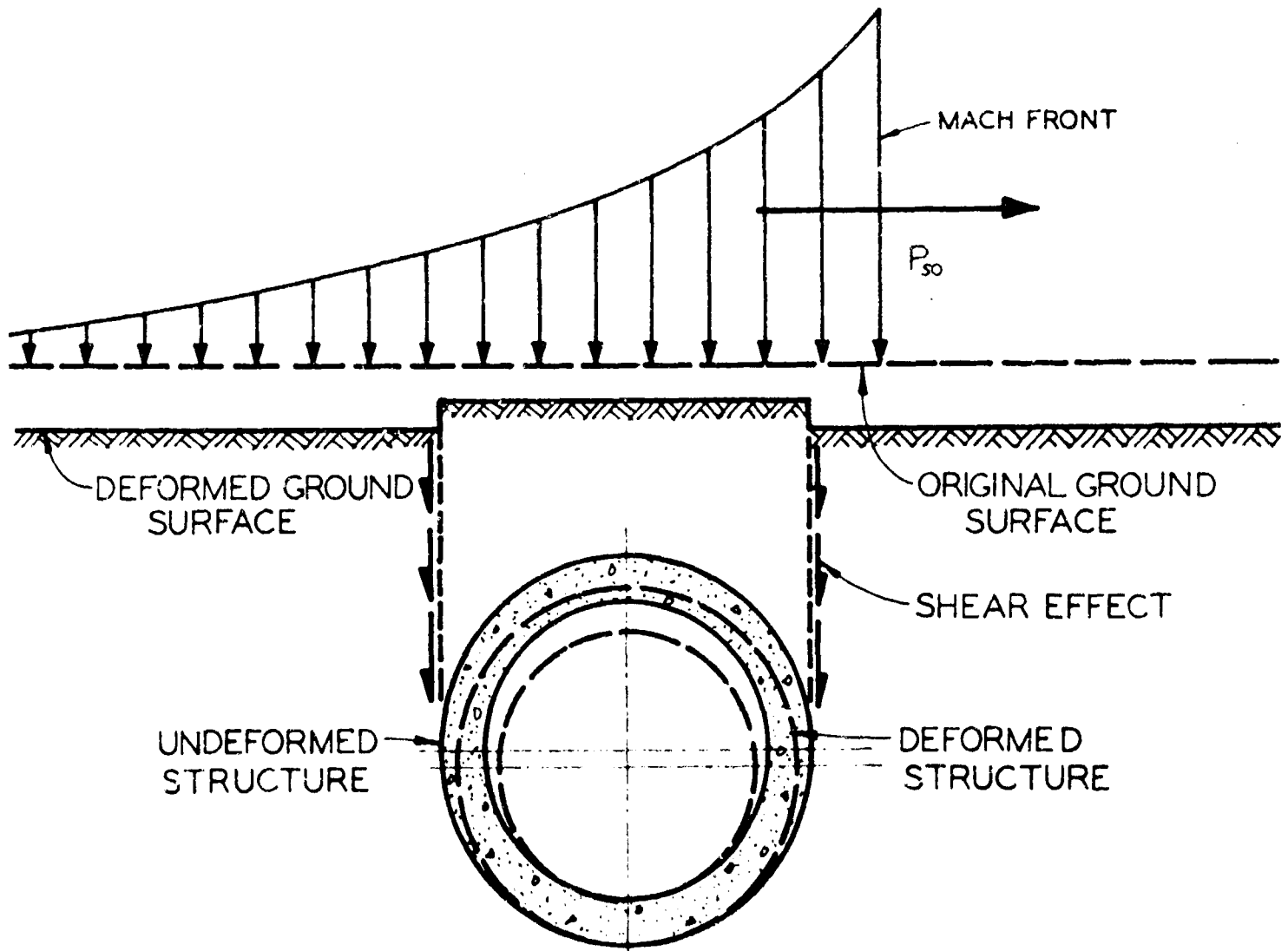


Figure C-2. Idealized Positive Settlement Ratio

The Negative Settlement Ratio. The negative settlement ratio by definition is associated with the change in geometry of the soil mass surrounding a buried structure such that the structure feels a vertical load which is less than the resultant of the dead and live loads immediately overhead.

The negative settlement ratio is shown visually in Figure C-4. It will be observed that the soil mass surrounding the structure deflects less than the vertical column of soil in which the structure is contained. As a result of this idealized geometrical discontinuity, vertical shearing forces are produced which subtract from the load that is normally experienced. The effective soil-structure interaction pressure for this situation is then smaller than that existing in an undisturbed soil at the same depth. As before, the sudden discontinuity does not exist and in reality soil arching takes place but the overall effect is the same.

Systems which produce negative settlement ratios are generally those which contain flexible structures. These flexible structures reduce the overall stiffness of the vertical column of soil in which they are contained. A simplified version of this result is shown in Figure C-5. If the same linear stress-strain relationship is assumed as that previously, the left column of soil will deflect an amount  $\Delta L_1 = pL/E$ , as before. The column of soil on the right, which contains the flexible structure, will deflect an amount  $\Delta L_2 = p(L-D)/E + \Delta D$ . If  $\Delta D$  is greater than  $pD/E$ , then  $\Delta L_2$  will be greater than  $\Delta L_1$ .  $\Delta D$  will always be greater than  $pD/E$  if the structure is more flexible than the soil mass it replaces. Flexible structures by definition are not as stiff as surrounding soil, therefore, they always produce negative settlement ratios.

Zero Settlement Ratio. A zero settlement ratio is defined as being associated with that condition when the surrounding soil mass and the soil column containing the structure deflect equal amounts. Under such conditions, the effective soil structure interaction pressure is equal to that existing in an undisturbed soil medium at the same point. Figure C-6 shows such a condition.

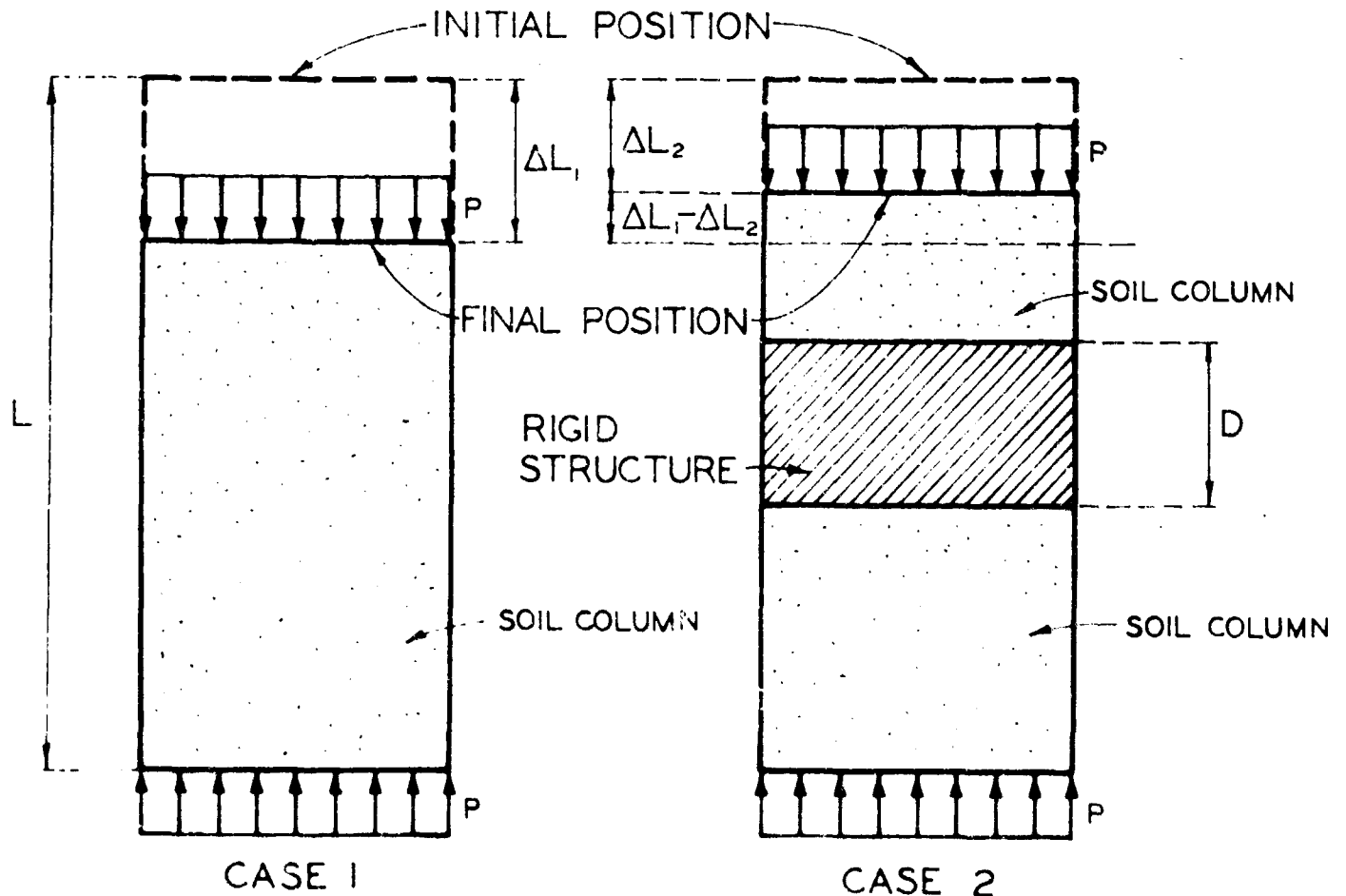


Figure C-3. Positive Settlement Ratio

These systems are those in which the soil and structure possess equal stiffnesses. Certain types of rigid, rigid-flexible, and flexible structures may at some point in their loading cycle exhibit this behavior. In general, such situations rarely happen throughout the entire loading cycle.

Soil-Structure Interactions

Rigid Fully-Buried Structures. Rigid fully-buried structures generally produce positive settlement ratio conditions, and as a result should be designed for pressures in excess of those existing at similar points in undisturbed soils. By definition, a rigid structure is one which undergoes negligible deformation on loading. According to the Air Force Design Manual (AFDM) definition, a fully buried structure is one which is buried sufficiently so that transient effects of shock wave loadings may be neglected. This arch, if corresponding to the fully-buried definition, can only undergo uniform compressive stress by virtue of its uniform pressure loadings. The only bending that can develop is due to the change in curvature associated with the uniform change in radius that results from this idealized loading.

Qualitative aspects of the behavior of this structure under a traveling pressure wave are shown in Figure C-7. At initial contact of the wavefront with the structure, non-uniform pressures are developed. These pressures deform the cylinder immediately with the result that passive earth pressures develop on the sides at right angles to the wavefront. Very rapidly, the situation degenerates or stabilizes into that shown in the later diagrams. Once the pressure is uniform, it then starts to decay somewhat proportional to the decaying surface wave.

A qualitative load-strain diagram for this shape is shown in Figure C-8. Note that such rigid structures generally fail suddenly on overload.

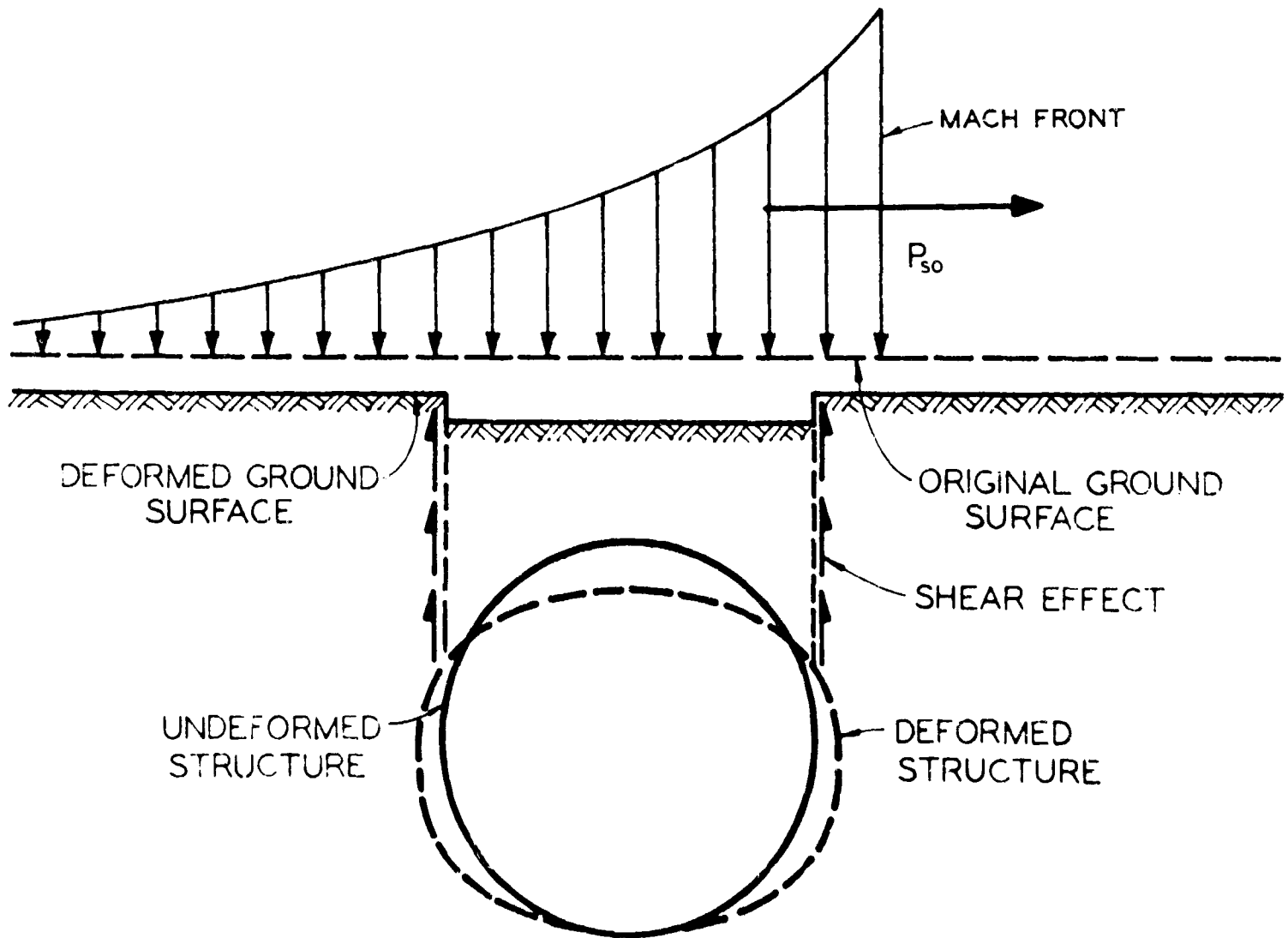


Figure C-4. Idealized Negative Settlement Ratio

**Flexible Buried Structures.** Flexible buried structures exhibit the opposite behavior to rigid structures. Yielding begins almost instantly with sign of overpressure and continues until such has been relieved. These structures contain yielding tension membranes as the roof and floor. Such structures will produce negative settlement ratios which rapidly attenuate blast overpressures.

A qualitative load-strain diagram for this shape is shown in Figure C-9. Note the large strain which follows a low load.

**Rigid-Flexible Buried Structures.** As the name implies, a rigid-flexible structure exhibits the qualities of each type during its loading cycle. As might be expected, positive settlement ratios immediately followed by negative ratios may develop. The qualitative load-strain picture for this structure may be seen in Figure C-10.

This structure is actually ambidextrous in that it may exhibit rigid, flexible, or rigid-flexible behavior depending on the nature of loading, type of backfill procedure, etc. Generally, however, it is quite rigid until either large elastic deformations or buckling takes over. Either of these latter effects are those of a flexible nature. Figure C-11 shows stable yield of this structure. Figure C-12 shows unstable yield.

**Summary of Effects.** The various types of structures, because of their various actions, feel different transmitted pressure waves. These waves, in their different forms, may be seen in Figure C-13. Note the immediate advantages of the rigid-flexible and flexible types.

Analysis Features

The stage has been set, by the previous qualitative discussions, for the statement that quantitative predictions of these soil-structure interaction loads are most difficult. Here we have a statically indeterminate structural problem of the worst type. Very little quantitative results of any kind are available to substantiate reliable magnitude

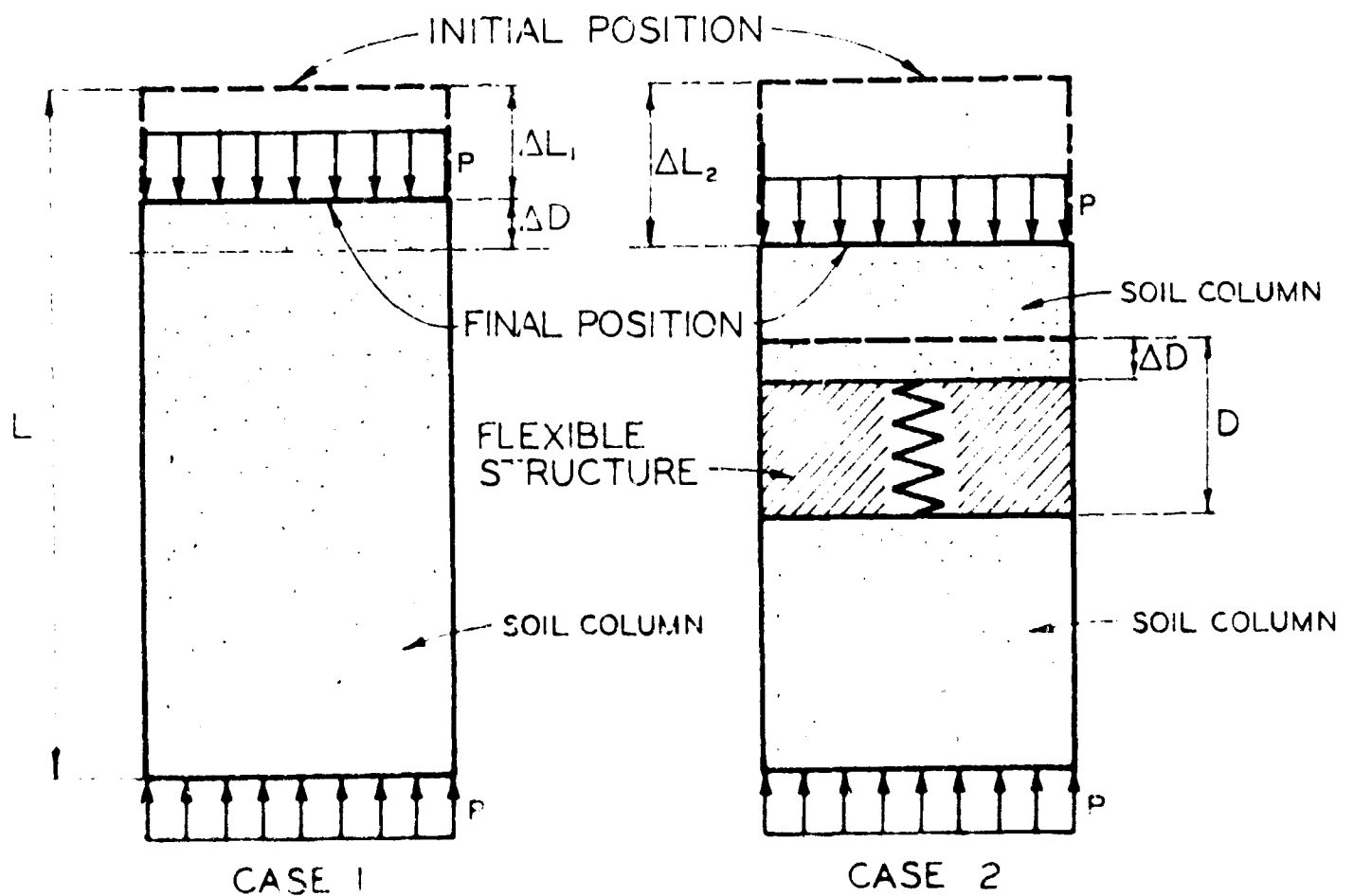


Figure C-5. Negative Settlement Ratio

predictions. There is a particularly intense need for more theoretical and experimental data on the soil-structure interaction phenomenon.

These quantitative predictions are necessary if hopes of meaningful analyses are real. Fortunately, designs may be produced from what limited knowledge we now have, if we are not overly concerned about being conservative.

### Design Features

The ultimate in structural analysis is to find an answer, such as stress and displacement; given a structure, its supports, and its loads. Obviously, for most physical systems there is generally but one answer. The analyst hopes to either find this answer exactly, or gain a close enough approximation so that his answer is acceptable. In short, the analyst is a problem solver. The ultimate in design is to create a given structure, to resist given loads, over given boundaries such that an analysis is not necessary to assure that this structure will perform satisfactorily. In short, then, the designer is a problem avoider.

A qualitative understanding of the general physical behavior of an underground structure, as we have just considered, is not sufficient for analysis. However, such an understanding is sufficient for design. Because so little is known about the quantitative behavior of underground structures, as compared with those above-ground, we

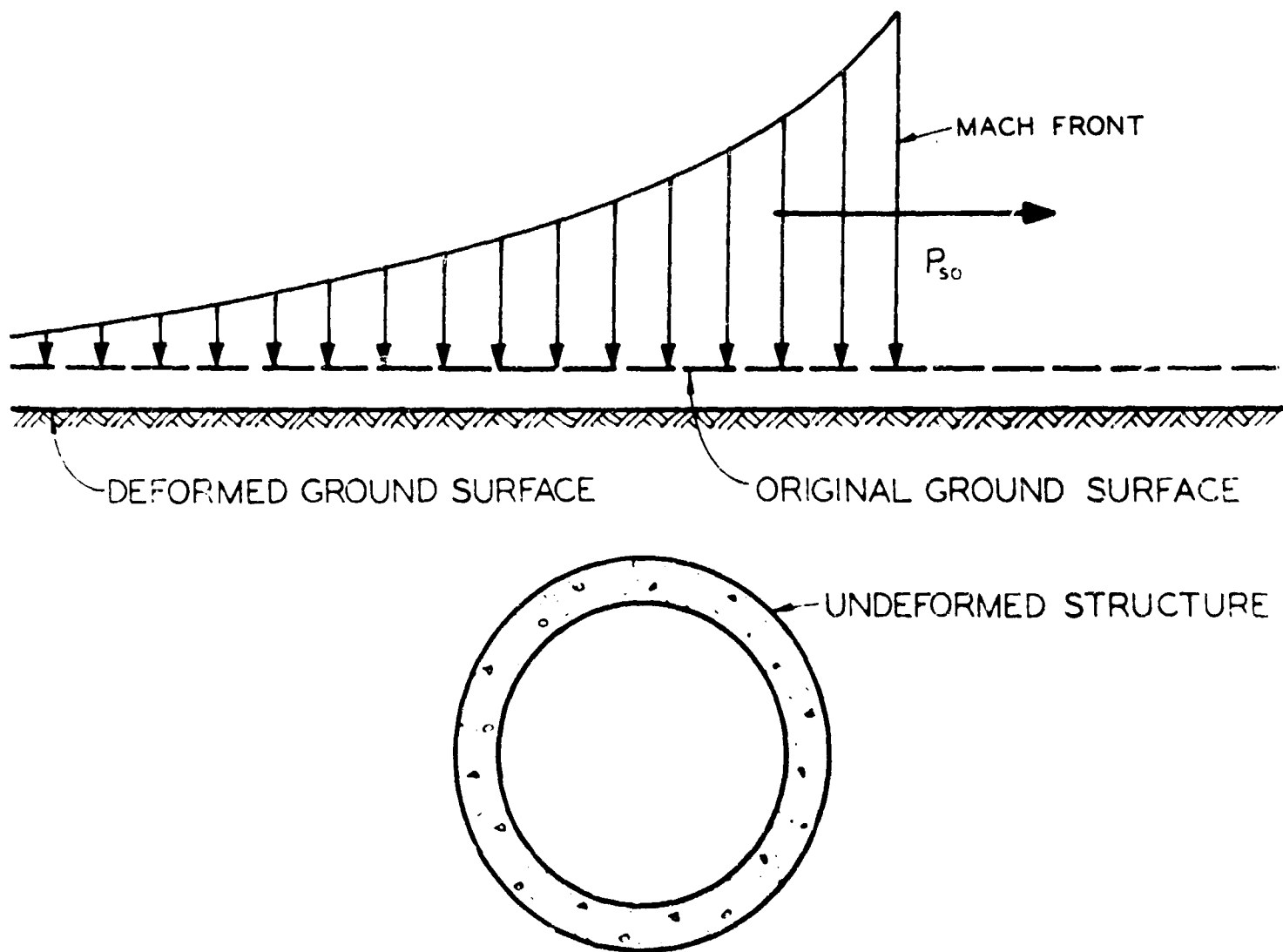


Figure C-6. Zero Settlement Ratio

unavoidably find that our designs are conservative. This is not altogether bad, however, because the source of conservatism is generally found in the supporting strength offered by the soil. For regions in which blast overpressures are considered, close-in fallout and initial radiation will almost assuredly be such that quite a lot of mass will be required for adequate shielding. There is no more economical mass for shielding than earth; and, therefore, in such regions, buried structures make sense from the fallout and radiation standpoint, certainly from the blast resistance standpoint.

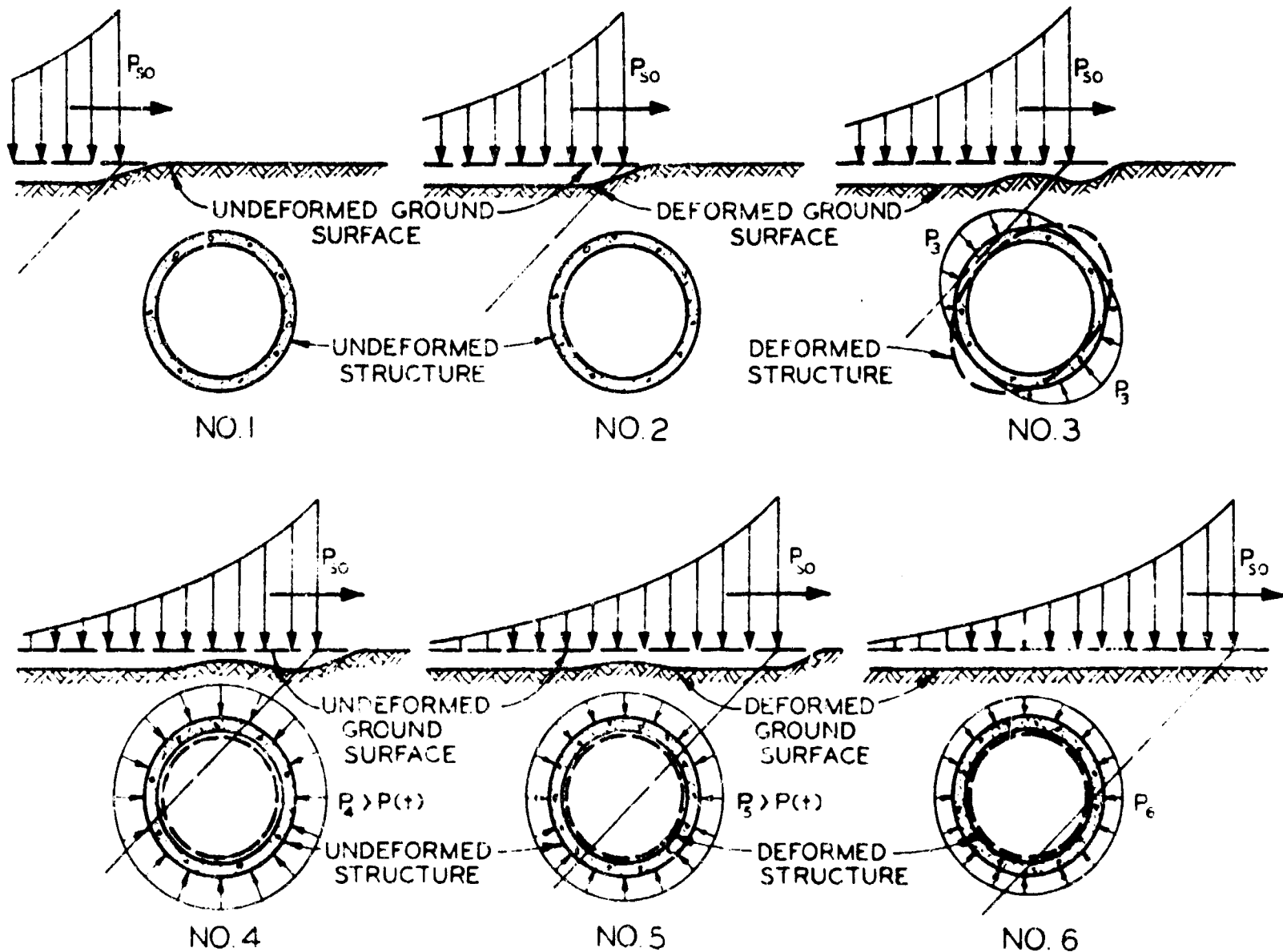


Figure C-7. A Structure Under a Traveling Pressure Wave

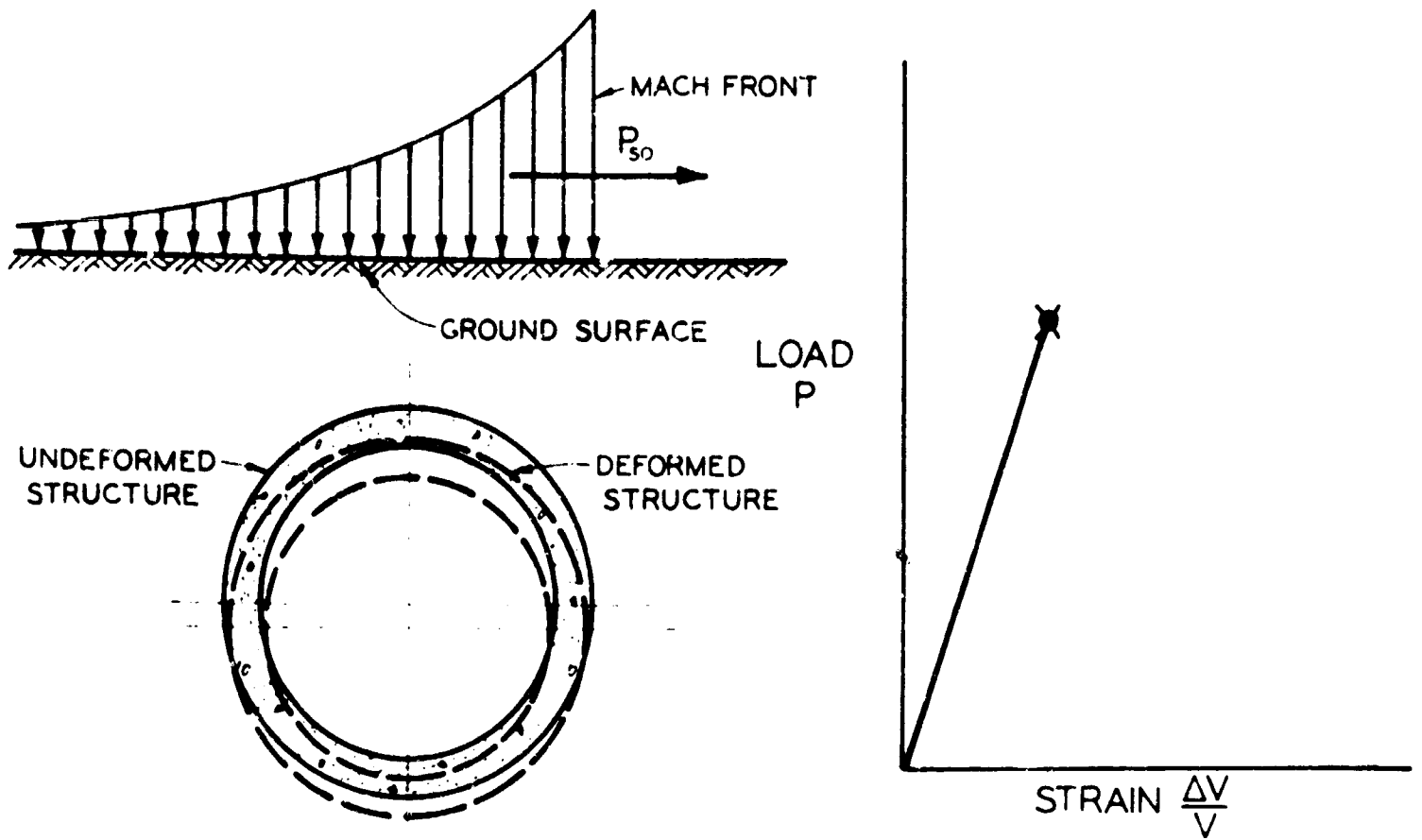


Figure C-8. Qualitative Load-Strain Diagram for Rigid Structures

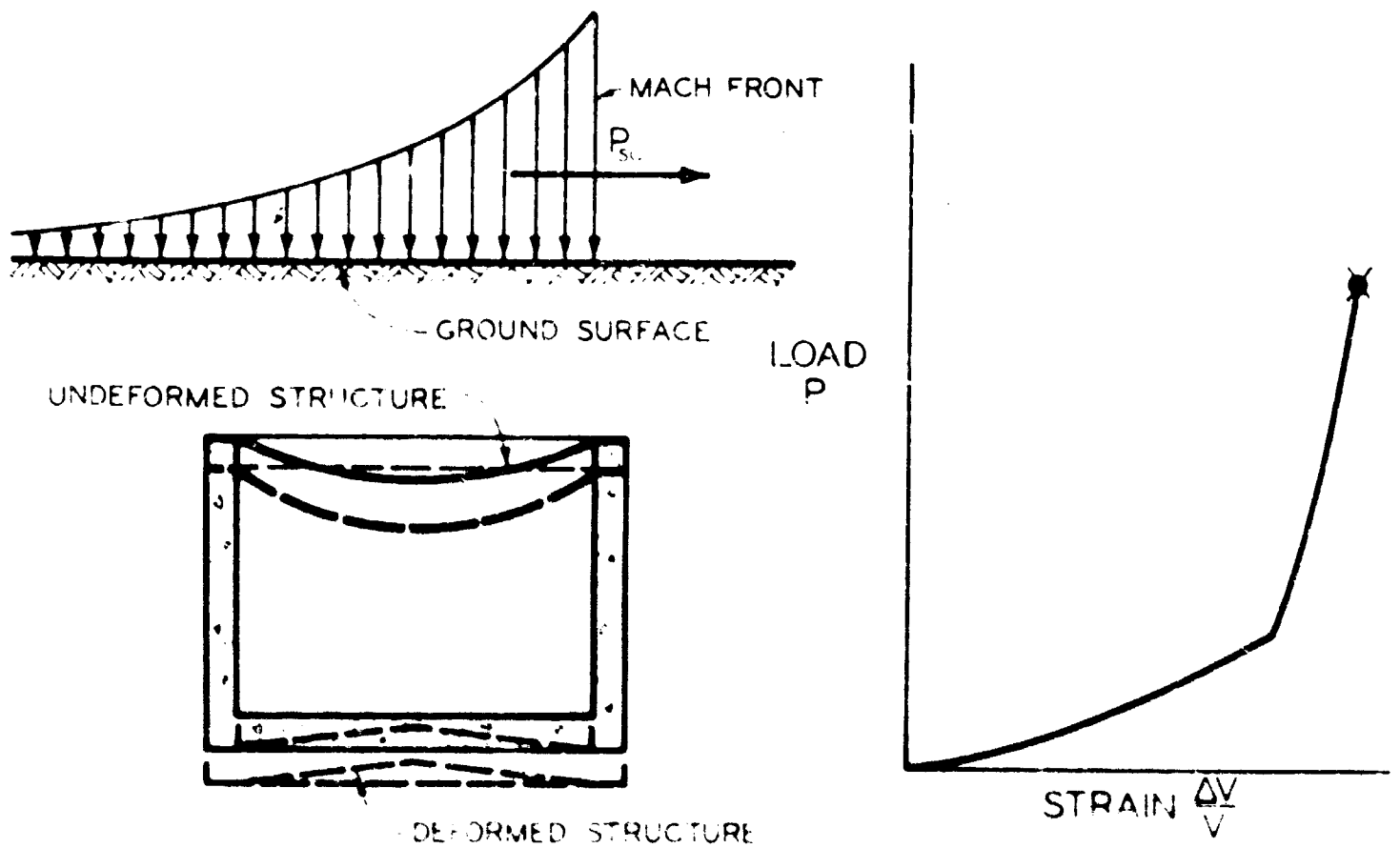


Figure C-9. Qualitative Load-Strain Diagram for Flexible Structures

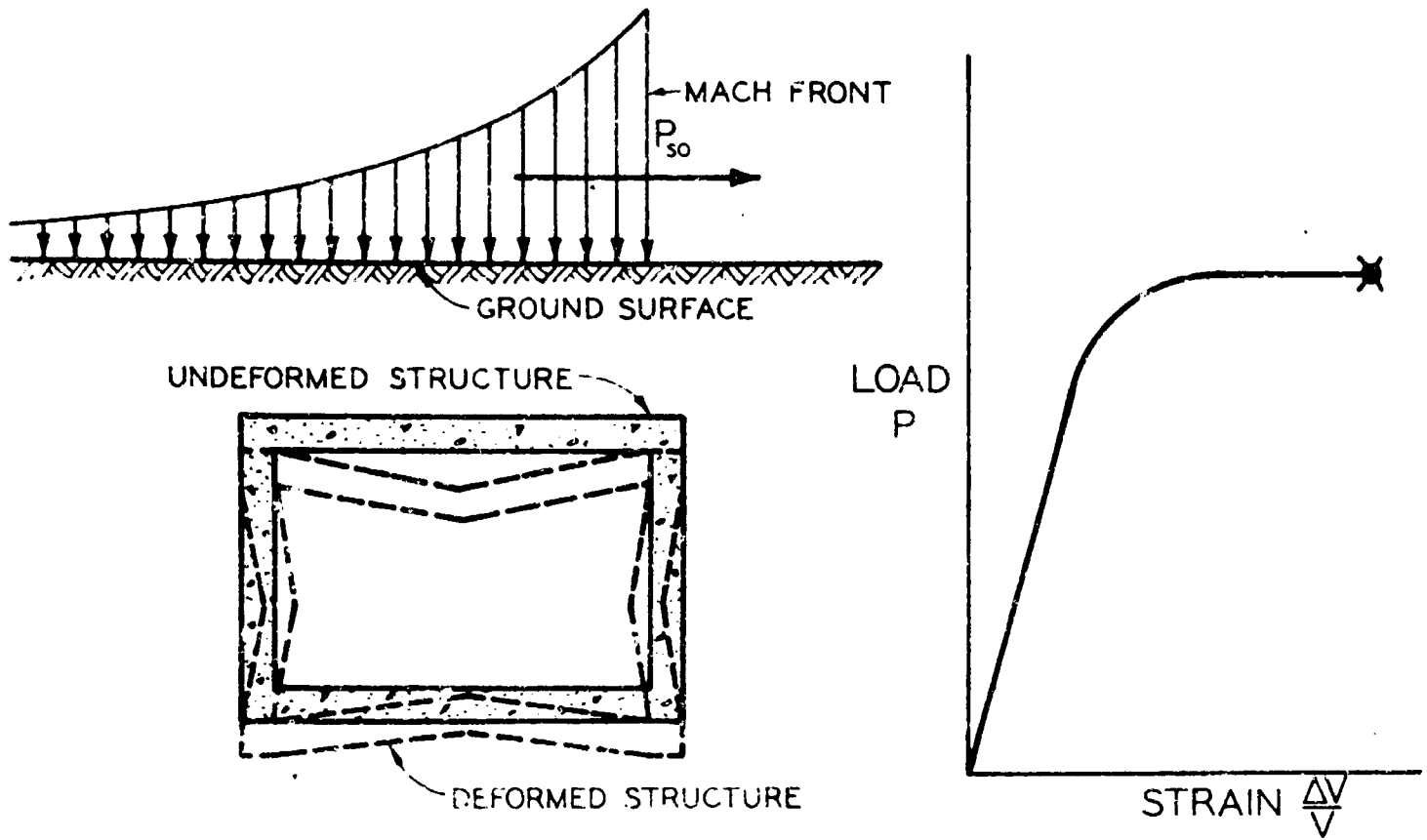


Figure C-10. Qualitative Load-Strain Diagram for Rigid-Flexible Structures

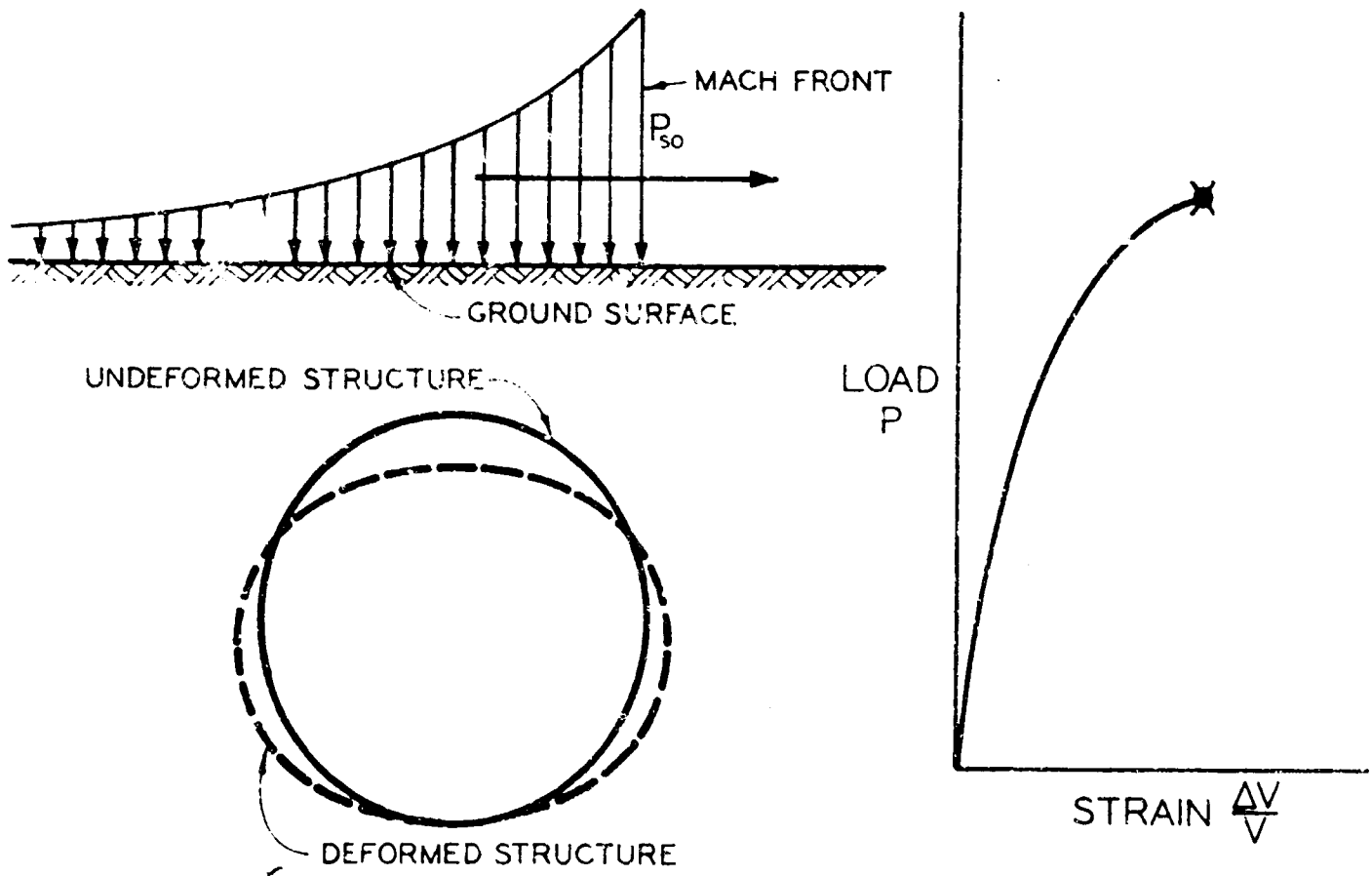


Figure C-11. Stable Yield of Culvert

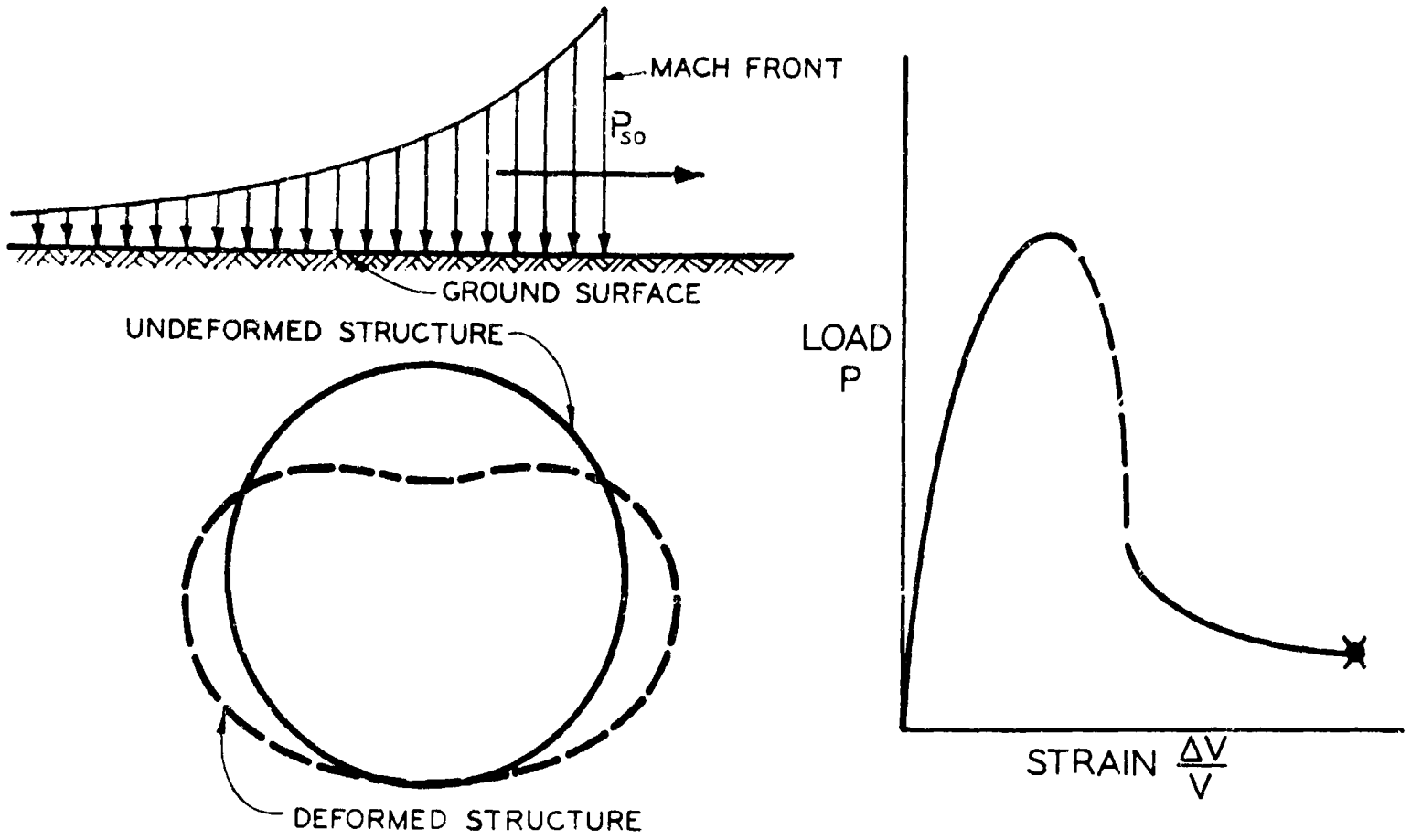


Figure C-12. Unstable Yield of Culvert

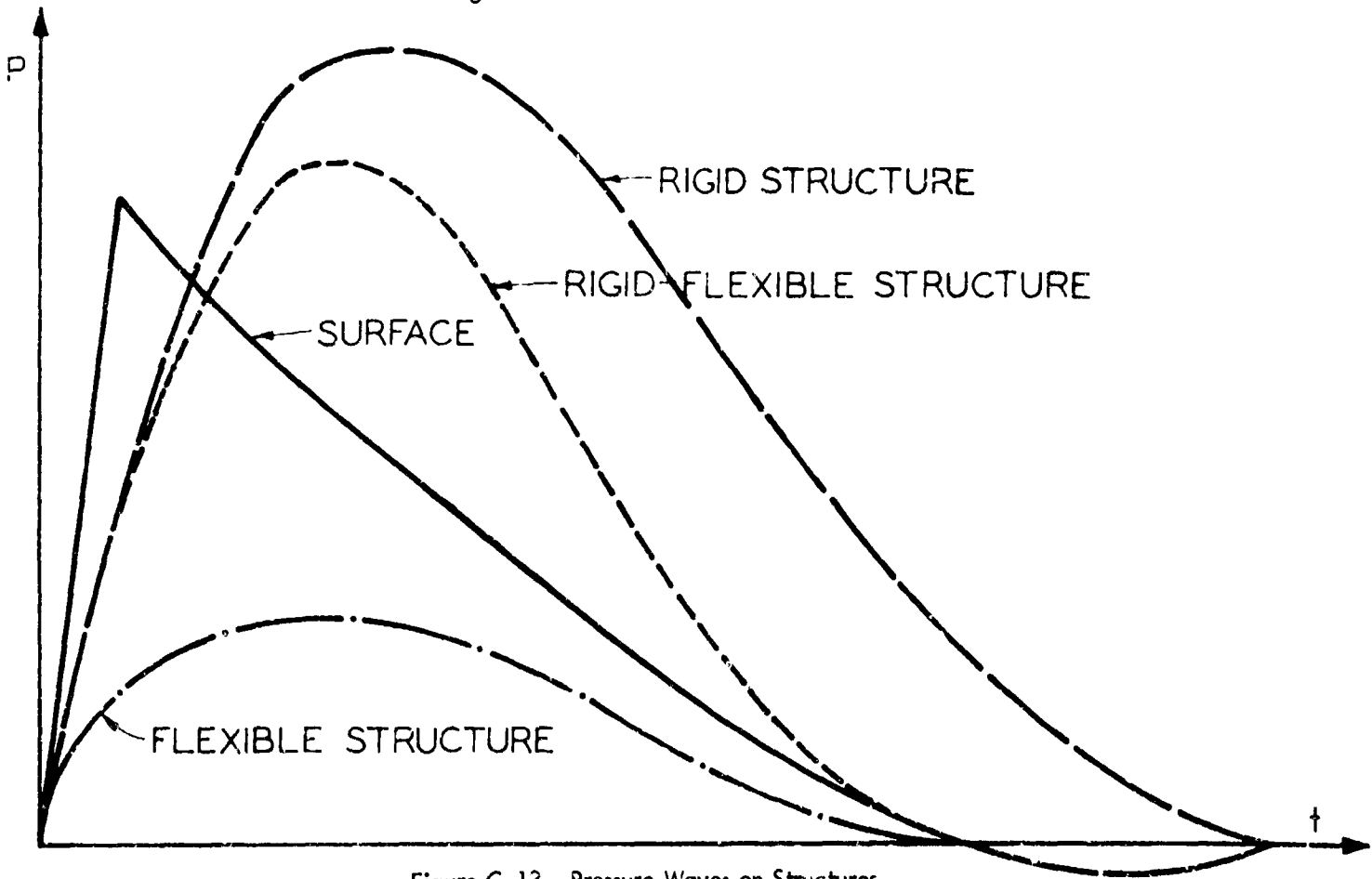


Figure C-13. Pressure Waves on Structures

APPENDIX D

HISTORICAL REVIEW OF MEMBRANE THEORY

A brief review of the development of large deflection theories of plates and the membrane theory of shells is offered in order to supplement the previous analyses. The review is not intended to be exhaustive in these fields, but rather a survey pointing out major contributions. A reasonably complete bibliography supplements the discussion.

In 1910, von Karman extended the linear theory of plates by taking into account the strain in the middle plane of the plate. He derived two non-linear differential equations, as follows:

$$\frac{\partial^4 w}{\partial x^4} + 2 \frac{\partial^2 w}{\partial x^2 \partial y^2} + \frac{\partial^4 w}{\partial y^4} = \frac{h}{D} \left[ \frac{q(x,y)}{h} + \frac{\partial^2 F}{\partial y^2} \frac{\partial^2 w}{\partial x^2} - 2 \frac{\partial^2 F}{\partial x \partial y} \frac{\partial^2 w}{\partial x \partial y} + \frac{\partial^2 F}{\partial x^2} \frac{\partial^2 w}{\partial y^2} \right] \quad (1)$$

$$\frac{\partial^4 F}{\partial x^4} + 2 \frac{\partial^2 F}{\partial x^2 \partial y^2} + \frac{\partial^4 F}{\partial y^4} = E \left[ \left( \frac{\partial^2 w}{\partial x \partial y} \right)^2 - \frac{\partial^2 w}{\partial x^2} \frac{\partial^2 w}{\partial y^2} \right] \quad (2)$$

In 1912, an exact solution of von Karman's equations for a thin, infinitely-long rectangular strip with clamped or supported edges was obtained by Boobnov.

In 1915, Hencky obtained an approximate solution of a laterally loaded circular membrane, or plate of negligible flexural rigidity, by a finite difference approach. Later (Hencky, 1921), he applied the same method to obtain an approximate solution of a laterally loaded rectangular membrane. This same problem was solved by F. Foppl in 1922. He reduced the von Karman equations to the following:

$$\frac{q(x,y)}{h} + \frac{\partial^2 F}{\partial x^2} \frac{\partial^2 w}{\partial y^2} - 2 \frac{\partial^2 F}{\partial x \partial y} \frac{\partial^2 w}{\partial x \partial y} + \frac{\partial^2 F}{\partial y^2} \frac{\partial^2 w}{\partial x^2} = 0 \quad (3)$$

$$\frac{\partial^4 F}{\partial x^4} + 2 \frac{\partial^2 F}{\partial x^2 \partial y^2} + \frac{\partial^4 F}{\partial y^4} = E \left[ \left( \frac{\partial^2 w}{\partial x \partial y} \right)^2 - \frac{\partial^2 w}{\partial x^2} \frac{\partial^2 w}{\partial y^2} \right] \quad (4)$$

Another approximate solution by A. Foppl and L. Foppl in 1924 made use of the Ritz method. They derived the following equation for the center deflection of a circular membrane with clamped edges:

$$\frac{w_o}{h} + 0.588 \left( \frac{w_o}{h} \right)^3 = \frac{3}{16} \frac{P}{E} \left( \frac{a}{h} \right)^4 (1 - \nu^2) \quad (5)$$

In 1925, Nadai derived an approximate solution to the circular membrane problem:

$$\frac{w_o}{h} + 0.583 \left( \frac{w_o}{h} \right)^3 = \frac{3}{16} \frac{P}{E} \left( \frac{a}{h} \right)^4 (1 - \nu^2) \quad (6)$$

And in 1928 Timoshenko used Nadai's approach with an assumed radial displacement and derived the following equation for the maximum deflection:

$$\frac{w_o}{h} + 0.488 \left( \frac{w_o}{h} \right)^3 = \frac{3}{16} \frac{P}{E} \left( \frac{a}{h} \right)^4 (1 - \nu^2) \quad (7)$$

In 1934, S. Way obtained a power series of von Karman's large deflection equations for the deflection equations, for the deflections of a circular plate. He carried the problem out to a center deflection-to-plate thickness ratio of 2/0. Later (Way, 1938), he obtained an approximate solution for a clamped rectangular plate using the Ritz energy method.

In 1936, Rudolf Kaiser reduced the general von Karman equations to five second-order differential equations; the flexural rigidity was taken as zero in one case. These five equations were solved numerically by the use of finite difference approximations for the solution of a square, simply supported, plate. The maximum center deflection-to-plate thickness ratio was 2/5.

From a summary of experimental and analytical research of flat plates under concentrated normal loads, R. G. Stum and R. L. Moore (Stum and Moore, 1937) concluded that when the deflection does not exceed one half the thickness of the plate, over 95 percent of the load may be assumed to be carried by bending. For deflections on the order of eight times the plate thickness, as little as 15 percent of the load is carried by bending.

Most of the theories of plates of negligible flexural rigidity limit the maximum deflection to about two to four times the thickness of the plate. This is certainly in the large deflection theory range but, in addition, these deflections also cause strains which are small enough to be within the elastic range.

A number of analytical studies have been conducted to determine the behavior of circular membranes (Hencky, 1915; Hill, 1950). Hill states that, for the special case when the radial and circumferential strains are equal, the strains vary approximately as the deflection.

Many circular membrane tests have been conducted (McPherson, et al, 1942; Sachs, et al, 1946; Brown and Sachs, 1948; Gleyzal, 1948; Brown and Thompson, 1949; Weil and Newmark, 1955). It can be noted here that, up to the initial point of secondary bulge at the center of the shell, the circumferential strains vary approximately as the deflection in the shell. The radial strain varies from about one half the center strain at the clamped edge, to the maximum at the center, (at the center, the radial and circumferential strains are equal). These tests were mainly interested in the "instability strains" or the strain at the start of the secondary bulge. This point is reached immediately before failure occurs. These tests also indicated that the circular membranes deflect to form a nearly spherical surface under uniform lateral pressure.

Only two of these circular membrane tests provided results which can be correlated with the material presented here (Gleyzal, 1948; Weil and Newmark, 1955). These are presented in Appendix A with Comparison of Results.

In an attempt to determine the plastic behavior of steel under a biaxial stress state, tests have been run on thin tubes (Fraenkel, 1948; Davis and Parker, 1948; Phillips and Kaechele, 1956).

In 1942, Samuel Levy and associates, working for the NACA, conducted a number of large deflection tests on thin rectangular plates (Levy, 1942a; Levy, 1942b; Ramberg, et al, 1942). In one of these tests the center deflection to plate thickness ratio was 12/2. The results of this test are shown in Figure D-1. A comparison with the present results is shown in Appendix A. The reports deal mainly with the solution of von Karman's fundamental equations for large deflections by Fourier series. However, in most cases the center deflection of the plate was less than four times the plate thickness and the permanent set was less than the thickness of the plate. It might be noted that they reached the conclusion that a plate with clamped edges having a length to span ratio of two, or greater, deflects substantially the same as a plate of infinite length.

The solution of von Karman's plate equations for a thin membrane, such that flexural rigidity is zero, has also been accomplished by Shaw and Perrone (Shaw and Perrone, 1954). They cast the problem in terms of displacement components  $u$ ,  $v$ , and  $w$  and thus obtained three simultaneous, non-linear, second-order, partial differential equations. These equations were solved by finite differences and a relaxation procedure. However, they dealt with relatively small deflections (stresses within the elastic range).

The point of interest here is that they solved for the vertical deflections ( $w$ ) with the horizontal displacements ( $u$  and  $v$ ) taken to be zero, and they also solved the complete problem for  $u$ ,  $v$ , and  $w$ . They noted then that the  $w$  displacements are large relative to  $u$  and  $v$  and that the solution for  $w$  only, holding  $u$  and  $v$  zero everywhere, does not vary appreciably from the  $w$  displacements obtained from the complete solution for  $u$ ,  $v$ , and  $w$ . That is, the solution for vertical displacements can be obtained accurately by considering equilibrium in the vertical direction only.

In 1959, W. Zema developed the equations that must be solved to calculate the stresses in a membrane shell which has a circular cross-section, at any point along its length (or width); and has the same angle with the horizontal at any point along its boundaries. The plan area may be quite irregular.

A series of tests for ultimate deflection and strain has been conducted by J. E. Greenspon (Greenspon, 1956). Only the results at failure are given in the comparison with present results (Appendix A).

In 1960, J. E. Greenspon considered the problem of large deflections in a plate and treated it as a membrane under uniform static pressure load:

$$\frac{\partial^2 w}{\partial x^2} + \frac{\partial^2 w}{\partial y^2} = -\frac{P}{S} \quad (8)$$

where  $P$  is the external lateral pressure and  $S$  is the tension per unit length. For the maximum deflection of a clamped rectangular plate he obtained:

$$w_{\max} = \frac{0.164 P a^2}{S \left[ 1 + \left( \frac{a}{b} \right)^2 \right]} \quad (9)$$

For the maximum strain at the middle of the long side  $x = 0, y = b/2$

$$\epsilon_{\max} = 0.132 h^2 \left[ \frac{\frac{Pb}{a}}{S \left[ 1 + \left( \frac{b}{a} \right)^2 \right]} \right]^2 \quad (10)$$

where  $S = \sigma_u t$ .

The concept of shell design by an inverse procedure has been suggested by a number of investigators (Poschl, 1927; Horne, 1945; Timoshenko, 1959; Flugge, 1960; Harrenstien, 1961). This concept is that of fitting the shape to which a shell must adapt, in order to carry prescribed normal pressure loads under uniform direct stress. Harrenstien assumed a uniform compressive membrane force ( $-S$ ) and reduced the equilibrium equations of a membrane shell (Wang, 1953) to one equation

$$\frac{1}{R_1} + \frac{1}{R_2} = \frac{P_3}{S} \quad (11)$$

He used the exact expression for the mean curvature of a circular membrane, and an almost exact expression for the mean curvature of a rectangular membrane, to solve for the shape a membrane must take to resist a lateral load completely by compressive membrane force.

Harrenstien used four approaches to solve the equations: (1) direct integration to obtain a closed form solution, (2) series solution, (3) numerical approximation by finite differences, and (4) membrane analogy. Shell structure models were built to conform to the dimensions predicted by the solutions of the equations. The presentation (Harrenstien, 1961) illustrated the strength of membrane shells designed by this method. Evidence of this fact may be observed by a

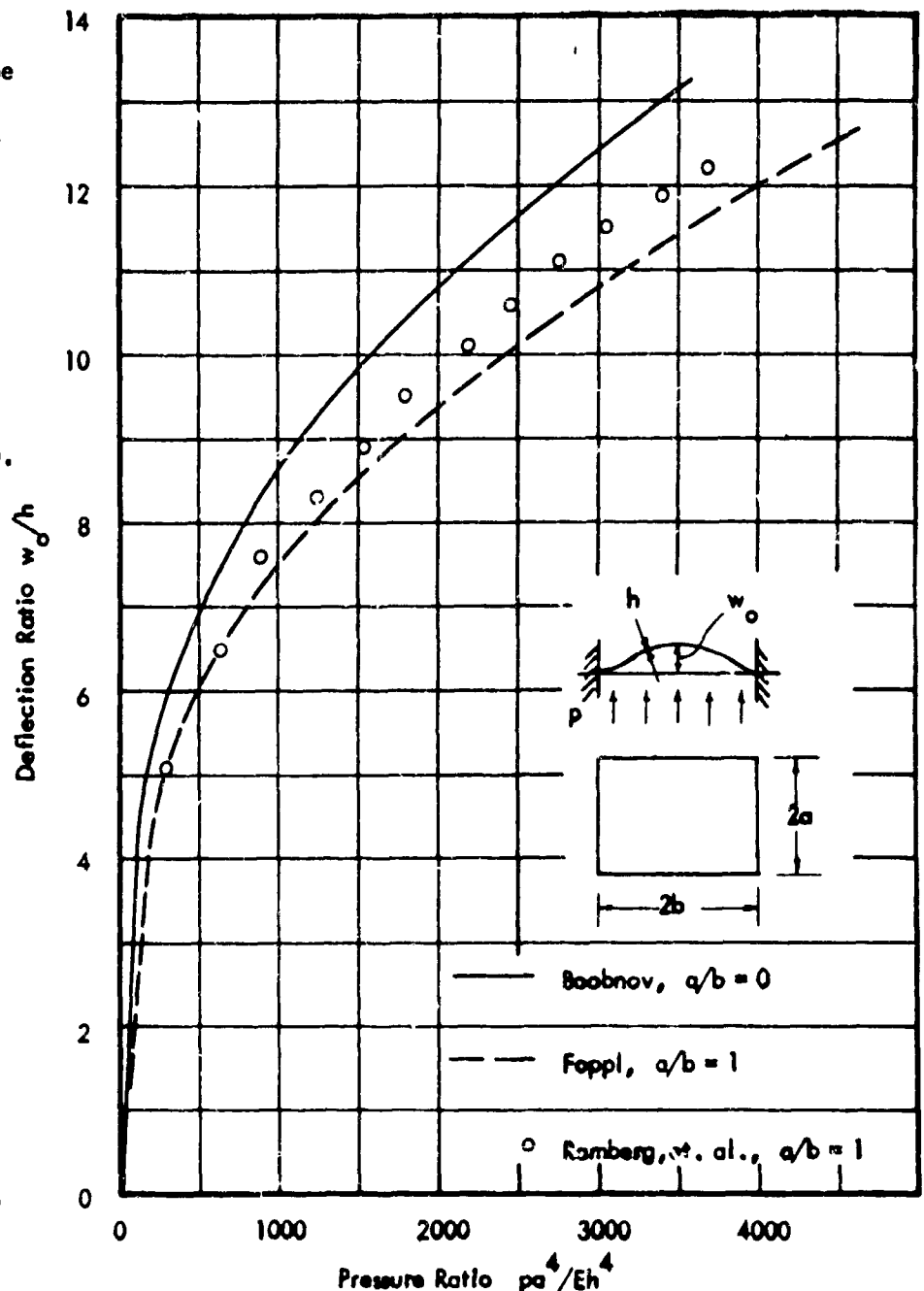


Figure D-1. Center Deflection versus Pressure for Rectangular Plates

consideration of the failure load exhibited by a 0.120 in. thick plaster-of-paris shell. This unreinforced shell, with a diameter of 12.0 in., and a center loading diameter of 2.4 in., resisted a center load of 685 lbs. before failing.

As can be observed from this review, some work has been done in the region of large plastic deflections of membrane. However, most of the work has been concerned with circular membranes. Little work has been accomplished concerning yielding rectangular membranes supported by yielding edge beams.

#### Bibliography

- Boobnov, Ivan G., "On the Stresses in a Ship's Bottom Plating Due to Water Pressure," Transactions of the Institute of Naval Architecture, Vol. 44, 1902, pp. 15-52.
- Brown, W. F., Jr. and G. Sachs, "Strength and Failure Characteristics of Thin Circular Membranes," Transactions of the American Society of Mechanical Engineers, Vol. 70, April, 1948, pp. 241-251.
- Brown, W. F., Jr. and F. C. Thompson, "Strength and Failure Characteristics of Metal Membranes in Circular Bulging," Transactions of the American Society of Mechanical Engineers, Vol. 71, July, 1949, pp. 575-585.
- Davis, H. E. and E. R. Parker, "Behavior of Steel Under Biaxial Stress as Determined by Tests on Tubes," Journal of Applied Mechanics, Vol. 15, September, 1948, pp. 201-215.
- Eisenhart, L. P., A Treatise on the Differential Geometry of Curves and Surfaces, Dover Publications, Inc., New York, 1960.
- Flugge, W., Statik and Dynamik der Schalen, 2nd Ed., Springer-Verlag, Berlin, 1957.
- Flugge, W., Stresses in Shells, Springer-Verlag, Berlin, 1960.
- Fraenkel, S. J., "Experimental Studies of Biaxially Stressed Mild Steel in the Plastic Range," Journal of Applied Mechanics, Vol. 15, September, 1948, pp. 193-200.
- Friedrichs, K. O., The Edge Effects in the Bending of Plates, Reissner Anniversary Volume, Edwards Bros., Inc., Ann Arbor, Michigan, 1949, pp. 197-210.
- Fung, Y. C. and W. H. Withrick, "A Boundary Layer Phenomenon in the Large Deflection of Thin Plates," Quarterly Journal of Mechanics and Applied Mathematics, Vol. 8, 1955, p. 191.
- Gleyzal, A., "Plastic Deformation of a Circular Diaphragm Under Pressure," Journal of Applied Mechanics, Vol. 15, No. 3, September, 1948, pp. 288-296.
- Greenspon, J. E., "An Approximation to the Plastic Deformation of a Rectangular Plate Under Static Load with Design Applications," International Shipbuilding Progress, Vol. 3, No. 22, June, 1956, pp. 329-340.
- Greenspon, J. E., "An Approximation to the Deflections and Strains in a Uniformly Loaded, Clamped Rectangular Panel Subjected to Very Large Plastic Deformations," Journal of the Aero/Space Sciences, Vol. 27, No. 5, May, 1960, pp. 392-393.
- Hansen, S. D., "Computer Program of the Large Deflection Membrane Equation," University of Arizona, November, 1963 (Unpublished).
- Harrenstien, H. P., "Configuration of Shell Structures for Optimum Stresses," Proceedings of the Symposium on Shell Research, Delft, August, 1961, pp. 232-249.
- Hencky, H., "Über den Spannungszustand in Dreisrunden Platten mit verschwingender Biegesteifigkeit," Zeitschrift für Mathematik und Physik, Vol. 63, 1915, p. 311.
- Hencky, H., "Die Berechnung dünner rechteckiger Platten mit verschwindender Biegesteifigkeit," Zeitschrift für Angewandte Mathematik und Mechanik, Vol. 1, April, 1921, pp. 81-89.

- Hill, R., "A Theory of the Plastic Bulging of a Metal Diaphragm by Lateral Pressure," Philosophical Magazine, 7th Series, Vol. 41, 1950, pp. 1133-1142.
- Home, M. R., "Shells with Zero Bending Stresses," Journal of the Mechanics and Physics of Solids, Vol. 2, 1945, pp. 117-126.
- Kaiser, R., "Rechnerische und experimentelle Ermittlung der Durchbiegungen und Spannungen von quadratischen Platten bei freier Auflagerung an den Rändern, gleichmäßig verteilter Last und grossen Ausbiegungen," Zeitschrift für Angewandte Mathematik, Vol. 16, 1936, pp. 73-98.
- Levy, S., "Bending of Rectangular Plates with Large Deflections," NACA Report No. 737, 1942.
- Levy, S., "Square Plate with Clamped Edges Under Normal Pressure Producing Large Deflections," NACA Report No. 740, 1942.
- McPherson, A. E., W. Ramberg, and S. Levy, "Normal Pressure Tests of Circular Plates with Clamped Edges," NACA Report No. 744, 1942.
- Phillips, A. and L. Kaechele, "Combined Stress Tests in Plasticity," Journal of Applied Mechanics, Vol. 23, 1956, p. 43.
- Poschl, T., "Kuppeln mit gleichen Normalspannungen," Der Bauingenieur, Vol. 8, 1927, pp. 624-628.
- Ramberg, W., A. E. McPherson and S. Levy, "Normal Pressure Tests of Rectangular Plates," NACA Report No. 749, 1942.
- Sachs, G., G. Espey and G. B. Kasik, "Circular Bulging of Aluminum-Alloy Sheet at Room and Elevated Temperatures," Transactions of the American Society of Mechanical Engineers, Vol. 68, February 1946, pp. 161-170.
- Shaw, F. S. and N. Perrone, "A Numerical Solution for the Nonlinear Deflection of Membranes," Journal of Applied Mechanics, Vol. 21, 1954, p. 117.
- Stum, R. G. and R. L. Moore, "The Behavior of Rectangular Plates Under Concentrated Load," Transactions of the American Society of Mechanical Engineers, Vol. 59, 1937.
- Timoshenko, S., "Deflections of a Uniformly Loaded Circular Plate with Clamped Edges," (1928), Collected Papers of Timoshenko, McGraw-Hill Book Co., Inc., New York, 1953.
- Timoshenko, S., Theory of Plates and Shells, McGraw-Hill Book Co., Inc., New York, 1959.
- Wang, Chi-Teh, Applied Elasticity, McGraw-Hill Book Co., Inc., New York, 1953, pp. 310-326.
- Way, S., "Bending of Circular Plates with Large Deflections," Transactions of the American Society of Mechanical Engineers, Vol. 56, 1934, p. 627.
- Way, S., "Uniformly Loaded, Clamped Rectangular Plates with Large Deflections," Proceedings of the Fifth International Congress of Applied Mechanics, Cambridge, Mass., 1938, p. 123.
- Weil, N. A. and N. M. Newmark, "Large Plastic Deformations of Circular Membranes," Journal of Applied Mechanics, Vol. 22, 1955, p. 533.
- Zerna, W., "The Calculations of Membrane Stresses in Doubly-Curved Shells of Arbitrary Plan," Ingenieur-Archiv, Vol. 28, March, 1959, pp. 363-365.

Unclassified

Security Classification

**DOCUMENT CONTROL DATA - R&D**

*(Security classification of title, body of abstract and indexing annotation must be entered when the overall report is classified)*

1. ORIGINATING ACTIVITY (Corporate author) University of Arizona Tucson, Arizona		2a. REPORT SECURITY CLASSIFICATION Unclassified	
		2b. GROUP N/A	
3. REPORT TITLE Yielding Membrane Elements in Protective Construction			
4. DESCRIPTIVE NOTES (Type of report and inclusive dates) Final Report			
5. AUTHOR(S) (Last name, first name, initial) H. Harrenstein                      J. Burns R. Gunderson                        J. Salmons S. Hanson                              D. Neilson			
6. REPORT DATE May 1965		7a. TOTAL NO. OF PAGES 121	7b. NO. OF REFS 36
8a. CONTRACT OR GRANT NO. OCD-OS-64-187		8a. ORIGINATOR'S REPORT NUMBER(S) ---	
b. PROJECT NO. Subtask 1122D		8b. OTHER REPORT NO(S) (Any other numbers that may be assigned this report) ---	
c.			
d.			
10. AVAILABILITY/LIMITATION NOTICES Distribution of this document is unlimited			
11. SUPPLEMENTARY NOTES ----		12. SPONSORING MILITARY ACTIVITY Office of Civil Defense Office of the Secretary of the Army Washington, D. C.	
13. ABSTRACT (U) The report covers an investigation of the feasibility of the application of doubly-curved shell structures to the problem of sheltering people from the blast effects of nuclear weapons. The steel shell works best in tension. Under certain conditions a 1/4 inch thick steel membrane will carry more load than a 19 inch thick concrete slab reinforced with steel at a rate of 4.08 inches per square foot. The membrane itself uses less steel than the reinforced concrete slab. Favorable soil-structure interaction effects are introduced with the yielding membranes. Boundary supports and full scale testing are items that need more attention as parts of future investigation.			

DD FORM 1473  
1 JAN 64

Unclassified

Security Classification

14. KEY WORDS	LINK A		LINK B		LINK C	
	ROLE	WT	ROLE	WT	ROLE	WT
Blast Shelters Shell structures Membranes Construction Yielding Membranes						

INSTRUCTIONS

1. **ORIGINATING ACTIVITY:** Enter the name and address of the contractor, subcontractor, grantee, Department of Defense activity or other organization (*corporate author*) issuing the report.
- 2a. **REPORT SECURITY CLASSIFICATION:** Enter the overall security classification of the report. Indicate whether "Restricted Data" is included. Marking is to be in accordance with appropriate security regulations.
- 2b. **GROUP:** Automatic downgrading is specified in DoD Directive 5200.10 and Armed Forces Industrial Manual. Enter the group number. Also, when applicable, show that optional markings have been used for Group 3 and Group 4 as authorized.
3. **REPORT TITLE:** Enter the complete report title in all capital letters. Titles in all cases should be unclassified. If a meaningful title cannot be selected without classification, show title classification in all capitals in parenthesis immediately following the title.
4. **DESCRIPTIVE NOTES:** If appropriate, enter the type of report, e.g., interim, progress, summary, annual, or final. Give the inclusive dates when a specific reporting period is covered.
5. **AUTHOR(S):** Enter the name(s) of author(s) as shown on or in the report. Enter last name, first name, middle initial. If military, show rank and branch of service. The name of the principal author is an absolute minimum requirement.
6. **REPORT DATE:** Enter the date of the report as day, month, year, or month, year. If more than one date appears on the report, use date of publication.
- 7a. **TOTAL NUMBER OF PAGES:** The total page count should follow normal pagination procedures, i.e., enter the number of pages containing information.
- 7b. **NUMBER OF REFERENCES:** Enter the total number of references cited in the report.
- 8a. **CONTRACT OR GRANT NUMBER:** If appropriate, enter the applicable number of the contract or grant under which the report was written.
- 8b, 8c, & 8d. **PROJECT NUMBER:** Enter the appropriate military department identification, such as project number, subproject number, system numbers, task number, etc.
- 9a. **ORIGINATOR'S REPORT NUMBER(S):** Enter the official report number by which the document will be identified and controlled by the originating activity. This number must be unique to this report.
- 9b. **OTHER REPORT NUMBER(S):** If the report has been assigned any other report numbers (*either by the originator or by the sponsor*), also enter this number(s).

10. **AVAILABILITY/LIMITATION NOTICES:** Enter any limitations on further dissemination of the report, other than those imposed by security classification, using standard statements such as:

- (1) "Qualified requesters may obtain copies of this report from DDC."
- (2) "Foreign announcement and dissemination of this report by DDC is not authorized."
- (3) "U. S. Government agencies may obtain copies of this report directly from DDC. Other qualified DDC users shall request through \_\_\_\_\_."
- (4) "U. S. military agencies may obtain copies of this report directly from DDC. Other qualified users shall request through \_\_\_\_\_."
- (5) "All distribution of this report is controlled. Qualified DDC users shall request through \_\_\_\_\_."

If the report has been furnished to the Office of Technical Services, Department of Commerce, for sale to the public, indicate this fact and enter the price, if known.

11. **SUPPLEMENTARY NOTES:** Use for additional explanatory notes.
12. **SPONSORING MILITARY ACTIVITY:** Enter the name of the departmental project office or laboratory sponsoring (*paying for*) the research and development. Include address.
13. **ABSTRACT:** Enter an abstract giving a brief and factual summary of the document indicative of the report, even though it may also appear elsewhere in the body of the technical report. If additional space is required, a continuation sheet shall be attached.

It is highly desirable that the abstract of classified reports be unclassified. Each paragraph of the abstract shall end with an indication of the military security classification of the information in the paragraph, represented as (TS), (S), (C), or (U).

There is no limitation on the length of the abstract. However, the suggested length is from 150 to 225 words.

14 **KEY WORDS:** Key words are technically meaningful terms or short phrases that characterize a report and may be used as index entries for cataloging the report. Key words must be selected so that no security classification is required. Identifiers such as equipment model designation, trade name, military project code name, geographic location, may be used as key words but will be followed by an indication of technical context. The assignment of links, rules, and weights is optional.